frontiers | Research Topics

Advances in crustacean research from the 10th International Crustacean Congress

Edited by
Kareen E. Schnabel and Rachael Peart

Published in
Frontiers in Marine Science

ISSN 1664-8714
ISBN 978-2-8325-5870-6
DOI 10.3389/978-2-8325-5870-6

About Frontiers

Frontiers is more than just an open access publisher of scholarly articles: it is a pioneering approach to the world of academia, radically improving the way scholarly research is managed. The grand vision of Frontiers is a world where all people have an equal opportunity to seek, share and generate knowledge. Frontiers provides immediate and permanent online open access to all its publications, but this alone is not enough to realize our grand goals.

Frontiers journal series

The Frontiers journal series is a multi-tier and interdisciplinary set of open-access, online journals, promising a paradigm shift from the current review, selection and dissemination processes in academic publishing. All Frontiers journals are driven by researchers for researchers; therefore, they constitute a service to the scholarly community. At the same time, the *Frontiers journal series* operates on a revolutionary invention, the tiered publishing system, initially addressing specific communities of scholars, and gradually climbing up to broader public understanding, thus serving the interests of the lay society, too.

Dedication to quality

Each Frontiers article is a landmark of the highest quality, thanks to genuinely collaborative interactions between authors and review editors, who include some of the world's best academicians. Research must be certified by peers before entering a stream of knowledge that may eventually reach the public - and shape society; therefore, Frontiers only applies the most rigorous and unbiased reviews. Frontiers revolutionizes research publishing by freely delivering the most outstanding research, evaluated with no bias from both the academic and social point of view. By applying the most advanced information technologies, Frontiers is catapulting scholarly publishing into a new generation.

What are Frontiers Research Topics?

Frontiers Research Topics are very popular trademarks of the *Frontiers journals series*: they are collections of at least ten articles, all centered on a particular subject. With their unique mix of varied contributions from Original Research to Review Articles, Frontiers Research Topics unify the most influential researchers, the latest key findings and historical advances in a hot research area.

Find out more on how to host your own Frontiers Research Topic or contribute to one as an author by contacting the Frontiers editorial office: frontiersin.org/about/contact

Advances in crustacean research from the 10th International Crustacean Congress

Topic editors

Kareen E. Schnabel — National Institute of Water and Atmospheric Research (NIWA), New Zealand

Rachael Peart — National Institute of Water and Atmospheric Research (NIWA), New Zealand

Citation

Schnabel, K. E., Peart, R., eds. (2025). *Advances in crustacean research from the 10th International Crustacean Congress*. Lausanne: Frontiers Media SA.

doi: 10.3389/978-2-8325-5870-6

Table of contents

frontiers | Frontiers in Marine Science

TYPE Editorial
PUBLISHED 17 December 2024
DOI 10.3389/fmars.2024.1529867

OPEN ACCESS

EDITED AND REVIEWED BY
Bronwyn M. Gillanders,
University of Adelaide, Australia

*CORRESPONDENCE
Rachael A. Peart
rachael.peart@niwa.co.nz

RECEIVED 18 November 2024
ACCEPTED 03 December 2024
PUBLISHED 17 December 2024

CITATION
Peart RA and Schnabel KE (2024) Editorial: Advances in crustacean research from the 10th International Crustacean Congress. *Front. Mar. Sci.* 11:1529867. doi: 10.3389/fmars.2024.1529867

Editorial: Advances in crustacean research from the 10th International Crustacean Congress

Rachael A. Peart* and Kareen E. Schnabel

Marine Biodiversity, National Institute of Water and Atmospheric Research, Wellington, New Zealand

KEYWORDS

editorial, Crustacea, New Zealand, international, congress

Editorial on the Research Topic
Advances in crustacean research from the 10th International Crustacean Congress

Introduction

Crustaceans are among the most abundant and diverse organisms on Earth. Due to their diversity and abundance and their occurrence in the terrestrial, freshwater, groundwater, marine and fossil environments, crustaceans are an integral part of ecosystems and ecosystem functioning. They are at the forefront of international studies of neurobiology, aquaculture, toxicology, biosecurity, biodiversity, evolution and many more. Crustaceans can also provide a signal for environmental change aiding the management of fisheries and other anthropogenic activity.

Every four years, the Crustacean Society (TCS) hosts an International Crustacean Congress (ICC), where international delegates share research covering a broad range of disciplines related to our world's Crustacea. In May 2023, the International Society of Invertebrate Reproduction and Development (ISIRD) and TCS jointly held the 10th ICC for the first time in Aotearoa New Zealand, hosted by the Museum of New Zealand Te Papa Tongarewa and the National Institute of Water & Atmospheric Research (NIWA).

The program was dedicated to the dissemination of all aspects of crustacean research and to promoting the exchange of information and ideas related to carcinology.

Summary of the topic papers

This Research Topic hosts some of the general proceedings of the conference and the results highlight the significance and importance of understanding the diversity and function of a globally critical group of organisms.

In this Research Topic, 11 papers by 42 authors collaboratively address issues related to a variety of crustacean topics. The papers covered a number of different groups of crustaceans; from peracarids to decapods and in a range of habitats, from freshwater to the deep-sea. Questions address environmental/climate factors such as the Southern Oscillation Index as drivers of

macrobenthic crustacean distribution, abundance and species richness in New Zealand estuaries (Lam-Gordillo et al.). Climate change as a driver of habitat change is also considered by Katharoyan et al. who examine its effects on South African mangrove and salt marsh crab populations. Freshwater prawns are considered in a study examining the cell metabolism of freshwater prawns providing a baseline for further cell culturing of crustaceans, with implications for fisheries and population sustainability (Sudarshan et al.). Aspects of crustacean larval biology are considered in an examination of how even at a larval stage the presence of marine protected areas can influence the abundance and resilience of crustacean communities (Landeira et al.). The influence of the immediate environment around crustaceans on their behaviour is examined concluding that fiddler crabs can learn complex routes in returning to their homebases (Chatterji and Layne). Fishery associated crustacean research was covered in the ICC10 congress proceedings, represented here by a study of artisanal fisheries in Northern Patagonia, concluding that there is a necessity to monitor the effects of seasonal variations on the reproductive cycle of crabs (Hamamé et al.). Geburzi et al. discuss the use of crustacean specific molecular probes (ultraconserved elements) in conservation genetics and evolutionary studies in both the shallow water and deep-sea environments. This approach provides opportunities to include poorly preserved and rare specimens in these types of studies. Different aspects of the deep-sea crustacean biology are considered by examining the connectivity between deep-sea biogeographic provinces (e.g. by the study of the tanaid superfamily Neotanaoidea), highlighting complex and generally understudied processes in the deep-sea (Theil and Błażewicz). Continuing the deep-sea focus, Casaubon and Riehl describe specific morphological measurement techniques to help understand functional morphology of deep-sea isopods collected from Icelandic waters. This Research Topic concludes with taxonomic descriptions of two new species: a ghost shrimp of the family Callianopsidae which is recorded for the first time from the waters off Aotearoa New Zealand (Schnabel and Peart), and a new species of *Pentaceration* isopod from the family Paramunnidae, also from the waters off Aotearoa New Zealand (Peart and Schnabel).

Gaps and perspectives

The global importance of the rich, unique and valuable biodiversity of crustaceans in ecosystems and global fisheries is undeniable. Unfortunately, it is this abundance, diversity and complexity that causes the most difficulties in studying these environments. Proportionally we know so little of the cell structure, functional morphology, biochemical responses, ecotoxicology and systematics of the crustaceans. It is essential to continually have conferences such as the International Crustacean Congress to inform and promote the world of crustacean research to try and fill these gaps.

Author contributions

RP: Conceptualization, Funding acquisition, Project administration, Writing – original draft, Writing – review & editing. KS: Conceptualization, Funding acquisition, Project administration, Writing – original draft, Writing – review & editing.

Acknowledgments

Special thanks are due to the editors, reviewers and all the staff who patiently and competently followed the entire process for the publication of this Research Topic.

Conflict of interest

The authors declare that the research was conducted in the absence of any commercial or financial relationships that could be construed as a potential conflict of interest.

The author(s) declared that they were an editorial board member of Frontiers, at the time of submission. This had no impact on the peer review process and the final decision.

Publisher's note

frontiers | Frontiers in Marine Science

TYPE Original Research
PUBLISHED 14 November 2023
DOI 10.3389/fmars.2023.1292849

OPEN ACCESS

EDITED BY
Meilin Wu,
Chinese Academy of Sciences (CAS), China

REVIEWED BY
Jibiao Zhang,
Guangdong Ocean University, China
Peng Zhang,
Guangdong Ocean University, China

*CORRESPONDENCE
Orlando Lam-Gordillo
orlando.lam-gordillo@niwa.co.nz

RECEIVED 12 September 2023
ACCEPTED 30 October 2023
PUBLISHED 14 November 2023

CITATION
Lam-Gordillo O, Lohrer AM, Douglas E, Hailes S, Carter K and Greenfield B (2023) Scale-dependent influence of multiple environmental drivers on estuarine macrobenthic crustaceans.
Front. Mar. Sci. 10:1292849.
doi: 10.3389/fmars.2023.1292849

Scale-dependent influence of multiple environmental drivers on estuarine macrobenthic crustaceans

Orlando Lam-Gordillo*, Andrew M. Lohrer, Emily Douglas, Sarah Hailes, Kelly Carter and Barry Greenfield

Coast and Estuaries, National Institute of Water and Atmospheric Research, Hamilton, New Zealand

Estuarine ecosystems are transitional environments, where land, freshwater, and marine ecosystems converge. Estuaries are also hotspots of ecological functioning and considered highly economically and culturally valuable for the ecosystem services they provide to humankind. However, multiple stressors (e.g., nutrient and sediment loading, pollution, climate change) are threatening the survival of estuarine organisms and therefore affecting the functions and services estuarine ecosystems provide. In this study, we investigated the influence of multiple environmental variables on long-term estuarine crustacean data across several estuaries in New Zealand. We focused on responses of specific crustacean groups and total crustacean abundance and richness to freshwater, ocean, and climate variables as drivers of change at large, medium, and fine spatial scales. Our analyses revealed that the abundance and richness of crustaceans, as well as the abundance of specific crustacean groups (i.e., Amphipoda, Decapoda, Cumacea, Tanaidacea), were influenced by unique combinations of environmental variables, resulting in scale dependent interactions. We also identified negative relationships between estuarine crustaceans and drivers, with decreased abundance and richness of crustaceans as the magnitude of drivers increased. Sea Surface Temperature (SST) and climate-related drivers (Southern Oscillation Index, SOI) were the dominant drivers affecting estuarine crustaceans, yet sediment muddiness negatively affected crustacean communities at all spatial scales assessed. Our research suggests that the combined effects of multiple environmental drivers such as increased muddiness, ocean warming, and climate change are likely to act in a concerted way to affect the health and functioning of estuarine ecosystems. The observed interactions between macrobenthic crustaceans and climatic and oceanic drivers have important implications for understanding climate change impacts on marine ecosystems and assist management and conservation efforts.

KEYWORDS

climate change, estuaries, ecosystems, environmental, GLM, New Zealand

1 Introduction

Estuarine ecosystems are considered hotspots for biodiversity, productivity, and biogeochemical cycling (Thrush et al., 2013; Villnäs et al., 2019). These ecosystems provide a range of ecosystem services (e.g., coastal protection, food production, tourism) and functions (Barbier et al., 2011; Thrush et al., 2013; Rullens et al., 2019; Hillman et al., 2020; Lam-Gordillo et al., 2022b).As ecotones between the land and sea, estuarine ecosystems act as buffer zones, filtering organic matter, nutrients, and sediments inputs from terrestrial sources (Seitzinger, 1988; Villnäs et al., 2019; O'Meara et al., 2020; Lam-Gordillo et al., 2022b). However, increasing inputs of sediments, inorganic nutrients, and other pollutants and contaminants linked to anthropogenic activities such as climate change are challenging the buffering capacity of the estuaries and therefore the functions and services these ecosystems provide (Chapman, 2016; Cloern et al., 2016; Villnäs et al., 2019; Malone and Newton, 2020; Lam-Gordillo et al., 2022a).

Estuarine ecosystems worldwide are under pressure from past and ongoing changes as a result of shipping and port development, the conversion of natural habitats to land for agriculture and forestry, excessive fishing and resource extraction, and industrialisation (Cloern et al., 2016; Villnäs et al., 2019; Thrush et al., 2021). Yet, these ecosystems are not only affected by human pressures (e.g., reduction of river flows, increased nutrient loads, eutrophication, pollution), but also by natural cycles, events, and trends associated with tides, storms, and broader climatic drivers (e.g., increasing air and water temperatures, sea level rise). These types of environmental stressors can act together to affect estuarine organisms and in turn the health and functioning of estuarine ecosystems (Cloern et al., 2016; Hewitt et al., 2016; Ellis et al., 2017; Goulding et al., 2021; Thrush et al., 2021; Lam-Gordillo et al., 2022b).

Estuarine ecosystems naturally experience huge shifts in conditions over short time spans due to tidal cycles and many organisms already exist close to their tolerance limits. Environmental variables determine the distributions and structure of organisms based on these tolerances but added stressors could constrain their distributions and challenge the survival of organisms. The effects of multiple environmental variables on the abundance and distribution of estuarine organisms, as well as on the health and functioning of these ecosystems, may not be strictly additive. Multiple stressors can act in a multiplicative manner, resulting in greater than expected (synergistic) or lower than expected (antagonistic) effects relative to additive combinations of individual stressor effects (Thrush et al., 2008b; Ellis et al., 2017; Carrier-Belleau et al., 2021; Clark et al., 2021). These multi-stressor interactions are predicted to increase as climate change (sea-level rise, altered rainfall patterns, and increased air and water temperatures) continues to unfold (Gunderson et al., 2016; Ellis et al., 2017; Clark et al., 2021). Understanding the interactions of changing environmental variables as drivers of estuarine communities is critical to inform policy and management to ensure healthy estuarine ecosystems (Simeoni et al., 2023). However, the influence of multiple stressors on estuarine communities is difficult to characterise, leading to uncertainties on predictions of community change and the consequent effects on ecosystem functioning (Thrush et al., 2008b; Hewitt et al., 2016; Ellis et al., 2017; Clark et al., 2021; Lam-Gordillo et al., 2021; Thrush et al., 2021).

Crustaceans, such as amphipods, cumaceans, decapods, isopods, and tanaids, represent one of the most abundant and important groups of benthic macrofauna (Sánchez-Moyano and García-Asencio, 2010; Medina-Contreras et al., 2022; De Grave et al., 2023; Nozarpour et al., 2023). These organisms have been recognised as effective bioindicators for assessing environmental change due to their sensitivity to various anthropogenic and natural disturbances (Borja et al., 2000; Dauvin et al., 2006; Sánchez-Moyano and García-Asencio, 2010). Crustaceans are also key contributors to the functioning of estuarine ecosystems (e.g., Needham et al., 2011; Needham et al., 2013; Agusto et al., 2022; Nozarpour et al., 2023). For example, crustaceans are involved in trophic dynamics transferring energy and matter from lower to higher trophic levels as food source for fish and birds (Zetina-Rejon et al., 2003; Bui and Lee, 2014; Medina-Contreras et al., 2022). These organisms also alter the sedimentary environment (e.g., topography, biogeochemistry, particle size) through biological processes such as bioturbation (Lohrer et al., 2004a; Needham et al., 2011; Needham et al., 2013; Fanjul et al., 2015; Agusto et al., 2022). Bioturbating crustaceans rework the sediment (e.g., bioirrigation, bioventilation), promoting sediment oxygenation, which ultimately enhances microbial activity responsible for organic matter decomposition and nutrient cycling (Welsh, 2003; Lohrer et al., 2004a; Kristensen et al., 2012; Lam-Gordillo et al., 2022a).

Crustaceans are prominent among taxa affecting ecosystem functioning (e.g., Nozarpour et al., 2023), and are sensitive to natural and anthropogenic disturbances (e.g., Borja et al., 2000). With case study analyses of crustaceans, we can improve our understanding of how coastal ecosystems respond to increasing temperatures, sea level rise, nutrient enrichment, pollution, and in general, how the crustacean communities inhabiting estuarine ecosystems respond to the influence of multiple stressors.

In recent decades, most studies of estuarine macrofauna have focused on evaluating individual effects of single stressors, while there has been less research assessing the influence of multiple stressors on estuarine macrobenthic communities (e.g., Thrush et al., 2008b; Ellis et al., 2017; Clark et al., 2021). Here we leveraged the availability of high-quality estuarine time-series data from three sites in each of three estuaries to investigate the influence of multiple environmental variables on long-term estuarine crustacean data across three different estuaries in New Zealand. We focused on (i) evaluating responses of crustacean communities to five environmental variables at large, medium, and fine scales, and (ii) assessing the influence of these multiple drivers on specific crustacean taxa groups. We hypothesised that (1) crustaceans will respond to multiple environmental predictors more often than to single predictors, (2) the influence of multiple drivers will be spatial scale dependent, and (3) specific crustacean groups will have differential responses to multiple drivers.

2 Materials and methods

2.1 Study area

Crustacean data were collected from nine sites total, with three sites in each of three estuaries (Kaipara: KaiB, KKF, NPC, Mahurangi: HL, JB, MH, and Manukau: AA, CB, CH) located on the North Island of New Zealand (Figure 1; Table 1). Kaipara Harbour opens to the Tasman Sea on the west coast and is one of the largest estuaries in the southern hemisphere, covering ~947 km^2 including vast extents of seagrass habitat (Heath, 1975; Pine et al., 2015; Bulmer et al., 2016). Recent intensification of agriculture and urban development in the catchment of the estuary has contributed to increased sediment loads and decreased water clarity (Ellis et al., 2004; Bulmer et al., 2016). Mahurangi Harbour, 24.7 km^2, is a relatively small estuary on the east coast (Thrush et al., 2008a; Oldman et al., 2009) with intertidal flats ranging from fine muddy sediments at the head of the harbour to coarse sands near the mouth. Pastoral farming, lifestyle blocks, and forestry occur in the catchment (Gibbs et al., 2005; Thrush et al., 2008a; Oldman et al., 2009). Manukau Harbour, to the south of Kaipara Harbour on the west coast, is the second largest estuary in New Zealand at 368 km^2 (Heath, 1975). It is a shallow estuary with a highly developed branching channel system and a mixture of habitats including intertidal mudflats, mangrove stands, and saltmarshes (Gorman and Neilson, 1999; Green et al., 2000; Bastakoti et al., 2019). Although adjacent to Auckland, New Zealand's largest city, the catchments draining into Manukau Harbour are small relative to estuary size and predominantly rural/pasture. All of the sites sampled in each estuary are Auckland Council ecological monitoring sites (Drylie, 2021). As such, the sites were selected for their relative similarity in terms of elevation relative to chart datum (mid-intertidal) and salinity at high tide (usually >32 PSU). However, sediment characteristics at each site varied from "muddy" to "sandy", often related to position of sites in upper versus lower estuary, respectively.

2.2 Data collection

2.2.1 Biological data

Crustacean data were retrieved from a long-term macrobenthic dataset (1989-2022) held by Auckland Council to assess the ecological health of estuaries. Collection of macrobenthic organisms, processing of samples, and sorting and identifications has followed standard protocols (Robertson et al., 2002; Hewitt et al., 2014) and strict quality assurance/quality control procedures (Hewitt et al., 2014; Greenfield et al., 2023), providing high confidence in the validity of data comparisons over time. Sampling of macrobenthic fauna was performed three-monthly from 2009 to 2022, years in which all 9 sites in the three estuaries were sampled (Table 1). Briefly, at each of the sampling sites, 12 replicate sediment samples for assessing macrobenthic fauna were collected using a hand-held PVC corer (13 cm diameter by 15 cm depth), sieved through a 0.5 mm mesh size, and preserved in 70% isopropanol. Benthic macrofauna were sorted, identified to the lowest possible taxonomic level (usually genus or species), and counted.

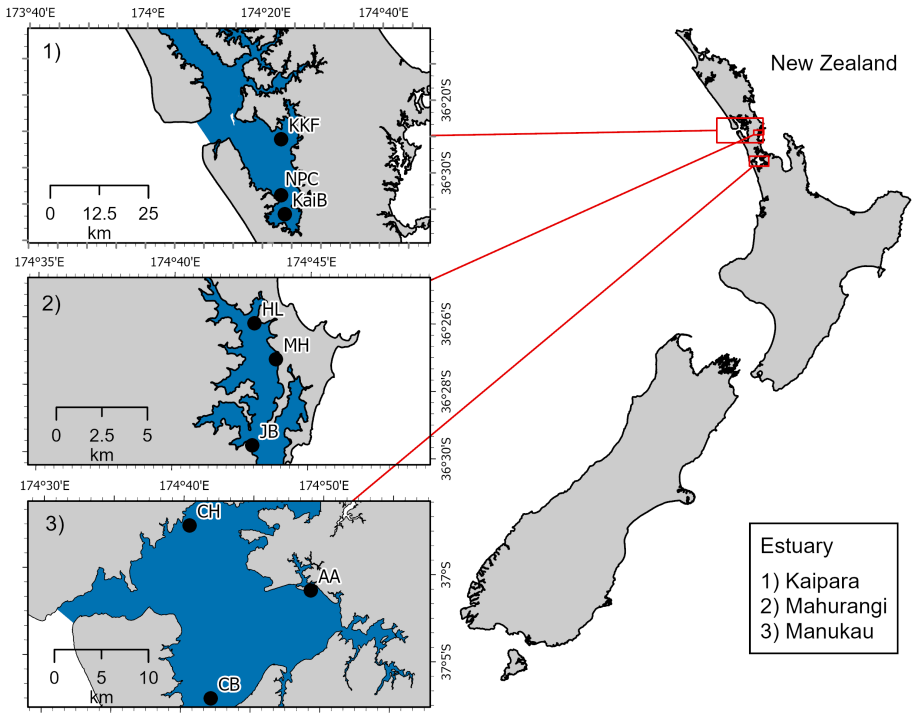

FIGURE 1
Map of the study area showing the nine sites across three estuaries in New Zealand from where crustacean samples were collected.

10.3389/fmars.2023.1292849

TABLE 1 Summary details of the macrobenthic and environmental data used in this study.

Estuary	Site	NZ coast	Time series (Macrofauna)	Sampling frequency	Collection	Source
Kaipara	KaiB	West	2009-2022	3 months	In-situ	Auckland Council
	KKF		2009-2022	3 months	In-situ	Auckland Council
	NPC		2009-2022	3 months	In-situ	Auckland Council
Mahurangi	HL	East	2009-2022	3 months	In-situ	Auckland Council
	JB		2009-2022	3 months	In-situ	Auckland Council
	MH		2009-2022	3 months	In-situ	Auckland Council
Manukau	AA	West	2009-2022	3 months	In-situ	Auckland Council
	CB		2009-2022	3 months	In-situ	Auckland Council
	CH		2009-2022	3 months	In-situ	Auckland Council
Environmental drivers		**Units**	**Time series**	**Sampling frequency**	**Collection**	**Source**
Chlorophyll *a*	Chl-a	mg/g	2009-2022	3 months	In-situ	NIWA
Organic matter content	OM	%	2009-2022	3 months	In-situ	NIWA
Mud content	Mud	%	2009-2022	3 months	In-situ	NIWA
Sea Surface Temperature	SST	°C	1984-2022	Monthly	Global	NOAA (https://www.cpc.ncep.noaa.gov)
Southern Oscillation Index	SOI	none	2009-2022	Monthly	Global	Ocean Color (https://oceancolor.gsfc.nasa.gov)

2.2.2 Environmental drivers

Five environmental variables with the potential to influence estuarine crustacean communities were available for analysis. All relate in some degree to anthropogenic activities, but the degree to which they are deleterious or beneficial often depends on magnitude and context. The five variables assessed were sediment chlorophyll *a* content (Chl-*a*); sediment organic matter content (OM); sediment mud content (muddiness, percent dry weight of silt and clay particles <63 um); sea surface temperature along the coast outside each estuary mouth (SST, degrees Celcius); and Southern Oscillation Index value (SOI, a general indicator of climate variability).

Chl-*a* is a photosynthetic pigment found in marine plants that is used as a proxy for soft-sediment microphytobenthos abundance. Microphytobenthos is an important source of labile food for macroinvertebrate crustaceans. *In situ* photosynthetic oxygen production by microphytobenthos can increase surface sediment oxygenation levels and biogeochemical rates (e.g., organic matter degradation, nitrification-denitrification). However, very high sediment Chl-*a* and organic matter levels are indicative of eutrophication, resulting from excessive nutrient loading from catchments and point sources. Microbially mediated organic matter remineralisation can deplete the dissolved oxygen in sediment pore water and contribute to toxic concentrations of ammonium and hydrogen sulphide.

Increased muddiness, resulting from increases in catchment-derived fine sediments, has had major impacts on the health and functioning of estuaries in New Zealand (Thrush et al., 2004). Estuary sedimentation is naturally high in New Zealand due to high rainfall and steep topography (Hicks et al., 2019), but changes in land-use have elevated soil erosion and export rates drastically relative to pre-human times (Hunt, 2019). Inverse relationships between sediment muddiness and macrofaunal abundance, richness and diversity are relatively well documented in New Zealand estuaries (Thrush et al., 2003b; Lohrer et al., 2004b; Lohrer et al., 2006; Lohrer et al., 2012; Thrush et al., 2017). Many anthropogenic contaminants bind to and are transported by fine sediment particles, and muddiness is often strongly correlated with sediment organic matter content (with fine sediments providing proportionally more surface area for the attachment of microbes than larger particles) (Douglas et al., 2018).

Climate change manifests locally in a variety of ways. For estuaries, this can be changes in prevailing winds, rainfall, and temperatures, which can affect exposure to wind-waves, turbidity, and heat stress and desiccation at low tide. There is worldwide concern about marine heat waves (Oliver et al., 2018; Oliver et al., 2021; Xu et al., 2022), including in New Zealand, where anomalously warm years have been occurring more often recently (Oliver et al., 2018; Behrens et al., 2022). Yet is possible that increasing sea surface temperatures may positively influence benthic macroinvertebrate growth and reproduction up to a point, whereafter negative impacts may ensue. We used both sea surface temperatures (SST) and the Southern Oscillation Index (SOI) as potential predictors of macroinvertebrate crustaceans in

our analysis. SOI is a measure of pressure variability between Tahiti and Darwin, Australia, associated with changes in weather and ocean current patterns worldwide. It is the index used to track the strength of El Niño (warm)/La Niña (cold) conditions. By definition, the SOI should not monotonically increase or decrease over time but will instead oscillate back and forth between positive and negative phases (occurring roughly every 2 to 7 years).

Methodological details for processing of Chl-*a*, OM, and grain size samples are described in full elsewhere (Douglas et al., 2017; Douglas et al., 2018; Drylie, 2021). Briefly, sediment samples for Chl-*a*, OM, and sediment grain size were collected using a smaller PCV corer (26 mm diameter, 20 mm deep core). Sediment from each small core was homogenised and sub-sampled for analysis of Chl a, OM, and sediment grain size. Chl-*a* was extracted from freeze dried sediments by boiling in 90% ethanol. The extract was measured spectrophotometrically, and an acidification step was included to separate degradation products (phaeophytin) from Chl-*a* (Sartory, 1982). Organic matter content was determined by drying the sediment at 60°C for 48 h and then combusting it at 400° C for 5.5 h, with OM expressed as percent dry weight lost on ignition. For sediment grain size, samples were homogenised and then digested in ~ 9% hydrogen peroxide until frothing ceases. Samples were wet sieved through 2000 µm, 500 µm, 250 µm and 63 µm mesh sieves. Pipette analysis was used to separate the <63 µm fraction into >3.9 µm and ≤3.9 µm. All fractions are then dried at 60°C until a constant weight is achieved (fractions are weighed at ~ 40 h and then again at 48 h) to obtain the percentage weight of gravel/shell hash (>2000 µm), coarse sand (500–2000 µm), medium sand (250–500 µm), fine sand (62.5–250 µm), silt (3.9–62.5 µm) and clay (≤3.9 µm).

Monthly SOI values were freely obtainable from the National Oceanographic and Atmospheric Administration - NOAA (https://www.cpc.ncep.noaa.gov). The same SOI time-series data were applied to all estuaries, as they are global scale metrics. Sea Surface Temperature (SST) data were obtained for each individual studied site. Monthly SST values for each site were generated from satellite imagery (Ocean Color - https://oceancolor.gsfc.nasa.gov) by extracting point-values from the grid-cell encompassing or closest to each site within each estuary studied.

2.3 Data analysis

To elucidate the patterns in the selected environmental variables over time, trend line analyses were performed for Chl-*a*, OM, Mud content, SOI, and SST individually. Linear regressions were performed and plotted using the package "ggpubr" (Kassambara, 2020) in R software (R-Core-Team, 2022).

To evaluate the influence of multiple predictors on estuarine crustaceans, we followed a spatial scale-based (i.e., large, medium, and fine scale) approach using Generalised Linear Models (GLMs). For the large scale (region), we used all the data available and evaluated the influence of all predictors on the abundance and richness of crustaceans, and the specific crustacean groups Amphipoda, Decapoda, Cumacean, and Tanaidacea. For the medium scale (estuary scale), we evaluated the influence of the multiple predictors on the abundance and richness of crustaceans, and specific crustacean groups, but separating all data by estuary (i.e., n=3). Lastly, for the fine scale (site scale) we evaluated the influence of all predictors on the abundance of estuarine crustaceans at each individual study site (n=9). All GLMs were constructed based on negative binomial regression model using the package "MASS" (Venables and Ripley, 2002). The GLM offers several advantages over conventional distance-based multivariate approaches, including accounting for species relationships, counts of rare species with zero-inflated abundance data, and the mean-variance relationship. Partial regression residual plots and forest (estimates) plots were created to investigate direct relationships between predictors and responses using the package "car" (Fox and Weisberg, 2019) and "sjPlot" (Lüdecke, 2023) respectively. Forest plots are a useful graphical means of summarising outcomes from GLMs, indicating the significance and direction (i.e., increase or decrease) of interactions between predictor and response variables. We did not use backward, forward, or stepwise techniques to determine final models, rather we used all five explanatory variables in each GLM and examined coefficient p-values to determine their significance. All the GLM and derived plots were performed using R software (R-Core-Team, 2022).

3 Results

A total of 56,751 crustacean organisms were collected from 2009 to 2022. The highest mean total abundance of crustaceans across sites and times in a harbour was recorded in Manukau Harbour (178 crustaceans), followed by Mahurangi (102 crustaceans), with the lowest mean total abundance recorded in Kaipara Harbour (60 crustaceans). Similarly, the highest mean total richness of crustaceans was found in Manukau Harbour (9 taxa), with the lowest richness found in Kaipara (7 taxa). At site level, CH (Manukau) was the site that showed the highest mean total abundance of crustaceans (302 crustaceans). The lowest mean total abundance was recorded at KaiB (Kaipara – 26 crustaceans). In terms of crustacean richness, JB (Mahurangi) showed the highest mean total richness (14 taxa), while the lowest mean total richness was observed at KaiB (5 taxa).

3.1 Trends in environmental drivers over time

Chlorophyll a (Chl-*a*) decreased over time at six of the nine sites studied (Table 2, Figure 2). In Kaipara Harbour, Chl-*a* increased at KaiB site, the site furthest from the estuary mouth, but decreased over time at the other sites (KKF and NPC; Table 2, Figure 2A). Similar trends were observed in Mahurangi Harbour: Chl-*a* increased over time at sites far from the estuary mouth (HL and MH) but decreased at the outermost site, JB. (Table 2, Figure 2B). In Manukau Harbour, Chl-*a* decreased over time at all the sites (Table 2, Figure 2C).

In contrast to Chl-*a*, organic matter content (OM) significantly increased over time (Table 3, Figure 3). In Kaipara and Mahurangi

10.3389/fmars.2023.1292849

TABLE 2 Summary results of regression line analyses showing trends in Chlorophyll a (Chl-*a*) over time at each site.

Site	Slope	p value	Significance	Direction
Kaipara				
KaiB	4.51E-04	3.54E-03	p<0.05	Increasing
KKF	-9.10E-04	1.62E-05	p<0.05	Decreasing
NPC	-1.40E-04	3.60E-01	p>0.10	Decreasing
Mahurangi				
HL	6.23E-04	0.068456	p<0.10	Increasing
JB	-4.30E-04	0.048782	p<0.05	Decreasing
MH	7.39E-04	0.000242	p<0.05	Increasing
Manukau				
AA	-1.70E-04	5.64E-01	p>0.10	Decreasing
CB	-1.16E-03	7.75E-05	p<0.05	Decreasing
CH	-7.00E-04	2.28E-02	p<0.05	Decreasing

Harbours, OM increased at all study sites (Table 3, Figures 3A, B). OM was low in Manukau Harbour compared to the other estuaries, with increases detected at AA and CH. Site CB in Manukau harbour was the only site exhibiting a decrease in OM over time (Table 3, Figure 3C).

Sediment mud content also generally increased over time in the study estuaries (Table 4, Figure 4). Mud content increased in all sites in Kaipara Harbour (Table 4, Figure 4A), at AA and CH in Manukau Harbour (Table 4, Figure 4C), and at HL in Mahurangi Harbour (Table 4, Figure 4B).

Long-term data (1984-2022) of the Southern Oscillation Index (SOI) revealed high variation of warm (El Niño) and cold (La Niña) climate (Figure 5). Analysis of the 1984-2022 data record indicates increasing SOI over time, with longer periods of warmer (El Niño) climate (Figure 5A). However, for the more recent period (i.e., the 2009-2022 timeframe of this study), SOI is trending downward, indicting longer and wider periods of cold (La Niña) climate (Figure 5B).

Seasonal cycles in Sea Surface Temperature (SST) were apparent at all sites, with warmer SST in austral summer and colder SST in austral winter (Figure 6). Linear trend analyses indicated an increase in SST of roughly 1°C at most study sites, with decreases through time at just two sites (HL and CH; Table 5, Figure 6).

3.2 Large (region) scale

GLM results showed how multiple environmental variables influenced crustacean communities at the large spatial scale, i.e., all the estuaries together (Figure 7, Supplementary Table 1). Crustacean abundance was significantly influenced by four variables (Figure 7A). Three of the four variables (SOI, SST and mud content) were inversely related to the abundance of crustaceans, i.e., with crustacean abundance decreasing as SOI, SST and mud content increased (Figure 7A, Supplementary Figure 1, Supplementary Table 1). Crustacean richness was influenced by SOI, mud and organic content (Figure 7B) and, as above, richness tended to decrease with increasing SOI and mud content (Figure 7B, Supplementary Figure 2, Supplementary Table 1).

The crustacean groups Amphipoda, Decapoda, Cumacean, and Tanaidacea were significantly influenced by distinct combinations of multiple environmental predictors (Figures 7C-F). Amphipoda abundance decreased with increasing SOI and mud content (Figure 7C, Supplementary Figure 3, Supplementary Table 1), while the abundance of Decapoda increased with increasing Chl-*a* and OM (Figure 7D, Supplementary Figure 4, Supplementary Table 1). SST and mud content influenced the abundance of Cumacea, showing a trend of decreasing abundance with increasing SST and mud content (Figure 7E, Supplementary Figure 5, Supplementary Table 1). A similar inverse relationship was found with Tanaidacea abundance and Chl-*a* (decreasing abundance with increasing Chl-*a*; Figure 7E, Supplementary Figure 6, Supplementary Table 1).

Organic content influenced all of the crustacean variables analysed with the exception of Cumacea abundance. Increases in OM generally resulted in increased crustacean abundance and richness, and increased abundance of Amphipoda, Decapoda, and Tanaidacea (Figure 7E, Supplementary Figures 1–6, Supplementary Table 1).

3.3 Medium (estuary) scale

Crustacean communities were also influenced by estuarine-scale variation in environmental predictors (Figures 8–10, Supplementary Tables 1–4). For Kaipara Harbour, the GLM results showed the abundance of crustaceans to be significantly influenced by SOI, SST, mud and organic content (Figure 8A). Similar to the large-scale patterns, crustacean abundance decreased with increases in SOI, SST

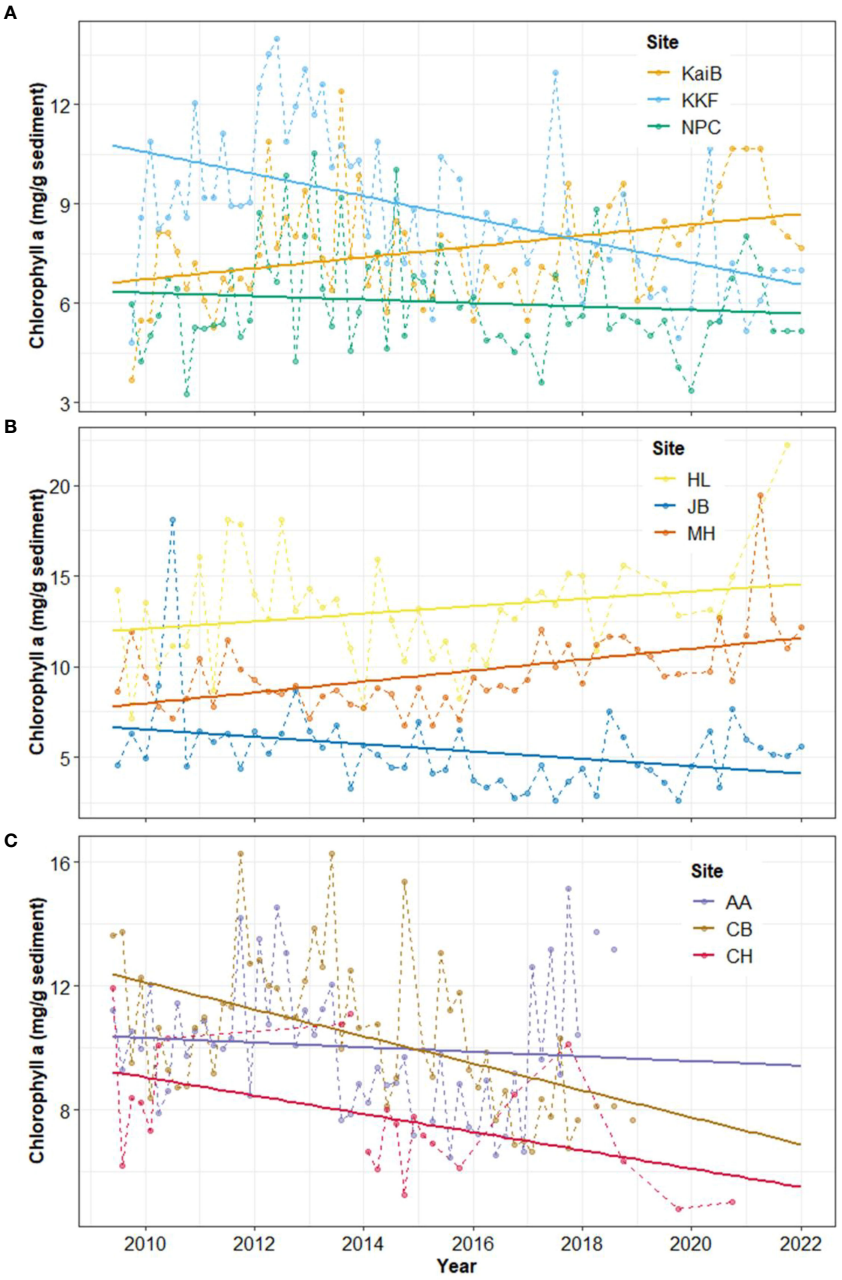

FIGURE 2
Time-series and linear trend analysis of Chlorophyll a in **(A)** Kaipara, **(B)** Mahurangi, and **(C)** Manukau estuary. Points and dashed lines depict data values and solid lines represent the regression. Note different Y-axis scales.

and mud content (Figure 8A, Supplementary Figure 7, Supplementary Table 2). Crustacean richness in Kaipara Harbour was influenced by fewer variables, increasing with Chl-*a* and decreasing with mud content but showing no relationship to SOI, SST or organic matter content (Figure 8B, Supplementary Figure 8, Supplementary Table 2). Amphipoda abundance in Kaipara followed the same pattern as crustacean abundance, i.e., decreasing with increasing SOI, SST and mud content (Figure 8C, Supplementary Figure 9, Supplementary Table 2) and increasing with OM. Decapoda abundance was also influenced by multiple variables, showing an increase in abundance with increasing Chl-*a*, mud, and OM (Figure 8D, Supplementary Figure 10, Supplementary Table 2). Cumacea abundance was inversely correlated with SOI, SST and mud content (Figure 8E, Supplementary Figure 11, Supplementary Table 2), while Tanaidacea abundance was not influenced by any of the multiple stressors assessed (Figure 8F, Supplementary Figure 12, Supplementary Table 2). Overall, mud content was the stressor that influenced the largest number of crustacean variables in Kaipara Harbour, with abundance and richness tending to decrease with increasing mud content in sediments.

Results from Mahurangi Harbour were similar to those in Kaipara. For example, crustacean abundance and richness were

10.3389/fmars.2023.1292849

TABLE 3 Summary results of the regression line analyses showing trends in sediment organic matter content (OM) over time at each site.

Site	Slope	p value	Significance	Direction
Kaipara				
KaiB	3.93E-04	6.36E-07	p<0.05	Increasing
KKF	2.69E-04	1.26E-06	p<0.05	Increasing
NPC	2.30E-04	1.66E-08	p<0.05	Increasing
Mahurangi				
HL	3.66E-05	0.690769	p>0.10	Increasing
JB	1.84E-04	0.007304	p<0.05	Increasing
MH	1.08E-04	0.063608	<0.10	Increasing
Manukau				
AA	9.11E-06	0.501916	p>0.10	Increasing
CB	-8.12E-05	0.252616	p>0.10	Decreasing
CH	1.81E-06	0.961861	p>0.10	Increasing

significantly influenced by Chl-*a*, mud, and OM (Figures 9A, B, Supplementary Table 3). Both of these response variables decreased when Chl-*a* and mud content increased (Figures 9A, B, Supplementary Figures 13, 14, Supplementary Tables 1–3). Chl-*a*, mud, and OM were also significant predictors of Amphipoda abundance (Figure 9C, Supplementary Figure 15, Supplementary Tables 1–3). Decapoda abundance in Mahurangi Harbour was only influenced by one environmental variable, SST (negatively; Figure 9D, Supplementary Figure 16, Supplementary Table 3), whereas Cumacea abundance was influenced by two different environmental variables, Chl-*a* and mud content (both negatively, Figure 9E, Supplementary Figure 17, Supplementary Table 3). As was the case in Kaipara Harbour, mud content was the environmental variable with the most pervasive negative effects on crustacean responses in Mahurangi Harbour.

The patterns observed in Manukau Harbour were rather different to those in Kaipara and Mahurangi (Figure 10, Supplementary Table 4). In Manukau Harbour, crustacean abundance decreased as SST and Chl-*a* increased (Figure 10A, Supplementary Figure 18, Supplementary Table 4). Richness was only influenced by one variable, responding positively (rather than negatively like abundance) to increased Chl-*a* (Figure 10B, Supplementary Figure 19, Supplementary Table 4). Amphipoda abundance decreased with increasing SOI, SST, and Chl-*a* (Figure 10C, Supplementary Figure 20, Supplementary Table 4), while OM positively influenced the abundance of Decapoda (Figure 10D, Supplementary Figure 21, Supplementary Table 4). Cumacean abundance decreased as SST, Chl-*a*, and mud content increased (Figure 10E, Supplementary Figure 22, Supplementary Table 4), while Tanaidacea was only influenced by Chl-*a*, with abundance inversely related to Chl-*a* (Figure 10F, Supplementary Figure 23, Supplementary Table 4). In Manukau Harbour, Chl-*a* influenced the greatest number of crustacean variables. Interestingly, the influence was negative for crustacean abundance and Amphipoda, Cumacea, and Tanaidacea abundance, whereas for crustacean richness the influence of Chl-*a* was positive.

3.4 Fine (site) scale

GLMs showed the significant influence of unique combinations of environmental variables on crustacean communities at each of the individual study sites (Figure 11, Supplementary Tables 5–7). Across all sites, SOI and SST were the most frequent variables influencing the abundance of crustaceans (Figure 11). Site KaiB was only influenced by SOI, showing a decrease in crustacean abundance with increasing SOI (Figure 11, Supplementary Figure 24, Supplementary Table 5). Almost all of the environmental variables influenced the abundance of crustaceans at KFF. Abundance tended to decrease with increasing SOI, SST and mud, while abundance increased with increased OM (Figure 11, Supplementary Figure 25, Supplementary Table 5). Abundance at the NPC site was only influenced by SST, showing a decrease in abundance with increased SST (Figure 11, Supplementary Figure 26, Supplementary Table 5).

The abundance of crustaceans at Site HL was significatively influenced by SOI, Chl-*a*, and mud content. Crustacean abundance decreased with increasing SOI and mud content and increased with increasing Chl-*a* (Figure 11, Supplementary Figure 27, Supplementary Table 6). At the JB site, SOI and OM influenced crustacean abundance, driving decreases and increases in crustacean abundance, respectively (Figure 11, Supplementary Figure 28, Supplementary Table 6). AA and CB were influenced by SST, with crustacean abundance at both sites tending to decrease with increasing SST (Figure 11, Supplementary Figures 30, 31, Supplementary Table 6). At Sites MH and CH, crustacean abundance was unable to be predicted with any of the environmental variables available (Figure 11, Supplementary Figures 29–31, Supplementary Table 6).

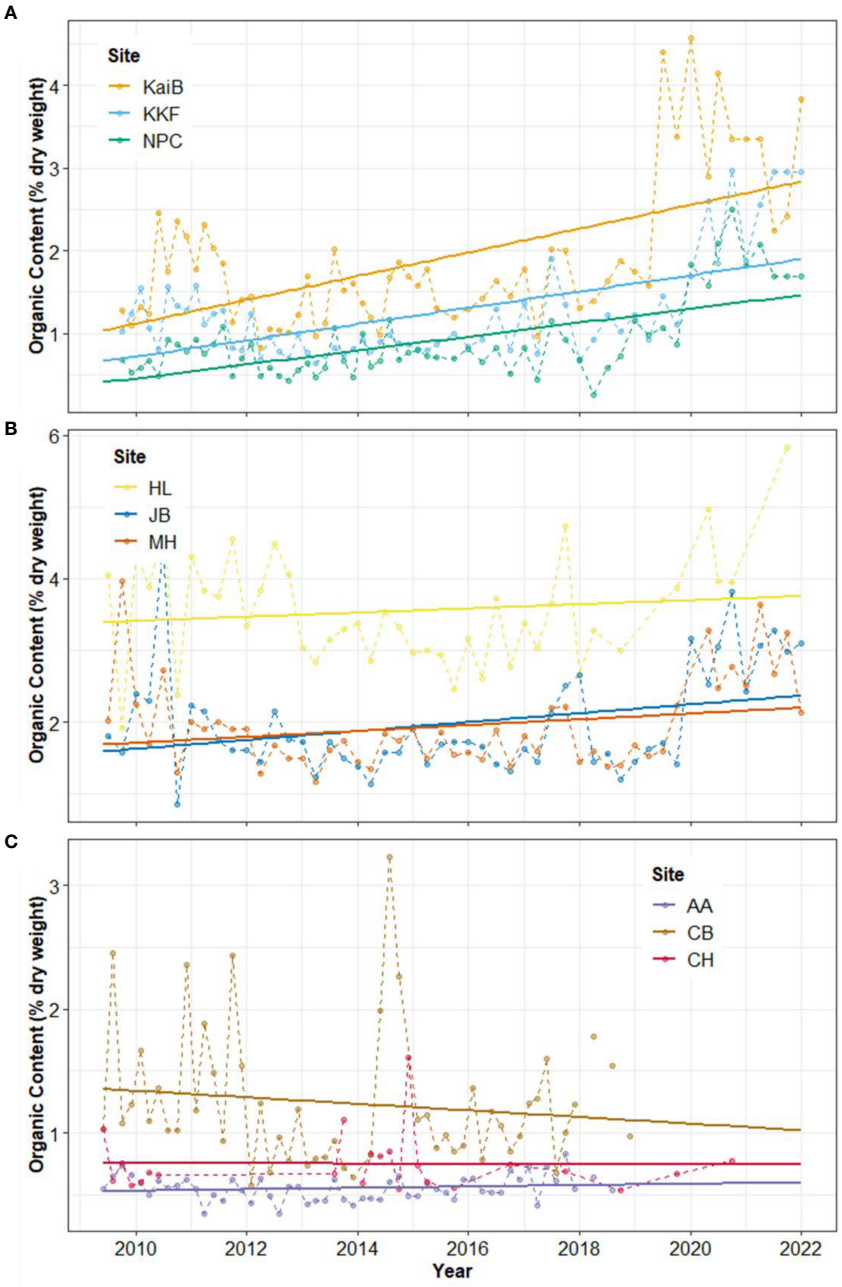

FIGURE 3
Time-series and linear trend analysis of sediment organic matter content in in **(A)** Kaipara, **(B)** Mahurangi, and **(C)** Manukau estuary. Points and dashed lines depict data values and solid lines represent the regression. Note different Y-axis scales.

4 Discussion

Climate change in combination with other environmental drives (e.g., nutrient and sediment inputs) are causing significant impacts on estuarine ecosystems (Kennish, 2021; Simeoni et al., 2023). The interaction of multiple environmental drivers, or multiple stressors, could exacerbate the deterioration of estuarine and coastal ecosystems, with negative consequences on living organisms, ecosystem functioning and services these important ecosystems provide (Kennish, 2021; Simeoni et al., 2023). The effects of multiple environmental drivers on estuarine ecosystems are occurring at accelerated rate, which challenges conservation and management efforts to improve the ecological health of these ecosystems. In this study, we analysed estuarine crustacean time-series data at three nested spatial scales—large (Auckland Region), medium (estuary within Auckland Region), and small (site within estuary)—to investigate the influence of multiple environmental variables related to freshwater, climate, and ocean drivers. There were trends over time in most of the environmental predictors, and our aim was to assess their potential effects on crustacean communities to improve prediction and our understanding of the interplay of multiple stressors. Our results showed that the

TABLE 4 Summary results of regression line analyses showing trends in sediment mud content over time at each site.

Site	Slope	p value	Significance	Direction
Kaipara				
KaiB	1.94E-03	3.44E-03	p<0.05	Increasing
KKF	1.29E-03	3.16E-06	p<0.05	Increasing
NPC	8.98E-04	1.95E-05	p<0.05	Increasing
Mahurangi				
HL	7.36E-04	0.480199	p>0.10	Increasing
JB	-1.93E-03	0.000837	p<0.05	Decreasing
MH	-1.52E-03	0.00047	p<0.05	Decreasing
Manukau				
AA	7.45E-05	0.065918	<0.10	Increasing
CB	-9.34E-04	0.155168	p>0.10	Decreasing
CH	2.12E-04	0.514888	p>0.10	Increasing

abundance and richness of crustaceans, as well as the abundance of specific crustacean groups (i.e., Amphipoda, Decapoda, Cumacean, Tanaidacea), were influenced by unique combinations of environmental variables, resulting in scale dependent interactions.

Across all the spatial scales studied, combinations of the five predictor variables influenced estuarine crustaceans in at least one case. Our first study hypothesis, that crustaceans will respond to multiple stressors more often than to single stressors, appears to have been supported. However, the combinations of variables that were significant changed across scales, supporting our second hypothesis that the influence of environmental predictor variables would be scale dependent. The large-scale outcomes showed that crustacean abundance was influenced by SST and SOI (climatic and oceanic stressors). Temperature of the ocean has been described as a key factor shaping the structure of benthic communities (Tittensor et al., 2010; Clark et al., 2021). We identified that SST has increased at these estuarine sites by ~1°C over the last 20 years, and demonstrated that the abundance of crustaceans tended to decrease with increasing SST, which is consistent with other studies suggesting that the increase of ocean temperature could affect the morphology, life history, abundance, and distribution of benthic communities (Hewitt et al., 2016; Dvoretsky and Dvoretsky, 2020; Clark et al., 2021). SOI is an indicator of environmental variability that has the potential to affect other environmental drivers (e.g., wind and current speeds, air and water temperature, cloudiness and precipitation, storm frequency and intensity). Our results showed that SOI influenced both abundance and richness of estuarine crustaceans. With increased SOI (and generally warmer conditions during El Nino phases), the abundance and richness of crustaceans decreased. Coupled with evidencing of increasing SST through time, this suggests that climate and ocean warming may be an important stressor affecting the abundance and richness of key macroinvertebrate estuarine organisms in New Zealand (Hewitt et al., 2016; Clark et al., 2021).

Sediment muddiness was another stressor influencing both abundance and richness of estuarine crustaceans. Sediment mud content in estuarine receiving environments has increased with elevated sediment loadings associated with human-alterations of coastal catchments, an environmental change that has had major impacts on estuarine assemblages and ecosystem functions (Thrush et al., 2003b; Douglas et al., 2019). We observed that above a threshold of about 10-20% mud content, further increases in muddiness coincided with rapid decreases in crustacean abundance and richness. This threshold aligns with previous studies describing negative impacts on diversity and ecosystem functioning above 25% sediment mud content (Thrush et al., 2003a; Lohrer et al., 2004b; Ellis et al., 2017; Douglas et al., 2018; Douglas et al., 2019; Pardo et al., 2022), but perhaps suggests that crustaceans as a group are slightly more sensitive than macrofauna as a whole.

Excessive organic matter can be an environmental stressor in estuarine systems, often due to its effects on sediment oxygen demand and the potential for bottom water hypoxia/anoxia. Here, sediment OM was the only environmental variable that was positively associated with the abundance and richness of estuarine crustaceans. This is likely because of the value of organic material as a food resource for macrofauna, especially deposit feeders, when present at low to moderate levels. However, beyond a critical point (4-5%), excessive organic matter content can initiate the onset of eutrophication symptoms (Ellis et al., 2017) and negatively impact estuarine crustaceans.

Highly variable interactions between multiple environmental variables and estuarine crustaceans were identified at the medium (estuary) scale. However, there were isolated cases of consistency. For example, SST was inversely correlated with the abundance of crustaceans in both Kaipara and Manukau Harbours. Both of these harbours are large, west coast estuaries. The prevailing wind and ocean swell arrives in New Zealand from the southwest, so perhaps these climate and ocean forcings are stronger on New Zealand's west coast relative to the east coast (Hewitt et al., 2016). Mahurangi Harbour (on the east coast) is smaller and more protected from prevailing

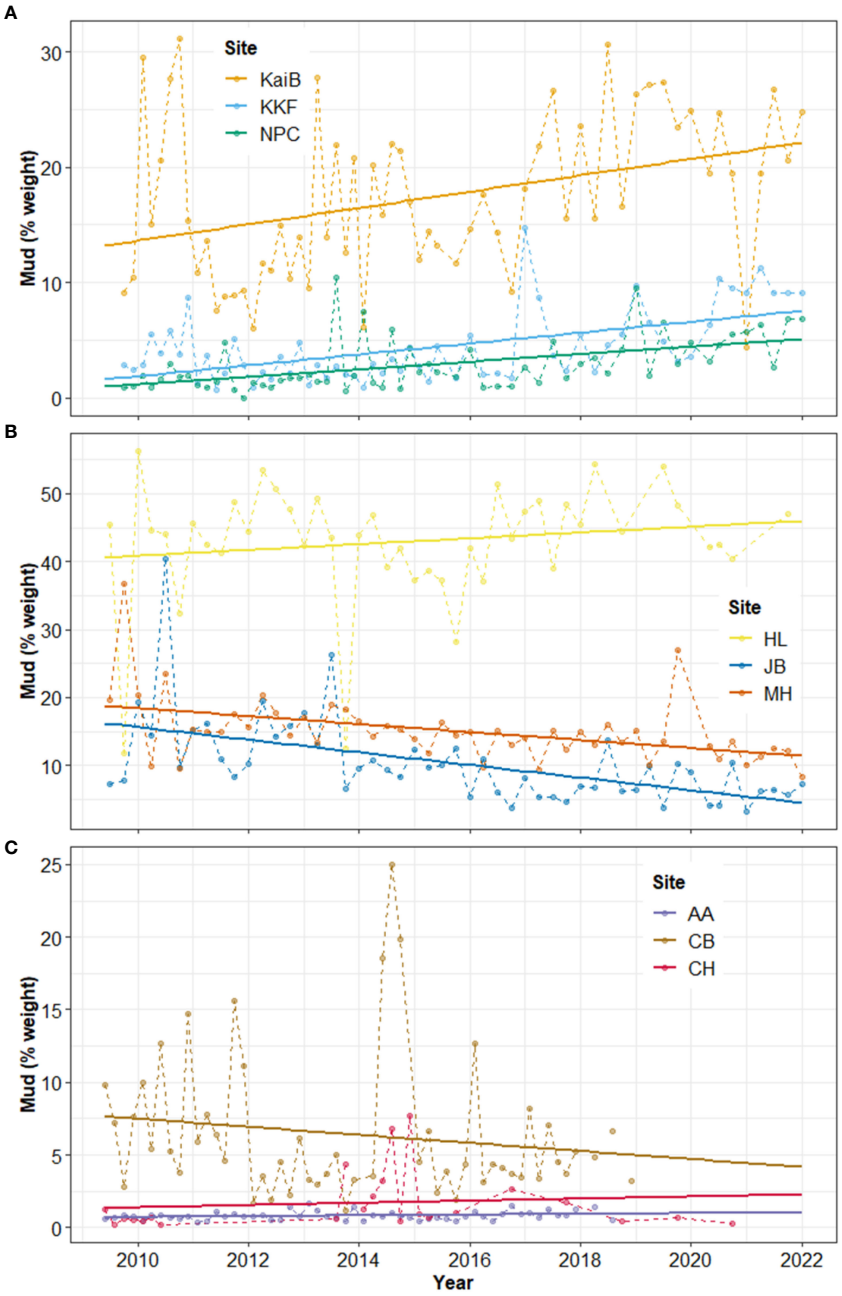

FIGURE 4
Time-series and linear trend analysis of sediment mud content in **(A)** Kaipara, **(B)** Mahurangi, and **(C)** Manukau estuary. Points and dashed lines depict data values and solid lines represent the regression. Note different Y-axis scales.

southwesterlies, and may therefore be less responsive to the ocean and climate proxy variables that we used as environmental predictors.

Sediment muddiness and OM content had similar effects on the abundance and richness of crustaceans in Kaipara and Mahurangi Harbours. Freshwater inputs deliver fine sediments and organic matter to estuaries. Relative to Manukau Harbour, Kaipara and Mahurangi have more riverine influence, have larger catchment size to estuary size ratios, and are closer together geographically (which may translate to comparable rainfall totals). This may explain the relatively similar responses to increased muddiness and OM observed in Kaipara and Mahurangi Harbours.

Mud content had a relatively consistent negative effect on the abundance and richness of crustaceans across scales, though it was most apparent and detectable at the largest scales. With >10% bed sediment muddiness, decreases in the abundance and richness of crustaceans were readily apparent, consistent with analyses of other macrofauna datasets in New Zealand (Thrush et al., 2003b; Lohrer et al., 2004b; Ellis et al., 2017; Douglas et al., 2018).

In contrast to mud, OM had a generally positive influence on the abundance and richness of crustaceans across estuaries. This result was generally apparent at the large and medium spatial scales assessed. The final sediment variable used as an

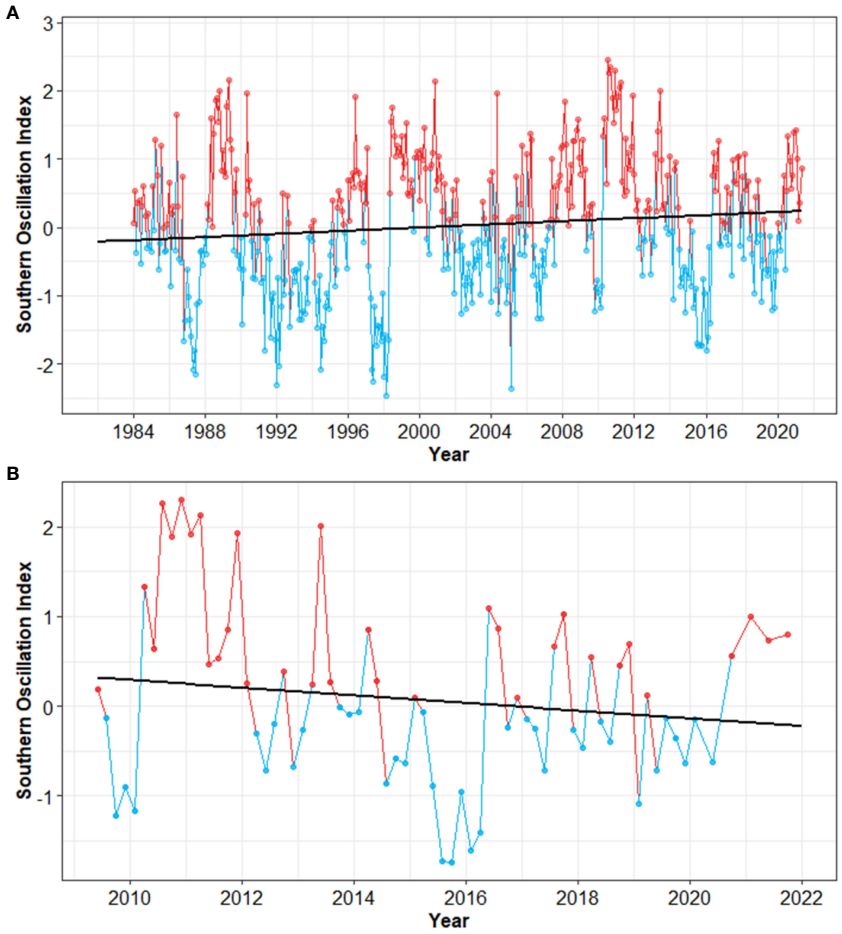

FIGURE 5
Time-series and linear trend analysis of the Southern Oscillation Index. **(A)** Long-term values (1984-2022), and **(B)** time frame of this study. Regression lines are indicated by solid black lines. Warm periods (El Niño) are in red, and cold periods (La Niña) in blue. Note different X-axis scales.

environmental predictor, Chl-*a*, was generally less influential. Significant effects of Chl-*a* at the estuary scale were only observed in Manukau Harbour. Manukau Harbour is a relatively turbid estuary and is large enough to have substantial wind-wave fetch. Both turbidity and wind-wave resuspension can limit microphytobenthos, a key food resource for the macroinvertebrate crustaceans investigated. This may explain why higher Chl-*a* resulted in higher crustacean abundance and richness in Manukau Harbour.

Results at the fine scale were highly site-specific, with crustacean responses generally influenced by fewer environmental variables and sometimes by only one predictor variable (or none). SST and SOI influenced crustacean abundance at the greatest number of individual sites (4/9 each). This outcome showed clear evidence of the potentially strong effects of climatic and oceanic drivers on estuarine communities (Hewitt et al., 2016; Clark et al., 2021). It is possible that the effects of the climate and ocean drivers are overriding the effects of sedimentary variables at the site scale (Thrush et al., 2008b; Hewitt et al., 2016; Ellis et al., 2017).

Our third study hypothesis was that different types of crustaceans (Amphipoda, Decapoda, Cumacea, Tanaidacea) would respond differently to multiple environmental predictors. We found some evidence of consistency in responses to multiple environmental drivers. For example, at the broader spatial scale, Amphipoda, Decapoda, and Tanaidacea were all influenced by OM, while Cumacea was influenced by stressors such as SST and sediment mud content. At the medium scale, results showed that Amphipoda and Cumacea were influenced by mud content, Decapoda was influenced by SST and OM, while Tanaidacea was not strongly influenced by any environmental variables at the medium scale. The mechanisms behind the differential responses of crustaceans to combinations of environmental variables are uncertain but could be linked to interactive effects and differences in the habitat requirements or tolerances of the four crustacean groups (Thrush et al., 2008b; Ellis et al., 2017; Dvoretsky and Dvoretsky, 2020; Clark et al., 2021).

It is important to highlight that the variance explained of estuarine crustaceans in our models was low (7%-51%).

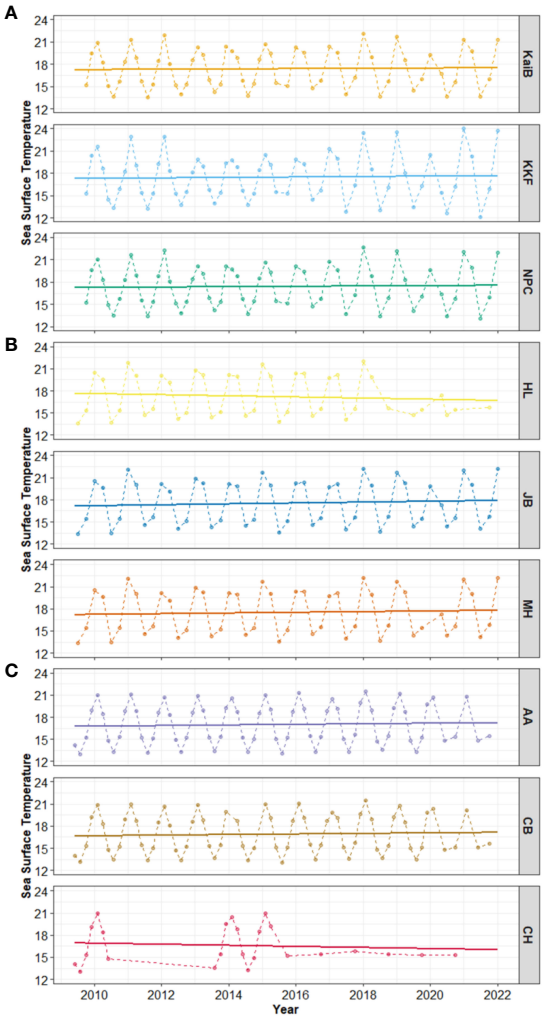

FIGURE 6
Time-series and linear trend analysis of Sea Surface Temperature in **(A)** Kaipara, **(B)** Mahurangi, and **(C)** Manukau estuary. Solid lines show the regression line, and points and dashed lines showed the data values. Right-hand Y-axis denotes site names.

However, it is increasingly recognised that weak relationships can be ecologically meaningful and that, in empirical studies, models often account for ~10% of the variability (Thrush et al., 2008b; Hewitt et al., 2016). More importantly, our results suggest a pathway to shift from examination of single environmental drivers (or stressor) effects to multiple environmental stressor effects. We also provide evidence of different responses of estuarine crustaceans to multiple environmental drivers at multiple spatial scales, which have important implications for how we should consider ecological responses to climate change and other anthropogenic pressures. Our result could be used for reducing uncertainty of the interactions between crustacean communities and environmental drivers improving prediction of ecological change, which is critical for management efforts and created informed approaches to mitigate multiple environmental drivers impacts.

5 Conclusion

This study elucidated how environmental drivers associated with freshwater, climate and ocean forcings can influence estuarine crustacean time-series variation across different spatial scales. Scale dependent responses to multiple environmental predictors were found, with SST and SOI (ocean and climate variables, respectively) the most common drivers of the abundance and richness of estuarine crustaceans overall. Notably, negative responses to two known stressors—elevated sediment muddiness and increasing SST—were identified, with mud content negatively affecting crustacean communities at all the spatial scales. Our results provide further evidence that catchment sediment loading may be impacting the health and functioning of estuarine ecosystems, with effects potentially exacerbated by increasing SST associated with a warming climate. The observed interactions between estuarine crustaceans and climatic, oceanic, and freshwater

TABLE 5 Summary results of regression line analyses showing Sea Surface Temperature (SST) over time at each site.

Site	Slope	p value	Significance	Direction
Kaipara				
KaiB	5.64E-05	0.828354	p>0.10	Increasing
KKF	8.64E-05	0.781832	p>0.10	Increasing
NPC	6.52E-05	0.812021	p>0.10	Increasing
Mahurangi				
HL	-3.61E-04	0.277098	p>0.10	Decreasing
JB	7.96E-05	0.784516	p>0.10	Increasing
MH	4.90E-05	0.868479	p>0.10	Increasing
Manukau				
AA	9.51E-05	0.703796	p>0.10	Increasing
CB	9.56E-05	0.692857	p>0.10	Increasing
CH	-4.39E-04	0.297892	p>0.10	Decreasing

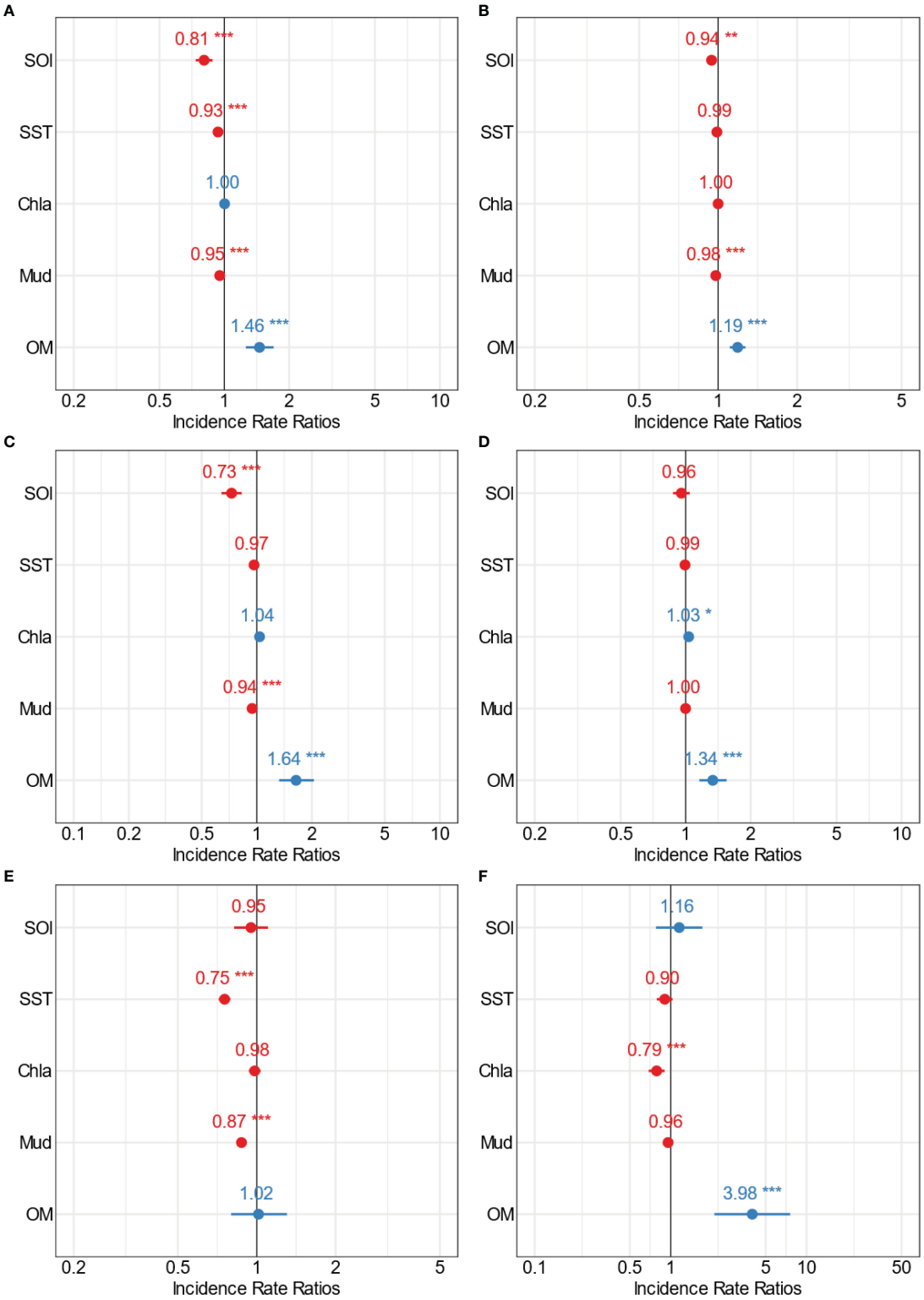

FIGURE 7
Forest plots summarising the outcomes from GLMs for the large-scale analysis showing the point estimates (Incidence Rate Ratios) for the relationships between multiple stressors and **(A)** total crustacean abundance, **(B)** crustacean richness, **(C)** Amphipoda, **(D)** Decapoda, **(E)** Cumacean, and **(F)** Tanaidacea abundance. The colour indicates positive (blue) and negative (red) significant (*p=0.5; **p=0.01; ***p=0.001) interactions of the point estimates.

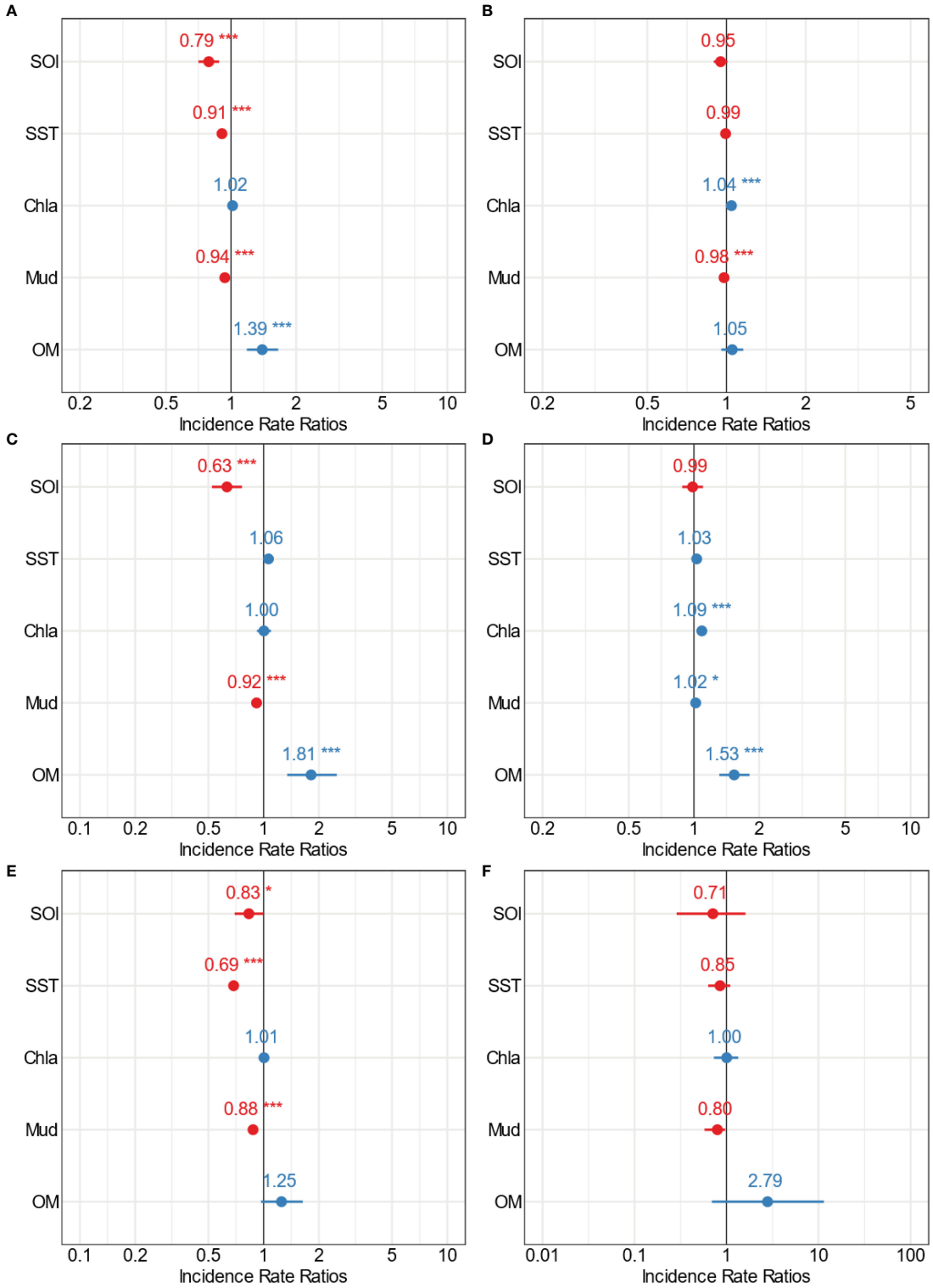

FIGURE 8
Forest plots summarising the outcomes from GLMs for Kaipara estuary (medium scale) showing the point estimates (Incidence Rate Ratios) for the relationships between multiple stressors and **(A)** total crustacean abundance, **(B)** crustacean richness, **(C)** Amphipoda, **(D)** Decapoda, **(E)** Cumacean, and **(F)** Tanaidacea abundance. The colour indicates positive (blue) and negative (red) significant (*p=0.5; **p=0.01; ***p=0.001) interactions of the point estimates.

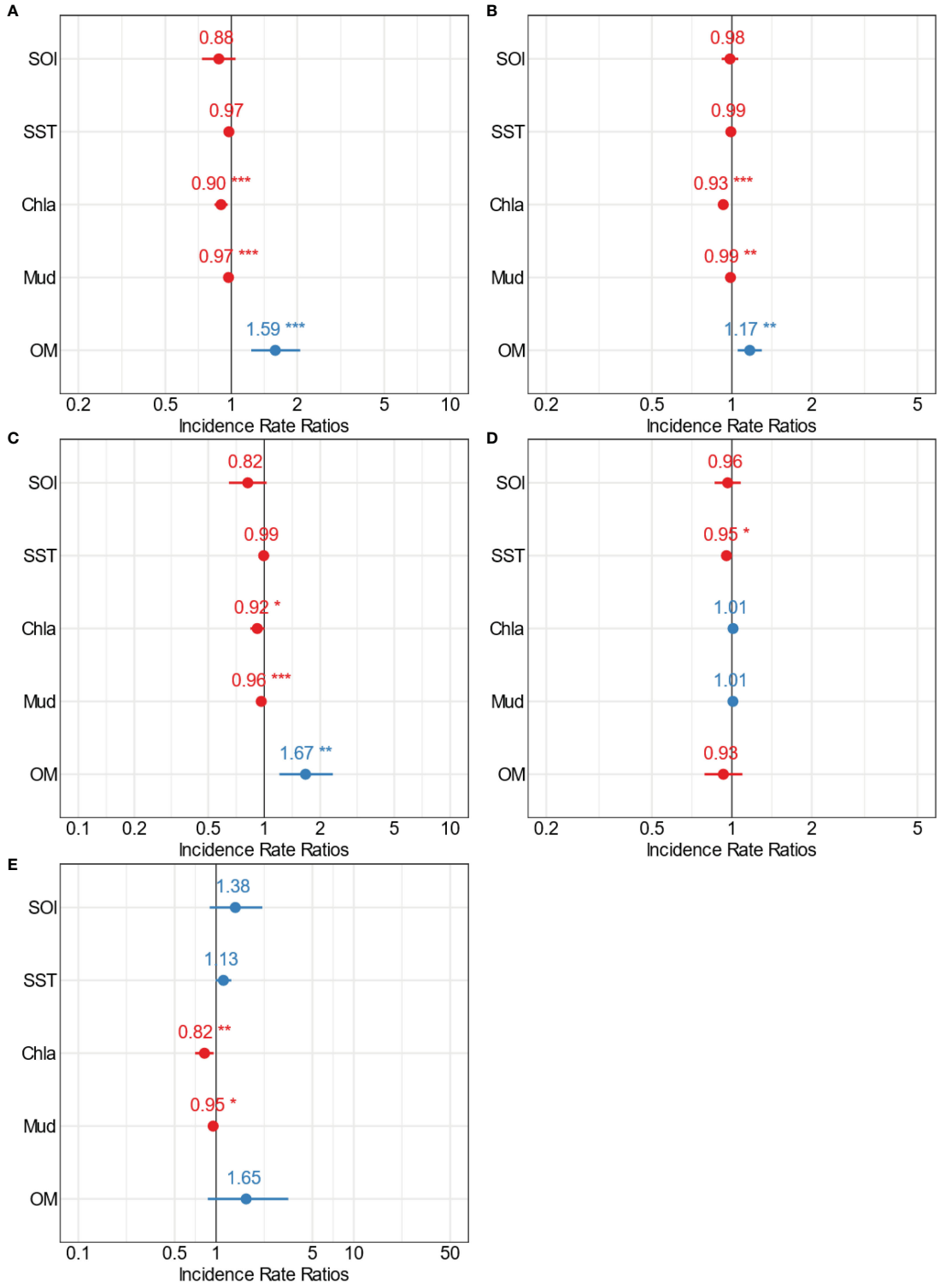

FIGURE 9
Forest plots summarising the outcomes from GLMs for Mahurangi estuary (medium scale) showing the point estimates (Incidence Rate Ratios) for the relationships between multiple stressors and **(A)** total crustacean abundance, **(B)** crustacean richness, **(C)** Amphipoda, **(D)** Decapoda, and **(E)** Cumacean abundance. The colour indicates positive (blue) and negative (red) significant (*p=0.5; **p=0.01; ***p=0.001) interactions of the point estimates.

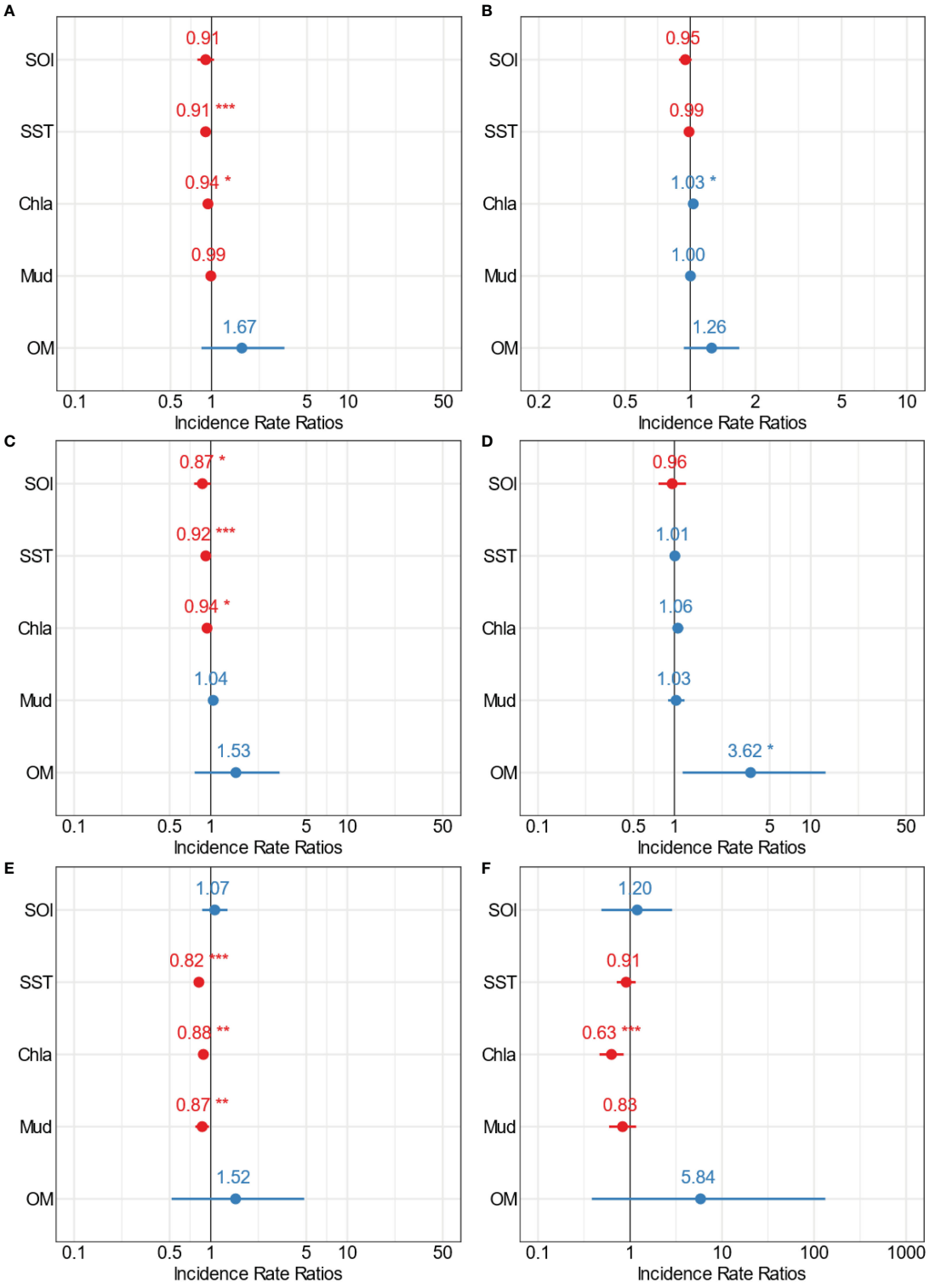

FIGURE 10
Forest plots summarising the outcomes from GLMs for Manukau estuary (medium scale) showing the point estimates (Incidence Rate Ratios) for the relationships between multiple stressors and **(A)** total crustacean abundance, **(B)** crustacean richness, **(C)** Amphipoda, **(D)** Decapoda, **(E)** Cumacean, and **(F)** Tanaidacea abundance. The colour indicates positive (blue) and negative (red) significant (*p=0.5; **p=0.01; ***p=0.001) interactions of the point estimates.

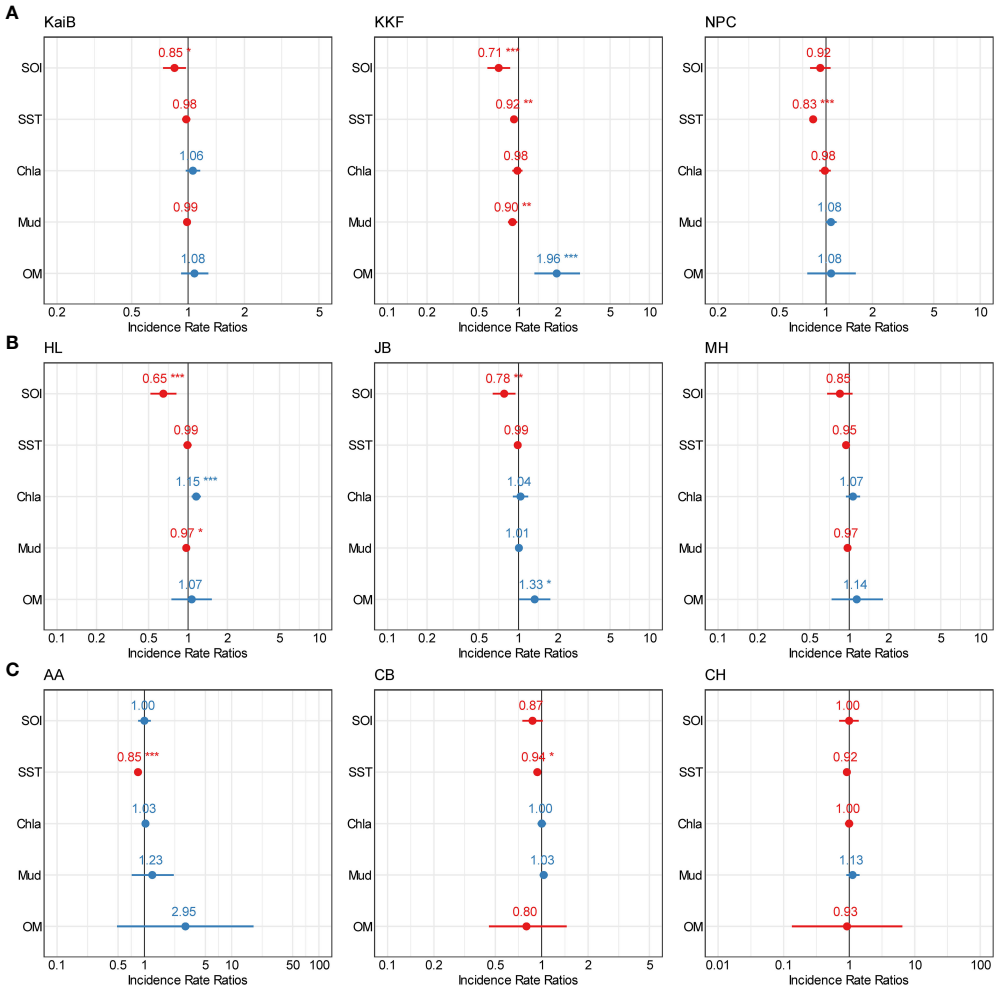

FIGURE 11
Forest plots summarising the outcomes from GLMs for each site (fine scale) showing point estimates (Incidence Rate Ratios) for relationships between multiple stressors and total crustacean abundance. **(A)** Kaipara estuary, **(B)** Mahurangi estuary, and **(C)** Manukau estuary. The colour indicates positive (blue) and negative (red) significant (*p=0.5; **p=0.01; ***p=0.001) interactions of the point estimates.

drivers have important implications for predicting the ecological consequences of climate change in coastal ecosystems. We also highlight the need for management and conservations efforts to reduce sediment inputs and mitigate the effects of increasing temperatures to maintain the ecological health and functioning of estuarine ecosystems.

Data availability statement

The original contributions presented in the study are included in the article/Supplementary Material. Further inquiries can be directed to the corresponding author.

Ethics statement

The manuscript presents research on animals that do not require ethical approval for their study.

Author contributions

OL-G: Conceptualization, Data curation, Formal Analysis, Methodology, Visualization, Writing – original draft, Writing – review & editing. AL: Conceptualization, Funding acquisition, Writing – review & editing, Formal Analysis. ED: Methodology, Writing – review & editing. SH: Data curation, Methodology, Writing – review & editing. KC: Data curation, Methodology, Writing – review & editing. BG: Data curation, Methodology, Writing – review & editing.

Funding

The author(s) declare financial support was received for the research, authorship, and/or publication of this article. Analysis was funded by NIWA Coasts & Oceans Strategic Science Investment Funding with additional support from Ministry for the Environment. Auckland Council funded data gathering (field work and sample collection/processing) at all of the study sites.

Acknowledgments

We would like to thank the many NIWA Marine Ecology technicians who have collected, processed and quality-checked estuarine macrofauna samples under contract from Auckland Council for decades. We thank the funders of data collection and analysis (Auckland Council, MfE, NIWA) and Auckland Council for permission to use the data.

Conflict of interest

The authors declare that the research was conducted in the absence of any commercial or financial relationships that could be construed as a potential conflict of interest.

Publisher's note

Supplementary material

The Supplementary Material for this article can be found online at: https://www.frontiersin.org/articles/10.3389/fmars.2023.1292849/full#supplementary-material

References

Agusto, L. E., Qin, G., Thibodeau, B., Tang, J., Zhang, J., Zhou, J., et al. (2022). Fiddling with the blue carbon: Fiddler crab burrows enhance CO2 and CH4 efflux in saltmarsh. *Ecol. Indic.* 144 (109538). doi: 10.1016/j.ecolind.2022.109538

Barbier, E. B., Hacker, S. D., Kennedy, C., Koch, E. W., Stier, A. C., and Silliman, B. R. (2011). The value of estuarine and coastal ecosystem services. *Ecol. Monogr.* 81 (2), 169–193. doi: 10.1890/10-1510.1

Bastakoti, U., Bourgeois, C., Marchand, C., and Alfaro, A. C. (2019). Urban-rural gradients in the distribution of trace metals in sediments within temperate mangroves (New Zealand). *Mar. pollut. Bull.* 149 (110614). doi: 10.1016/j.marpolbul.2019.110614

Behrens, E., Rickard, G., Rosier, S., Williams, J., Morgenstern, O., and Stone, D. (2022). Projections of future marine heatwaves for the oceans around New Zealand using New Zealand's earth system model. *Front. Climate* 4. doi: 10.3389/fclim.2022.798287

Borja, A., Franco, J., and Pérez, V. (2000). A marine biotic index to establish the ecological quality of soft-bottom benthos with European estuarine and coastal environments. *Mar. pollut. Bull.* 40, 1100–1114. doi: 10.1016/S0025-326X(00)00061-8

Bui, T. H. H., and Lee, S. Y. (2014). Does "you are what you eat" apply to mangrove grapsid crabs? *PloS One* 9. doi: 10.1371/journal.pone.0089074

Bulmer, R. H., Kelly, S., and Jeffs, A. G. (2016). Light requirements of the seagrass, Zostera muelleri, determined by observations at the maximum depth limit in a temperate estuary, New Zealand. *New Z. J. Mar. Freshw. Res.* 50 (2), 183–194. doi: 10.1080/00288330.2015.1120759

Carrier-Belleau, C., Drolet, D., McKindsey, C., and Archambault, P. (2021). Environmental stressors, complex interactions and marine benthic communities' responses. *Sci. Rep.* 11. doi: 10.1038/s41598-021-83533-1

Chapman, P. M. (2016). Assessing and managing stressors in a changing marine environment. *Mar. pollut. Bull.* 124 (2), 587–590. doi: 10.1016/j.marpolbul.2016.10.039

Clark, D. E., Stephenson, F., Hewitt, J. E., Ellis, J. I., Zaiko, A., Berthelsen, A., et al. (2021). Influence of land-derived stressors and environmental variability on compositional turnover and diversity of estuarine benthic communities. *Mar. Ecol. Prog. Ser.* 666, 1–18. doi: 10.3354/meps13714

Cloern, J. E., Abreu, P. C., Carstensen, J., Chauvaud, L., Elmgren, R., Grall, J., et al. (2016). Human activities and climate variability drive fast-paced change across the world's estuarine–coastal ecosystems. *Globlal Change Biol.* 22, 513–529. doi: 10.1111/gcb.13059

Dauvin, J. C., Desroy, N., Janson, A. L., Vallet, C., and Duhamel, S. (2006). Recent changes in estuarine benthic and suprabenthic communities resulting from the development of harbour infrastructure. *Mar. pollut. Bull.* 53, 80–90. doi: 10.1016/j.marpolbul.2005.09.020

De Grave, S., Decock, W., Dekeyzer, S., Davie, P. J. F., Fransen, C. H. J. M., Boyko, C. B., et al. (2023). Benchmarking global biodiversity of decapod crustaceans (Crustacea: Decapoda). *J. Crustacean Biol.* 43 (3), 1–9. doi: 10.1093/jcbiol/ruad042

Douglas, E. J., Lohrer, A. M., and Pilditch, C. A. (2019). Biodiversity breakpoints along stress gradients in estuaries and associated shifts in ecosystem interactions. *Sci. Rep.* 9 (1), 17567. doi: 10.1038/s41598-019-54192-0

Douglas, E. J., Pilditch, C. A., Kraan, C., Schipper, L. A., Lohrer, A. M., and Thrush, S. F. (2017). Macrofaunal functional diversity provides resilience to nutrient enrichment in coastal sediments. *Ecosystems* 20 (7), 1324–1336. doi: 10.1007/s10021-017-0113-4

Douglas, E. J., Pilditch, C. A., Lohrer, A. M., Savage, C., Schipper, L. A., and Thrush, S. F. (2018). Sedimentary environment influences ecosystem response to nutrient enrichment. *Estuaries Coasts* 41, 1994–2008. doi: 10.1007/s12237-018-0416-5

Drylie, T. P. (2021). *Marine ecology state and trends in Tāmaki Makaurau / Auckland to 2019. State of the environment reporting* (Auckland, New Zealand: Auckland Council technical report). TR2021/09.

Dvoretsky, A. G., and Dvoretsky, V. G. (2020). Effects of environmental factors on the abundance, biomass, and individual weight of juvenile red king crabs in the barents sea. *Front. Mar. Sci.* 7 (726). doi: 10.3389/fmars.2020.00726

Ellis, J., Nicholls, P., Craggs, R., Hofstra, D., and Hewitt, J. (2004). Effects of terrigenous sedimentation on mangrove physiology and associated macrobenthic communities. *Mar. Ecol. Prog. Ser.* 270, 714–782. doi: 10.3354/meps270071

Ellis, J. I., Clark, D., Atalah, J., Jiang, W., Taiapa, C., Patterson, M., et al. (2017). Multiple stressor effects on marine infauna: responses of estuarine taxa and functional traits to sedimentation, nutrient and metal loading. *Sci. Rep.* 7 (12013). doi: 10.1038/s41598-017-12323-5

Fanjul, E., Escapa, M., Montemayor, D., Addino, M., Alvarez, M. F., Grela, M. A., et al. (2015). Effect of crab bioturbation on organic matter processing in South West Atlantic intertidal sediments. *J. Sea Res.* 95, 206–216. doi: 10.1016/j.seares.2014.05.005

Fox, J., and Weisberg, S. (2019). "An R Companion to Applied Regression,", *3rd ed.* (Thousand Oaks CA: Sage).

Gibbs, M., Funnell, G., Pickmere, S., Norkko, A., and Hewitt, J. (2005). Benthic nutrient fluxes along an estuarine gradient: influence of the pinnid bivalve Atrina zelandica in summer. *Mar. Ecol. Prog. Ser.* 288, 151–164. doi: 10.3354/meps288151

Gorman, R. M., and Neilson, C. G. (1999). Modelling shallow water wave generation and transformation in an intertidal estuary. *Coast. Eng.* 36 (3), 197–217. doi: 10.1016/S0378-3839(99)00006-X

Goulding, T., Sousa, P. M., Silva, G., Medeiros, J. P., Carvalho, F., Metelo, I., et al. (2021). Shifts in estuarine macroinvertebrate communities associated with water quality and climate change. *Front. Mar. Sci.* 8. doi: 10.3389/fmars.2021.698576

Green, M. O., Bell, R. G., Dolphin, T. J., and Swales, A. (2000). Silt and sand transport in a deep tidal channel of a large estuary (Manukau Harbour, New Zealand). *Mar. Geol.* 163, 217–240. doi: 10.1016/S0025-3227(99)00102-4

Greenfield, B. L., Hailes, S., MacLean, F., Peart, R., Read, G. B., Marshall, B., et al. (2023). "Protocol for the Identification of Benthic Estuarine and Marine Macroinvertebrates: A guide for parataxonomists," in *C-SIG Coastal Taxonomic Resource Tool*. Wellington, New Zealand. vol. 40.

Gunderson, A. R., Armstrong, E. J., and Stillman, J. H. (2016). Multiple stressors in a changing world: the need for an improved perspective on physiological responses to the dynamic marine environment. *Annu. Rev. Mar. Sci.* 8, 357–378. doi: 10.1146/annurev-marine-122414-033953

Heath, R. A. (1975). Stability of some New Zealand coastal inlets. *New Z. J. Mar. Freshw. Res.* 9, 449–457. doi: 10.1080/00288330.1975.9515580

Hewitt, J. E., Ellis, J. I., and Thrush, S. F. (2016). Multiple stressors, nonlinear effects and the implications of climate change impacts on marine coastal ecosystems. *Global Change Biol.* 22, 2665–2675. doi: 10.1111/gcb.13176

Hewitt, J. E., Hailes., S. F., and Greenfield, B. L. (2014). Protocol for processing, identification and quality assurance of New Zealand marine benthic invertebrate samples. *Prepared Northland Regional Council* 36, 1–36.

Hicks, M., Semadeni-Davies, A., Haddadchi, A., Shankar, U., and Plew, D. (2019). *Updated sediment load estimator for New Zealand. Prepared for the Ministry for the Environment*. Hamilton, New Zealand. 190, *NIWA Client Report 2018341CH*.

Hillman, J. R., Lundquist, C. J., O'Meara, T. A., and Thrush, S. F. (2020). Loss of large animals differentially influences nutrient fluxes across a heterogeneous marine intertidal soft-sediment ecosystem. *Ecosystems* 24 (2), 272–283. doi: 10.1007/s10021-020-00517-4

Hunt, S. (2019). *Summary of historic sedimentation measurements in the Waikato region and formulation of a historic baseline sedimentation rates, WRC Tech. Report 2019/08.*

Kassambara, A. (2020) *ggpubr: 'ggplot2' Based Publication Ready Plots*. Available at: https://CRAN.R-project.org/package=ggpubr.

Kennish, M. J. (2021). Drivers of change in estuarine and coastal marine environments: an overview. *Open J. Ecol.* 11 (3), 224–239. doi: 10.4236/oje.2021.113017

Kristensen, E., Penha-Lopes, G., Delefosse, M., Valdemarsen, T., Quintana, C. O., and Banta, G. T. (2012). What is bioturbation? The need for a precise definition for fauna in aquatic sciences. *Mar. Ecol. Prog. Ser.* 446, 285–302. doi: 10.3354/meps09506

Lam-Gordillo, O., Baring, R., and Dittmann, S. (2021). Taxonomic and functional patterns of benthic communities in Southern temperate tidal flats. *Front. Mar. Sci.* 8. doi: 10.3389/fmars.2021.723749

Lam-Gordillo, O., Huang, J., Barcelo, A., Kent, J., Mosley, L. M., Welsh, D. T., et al. (2022a). Restoration of benthic macrofauna promotes biogeochemical remediation of hostile sediments; An in *situ* transplantation experiment in a eutrophic estuarine-hypersaline lagoon system. *Sci. Total Environ.* 833, 155201. doi: 10.1016/j.scitotenv.2022.155201

Lam-Gordillo, O., Mosley, L. M., Simpson, S. L., Welsh, D. T., and Dittmann, S. (2022b). Loss of benthic macrofauna functional traits correlates with changes in sediment biogeochemistry along an extreme salinity gradient in the Coorong lagoon, Australia. *Mar. pollut. Bull.* 174, 113202. doi: 10.1016/j.marpolbul.2021.113202

Lohrer, A. M., Hewitt, J. E., and Thrush, S. F. (2006). Assessing far-field effects of terrigenous sediment loading in the coastal marine environment. *Mar. Ecol. Prog. Ser.* 315), 13–18. doi: 10.3354/meps315013

Lohrer, A., Thrush, S., and Gibbs, M. (2004a). Bioturbators enhance ecosystem function through complex biogeochemical interactions. *Nature* 431, 1092–1095. doi: 10.1038/nature03042

Lohrer, A. M., Thrush, S. F., Hewitt, J. E., Berkenbusch, K., Ahrens, M., and Cummings, V. J. (2004b). Terrestrially derived sediment: response of marine macrobenthic communities to thin terrigenous deposits. *Mar. Ecol. Prog. Ser.* 273), 121–138. doi: 10.3354/meps273121

Lohrer, A. M., Townsend, M., Rodil, I. F., Hewitt, J. E., and Thrush, S. F. (2012). Detecting shifts in ecosystem functioning: the decoupling of fundamental relationships with increased pollutant stress on sandflats. *Mar. pollut. Bull.* 64 (12), 2761–2769. doi: 10.1016/j.marpolbul.2012.09.012

Lüdecke, D. (2023). *sjPlot: Data Visualization for Statistics in Social Science*. Available at: https://strengejacke.github.io/sjPlot/.

Malone, T. C., and Newton, A. (2020). The globalization of cultural eutrophication in the coastal ocean: causes and consequences. *Front. Mar. Sci.* 7 (670). doi: 10.3389/fmars.2020.00670

Medina-Contreras, D., Arenas, F., Cantera-Kintz, J., Sánchez, A., and Lázarus, J.-F. (2022). Carbon sources supporting macrobenthic crustaceans in tropical eastern pacific mangroves. *Food Webs* 30, e00219. doi: 10.1016/j.fooweb.2022.e00219

Needham, H. R., Pilditch, C. A., Lohrer, A. M., and Thrush, S. F. (2011). Context-specific bioturbation mediates changes to ecosystem functioning. *Ecosystems* 14 (7), 1096–1109. doi: 10.1007/s10021-011-9468-0

Needham, H. R., Pilditch, C. A., Lohrer, A. M., and Thrush, S. F. (2013). Density and habitat dependent effects of crab burrows on sediment erodibility. *J. Sea Res.* 76, 94–104. doi: 10.1016/j.seares.2012.12.004

Nozarpour, R., Shojaei, M. G., Naderloo, R., and Nasi, F. (2023). Crustaceans functional diversity in mangroves and adjacent mudflats of the Persian Gulf and Gulf of Oman. *Mar. Environ. Res.* 186, 105919. doi: 10.1016/j.marenvres.2023.105919

Oldman, J. W., Black, K. P., Swales, A., and Stroud, M. J. (2009). Prediction of annual average sedimentation rates in an estuary using numerical models with verification against core data – Mahurangi Estuary, New Zealand. *Estuarine Coast. Shelf Sci.* 84 (4), 483–492. doi: 10.1016/j.ecss.2009.05.032

Oliver, E. C. J., Benthuysen, J. A., Darmaraki, S., Donat, M. G., Hobday, A. J., Holbrook, N. J., et al. (2021). Marine heatwaves. 13 (1), 313–342. doi: 10.1146/annurev-marine-032720-095144

Oliver, E. C. J., Donat, M. G., Burrows, M. T., Moore, P. J., Smale, D. A., Alexander, L. V., et al. (2018). Longer and more frequent marine heatwaves over the past century. *Nat. Commun.* 9, 1324. doi: 10.1038/s41467-018-03732-9

O'Meara, T. A., Hewitt, J. E., Thrush, S. F., Douglas, E. J., and Lohrer, A. M. (2020). Denitrification and the role of macrofauna across estuarine gradients in nutrient and sediment loading. *Estuaries Coasts* 43 (6), 1394–1405. doi: 10.1007/s12237-020-00728-x

Pardo, J. C. F., Poste, A. E., Frigstad, H., Quintana, C. O., and Trannum, H. C. (2022). The interplay between terrestrial organic matter and benthic macrofauna: Framework, synthesis, and perspectives. *Ecosphere* 14, e4492. doi: 10.1002/ecs2.4492

Pine, M. K., Radford, C. A., and Jeffs, A. G. (2015). Eavesdropping on the Kaipara Harbour: characterising underwater soundscapes within a seagrass bed and a subtidal mudflat. *New Z. J. Mar. Freshw. Res.* 49 (2), 247–258. doi: 10.1080/00288330.2015.1009916

R-Core-Team (2022). *R: A language and environment for statistical computing* (Vienna, Austria: R Foundation for Statistical Computing). Available at: https://www.R-project.org/.

Robertson, B. M., Gillespie, P. A., Asher, R. A., Frisk, S., Keeley, N. B., Hopkins, G. A., et al. (2002). Estuarine environmental assessment and monitoring: A national protocol. *Prepared support. Councils Ministry Environ. Sustain. Manage. Fund.* 5096, 93–159.

Rullens, V., Lohrer, A. M., Townsend, M., and Pilditch, C. A. (2019). Ecological mechanisms underpinning ecosystem service bundles in marine environments – A case study for shellfish. *Front. Mar. Sci.* 6. doi: 10.3389/fmars.2019.00409

Sánchez-Moyano, J. E., and García-Asencio, I. (2010). Crustacean assemblages in a polluted estuary from South-Western Spain. *Mar. pollut. Bull.* 60, 1890–1897. doi: 10.1016/j.marpolbul.2010.07.016

Sartory, D. P. (1982). *Spectrophotometric Analysis of Chlorophyll a in Freshwater Phytoplankton. . Report No. TR 115* (Pretoria: Hydrological Research Institute, Department of Environment Affairs), 163.

Seitzinger, S. P. (1988). Denitrification in freshwater and coastal marine ecosystems: Ecological and geochemical significance. *Limnol. Oceanogr.* 33 (4), 702–724. doi: 10.4319/lo.1988.33.4_part_2.0702

Simeoni, C., Furlan, E., Pham, H. V., Critto, A., de Juan, S., Trégarot, E., et al. (2023). Evaluating the combined effect of climate and anthropogenic stressors on marine coastal ecosystems: Insights from a systematic review of cumulative impact assessment approaches. *Sci. Total Environ.* 861, 160687. doi: 10.1016/j.scitotenv.2022.160687

Thrush, S. F., Halliday, J., Hewitt, J. E., and Lohrer, A. M. (2008a). The effects of habitat loss, fragmentation, and community homogenization on resilience in estuaries. *Ecol. Appl.* 18 (1), 12–21. doi: 10.1890/07-0436.1

Thrush, S. F., Hewitt, J. E., Cummings, V. J., Ellis, J. I., Hatton, C., Lohrer, A., et al. (2004). Muddy waters: elevating sediment input to coastal and estuarine habitats. *Front. Ecol. Environ.* 2 (6), 299–306. doi: 10.1890/1540-9295(2004)002[0299:MWESIT]2.0.CO;2

Thrush, S. F., Hewitt, J. E., Gladstone-Gallagher, R. V., Savage, C., Lundquist, C., O'Meara, T., et al. (2021). Cumulative stressors reduce the self-regulating capacity of coastal ecosystems. *Ecol. Appl.* 31 (1), e02223. doi: 10.1002/eap.2223

Thrush, S. F., Hewitt, J. E., Hickey, C. W., and Kelly, S. (2008b). Multiple stressor effects identified from species abundance distributions: Interactions between urban contaminants and species habitat relationships. *J. Exp. Mar. Biol. Ecol.* 366, 160–168. doi: 10.1016/j.jembe.2008.07.020

Thrush, S. F., Hewitt, J. E., Kraan, C., Lohrer, A. M., Pilditch, C. A., and Douglas, E. (2017). Changes in the location of biodiversity-ecosystem function hot spots across the seafloor landscape with increasing sediment nutrient loading. *Proc. Biol. Sci.* 284 (1852). doi: 10.1098/rspb.2016.2861

Thrush, S. F., Hewitt, J. E., Norkko, A., Cummings, V. J., and Funnell, G. A. (2003a). Macrobenthic recovery processes following catastrophic sedimentation on estuarine sandflats. *Ecol. Appl.* 13, 1433–1455. doi: 10.1890/02-5198

Thrush, S. F., Hewitt, J. E., Norkko, A., Nicholls, P. E., Funnell, G. A., and Ellis, J. I. (2003b). Habitat change in estuaries: predicting broad-scale responses of intertidal macrofauna to sediment mud content. *Mar. Ecol. Prog. Ser.* 263, 113–125. doi: 10.3354/meps263101

Thrush, S. F., Townsend, M., Hewitt, J. E., Davies, K., Lohrer, A. M., Lundquist, C., et al. (2013). *The many uses and values of estuarine ecosystems. Ecosystem services in New Zealand–conditions and trends* (Lincoln, New Zealand: Manaaki Whenua Press), 226–237.

Tittensor, D. P., Mora, C., Jetz, W., Lotze, H. K., Ricard, D., Berghe, E. V., et al. (2010). Global patterns and predictors of marine biodiversity across taxa. *Nature* 466, 1098–1101. doi: 10.1038/nature09329

Venables, W. N., and Ripley, B. D. (2002). *Modern Applied Statistics with S-Plus. 4th ed.* (New York: Springer), ISBN: .

Villnäs, A., Janas, U., Josefson, A. B., Kendzierska, H., Nygård, H., Norkko, J., et al. (2019). Changes in macrofaunal biological traits across estuarine gradients: implications for the coastal nutrient filter. *Mar. Ecol. Prog. Ser.* 622, 31–48. doi: 10.3354/meps13008

Welsh, D. T. (2003). It's a dirty job but someone has to do it: the role of marine benthic macrofauna in organic matter turnover and nutrient recycling to the water column. *J. Chem. Ecol.* 19, 321–324. doi: 10.1080/0275754031000155474

Xu, T., Newman, M., Capotondi, A., Stevenson, S., Di Lorenzo, E., and Alexander, M. A. (2022). An increase in marine heatwaves without significant changes in surface ocean temperature variability. *Nat. Commun.* 13 (7396). doi: 10.1038/s41467-022-34934-x

Zetina-Rejon, M. J., Arreguín-Sanchez, F., and Chavez, E. A. (2003). Trophic structure and flows of energy in the Huizache-Caimanero lagoon complex on the Pacific coast of Mexico. *Estuarine Coast. Shelf Sci.* 57, 803–815. doi: 10.1016/S0272-7714(02)00410-9

frontiers | Frontiers in Marine Science

TYPE Original Research
PUBLISHED 31 January 2024
DOI 10.3389/fmars.2023.1322744

OPEN ACCESS

EDITED BY
Giovanna Romano,
Anton Dohrn Zoological Station, Italy

REVIEWED BY
Filomena Ristoratore,
Zoological Station Anton Dohrn, Italy
Ernesto Maldonado,
National Autonomous University of Mexico, Mexico

*CORRESPONDENCE
Amir Sagi
sagia@bgu.ac.il

RECEIVED 17 October 2023
ACCEPTED 18 December 2023
PUBLISHED 31 January 2024

CITATION
Sudarshan G, Weil S, Manor R, Goldstein O, Sultan E, Aflalo ED, Ofir R, Zimin SV, Rosental B and Sagi A (2024) Development of long-term primary cell culture of *Macrobrachium rosenbergii*: morphology, metabolic activity, and cell-cycle analysis. *Front. Mar. Sci.* 10:1322744. doi: 10.3389/fmars.2023.1322744

Development of long-term primary cell culture of *Macrobrachium rosenbergii*: morphology, metabolic activity, and cell-cycle analysis

Gurucharan Sudarshan[1], Simy Weil[1], Rivka Manor[1], Oron Goldstein[2,3], Eliya Sultan[3], Eliahu D. Aflalo[1,4], Rivka Ofir[3,5], Sean V. Zimin[1], Benyamin Rosental[2,3] and Amir Sagi[1,6]*

[1]Department of Life Sciences, Ben-Gurion University of the Negev, Beer Sheva, Israel, [2]The Shraga Segal Department of Microbiology, Immunology, and Genetics, Faculty of Health Sciences, Ben-Gurion University of the Negev, Beer Sheva, Israel, [3]Regenerative Medicine and Stem Cell Research Center, Ben-Gurion University of the Negev, Beer Sheva, Israel, [4]Department of Life Sciences, Achva Academic College, Arugot, Israel, [5]Dead Sea and Arava Science Center, Central Arava Branch, Yair Farm, Beer Sheva, Israel, [6]National Institute for Biotechnology in the Negev, Ben-Gurion University of the Negev, Beer Sheva, Israel

This study describes our attempts to generate a sustainable cell culture of *Macrobrachium rosenbergii*. We present here a continuous longitudinal study on the embryonic primary cell culture of freshwater prawn *M. rosenbergii* that was uniquely monitored for up to 90 days with regard to its morphology, metabolic activity, and cell-cycle parameters. The daily monitoring of cells' wellbeing and morphology showed seeded cells to be changing from attached singular diverse-sized cells after days 4–10 to interconnected clusters of cells, which apparently increased in number as detected by their density in the well. Moreover, the cultures demonstrated an autonomous transition during days 7–10, from completely two-dimensional (2D) morphology to a combination of 2D and three-dimensional (3D) growing structures, leading to the formation of multilayered spheroid-like cell masses. The metabolic activity of cultures showed a non-linear elevated pattern peaking on day 26, demonstrating proliferation and increment in the number of cells, retaining statistically significant elevated metabolic activity up to 40 days, and thereafter gradually declining. In parallel, cell-cycle analyses performed through florescence-activated cell sorting (FACS) showed that the G0/G1 and S phases were inversely proportional to each other. Proliferation, based on metabolic activity, in the cultures was sustained by a significant increase in the portion of cells arrested in the S phase, from day 4 up to day 24, and then a decrease between days 45 and 90. Sorting the populations in the *M. rosenbergii* primary embryonic cell culture on days 3 and 24 revealed eight seeded populations, most of them expressing the putative proliferation markers *MrMYC* and *MrPCNA*, while six of them expressed also the putative stem-cell markers *MrOct-4* and *MrSox-2/3*. Therefore, assuming the increment in cell density and metabolic activity and the reduction in G0/G1 distribution toward S, as well as the increment in G2/M, all pointing toward proliferation, we further hypothesized that splitting the cultures along the experiment at the high-proliferating mitotic ratio peaks would enable successful passages. Indeed, in prawn embryonic primary cell culture, we

succeeded in executing two consecutive passages: the first after 8 days in culture and the second 4 days following the first passage. Cells after both passages expressed the species-specific *Mr18S*, along with the proliferative markers *MrMYC* and *MrPCNA* and the stem-cell markers *MrOct-4* and *MrSox-2/3*. After several decades of research efforts to establish a crustacean cell line—with no published success—here, we present *M. rosenbergii* cultures composed of putative proliferating/stem-cell subpopulations or appearing like clones. These mix-population prawn embryonic primary cell cultures could serve as a basic platform for immortalization and contribute to the long-term goal of establishing sustainable cell-culture lines.

KEYWORDS

cell cycle analysis, *Macrobrachium rosenbergii*, metabolic activity, passages, primary embryonic cell culture

Introduction

Despite several decades of research, a prawn cell line is still not available, and the optimal conditions for successful crustacean *in vitro* cell cultures are yet to be established. *In vitro* primary cell culture proliferation and passage achievements have gained attention in crustacean research as tools to manage and conserve valuable genetic resources, develop sustainable aquaculture practices, and support scientific investigations (Ma et al., 2017). Researchers have made notable progress in developing primary cell cultures and organ explants for various crustacean species (Jayesh et al., 2012; Anoop et al., 2021). However, maintaining the delicate balance between cell proliferation, differentiation, and cell–cell-interaction microenvironment still requires continuous efforts to refine culture media and conditions. Addressing critical factors such as optimal osmolality, vital-pathway metabolites as nutrient additives, and adequate addition of both growth and mitogenic factors still constitutes major challenges. In the present work, we adapted the commercial Opti-MEM medium (MEM-based medium) to optimal salinity for cells of the prawn *Macrobrachium rosenbergii* (420 mOsm; Frerichs, 1996). We also included metabolic precursors that facilitate the growth of adherent epithelial, smooth muscle, and primary fibroblast human cells including the selected medium used for stem cell research (Lee et al., 1996). In our previous study, the effectiveness of Opti-MEM in embryonic primary cell cultures was demonstrated for up to 14 days of culture (Sudarshan et al., 2023a). A disinfection protocol developed for fertilized eggs prior to cell isolation (Molcho et al., 2022) enabled the continuation of culture for longer periods. As a source of growth and attachment factors, lipids, hormones, and binding and transfer proteins, fetal bovine serum was adjusted up to 10% of the medium (Jochems et al., 2002).

In general, primary cell cultures have a limitation: they lose their ability to divide and proliferate after a certain number of divisions (Grimes and Chandra, 2009). Immortality can be achieved only when cells retain the ability to continuously and indefinitely divide, without undergoing senescence or cell death—a hallmark of cancer cells. Stem cells exhibit a phenomenon known as neoplasticity: the ability to self-renew independently. They show extended life spans and continue to divide for longer periods compared to differentiated cells, which stop dividing once differentiated (Hanahan and Weinberg, 2011). Upon continuous repetition of the complex animal cell cycle under optimal balance of nutrition and growth factors, genes like *MYC*, which upregulates *Cyclin B*, take center stage in orchestrating the rhythm of proliferation, while *PCNA* ensures precision in DNA replication (Shivji et al., 1992; Porter and Donoghue, 2003). Meanwhile, in the world of stem cells, *Oct4* and *Sox2* perform a delicate duet, harmonizing the balance between self-renewal and differentiation, thereby guiding the cell's destiny (Boyer et al., 2005). The expression of transcription factors like OCT4 and SOX3 is commonly associated with the maintenance of pluripotency in vertebrate embryonic stem cells (ESCs) (Archer et al., 2011). These two transcription factors work together in a complex to regulate genes important for maintaining the undifferentiated state of stem cells. When undergoing differentiation, they exhibit a dynamic change in markers (downregulation of *OCT4* and *SOX2*) as they progress toward their specialized cell fates (Swain et al., 2020). These stem-cell markers are expressed in the early stages of embryo development, much before the development and differentiation of lineages. Other than the genes above, *MYC* is known to be expressed in a variety of cancers. *MYCN*, a *MYC* paralog widely known as a proto-oncogene, is expressed in neuroblastoma (Ahmadi et al., 2021). *MYC* also supports high proliferation rates in mesenchymal stem cells. However, it is also involved in differentiation, cell-cycle progression, and cellular transformation (Melnik et al., 2019).

In the present work, we checked for the presence of the stem-cell markers listed above in an embryonic *M. rosenbergii* primary cell culture, showing supportive evidence from our embryonic *M. rosenbergii* transcriptomic libraries (Sharabi et al., 2016; Abayed

et al., 2019; Grinshpan et al., 2022). We hypothesized that harvesting embryonic primary cells for culture, with both high proliferative properties and including populations that originated from embryonic stem cells from all germ layers, presents an opportunity to obtain prolonged *in vitro* culture and even achieve a few passages before the culture reaches senescence.

Materials and methods

Animals

M. rosenbergii prawns were grown to maturity in artificial ponds at Ben-Gurion University of the Negev, Beer Sheva, Israel. Thereafter, to ensure a constant supply of embryos for primary embryonic cell isolation, gravid females were obtained by housing four to six mature females with a blue-claw male in 500-L tanks. The tanks were checked daily for the typical male reproductive guarding behavior to identify fertilized females (Molcho et al., 2022). Experiments were performed on embryos 10–16 days post-fertilization.

Mining genes from *M. rosenbergii* transcriptomic libraries

Data from three transcriptomic libraries, all of which were established in our laboratory, were used. One of the transcriptomic libraries includes various embryonic developmental stages (Abayed et al., 2019; Wahl et al., 2022), and the other includes larvae, post-larvae, and specific adult tissues (Sharabi et al., 2016; Abayed et al., 2019; Grinshpan et al., 2022). Homologs were mined from the libraries using a tBLASTn search using the amino acid sequence of OCT-4 from *Oreochromis mossambicus* (ALM89054.1), SOX-2/3 from *Penaeus mondon* (XP_037784358.1), MYC from *Homarus americanus* (XP_042210132.1), and PCNA from *Drosophila melanogaster*. mRNA sequences were aligned to the transcriptomic libraries, and putative protein sequences were compared using various NCBI BLAST algorithms (accessed during March and April 2023, https://blast.ncbi.nlm.nih.gov/Blast.cgi).

Isolation of *M. rosenbergii* primary embryonic cells for culture

In our laboratory, a highly effective protocol for isolating primary cells from prawn embryonic primary cell cultures was developed. This well-established method ensures the reliable harvesting of these vital cells for further research and experimentation (Molcho et al., 2022; Sudarshan et al., 2023a; Sudarshan et al., 2023b). Briefly, gravid females holding laid eggs on their swimming legs were disinfected for surface sterilization by submerging the animals in an aqueous solution of methylene blue (3 ppm) overnight, prior to cell isolation. On the following day, the embryos were removed from the females' swimming legs using forceps, washed with a sterile saline solution (420 mOsm), and supplemented with antibiotics penicillin–streptomycin solution (PS; 1 mg/ml, Cat. No. 03-031-1B, Biological Industries, Beit HaEmek, Israel) and tetracycline (T; 25 µg/ml, Cat. No. T-9823, Merck, Rahway, NJ, USA) and antimycotic reagent voriconazole (V; 0.5 µg/ml, Cat. No. PZ0005, Merck, USA)—referred henceforth as salineX1. The separated eggs were further disinfected in salineX1 with formalin (1%, Cat. No. 252549, 420 mOsm, Sigma-Aldrich, St. Louis, MO, USA) for 1 min followed by iodophor (1 ppm polydine, Dr. Fisher, Israel) for 3 min, then rinsed again with fresh salineX1, and rotated for 10 min at room temperature (RT). The embryonic cells were obtained by short homogenization of fertilized eggs in PSTV containing a protease and phosphatase inhibitor cocktail (Halt™ Protease Inhibitor, Cat. No. 87785, Thermo Fisher Scientific, Waltham, MA, USA). The total homogenate obtained, which consisted of whole embryo tissue, dispersed cells, and yolk protein, was passed through a 70-µm cell strainer to separate the egg envelopes and non-broken eggs from the dispersed cells. The filtrate was then pelleted by centrifugation at 850 g for 6 min at 18° C. The residue remaining in the cell strainer was transferred to Eppendorf tubes, each containing 1 mg/ml collagenase type I and 1 mg/ml collagenase IV (Cat. No. C0130 and C5138, respectively, Sigma-Aldrich, USA) and incubated for 30 min at room temperature (Waterhouse et al., 2009) with constant rotation. The extracellular matrix digestion was stopped by centrifugation as above, and the pellet was washed with medium containing 10% fetal bovine serum (FBS; Cat. No. F7524, Gibco, Grand Island, NY, USA) and combined with a filtrated cell pellet. The total cell pellet was resuspended in 2 ml of salineX1, slowly poured into an animal physiological Percoll step gradient (Cat. No. 17-0891-01, GE Healthcare Bio-Sciences AB, Uppsala, Sweden) prepared with crustacean salineX1 for osmolarity (100%, 1.062 g/ml; 50%, 0.565 g/ml; 25%, 0.282 g/ml; and 12.5%, 0.141 g/ml) and centrifuged again at 1,000 *g* for 15 min at 18°C with minimal deceleration. The Percoll gradient was used to separate the different embryonic cell types from the bulky yolk proteins (early embryonic nutrition). The yolk proteins appeared at 12.5% Percoll, while the cells migrated down the gradient and spread between 12.5% and 50% Percoll. All cell types were pooled and used for culture, transferred to a new 15-ml tube, centrifuged, and washed from Percoll with up to 10 ml of salineX1. The cells obtained were reconstituted in 1 ml Opti-MEM medium (Cat. No. 31985-047, Gibco, USA) supplemented as described above for salineX1, then visualized by trypan blue exclusion (0.2% final concentration, Cat. No. 03-102-1B, Biological Industries, Israel), and counted using a hemocytometer.

Morphological description and metabolic activity

Freshly isolated cells were seeded at a density of 10^6 cells/well in 24-well plates. The cells were cultured overnight in Dulbecco's modified Eagle medium (DMEM) high glucose (supplemented with PSTV, 10% FBS, non-essential amino acids (Cat. No. M7145, Sigma-Aldrich, Darmstadt, Germany) sodium pyruvate (Cat. No. S8636, Sigma-Aldrich, Germany), and glutamax (Cat. No.

35050061, Thermo Fisher Scientific, Oxford, UK)) at 28°C with 5% CO_2, our upgrading to the published protocol, to facilitate the attachment of higher numbers of cells to the plate (Sudarshan et al., 2023b). On day 1, the culture media were gently changed to Opti-MEM supplemented with 10% FBS and salineX1 PSTV and osmolarity-adjusted to 420 mOsm—referred to as growing medium (Frerichs, 1996). The culture plates were incubated in a 75% humidified incubator at 28°C with 5% CO_2 with 200 µl of growing medium overnight. The medium was then gently removed and refreshed with 200 µl of fresh growing medium to retain only the attached populations. Cells were monitored using an inverted microscope (Olympus CK40, Tokyo, Japan) and imaged using a digital eyepiece camera (Dino-Eye AM4023) and imaging software (DinoCapture 2.0, Dino-Lite, Netherlands) at each time point for morphological difference. The metabolic rate of the cultured cells was measured using a CCK-8 proliferation kit (Cat. No. 96992, Merck, Darmstadt, Germany) according to the manufacturer's protocol. The CCK-8 kit is based on the bio-reduction of WST-8 (2-(2-methoxy-4-nitrophenyl)-3-(4-nitrophenyl)-5-(2,4-disulfophenyl)-2*H*-tetrazolium, monosodium salt by cellular dehydrogenases to an orange formazan product that is directly proportional to the number of living cells (correlated to [3*H*]-thymidine incorporation assay). After 3 h of incubation in an incubator, the absorbance was read at 450 nm using a Tecan spectrophotometer (Tecan, Männedorf, Switzerland) and analyzed using Magellan software (Tecan, Switzerland). Significance between specific time points was determined using generalized additive models (GAMs) (Mundo et al., 2022), which are used in data analysis for understanding (especially non-linear) relationships between variables, resulting in smooths marking the confidence interval. For each time of metabolic activity, the cells were stored for cell-cycle analysis (CCA).

Cell-cycle analysis

For CCA, cells from the plate were detached using Accutase (Cat. No. 00-4555-56, Sigma-Aldrich, USA) for 15 min at 28°C, pipetted gently to detach from the plate, then transferred to Eppendorf tubes, centrifuged at 850 g for 5 min, and eluted with growing medium. Cells were washed twice with salineX1, pelleted, and fixed in 4% paraformaldehyde (PFA). Post-fixation, the cells were washed twice with fresh salineX1 and stored in a cryo-preservative (10% dimethyl sulfoxide (DMSO), 90% FBS). Later, cells were pelleted and permeabilized using permeabilization buffer X1 (Cat. No. 00-8333-56, Thermo Fisher Scientific, USA) for 20 min, stained with propidium iodide (PI; 50 µg/ml; Cat. No. 81845, Merck, Germany), and analyzed using a flow cytometer (Gallios, Beckman Coulter, Brea, CA, USA). To analyze the phases of CCA, the events were gated based on PI positives into three separate phases. The flow cytometry results were displayed using CytExpert v2.5 software (Beckman Coulter, USA). Each cell-cycle phase of the parent population was normalized to 100% in every biological triplicate at each time point. The significance between the cell-cycle phases along specific time points was determined using GAM (Mundo et al., 2022).

RNA isolation and PCR analysis

RNA was extracted using TRI reagent (Cat. No. T3934, Sigma-Aldrich, USA), and 1 µg of total RNA was converted into cDNA by following the protocol of the qScript cDNA synthesis kit (Cat. No. 95047-100, Quantabio, Beverly, MA, USA). PCR was performed using the following primers for stem-cell markers: *MrOCT-4* F: CTGGTGGGTGTAAGTGGGAT, *MrOCT-4* R: CCAGGGAAGGAAACGCAAAA (57°C), *MrSOX-2/3 F*: CGTGTTAGTTAGCGCTGGTC, *MrSOX-2/3* R: ACACTTCGGATTTTGGGCAC (56°C) and for proliferating gene markers: *MrPCNA* F: TGTCTCCCTCGTCTCTCTCA, *Mr PCNA* R: GCTGCTGAGAATTTCACCCC (56°C), *MrMYC* F: GCAGTTTGCCTGAAGACCTC and *MrMYC* R: ACAGGAGGTCGGATATGTGC (58°C) using cDNA as templates. For the sorted cell populations, when the available number of cells ranged between 15 and 30 K, the TRI reagent kit was used for RNA extraction, and the cDNA reaction was performed using 0.5 µg of total RNA.

Sorting for putative stem-cell and proliferative populations in *M. rosenbergii* primary embryonic cell cultures

Freshly isolated cells were seeded at a density of 10^6 cells/well in 24-well plates. The cells were cultured in DMEM high glucose (supplemented with PSTV, 10% FBS, non-essential amino acids, sodium pyruvate, and glutamax) overnight at 28°C with 5% CO_2 to facilitate the attachment of higher numbers of cells to the plate. DMEM high glucose was then gently removed along with non-attached cells and debris and refreshed with 500 µl of fresh growing medium to retain only the attached populations. Cells were cultured up to two time points, 3 days and 24 days, for comparison of population content in the fast-growing metabolic-activity phase in culture. For subjecting the cultured cells to florescence-activated cell sorting (FACS), the cells were harvested by enzymatic treatment using Accutase as described above. As opposed to 3 days in culture, after 24 days, with elevated numbers of clusters of interconnected cells, the enzymatic protocol was prolonged for harvesting single detached cells, as required for FACS. The cells were stained with PI to estimate cell viability and sorted through FACS (SH800S, Sony, Tokyo, Japan). The cells were sorted into distinct populations in separate tubes containing either Opti-MEM for morphology or TRI reagent for RNA isolation.

Cell proliferation and passages

Newly isolated embryonic primary cells were seeded at a density of 10^6 cells/well in 24-well plates with DMEM high glucose. On the next day, non-attached cells were removed and fed overnight with a growing medium. After 8 days in culture, the density reached approximately 80% confluency. The cells were treated with Accutase for 15 min at 28°C and pipetted gently to detach from the plate, transferred to Eppendorf tubes, and centrifuged at 850 g for

5 min. This was followed by washing with 100 µl growing medium, centrifugation, and reconstitution with 100 µl Opti-MEM, with 5 µl saved for trypan-blue exclusion staining. For RNA extraction, 10^6 cells were saved, and for CCA, 300 K were fixed as described earlier. The remaining cells were reseeded at a density of 10^6 cells/well in 24-well plates as passage 1—the same original density. After 4 days in culture as passage 1, when the wells were almost confluent, a new passage was performed, and the attached cell's extracellular matrix was enzymatically digested. A short incubation of 7 min at 28°C with Accutase was effective in obtaining single dispersed cells detached from the plate. The cells were transferred to Eppendorf tubes, centrifuged at 850 g for 5 min, washed with growing medium, centrifuged again, reconstituted with 100 µl Opti-MEM, and counted using trypan blue. The harvested cells were reseeded in a new 24-well plate at a 10^6 cells/well density and cultured at the same conditions as passage 2. Both passages 1 and 2 were further analyzed through FACS after 8 days and 4 days after passage, respectively. The sorted cells were separated into different populations and directly added to the TRI reagent for RNA isolation as described above.

Results

Morphology of *M. rosenbergii* primary embryonic cells during 90 days in culture

On the day of seeding, cells were allowed to settle and attach to the plate. Most cells were isolated and round in morphology (Figure 1A). On the following day, after removing the debris, aggregates and clusters of diverse sizes were already visible (Figure 1B). A notable presence of extracellular vesicle-like structures was observed among the cultures, mostly crowdedly located surrounding the elongated cell–cell connections. From day 4 onward, the connections between the cell clusters formed a net-like structure of intercellular bridges (Figures 1C–H) and thinner single connection (black bracket) or, alternatively, groups (yellow bracket) of finger-like projections (Figures 1C–H). Additionally, cells embedded in apparent connective-tissue-like morphology were noted from 60 days in culture (Figure 1G). Interestingly, the culture was mainly spread as two-dimensional (2D) on day 4, but from day 16 onward (till day 90), it assumed a three-dimensional (3D) spheroid-like architecture (Figures 1B–H).

Long-term metabolic activity of *M. rosenbergii* primary embryonic cell culture

Spikes in the metabolic activity of the cells were detected on days 4, 12, and 26. The highest metabolic activity was seen on day 26, followed by a gradual decline until day 90, at which point it was still higher than on day 1. Based on OD values, the metabolic activity was significantly higher in the first 33 days of the culture, reaching more than 10 times the seeded culture's OD. After 3 months, a fivefold metabolic activity was measured as compared to the seeded culture (Figure 2A). The metabolic activity was significantly higher in the first month of the culture based on the GAM statistical analysis (upper yellow mark). A significant decline was observed between days 50 and 75 (lower yellow mark) and until the end of the experiment (Figure 2B).

Cell-cycle analysis of *M. rosenbergii* primary embryonic cell culture

Higher metabolic activity is directly proportional to the number of living cells. FACS-mediated cell-cycle analysis allows us to

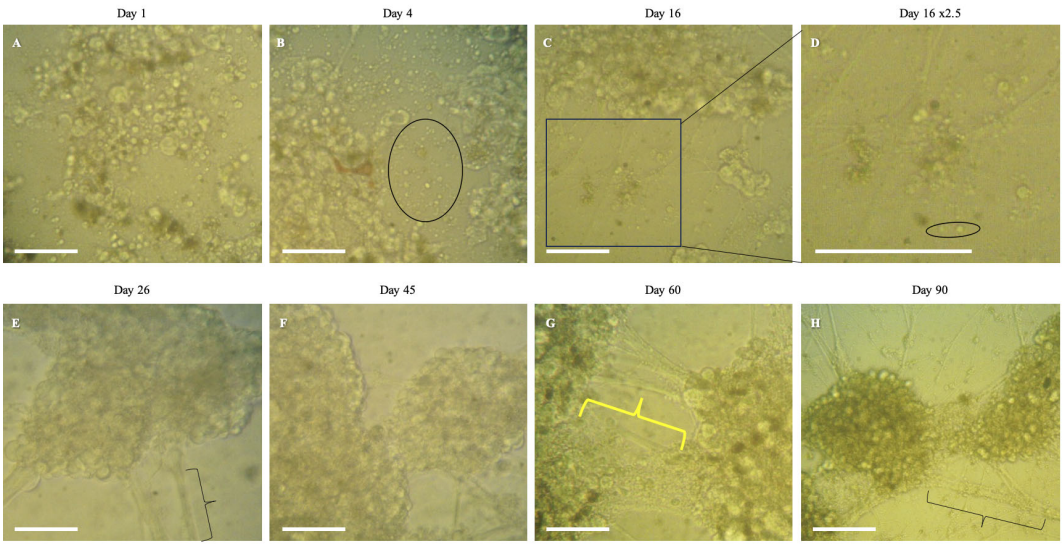

FIGURE 1
Morphology of long-term *Macrobrachium rosenbergii* embryonic primary cell culture. Representative days in culture: **(A)** day 1, **(B)** day 4, **(C)** day 16, **(D)** zoomed-in images of day 16 depicting extracellular vesicle-like morphology, **(E)** day 26, **(F)** day 45, **(G)** day 60, and **(H)** day 90. Black brackets denote prominent connections between clusters that look like intercellular bridges. The oval box denotes extracellular vesicle-like structures. The yellow bracket shows cells embedded in apparent connective-tissue-like morphology. Bar = 50 µm, **(A–C)** and **(E–H)**. Bar = 125 µm, **(D)**.

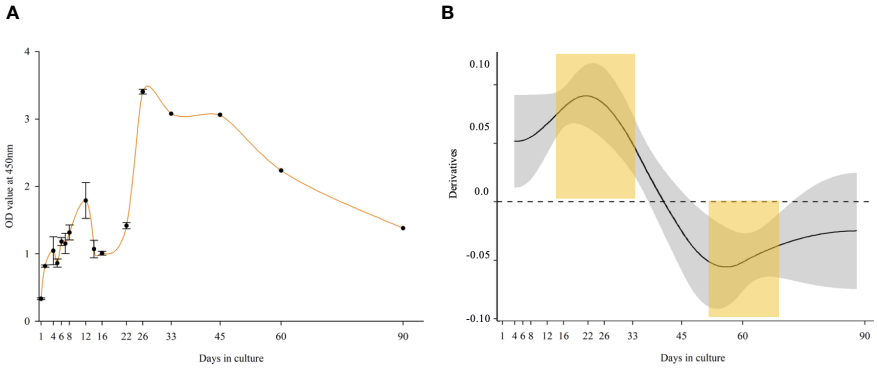

FIGURE 2
Metabolic activity of long-term Macrobrachium rosenbergii embryonic primary cell culture. **(A)** OD values (CCK-8 proliferation kit) of Opti-MEM culture up to 90 days. **(B)** Derivatives of a GAM-smooth fitted for OD values ($p < 0.001$), indicating a significant (CI excluding zero) positive trend up to Day 33, and a significant negative one from Day 45. Statistically significant different time points are marked in yellow regions.

determine the portion of cells arrested in each phase, in turn allowing us to determine the mitotic ratio. The FACS gating is depicted in Figure 3A, indicating that at the seeding point, the ratio between G0/G1 and S+G2+M was 75:25. The portion of cells in G0/G1 ranged between 51% and 78% throughout the experiment, showing a significant decrease between 2 and 22 days. The S phase ratio increased between days 12 and 33, peaked on day 26, and gradually decreased until day 90. G2/M cells were at 10% on the seeding day and maintained a steady ratio with minor fluctuations, and in the last two time points, they dropped to 3% (Figure 3B). GAM analyses applied to the cell-cycle phases showed an inverted mirror image between the statistical significance patterns of the G0/G1 and S phases of the cells (Supplementary Figure 1, left and middle). The distribution of cells at G0/G1 decreased significantly during the start of the culture, while the S phase was highly increased, and vice versa between days 50 and 90. Toward the end of the experiment, the ratio was inversed: the cells at the S phase decreased, while cells at G0/G1 increased significantly. Statistically, cells at G2/M (the shortest time period of the cell cycle) showed no significant difference throughout the culture (Supplementary Figure 1, right). In order to determine the changes in the proliferation pattern of the cells during the experiment, we calculated the mitotic ratio (the sum of the S, G2, and M phases divided by the sum of the G0 and G1 phases) of the cells from the CCA results. On day 1, the mitotic ratio was 35, increasing on days 2, 8, 16, 22–26, and 45, and then gradually declining toward day 90 to a lower value than on seeding day (~20) (Figure 3C).

Sorting of *M. rosenbergii* primary embryonic cell culture to eight subpopulations

Both metabolic activity and CCA show evidence for proliferation in this long-lasting culture. However, it is still an open question whether this culture contained putative stem-cell clones with the potential to become sustainable in culture in the future. To address this, we performed FACS for live cells on days 3 and 24 (Figures 4A–D). Survival of cells according to PI staining was 70% and 35% on days 3 and 24, respectively. The gating strategy

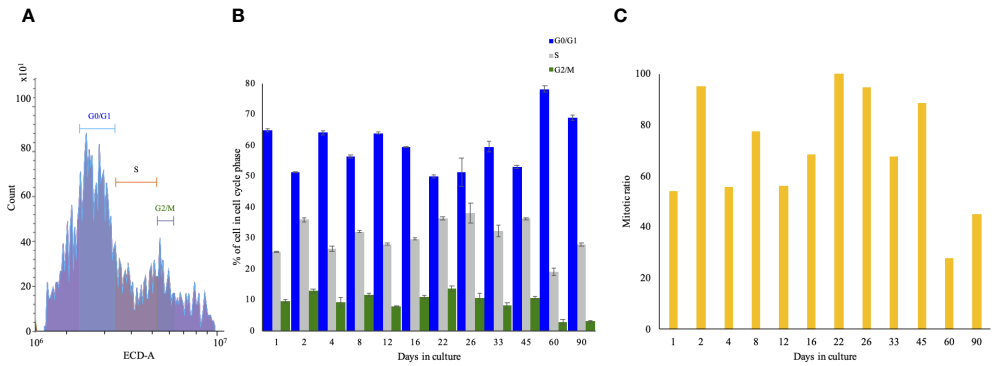

FIGURE 3
Cell-cycle analysis of long-term *Macrobrachium rosenbergii* embryonic primary cell culture through FACS. **(A)** Gating strategy of cell-cycle phases. The x-axis denotes the intensity of PI, and the y-axis denotes the count of events. **(B)** Normalized cell-cycle-phase distribution during the study. **(C)** Calculated cell-cycle mitotic ratio (S+G2+M)/(G0+G1) of cells at specific time points. FACS, florescence-activated cell sorting; PI, propidium iodide.

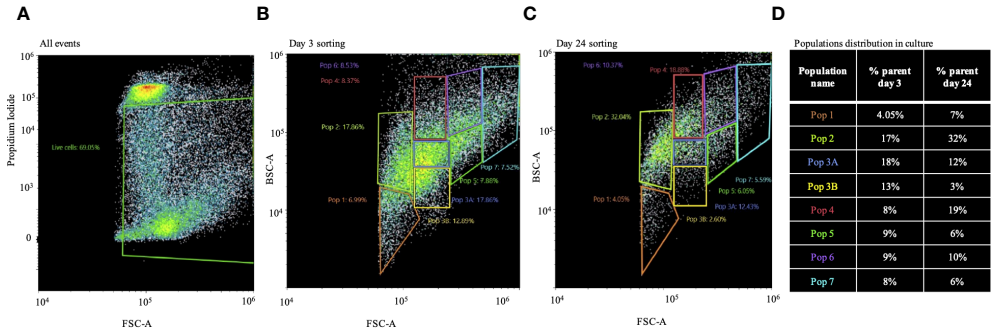

Population name	% parent day 3	% parent day 24
Pop 1	4.05%	7%
Pop 2	17%	32%
Pop 3A	18%	12%
Pop 3B	13%	3%
Pop 4	8%	19%
Pop 5	9%	6%
Pop 6	9%	10%
Pop 7	8%	6%

FIGURE 4
Population distribution of long-term *Macrobrachium rosenbergii* embryonic primary cell cultures. **(A)** FACS of live cells based on PI negatives and gating strategy based on cell size and granularity. **(B)** Distribution of populations 1–7 from 3-day cultured cells. **(C)** Same as in panel B, but from 24-day cultured cells. **(D)** Table describing changes in population distribution in cultures on day 3 and day 24 as percentages of sorted cell populations. FACS, florescence-activated cell sorting; PI, propidium iodide.

was based on different cell sizes and granularity, resulting in eight different populations detected for day 3 or 24 (Figures 4B, C). As shown in Figure 4D, there was no dramatic change in the percentage distribution of populations 1, 3A, 5, 6, and 7 between culture days 3 and 24. However, populations 2 and 4 were almost twice as high on day 24 as compared to day 3, and population 3B was higher on day 3 compared to day 24. The morphology of the different populations of cells after sorting did not differ between day 3 and day 24 (Supplementary Figure 2).

Screening for putative stem cells and proliferative populations in *M. rosenbergii* primary embryonic cell culture

Mining the *M. rosenbergii* transcriptomic libraries for expression of putative stem-cell and proliferation markers resulted in identifying orthologs of *MrSOX-2/3*, *MrOCT-4*, *MrMYC*, and *MrPCNA*. The putative stem-cell markers were expressed in the early stages of embryo development, much before the development and differentiation of lineages. Proliferative genes *MYC* and *PCNA* were also expressed at the early embryonic developmental stages at very high levels, thus giving us the liberty to use them as embryonic stem-cell proliferation marker genes (Supplementary Figure 3). The sorted cell populations were checked for the expression of *MrSOX-2/3* and *MrOCT-4* putative stem-cell markers and *MrMYC* and *MrPCNA* proliferation markers. cDNA from embryos aged 1 and 12 days and cultured cells at isolation days 0 and 1 served as positive control. As shown in the PCR agarose gel (Figure 5), all cells expressed both putative stem-cell and proliferative genes. *Mr18S* served as a housekeeping gene for the RNA content of samples and species identification, being expressed in all samples.

In the 3-day group, we found *MrOCT-4* expression in some specific sets of cells: 3A, 4, 5, 6, and 7. However, in the 24-day group, *MrOCT-4* appeared in slightly different sets: 3A, 3B, 4, 5, and 7. *MrSOX-2/3* was present in several groups of cells in the 3-day group: 1, 2, 3A, 3B, 6, and 7; in the 24-day group, it was only in

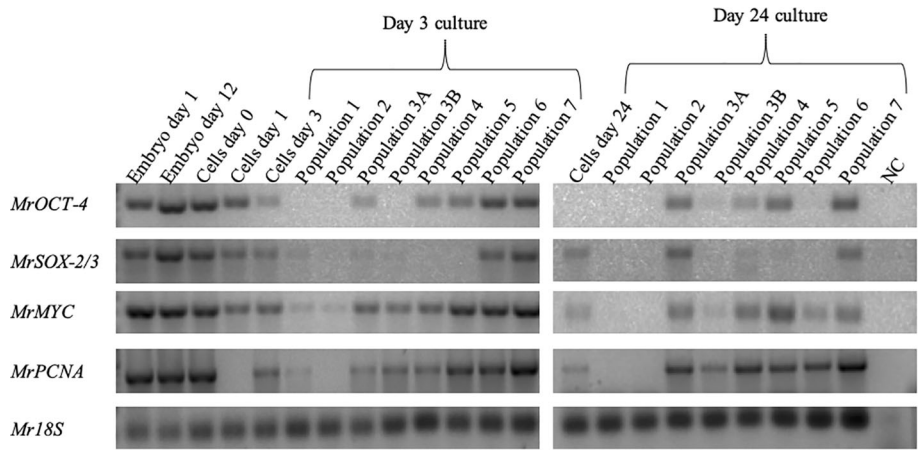

FIGURE 5
Identification of putative stem-cell and proliferative-cell populations in cultured cells. Agarose gels showing expression of stem-cell pluripotency markers (*MrSOX-2/3*, 316 bp; *MrOCT-4*, 327 bp) and proliferation genes (*MrMYC*, 330 bp; *MrPCNA*, 384 bp; *Mr18S*, 124 bp) served as housekeeping gene for RNA extraction and species identification.

groups 3A, 4, 5, and 7. *MrMYC* was expressed in all populations on day 3; on day 24, it was not present only in populations 1 and 2. Another proliferation marker, *MrPCNA*, was not expressed in cells on day 1 and in population 2 of the sorted cells on day 3. On day 24, the sorted population expressed a similar pattern as *MrMYC*.

Cell proliferation and passages of *M. rosenbergii* primary embryonic cell culture

Cultures on day 8 exhibited a morphology of 2D and 3D clusters of interconnected cells (Figure 6A). Before passage splitting, the number of cells counted was 1.9×10^6 per well. After 2 days of passage 1, the reseeded cells retained the same morphology as before the passage (Figure 6A, middle). The second passage of cells had a count of 1.3×10^6 per well. After 12 days from the first passage, attached round cells were noted, and over time, they became crowded in the center of the well but were not confluent in the contour of the well (Figure 6A, right). After sorting the cultures, the majority of the cells were in population 2 (almost 50%), and population 4 was the second most abundant (20%–23%). The less abundant populations were 1 and 6 (8%–4% and 6%–7%, respectively) (Figure 6B). Cells at both consecutive passages expressed the species-specific *Mr18S* (Figure 6C). *MrOCT-4* was expressed in almost all populations of both passages except for populations 1 and 2, while *MrSOX-2/3* was expressed only in populations 3A, 3B, 5, and 7 of passage 1 and in 3B, 6, and 7 of passage 2 (Figure 6C).

Discussion

With the longstanding aim of establishing a sustainable crustacean cell line, we reached a long-term primary culture of 90 days and two consecutive passages using an *M. rosenbergii* primary embryonic cell culture. Such processes are generally initiated by the establishment of adherent 2D cultures in which cells grow as a

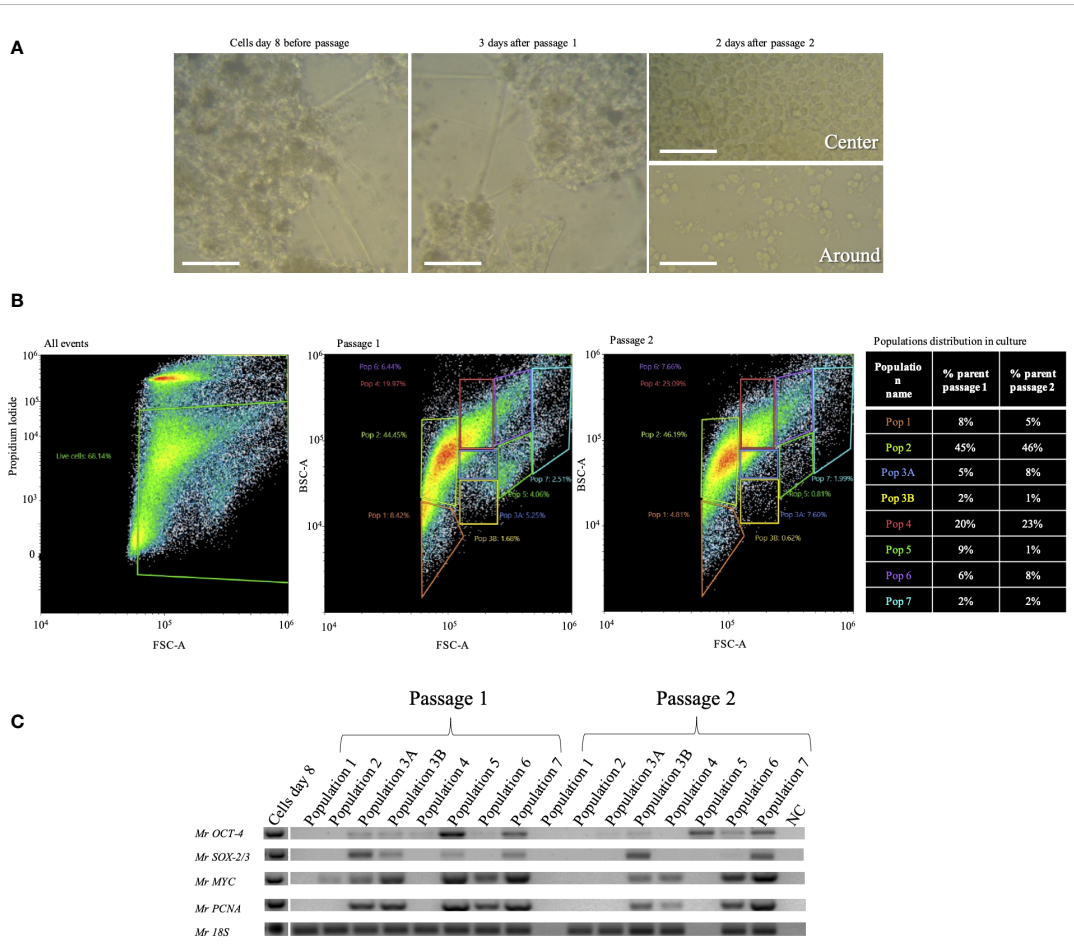

FIGURE 6
Two consecutive passages of *Macrobrachium rosenbergii* embryonic primary cell cultures. **(A)** Morphology of the culture on day 1 (left), 3 days into passage 1 (middle), and 2 days into passage 2. Above: image from the center of the well; below: image from the contour of the well. **(B)** Population distribution of *M. rosenbergii* embryonic primary cell subcultures, passages 1 and 2 through FACS of live cells, based on PI negatives and gating strategy based on cell size and granularity (left). Distribution of populations 1–7 from passages 1 and 2 (middle). Table describing changes in population distribution in passages, presented as percentage of PI-stained cells from total stained events (% parents, right). **(C)** Agarose gels showing expression of putative stem-cell pluripotency markers (*MrSOX-2/3*, 316 bp; *MrOCT-4*, 327 bp) and proliferation genes (*MrMYC*, 330 bp; *MrPCNA*, 384 bp). *Mr18S* (124 bp) served as a housekeeping gene for RNA extraction and species identification. FACS, florescence-activated cell sorting; PI, propidium iodide.

monolayer in a culture flask or a flat well plate, attached to a plastic surface as depicted in the initial step of our culture after removing the dead and non-attached cells. The later-emerging interconnected morphology of cell clusters featured a combination of 2D and 3D growing structures that led to the formation of multilayered spheroid-like cell masses, mimicking aspects of tumor architecture (Zani and Edelman, 2010; Mattes and Scholpp, 2018; Pizon et al., 2022). Under these optimized conditions, the 3D sphere-like morphology was retained for the first time (to the best of our knowledge of the peer-reviewed literature) for such a long period in an *M. rosenbergii* primary embryonic cell culture.

The elongated cell connections formed could be related to cell-signaling traffic enabling the transport of vital elements for sustainability and growth (Zani and Edelman, 2010; Mattes and Scholpp, 2018). As cells proliferate, they tend to make use of the intricate connections as pathways, to move from one cluster to another, or for the exchange of growth factors and essential elements (Bagheri et al., 2020). The cells that formed 3D patterns growing like mushrooms look similar to HER2-positive breast cancer cell lines cultured in 3D (Breslin and O'Driscoll, 2016). We suspect that cells in the innermost part of our observed clusters might not receive as much nutrients as those on the outer edges. The outer cells, being more exposed to the culture medium, tend to divide and multiply rapidly, while the inner cells remain less active, similar to cancer tumors (Bowden et al., 2020). Moreover, the notable presence of extracellular vesicle (EV)-like structures located mostly surrounding the elongated cell–cell cluster connections are suggested to be derived from the different types of embryonic stem cells, carrying cargo that influences the differentiation of target cells as described in vertebrates (Gong et al., 2021). EV research in crustaceans revealed their roles in intercellular communication, immune responses, and reproductive processes (Bowden et al., 2020). The presence of EV might suggest signaling-molecule transport, but this remains to be further studied.

The non-linear elevated fluctuation pattern in the metabolic activity can be related to energetic pathways exhibited by the cells. Cells can switch between different metabolic pathways based on their microenvironment and needs. Cancer cells at certain periods used aerobic glycolysis to convert glucose into energy (Tripathi et al., 2022). Based on the drop-in metabolic activity of cells in culture, such a process might occur on days 4, 8, 12, and 26 in the prawn embryonic primary cell culture. At these higher peaks, high proliferation of cells is suggested; hence, more efficient oxidative-phosphorylation respiration is needed to facilitate the uptake and incorporation of nutrients into biomass. Nucleotides, amino acids, and lipids are needed to produce new cells in culture, cell membranes, and other components (Vander Heiden et al., 2009). This aligns with the peak in metabolic activity, suggesting that the latter might represent an optimal state for cell growth and proliferation. We suggest that the abundant extracellular vesicles we showed in our culture could explain the increment in phosphatidylcholine, phosphatidylserine, and palmitate detected in the culture media correlating with the peak in metabolic activity (Sudarshan et al., 2023b). Organic solvents used for metabolic extraction could easily solubilize the extracellular vesicle membrane and elute the metabolites in the extracellular vesicle's cargo, suggesting that these metabolites are involved in inducing proliferation.

As mentioned earlier, our cells formed 3D mushroom-like structures. Cells in the inner mass need to rely on aerobic glycolysis to produce energy and are not stimulated by growth factors or inducers available in the medium. In contrast, cells in the outer layer are in direct contact with the medium and are hence supplied with the necessary growth hormones, inducers, and mitogenic factors and might be in a constant state of proliferation (Fontana et al., 2020; Zanoni et al., 2020). This allows us to determine the phase of the cell by morphological appearance. The peak in metabolic activity on days 12 to 26 was found to be associated with the peak in the S phase from days 8 to 33 based on cell-cycle analysis, thus providing insights into cell-division dynamics within the culture. The rise in the abundance of S-phase cells indicates active DNA synthesis, followed by a gradual decrease. This evidence suggests a burst of cell proliferation followed by stabilization, exhibiting a high mitotic ratio for a relatively long time in culture. The proliferation potential of the primary cell culture is suggested by the results to be similar to that of cancerous cell lines like HT-29 colorectal adenocarcinoma, Jurkat cells, and lung carcinoma epithelial cells A549 (Begum et al., 2013).

We infer that whenever a sorted cell population does not express putative stem-cell markers, it is in a state of differentiation. From the sorted 3-day *M. rosenbergii* primary culture results, it seems that populations 3A, 6, and 7 are probably self-renewing putative stem cells in nature, as was supported by their gene-expression patterns, which are similar to populations 3A, 4, 5, and 7 in 24-day sorted cultures. Studies in humans have shown that when Sox-3 is expressed alone in a cell, it can bind to specific DNA sequences called Sox-binding sites and regulate the expression of target genes. Sox-3 is known to be involved in various cellular processes, including embryonic development and neural differentiation (Archer et al., 2011). Nevertheless, the expression of Sox-3 alone in our cultures may suggest that these cell populations are already differentiated (Wang et al., 2006). Future work, using specific cell markers, may make it possible to point toward the exact types of differentiated cells, e.g., differentiated neural cells like in humans.

In our culture, almost all sorted populations were in a state of proliferation on days 3 and 24. This suggests that our conditioning of the medium (Sudarshan et al., 2023a) supported the culture of *M. rosenbergii* cells in sustaining the stemness of the embryonic cells by self-renewing and differentiation of specific lineages. The only populations that expressed neither stem-cell markers nor typical proliferation genes had the smallest (7–10 μm) size compared to other populations, which might suggest that they originated from the hematopoietic lineage, which does not proliferate and contains the smallest cells of the organism (Matozzo and Marin, 2010).

We hypothesized that interfering along the experiment at points of high-proliferating mitotic-ratio peaks, for example, after 8 days, would result in a successful passage. Diluting cell densities for the first and second subculturing passages resulted in increased embryonic subpopulations that expressed the *M. rosenbergii*-specific *Mr18S* gene and which proliferated and also expressed putative stem-cell markers. Other than a study on *M. rosenbergii* heart cell explants, which, to the best of our knowledge, did not mature into a continuous cell line (Goswami et al., 2010), and a

patent application of a commercial company (SHIOK meats) that was not scientifically published, our report seems to have a promising potential in reaching immortalization and contributing to the long-time goal of establishing sustainable crustacean cell-culture lines (Sriram and Ling, 2020).

In conclusion, the results of the present study suggest that our *M. rosenbergii* primary embryonic cell culture undergoes significant changes in morphology, metabolic activity, and cell-cycle dynamics over time. Understanding these changes and their implications can be valuable for further studies and applications involving *M. rosenbergii* primary embryonic cell cultures.

Data availability statement

The datasets presented in this study can be found in online repositories. The names of the repository/repositories and accession number(s) can be found in the article/Supplementary Material.

Ethics statement

The manuscript presents research on animals that do not require ethical approval for their study.

Author contributions

GS: Conceptualization, Data curation, Formal analysis, Methodology, Validation, Visualization, Writing – original draft, Writing – review & editing. SW: Conceptualization, Investigation, Methodology, Project administration, Resources, Supervision, Validation, Visualization, Writing – review & editing. RM: Investigation, Project administration, Resources, Software, Supervision, Validation, Visualization, Writing – review & editing. OG: Methodology, Software, Supervision, Validation, Writing – review & editing. ES: Formal analysis, Methodology, Software, Writing – review & editing. EA: Conceptualization, Formal analysis, Investigation, Methodology, Project administration, Software, Supervision, Writing – review & editing. RO: Conceptualization, Investigation, Project administration, Supervision, Visualization, Writing – review & editing. SZ: Data curation, Formal analysis, Methodology, Software, Writing – review & editing. BR: Formal analysis, Investigation, Methodology, Project administration, Supervision, Validation, Visualization, Writing – review & editing. AS: Conceptualization, Funding acquisition, Project administration, Resources, Supervision, Visualization, Writing – review & editing.

Funding

The author(s) declare financial support was received for the research, authorship, and/or publication of this article. Funding for this study was granted by the Ministry of Science and Technology, Israel-Taiwan collaboration 00019994. The work of BR was supported by the Israel Science Foundation (ISF, Grants Nos. 1416/19 and 2841/19). The authors declare no competing financial interests.

Acknowledgments

We would like to thank Enzootic Ltd. and Colors Farm for the supply of embryos for the study. We would like to thank Prof. Ofer Ovadia, Dept. of Life Sciences, BGU, for the discussion regarding statistical analyses.

Conflict of interest

The authors declare that the research was conducted in the absence of any commercial or financial relationships that could be construed as a potential conflict of interest.

Publisher's note

All claims expressed in this article are solely those of the authors and do not necessarily represent those of their affiliated organizations, or those of the publisher, the editors and the reviewers. Any product that may be evaluated in this article, or claim that may be made by its manufacturer, is not guaranteed or endorsed by the publisher.

Supplementary material

The Supplementary Material for this article can be found online at: https://www.frontiersin.org/articles/10.3389/fmars.2023.1322744/full#supplementary-material

References

Abayed, F. A. A., Manor, R., Aflalo, E. D., and Sagi, A. (2019). Screening for Dmrt genes from embryo to mature *Macrobrachium rosenbergii* prawns. *Gen. Comp. Endocrinol.* 282, 113205. doi: 10.1016/j.ygcen.2019.06.009

Ahmadi, S. E., Rahimi, S., Zarandi, B., Chegeni, R., and Safa, M. (2021). MYC: a multipurpose oncogene with prognostic and therapeutic implications in blood Malignancies. *J. Hematol. Oncol.* 14, 121. doi: 10.1186/s13045-021-01111-4

Anoop, B. S., Puthumana, J., Vazhappilly, C. G., Kombiyil, S., Philip, R., Abdulaziz, A., et al. (2021). Immortalization of shrimp lymphoid cells by hybridizing with the continuous cell line *Sf9* leading to the development of '*PmLyO-Sf9*'. *Fish Shellfish Immunol.* 113, 196–207. doi: 10.1016/j.fsi.2021.03.023

Archer, T. C., Jin, J., and Casey, E. S. (2011). Interaction of Sox1, Sox2, Sox3 and Oct4 during primary neurogenesis. *Dev. Biol.* 350, 429–440. doi: 10.1016/j.ydbio.2010.12.013

Bagheri, H. S., Bani, F., Tasoglu, S., Zarebkohan, A., Rahbarghazi, R., and Sokullu, E. (2020). Mitochondrial donation in translational medicine; from imagination to reality. *J. Trans. Med.* 18, 367. doi: 10.1186/s12967-020-02529-z

Begum, J., Day, W., Henderson, C., Purewal, S., Cerveira, J., Summers, H., et al. (2013). A method for evaluating the use of fluorescent dyes to track proliferation in cell lines by dye dilution. *Cytometry. Part A*, 83 (12), 1085–1095.

Bowden, T. J., Kraev, I., and Lange, S. (2020). Extracellular vesicles and post-translational protein deimination signatures in haemolymph of the American lobster (Homarus americanus). *Fish Shellfish Immunol.* 106, 79–102. doi: 10.1016/j.fsi.2020.06.053

Boyer, L. A., Lee, T. I., Cole, M. F., Johnstone, S. E., Levine, S. S., Zucker, J. P., et al. (2005). Core transcriptional regulatory circuitry in human embryonic stem cells. *Cell* 122, 947–956. doi: 10.1016/j.cell.2005.08.020

Breslin, S., and O'Driscoll, L. (2016). The relevance of using 3D cell cultures, in addition to 2D monolayer cultures, when evaluating breast cancer drug sensitivity and resistance. *Oncotarget* 7, 45745–45756. doi: 10.18632/oncotarget.9935

Fontana, F., Raimondi, M., Marzagalli, M., Sommariva, M., Gagliano, N., and Limonta, P. (2020). Three-dimensional cell cultures as an *in vitro* tool for prostate cancer modeling and drug discovery. *Int. J. Mol. Sci.* 21, 6806. doi: 10.3390/ijms21186806

Frerichs, G. N. (1996). *In vitro* culture of embryonic cells from the freshwater prawn *Macrobrachium rosenbergii*. *Aquaculture* 143, 227–232. doi: 10.1016/0044-8486(96)01281-1

Gong, Y., Wei, X., Sun, W., Ren, X., Chen, J., Aweya, J. J., et al. (2021). Exosomal miR-224 contributes to hemolymph microbiota homeostasis during bacterial infection in crustacean. *PloS Pathog.* 17, e1009837. doi: 10.1371/journal.ppat.1009837

Goswami, M., Lakra, W. S., Rajaswaminathan, T., and Rathore, G. (2010). Development of cell culture system from the giant freshwater prawn *Macrobrachium rosenbergii* (de Man). *Mol. Biol. Rep.* 37, 2043–2048. doi: 10.1007/s11033-009-9659-3

Grimes, A., and Chandra, S. B. (2009). Significance of cellular senescence in aging and cancer. *Cancer Res. Treat* 41, 187–195. doi: 10.4143/crt.2009.41.4.187

Grinshpan, N., Abayed, F. A. A., Wahl, M., Ner-Gaon, H., Manor, R., Sagi, A., et al. (2022). The transcriptional landscape of the giant freshwater prawn: Embryonic development and early sexual differentiation mechanisms. *Front. Endocrinol.* 13. doi: 10.3389/fendo.2022.1059936

Hanahan, D., and Weinberg, R. A. (2011). Hallmarks of cancer: the next generation. *Cell* 144, 646–674. doi: 10.1016/j.cell.2011.02.013

Jayesh, P., Seena, J., and Singh, I. S. (2012). Establishment of shrimp cell lines: perception and orientation. *Indian J. Virol.* 23, 244–251. doi: 10.1007/s13337-012-0089-9

Jochems, C. E. A., van Der Valk, J. B. F., Stafleu, F. R., and Baumans, V. (2002). The use of fetal bovine serum: ethical or scientific problem? *Alternatives to Lab. Anim.* 30, 219–227.

Lee, J. H., Jang, S. I., Yang, J. M., Markova, N. G., and Steinert, P. M. (1996). The proximal promoter of the human transglutaminase 3 gene. Stratified squamous epithelial-specific expression in cultured cells is mediated by binding of Sp1 and ets transcription factors to a proximal promoter element. *J. Biol. Chem.* 271, 4561–4568. doi: 10.1074/jbc.271.8.4561

Ma, J., Zeng, L., and Lu, Y. (2017). Penaeid shrimp cell culture and its applications. *Rev. Aquaculture* 9, 88–98. doi: 10.1111/raq.12106

Matozzo, V., and Marin, M. G. (2010). First cytochemical study of haemocytes from the crab Carcinus aestuarii (Crustacea, Decapoda). *Eur. J. Histochem.* 54, e9. doi: 10.4081/ejh.2010.e9

Mattes, B., and Scholpp, S. (2018). Emerging role of contact-mediated cell communication in tissue development and diseases. *Histochem. Cell Biol.* 150, 431–442. doi: 10.1007/s00418-018-1732-3

Melnik, S., Werth, N., Boeuf, S., Hahn, E.-M., Gotterbarm, T., Anton, M., et al. (2019). Impact of c-MYC expression on proliferation, differentiation, and risk of neoplastic transformation of human mesenchymal stromal cells. *Stem Cell Res. Ther.* 10, 73. doi: 10.1186/s13287-019-1187-z

Molcho, J., Manor, R., Shamsian, M., Sudarshan, G., Ofir, R., Parker, D., et al. (2022). On genome editing in embryos and cells of the freshwater prawn *Macrobrachium rosenbergii*. *Aquaculture* 558, 738391. doi: 10.1016/j.aquaculture.2022.738391

Mundo, A. I., Tipton, J. R., and Muldoon, T. J. (2022). Generalized additive models to analyze nonlinear trends in biomedical longitudinal data using R: Beyond repeated measures ANOVA and linear mixed models. *Stat Med.* 41, 4266–4283. doi: 10.1002/sim.9505

Pizon, M., Schott, D., Pachmann, U., Schobert, R., Pizon, M., Wozniak, M., et al. (2022). Chick chorioallantoic membrane (CAM) assays as a model of patient-derived xenografts from circulating cancer stem cells (cCSCs) in breast cancer patients. *Cancers (Basel)* 14. doi: 10.3390/cancers14061476

Porter, L. A., and Donoghue, D. J. (2003). Cyclin B1 and CDK1: nuclear localization and upstream regulators. *Prog. Cell Cycle Res.* 5, 335–347.

Sharabi, O., Manor, R., Weil, S., Aflalo, E. D., Lezer, Y., Levy, T., et al. (2016). Identification and characterization of an insulin-like receptor involved in crustacean reproduction. *Endocrinology* 157, 928–941. doi: 10.1210/en.2015-1391

Shivji, M. K. K., Kenny, M. K., and Wood, R. D. (1992). Proliferating cell nuclear antigen is required for DNA excision repair. *Cell* 69, 367–374. doi: 10.1016/0092-8674(92)90416-A

Sriram, S., and Ling, K. Y. (2020). Isolation and cultivation of muscle and fat cells from crustaceans. International patent WO 2020/149791 A1, filled and issued. (Singapore).

Sudarshan, G., Weil, S., Jasińska, W., Manor, R., Goldstein, O., Aflalo, E. D., et al. (2023a). Correlation between metabolomic profile and proliferation of Macrobrachium rosenbergii primary embryonic cell culture. *Front. Mar. Sci.* 10. doi: 10.3389/fmars.2023.1270491

Sudarshan, G., Weil, S., Rotem-Dai, N., Manor, R., Greenshpan, Y., Goldstein, O., et al. (2023b). Enhanced proliferation in a prawn embryonic primary cell culture ectopically expressing mutated Ras. *Front. Mar. Sci.* 9. doi: 10.3389/fmars.2022.1100971

Swain, N., Thakur, M., Pathak, J., and Swain, B. (2020). SOX2, OCT4 and NANOG: The core embryonic stem cell pluripotency regulators in oral carcinogenesis. *J. Oral. Maxillofac. Pathol.* 24, 368–373. doi: 10.4103/jomfp.JOMFP_22_20

Tripathi, S., Park, J. H., Pudakalakatti, S., Bhattacharya, P. K., Kaipparettu, B. A., and Levine, H. (2022). A mechanistic modeling framework reveals the key principles underlying tumor metabolism. *PloS Comput. Biol.* 18, e1009841. doi: 10.1371/journal.pcbi.1009841

Vander Heiden, M. G., Cantley, L. C., and Thompson, C. B. (2009). Understanding the Warburg effect: the metabolic requirements of cell proliferation. *Science* 324, 1029–1033. doi: 10.1126/science.1160809

Wahl, M., Levy, T., Manor, R., Aflalo, E. D., Sagi, A., and Aizen, J. (2022). Genes encoding the glycoprotein hormone GPA2/GPB5 and the receptor LGR1 in a female prawn. *Front. Endocrinol.* 13. doi: 10.3389/fendo.2022.823818

Wang, T. W., Stromberg, G. P., Whitney, J. T., Brower, N. W., Klymkowsky, M. W., and Parent, J. M. (2006). Sox3 expression identifies neural progenitors in persistent neonatal and adult mouse forebrain germinative zones. *J. Comp. Neurol.* 497, 88–100. doi: 10.1002/cne.20984

Waterhouse, A. M., Procter, J. B., Martin, D. M., Clamp, M., and Barton, G. J. (2009). Jalview Version 2–a multiple sequence alignment editor and analysis workbench. *Bioinformatics* 25, 1189–1191. doi: 10.1093/bioinformatics/btp033

Zani, B. G., and Edelman, E. R. (2010). Cellular bridges: Routes for intercellular communication and cell migration. *Communicative Integr. Biol.* 3, 215–220. doi: 10.4161/cib.3.3.11659

Zanoni, M., Cortesi, M., Zamagni, A., Arienti, C., Pignatta, S., and Tesei, A. (2020). Modeling neoplastic disease with spheroids and organoids. *J. Hematol. Oncol.* 13, 97. doi: 10.1186/s13045-020-00931-0

frontiers | Frontiers in Marine Science

TYPE Original Research
PUBLISHED 25 April 2024
DOI 10.3389/fmars.2024.1371782

OPEN ACCESS

EDITED BY
Rachael Peart,
National Institute of Water and Atmospheric Research (NIWA), New Zealand

REVIEWED BY
Ajit Kumar Mohanty,
Indira Gandhi Centre for Atomic Research (IGCAR), India
Henrique Queiroga,
University of Aveiro, Portugal

*CORRESPONDENCE
José M. Landeira
jose.landeira@ulpgc.es

†Deceased

RECEIVED 17 January 2024
ACCEPTED 10 April 2024
PUBLISHED 25 April 2024

CITATION
Landeira JM, Fatira E, Cuesta JA, Schubart CD, Moreno-Borges S and Rodríguez A (2024) Larval dynamics suggest phenological strategies and positive effect of marine protected areas controlling indigenous and non-indigenous crab populations.
Front. Mar. Sci. 11:1371782.
doi: 10.3389/fmars.2024.1371782

Larval dynamics suggest phenological strategies and positive effect of marine protected areas controlling indigenous and non-indigenous crab populations

José M. Landeira[1*], Effrosyni Fatira[1], Jose A. Cuesta[2], Christoph D. Schubart[3†], Sergio Moreno-Borges[4] and Adriana Rodríguez[4]

[1]Instituto de Oceanografía y Cambio Global, IOCAG, Universidad de Las Palmas de Gran Canaria, Las Palmas de Gran Canaria, Spain, [2]Department of Ecology and Coastal Management, Instituto de Ciencias Marinas de Andalucía (ICMAN-CSIC), Cádiz, Spain, [3]Institute of Zoology, University of Regensburg, Regensburg, Germany, [4]Biodiversidad, Ecología marina y Conservación Research Group (BIOECOMAC) Research Group, Universidad de La Laguna, San Cristobal de La Laguna, Spain

The early life of most decapod crustaceans takes place in the water column as larvae before they settle in benthic habitats. The spatial and temporal variability in the settling of larval stages offers valuable insights into the potential recruitment of natural populations. To explore this, we studied megalopa assemblages at various segments of coastline on El Hierro and Lanzarote islands, both within and outside the Marine Protected Areas (MPAs) of each island. The study spanned four consecutive oceanographic periods in the Canary Islands (NW Africa), employing light traps for sample collection. The low number of recorded species suggested that light traps exhibit selectivity, particularly for megalopae belonging to Portunidae and Grapsidae. El Hierro, which experienced warmer sea surface temperatures, displayed higher megalopa abundance values than Lanzarote and distinct larval assemblages was observed between these two islands. Similarly, we identified significant variations in abundance and species composition between stratified and mixing seasons. These seasonal differences were influenced by the dominance of *Achelous hastatus*, *Percnon gibbesi*, and *Cronius ruber* during the stratified season. In Lanzarote, *C. ruber* was not recorded during the mixing season, suggesting that the colder conditions there may constrain its reproduction. Interestingly, we observed that species traditionally harvested from the intertidal zone for human consumption (*Plagusia depressa*) or used as bait for recreational fishing (*Pachygrapsus* spp. and *P. gibbesi*) exhibited higher megalopa abundances within the MPAs. In contrast, we noted lower megalopa densities of the non-indigenous species *C. ruber* within the protected areas. These results indicate a positive effect of MPAs controlling indigenous and non-indigenous crab populations. Moreover, the study provides novel data, showing that light traps are suitable for monitoring the temporal occurrence, abundance, and spatial distribution of non-indigenous and commercially exploited species. This is key for adopting an ecosystem-based approach to manage marine resources.

KEYWORDS

megalopa, light trap, phenology, recruitment, protection, Canary Islands

1 Introduction

Marine brachyuran crabs have a complex life-cycle consisting of two main phases: one that occurs in the benthic environment during the juvenile-adult period and another in the pelagic realm as larvae (Anger, 2006). Both phases are crucial and interdependent as the larval success depends on the maternal investment, and the maintenance of adult populations requires a sufficient level of larval recruitment (Oliphant & Thatje, 2021). The larval phase consists of a series of zoea stages, which are specialized for the planktonic life and finish with a megalopa stage. This last stage emerges after a metamorphosis to prepare the larvae in the transition plankton-benthos. Although these larval stages have limited size and swimming capabilities, they have developed different morphologies and behaviors to ensure an optimum foraging, growth, and predator avoidance to survive (Bashevkin et al., 2020).

The interdependence of pelagic and benthic phases makes the study of planktonic larval stages of paramount importance to understand changes at population-level (Hjort, 1914). Consequently, many efforts have been made to increase our knowledge of early life stages of decapod crustaceans. These include the analyses of the biodiversity in sensitive ecosystems (Brandão et al., 2016), the investigation of reproductive phenology (González-Gordillo & Rodríguez, 2003; Landeira & Lozano-Soldevilla, 2018), the identification of transport pathways and population connectivity (Pires et al., 2020; Clavel-Henry et al., 2021), the early detection of non-indigenous species (Torres et al., 2012; Marco-Herrero et al., 2018), the assessment of the effectiveness of Marine Protected Areas (MPAs) (Whomersley et al., 2018), and the examination of the impact of climate change (Lindley et al., 2010). Considering their significance, a comprehensive understanding of the early life stages of decapods is a prerequisite for adopting an ecosystem-based approach to management. This is particularly crucial under the EU Marine Strategy Framework Directive (MSFD - Directive 2008/56/EC), where understanding of the early life stages serves as a descriptor for determining good environmental status and plays a role in establishing MPAs. Additionally, it is essential for monitoring the temporal occurrence, abundance, and spatial distribution of non-indigenous and commercially exploited species.

The Canary Islands archipelago is an interesting region to investigate larval dynamics of marine invertebrates. The archipelago is located in a subtropical transition area in the NE Atlantic and shows clear signs of tropicalization due to ongoing warming of the waters (González et al., 2017; González-Delgado et al., 2018). In terms of faunistic composition, it presents high diversity of marine species, and the decapod crustaceans are well studied comprising more than 374 species reported (González, 2018). To preserve and restore the biodiversity, as well as to enhance the total biomass of commercial species and therefore, support the local artisanal fisheries, the Canary Island government has established MPAs in the islands of Lanzarote, La Palma and El Hierro (Sanabria-Fernandez et al., 2019). The Canary Islands extends westward from near the NW African coast to the open ocean, acting as a barrier to the flow of both the Canary Current and the Trade winds inducing an intense mesoscale activity southward the islands (Barton et al., 1998). This mesoscale activity is a major driver in the distribution of decapod larvae in the open waters. Eddies and the lee zone formed downstream of the archipelago due to the island-mass effect (Sangrà et al., 2007) serve as retention zones for larvae of neritic species (Landeira et al., 2009, Landeira et al., 2010, Landeira et al., 2013). Moreover, it has been observed that upwelling filaments from the continental shelf transport larvae from African populations towards the island coasts, serving as potential pathways of connectivity (Landeira et al., 2012; Landeira et al., 2017). The year-round upwelling system off NW Africa generates high variability in the physical, chemical, and biological conditions (Arístegui et al., 2009). Thus, islands closer to Africa are more influenced by the upwelling system, showing colder and nutrient-richer waters than the western side of the archipelago. Moreover, the temporal variability of the oceanographic conditions characterizes two distinct seasons in the region. The productive season (Late Winter Bloom) takes place from January to May due to surface waters cooling and vertical mixing of nutrients (Arístegui et al., 2001). The rest of the year (from late spring to autumn) the region is characterized by a strong stratification of the water column giving rise to surface warming and oligotrophy (Couret et al., 2023a). This seasonality determines temporal changes in plankton biomass and composition (Schmoker et al., 2012; Couret et al., 2023b), and reproductive strategies of decapod crustaceans (Landeira & Lozano-Soldevilla, 2018).

Despite the advances in understanding the planktonic dynamics of decapod crustacean larvae over the past decade, spatial and temporal patterns of settlement larval stages near the coast remain poorly known in the Canary Island region. Only observations on colonizing artificial collectors in different habitats have provided insights on the settlement preferences of post-larval stages of decapod crustaceans through an annual cycle (García-Sanz et al., 2014; Herrera et al., 2014). Filling the gap of knowledge is fundamental for understanding recruitment processes and population functioning. Ultimately, it can serve as a valuable tool for policymakers to improve the capacities for the management of marine resources and ecosystem services. This study aimed to provide information on spatial and temporal variability of the abundance, composition, and assemblages of settlement stage of brachyuran crabs in the Canary Islands by sampling with light traps during four consecutive environmental seasons. Moreover, we investigated the possible effect of MPAs controlling larval assemblages in relation to non-indigenous species and indigenous species with commercial interest.

2 Material and methods

2.1 Decapod larvae collection

Settlement stages of decapod crustaceans (referred to megalopa) were collected with the Ecocean CARE® light trap. The CARE light trap consisted of a float with a watertight block containing a rechargeable light, and a 2 m conical net (2 mm mesh size) hanging 1.5 m below the sea surface (Lecaillon, 2004). The sampling was designed to ensure segments of coastline with contrasting environmental conditions in the Canary Islands

(Central Atlantic, NW Africa, Figure 1A). Considering the longitudinal gradient of temperature and productivity generated by the NW African upwelling system, we targeted the islands of Lanzarote (eastern side of the archipelago, with high upwelling influence) and El Hierro (westernmost island, non-upwelling influence) (Figure 2; Table 1). Thus, samples were collected during the stratified-warm season (years 2019 and 2020) and mixing-cold season (years 2020 and 2021) at 4 segments of coastline in Lanzarote and 4 in El Hierro (Figures 1B, C; Table 1). Two of those segments were placed inside each MPA of "Isla de La Graciosa e Islotes del Norte" in Lanzarote, and of "La Restinga-Mar de las Calmas" in El Hierro (Figures 1B, C; Table 1). Samples were not obtained at Lanzarote's MPA stations (traps A1-3, F1-3) because of adverse weather conditions during the 2019 campaign. Furthermore, one sample was lost during the 2021 campaign due to a mesh breakage in the trap Q2. At each segment of coastline, three light traps were moored nearshore, at 10-25 m depth and at 20-300 m from the coastline. The traps were set maintaining a minimum distance of 300 m apart from each other to prevent light overlapping (Félix-Hackradt et al., 2013; Moreno-Borges et al., in press). Traps were left overnight; usually deployed and retrieved 1-2 hours before the sunset and after sunrise, respectively. Thus, for each campaign (seasonal sampling on an island), the segments of coastlines were sampled on consecutive days. For example, during the stratified sampling season of 2019 on El Hierro island, the Orchilla coastline segment was sampled on October 20th, Bonanza on the 21st, Tacorón on the 22nd, and Bahía de Naos on the 23rd. On board, the samples were recovered, labelled, and preserved in 95% ethanol. In the laboratory, decapod larvae from each sample were sorted and transferred to new preservation liquid (ethanol 95%) for posterior taxonomic identifications.

2.2 Taxonomic identifications

Most of the larvae collected were in megalopa stage; however, occasionally few zoea stage larvae occurred in the catches. As this study is focused on settlement stages, only the megalopa was analyzed. In the laboratory, each megalopa was identified using a stereomicroscope and following the taxonomic key of Ingle (1992) and Marco-Herrero (2015), as well as specific larval morphology descriptions of decapod crustaceans recommended by González-Gordillo et al. (2001). As the knowledge on the morphology of megalopae is limited in subtropical areas such as the Canary Islands, we removed the fifth pereiopod of those unidentified megalopae with distinct phenotype for molecular identification.

2.3 Molecular identification

The identification of the megalopae, and one adult specimen of *Thalamita poissonii*, was based on partial sequences of the 16S rRNA or

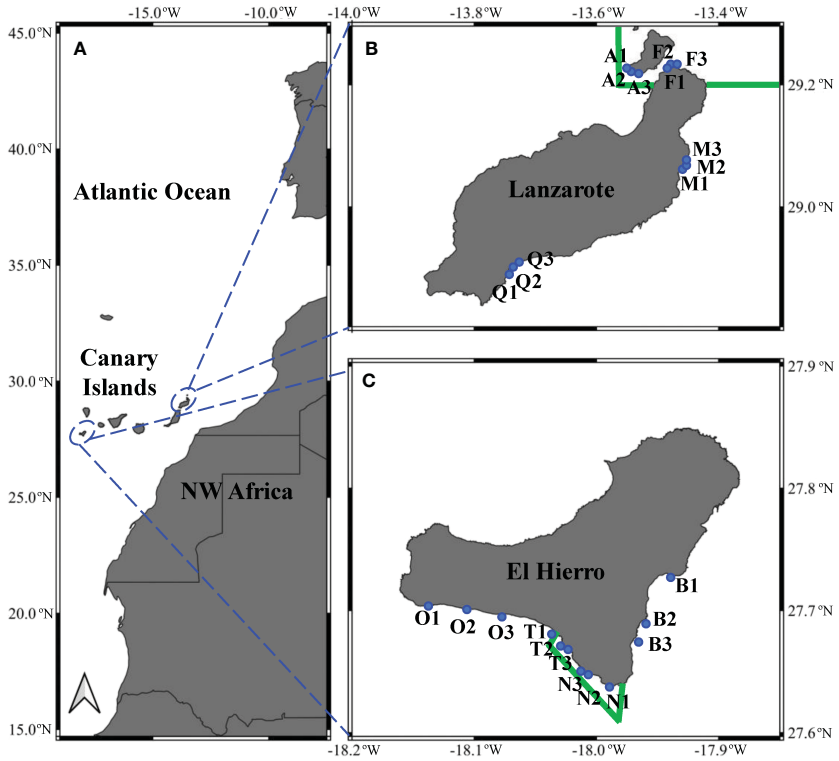

FIGURE 1
Location of the sampling stations in the Canary Islands, NW Africa **(A)**. Green lines delimit the boundaries of the Marine Protected Areas in Lanzarote **(B)** and El Hierro **(C)** islands. Blue dots stand for section of coastline: A = Montaña Amarilla, F = Punta Fariones, M = Mala, P = Playa Quemada, B = Bonanza, N = Bahía de Naos, T = Tacorón, O = Orchilla.

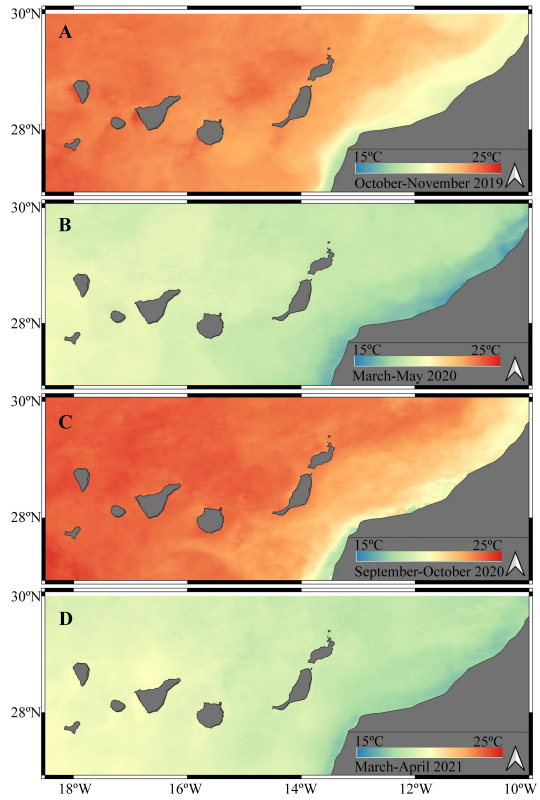

FIGURE 2
Sea surface temperature derived from satellite data. Maps correspond to averaged values of sea surface temperature during each sampling period: October-November 2019 **(A)**, March-May 2020 **(B)**, September-October 2020 **(C)**, March-April 2021 **(D)**.

cytochrome oxidase unit I (COI) mitochondrial genes. Total genomic DNA of the megalopa specimen, and the adult, was extracted from a pereiopod following a modified Chelex 10% protocol by Estoup et al. (1996). The 16S rRNA and COI genes were amplified with polymerase chain reaction (PCR) using the following cycling conditions: 2 min at 95°C, 35 cycles of 20s at 95°C, 20s at 45-48°C, 45s (16S) or 47s (COI) at 72°C, and 5 min at 72°C. The primers 1472 (5'-AGA TAG AAA CCA ACC TGG-3') (Crandall & Fitzpatrick, 1996) and 16L2 (5'-TGC CTG TTT ATC AAA AAC AT-3') (Schubart et al., 2002) were used to amplify a maximum of 545 bp of 16S rRNA, and for the COI gene the primers COH6 (5′-TAD ACT TCD GGR TGD CCA AAR AAY CA-3′) and COL6b (5'-ACA AAT CAT AAA GAT ATY GG-3') (Schubart & Huber, 2006) were used to amplify a maximum of 670 bp.

PCR products were sent to Stab Vida company to be purified and then bidirectionally sequenced. Sequences were edited using the software Chromas version 2.0. With the obtained final DNA sequences were performed a BLAST (Basic Local Alignment Search Tool) on NCBI (National Center for Biotechnology Information) web facility on GenBank sequences database (http://www.ncbi.nlm.nih.gov/genbank/) to get the best matches for identification. The COI sequences were also searched in the official Barcode of Life database (BOLD) (http://v3.boldsystems.org/index.php/IDS_OpenIdEngine). Identifications were considered as positive when retrieved sequences showed similarity values greater than 99%, only differed in 1–3 or 1–7 mutations in 16S or COI, respectively. This is a more conservative limit than other previous works identifying decapod larvae considering > 98% (Brandão et al., 2016). Larval sequences for both genes are deposited in Genbank, and the megalopa and adult specimens DNA vouchers were deposited in "Museos de Tenerife - Naturaleza y Arqueología" (MUNA).

2.4 Data analysis and statistics

Sea surface temperature derived from long-wave (11-12 μm) thermal radiation satellite data were obtained from the Ocean Color web site (https://oceancolor.gsfc.nasa.gov/) using long-wave infrared algorithm and Aqua MODIS information (Kilpatrick et al., 2015). Averaged data were computed for the study period of each sampling season and plotted using the geographic information system QGIS 3.18 (QGIS Development Team, 2022).

Abundance of megalopa were standardized into catch per unit of effort (CPUE), with 'effort' being both number of traps and time fished (megalopae per trap x night) (Félix-Hackradt et al., 2013). This standardization was important in those samplings with trap failures. The Shannon–Wiener diversity index (H′), $H' = \sum_{i=1}^{S} p_i \ln p_i$ (where S is the number of taxa and p_i is the proportion of individuals in taxa i), was based on all identified taxa.

TABLE 1 Sampling information for segment of coastline and study period.

Island	Segment of coastline	Trap code	2019 stratified	2020 mixing	2020 stratified	2021 mixing	MPA
El Hierro	Orchilla	O1, O2, O3	20 Oct.	25 May	18 Oct.	11 Apr.	No
	Bonanza	B1, B2, B3	21 Oct.	27 May	16 Oct.	14 Apr.	No
	Tacorón	T1, T2, T3	22 Oct.	26 May	19 Oct.	12 Apr.	Yes
	Bahía de Naos	N1, N2, N3	23 Oct.	28 May	17 Oct.	13 Apr.	Yes
Lanzarote	Playa Quemada	Q1, Q2, Q3	27 Nov.	12 Mar.	20 Sept.	12 Mar.	No
	Mala	M1, M2, M3	28 Nov.	13 Mar.	19 Sept.	13 Mar.	No
	Punta Fariones	F1, F2, F3	–	17 Mar.	22 Sept.	25 Mar.	Yes
	Montaña Amarilla	A1, A2, A3	–	18 Mar.	23 Sept.	24 Mar.	Yes

MPA stands for Marine Protected Area.

Regarding statistical analysis, 3-way PERMANOVA (Anderson et al., 2008), based on Bray-Curtis distances matrix calculated from log (x+1) transformed CPUE data of each taxon. PERMANOVA tested differences in the CPUE of megalopa assemblages between islands (El Hierro vs Lanzarote), level of protection (inside vs outside the MPA) and sampling season (mixing vs stratified). In this model design, "island", "season", and "protection" were fixed factors, being "protection" nested in "island". P-values were calculated from 999 unrestricted permutations of the data. Multivariate analysis of assemblage structure using multidimensional scaling (MDS) was applied to visualize differences in the structure of the entire community, and the individual contribution of each species to the dissimilarity for each factor (island, season, and protection) was calculated by the SIMPER routine (Clarke et al., 2014). All statistical analyses were carried out using the software PRIMER 7.0.23 + PERMANOVA routine.

3 Results

3.1 Environmental conditions

Satellite imagery pictured the spatio-temporal variability of sea surface temperature (SST) in the Canary Islands region (Figure 2). Upwelling waters were present in the African shelf showing cold SST (16.68-18.03 °C). The limited longitudinal extension of the upwelled waters generated a westward increase of SST in the study region up to 4-5 °C during the stratified season and 3-3.5 °C during the mixing season. Thus, El Hierro exhibited warmer SST values than Lanzarote in both seasons. For example, during the stratified season Lanzarote showed a mean SST of 22.48 ± 0.36 °C, whereas in El Hierro the mean SST was 23.67 ± 0.41 °C (Figures 2A, C). During the mixing season, typical lower SST values were observed in Lanzarote (18.96 ± 0.42 °C) and El Hierro (19.72 ± 0.30 °C) (Figures 2B, D).

3.2 Molecular identification

We identified a subset of megalopae as *A. hastatus* by matching their sequences with those deposited by Mantelatto et al. (2009); Schubart & Reuschel (2009), and Marco-Herrero et al. (2021). Additionally, using sequences published by González et al. (2017), we identified other portunid megalopae as *C. ruber*. Sequences obtained from two adult specimens we deposited in the MUNA allowed us to identify further megalopae as *T. poissonii*. Big-sized grapsid megalopae aligned with sequences of *Grapsus adscensionis* from Schubart (2011). Molecular analysis revealed significant similarity between a group of megalopae and sequences of *Cryptosoma* spp. from GenBank, as well as with sequences of *Dromia erythropus* submitted by Mantelatto et al. (2018). Considering the known distribution of these species and the species documented in the Canary Islands (González, 2016), we assigned our sequences to *C. cristatum* and *D. marmorea*. For comprehensive details on the molecular identifications, please refer to Supplementary Material 1.

3.3 Spatio-temporal patterns of megalopa larvae

In the framework of this study, light traps collected a total of 65,639 crab megalopae belonging to 12 different taxa (Table 2). The maximum abundance value of 8,832 megalopae per trap x night occurred in El Hierro Island within the Marine Protected Area at Tacorón (T3 trap) during the stratified season of 2019. In contrast, significantly lower megalopa catches were observed in Lanzarote, averaging 78.75 megalopae per trap x night, compared to El Hierro, where the average was 1,300 megalopae per trap x night. In terms of seasonality, megalopae were more abundant during the stratified period (averaging 1,375.64 megalopae per trap x night) than during the mixing period (averaging 160.64 megalopae per trap x night). With respect to total abundance, more larvae were collected outside the MPA (averaging 868.81 megalopae per trap x night) than inside (averaging 590.59 megalopae per trap x night). Shannon diversity index was low (ranging from 0.43 to 1.99) due to the limited number of taxa found. Similar diversity values were observed between seasons (mixing: 1.19; stratified: 1.27) and islands (El Hierro: 1.22; Lanzarote: 1.17). However, there was a weak difference in level of protection where the average value of diversity was higher (1.35) inside the MPA than outside (1.13).

Permutational multivariate analysis of variance (PERMANOVA) revealed significant differences in megalopae abundance and species

TABLE 2 Similarity percentage (SIMPER) results for seasonal, protection, and island assemblages, showing the most important species contributing to each group (cut-off for lower contributions 70%).

	Seasonality stratified vs mixing		Protection inside vs outside MPA		Island el Hierro vs Lanzarote	
Taxa	Diss/SD	Contrib%	Diss/SD	Contrib%	Diss/SD	Contrib%
Achelous hastatus	1.2	23.36	1.1	24.06	1.54	27.68
Percnon gibbesi	1.23	18.32	0.77	8.32	1.36	16.31
Pachygrapsus spp.	1.04	14.76	1.08	15.76	1.30	14.93
Cronius ruber	1.17	10.36	1.25	10.28	1.18	8.89
Plagusia depressa	0.77	7.54	1.07	15.85	0.78	7.43

The ratio between the contribution (Contrib%) of each species to the average dissimilarity within the group to the standard deviation (Diss/SD ratio) helps pointing out the key species for each assemblage.

composition for factors "seasonality" (PERMANOVA pseudo-F=27.87; P=0.001), "islands" (PERMANOVA pseudo-F=51.00; P=0.001) and "protection" (PERMANOVA pseudo-F=5.69; P=0.001). The non-metric multidimensional scaling analysis (nMDS), based on species composition and abundance, separated the samples among both seasons and islands (Figures 3A, B). However, when considering the factor "protection", the nMDS did not show a clear separation, despite the significant differences detected in the PERMANOVA analysis (Figure 3C). Moreover, overlaying the total megalopa abundance on the nMDS plots not only aided in visualizing the higher values both during the stratified season (Figure 3D) and in El Hierro island (Figure 3E), but also the weak separation of sample collected inside and outside the MPAs (Figure 3F). Similarly, overlaying the Shannon diversity indexes confirmed the similar values across factors (Figures 3G–I).

Spatial and temporal distributions of five taxa accounted for 70% of the differences observed in both "seasonality" and "level of protection" (Table 2). The SIMPER analysis showed the high contribution of *A. hastatus*, *P. gibessi*, *C. ruber*, *Pachygrapsus* spp. and *P. depressa* to the average dissimilarity between seasons (57.93%) and islands (61.06%) (Table 2). Temporal distribution of *A. hastatus*, *P. gibessi*, *C. ruber* indicated a dominance during the stratified season (Figures 4, 5). Interestingly, megalopae of *A. hastatus*, the most abundant taxa, and *P. gibessi* occurred in both seasons, but exhibited a clear seasonality in El Hierro (Figure 4) that was not so evident in Lanzarote (Figure 5). In the case of *C. ruber*, the phenological seasonality was observed in both islands. However, its megalopae occurred year-round in El Hierro (Figure 4), whereas in Lanzarote they were present only during the stratified period (Figure 5). On the other hand, the higher abundance of *Pachygrapsus* spp., *P. depressa*, and *P. gibessi*, and the lower abundance of *C. ruber* inside the MPA (Figures 6, 7) contributed to differentiate the community assemblages based on the protection level, exhibiting an average dissimilarity of 56.56% (Table 2). Again, this pattern of protection was less consistent in Lanzarote (Figure 7).

4 Discussion

4.1 Methodological considerations

Light traps offer a passive sampling method suitable for shallow coasts and reefs where working with plankton nets can be challenging. Their ability to collect undamaged and even live specimens at a low cost has led to their widespread utilization in the collection of larval stages of marine organisms (McLeod & Costello, 2017). While light traps have predominantly been employed for the collection of fish larvae (e.g. Félix-Hackradt et al., 2013), their effectiveness in capturing invertebrate larvae, including decapod crustaceans, has also been demonstrated (Reyns & Sponaugle, 1999; Jeffs et al., 2003; Miller and Shanks, 2004; Herter & Eckert, 2008; Sigurdsson et al., 2014; Moreno-Borges et al, in press). Previous studies on decapod larvae have involved adaptations of the common box traps, cylindrical traps, quatrefoil traps, and tube traps. However, only the sampling framework analyzed in the present study utilized a net trap like the CARE light trap (see Moreno-Borges et al., in press) for additional methodological information). Interestingly, despite the utilization of different collecting methods, it appears that all light traps exhibited high selectivity for individuals in settlement stage. In terms of selectivity, the light traps also captured various organisms, including fish larvae, hyperbenthic taxa (mysids, amphipods, and isopods), as well as certain planktonic copepods and ostracods. Nevertheless, it is noteworthy that the light traps showed remarkable selectivity towards the megalopa stage of crabs,

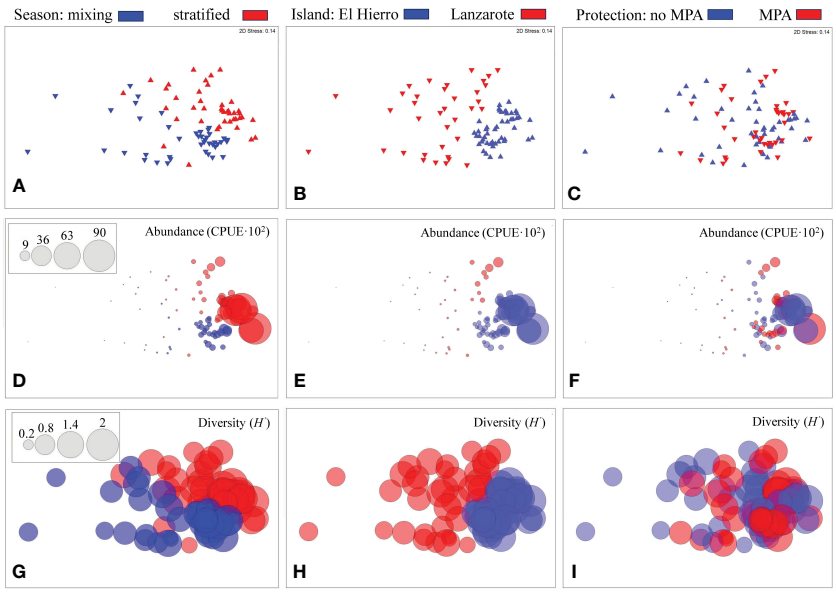

FIGURE 3
Non-metric Multidimensional Scaling (nMDS) plots based on megalopae abundance and composition for each factor: season **(A, D, G)**, islands **(B, E, H)** and protection **(C, F, I)**. Bubble size stand for total abundance, CPUE·10^{-2} **(D, E, F)** or Shannon diversity index, *H'* **(G, H, I)**.

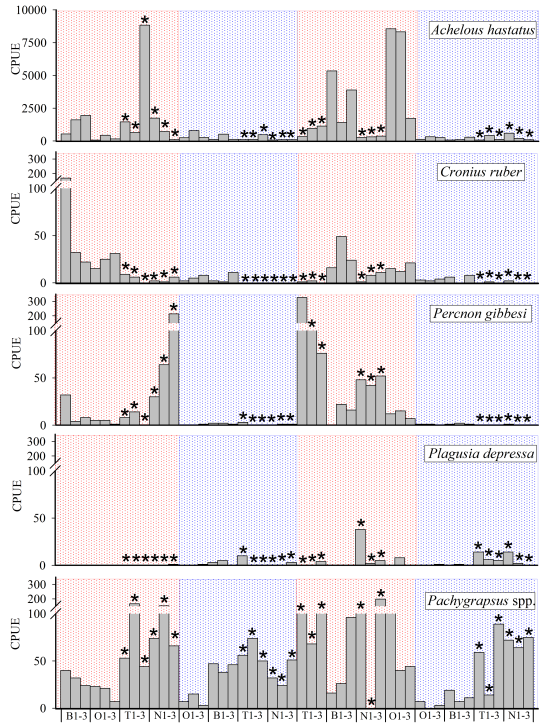

FIGURE 4
Temporal distribution of megalopae abundance (CPUE·10^{-2}) for key species in El Hierro. Asterisks stand for samples collected inside the Marine Protected area (MPA). Red and blue areas stand for mixing and stratified periods, respectively.

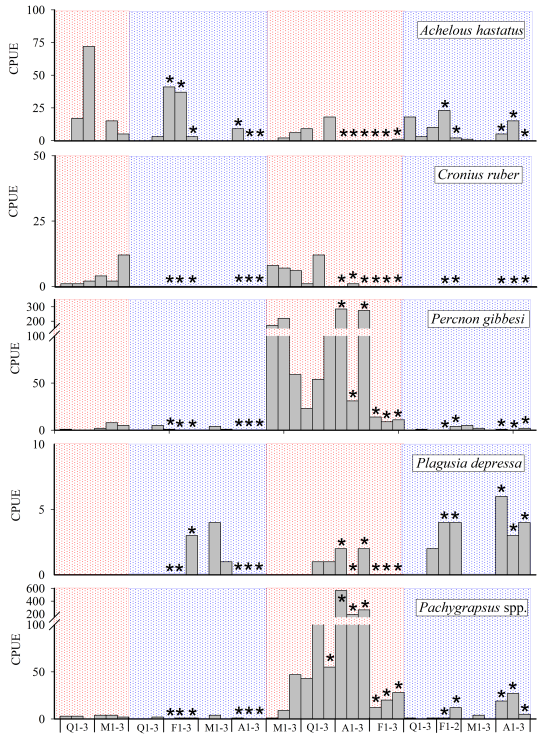

FIGURE 5
Temporal distribution of megalopa abundance (CPUE·10^{-2}) for key species in Lanzarote. Asterisks stand for samples collected inside the Marine Protected area (MPA). Red and blue areas stand for mixing and stratified periods, respectively.

comprising a dominant proportion exceeding 95% of the total yield of decapod larvae. Indeed, when Porter et al. (2008) conducted a comparative analysis of the effectiveness of light traps and plankton tows for sampling brachyuran crab larvae, they observed that traps were more efficient at capturing fast-swimming megalopae, which possessed the ability to evade the nets. This observation is substantiated by the limited presence of megalopae in plankton samples previously examined in the Canary Islands region (Landeira et al., 2013, Landeira et al., 2017; Landeira & Lozano-Soldevilla, 2018). Hence, the concurrent utilization of both plankton nets and light traps appears to be a suitable approach for investigating dispersive and settling processes of zoea and megalopa larval stages. However, the ability of the CARE light trap to capture a broad spectrum of species is limited. Given the presence of 132 crab species within the marine fauna of the Canary Islands (González, 2016) and the identification of approximately 40 species from plankton samples (Landeira et al., 2013, Landeira et al., 2017; Landeira & Lozano-Soldevilla, 2018), the identification of only 12 taxa from light traps appear to be a relatively limited number.

On the contrary, the low number of species may also indicate that light traps are very selective for certain species. More specifically, we collected high numbers of portunid megalopae, with *A. hastatus* as the most abundant species, as well as grapsoid megalopae particularly represented by *Pachygrapsus* spp. Similarly, using quatrefoil traps in Caribbean coral reefs, Reyns and Sponaugle (1999) found in the catches a significant contribution of the families Portunidae and Grapsidae along with Majidae. As light traps are designed to attract (McLeod & Costello, 2017), it is reasonable to infer that the megalopa stage of these two families may exhibit a phototaxis behavior that attracts them towards the trap amidst the darkness. Portunidae is one of the crab families that encompasses a higher number of non-indigenous species worldwide. Their large body size, swimming ability and aggressive behavior, as well as its high fecundity and broad environmental tolerance have facilitated the expansion of several species far from their distribution ranges such as *Callinectes sapidus* in the Mediterranean Sea and Atlantic Ocean (González-Ortegón et al., 2022), *Charybdis japonica* in New Zealand (Fowler and McLay, 2013) or *C. ruber* in the Canary Islands (González et al., 2017). Hence, we suggest employing light traps for the monitoring or early detection of non- indigenous portunid species, that can enable a prompt response for the management and mitigation of the potential invasion. Our study demonstrates that for non- indigenous species lacking taxonomic descriptions of larval morphology, such as *C. ruber*, the combination of light trap sampling and molecular identification can indeed serve as a potent tool.

4.2 Spatial and seasonal patterns

The study was designed to test differences in species composition between distant islands with contrasting oceanographic conditions. The oceanographic gradient from east to west across the archipelago plays a significant role in shaping the distribution of biota (Brito et al.,

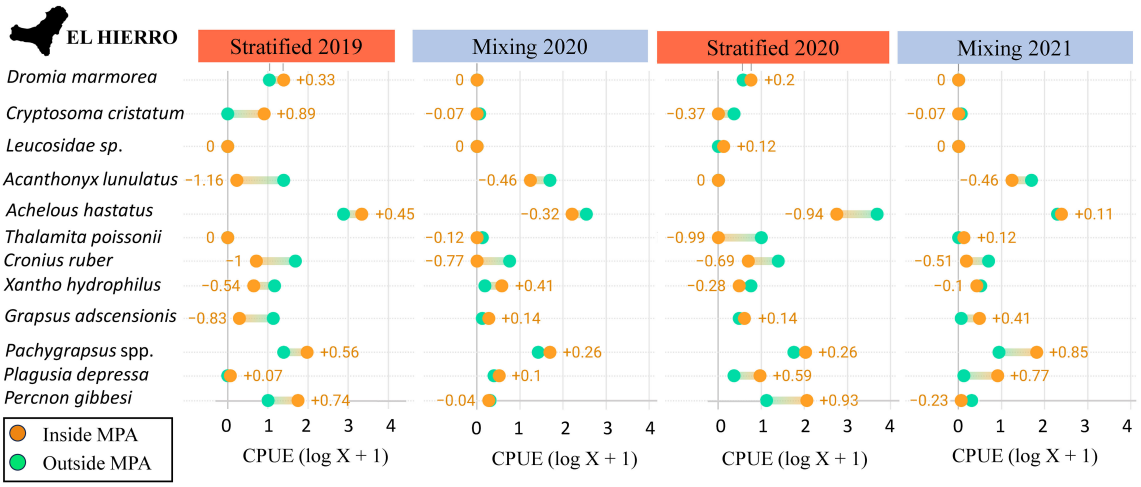

FIGURE 6
Mean abundance values, log (CPU +1), of each taxon within and outside the Marine Protected Area (MPA) for each sampling period in El Hierro. Orange values are obtained subtracting the abundance within the MPA from the abundance outside the MPA.

2001). In the western islands, characterized by warmer waters, there is a greater prevalence of tropical species. Conversely, in the eastern islands with temperate waters, species exhibiting temperate affinities are more commonly found (Tuya et al., 2004; Sangil et al., 2012a). As expected, we observed warmer temperatures in El Hierro than in Lanzarote which was clearly influenced by colder waters from the NW African upwelling (Barton et al., 1998). The relatively low number of species observed in the samples, resulted from the high light trap's selectivity for capturing megalopae of certain species, hindered the ability to characterize the expected east-west diversity gradient. However, differences in megalopa abundance *A. hastatus*, *C. ruber*, *Pachygrapsus* spp., *P. gibbesi*, and *P. depressa* allowed the separation of two distinct assemblages for Lanzarote and El Hierro.

The seasonality of decapod larvae in the plankton is primarily governed by the reproductive phenology of adult populations. In the present study, we found significant differences in megalopae abundance and species composition between stratified and mixing seasons. Data derived from plankton nets in the Canary Islands has indicated that most decapod species exhibit continuous reproduction throughout the year, with peaks in abundance coinciding with periods of water stratification and mixing (Landeira & Lozano-Soldevilla, 2018). Consistent with our findings, colonization experiments conducted in various habitats including, seagrass meadows, sandy patches, and macroalgal-dominated beds on Gran Canaria Island (located centrally in the archipelago) have likewise noted a seasonality in the settlement of postlarval stages of decapods linked to warm and cold periods of the year (García-Sanz et al., 2014; Herrera et al., 2014). In the Atlantic Ocean, this seasonality becomes progressively more pronounced as one moves northward (González-Gordillo & Rodríguez, 2003; Pan

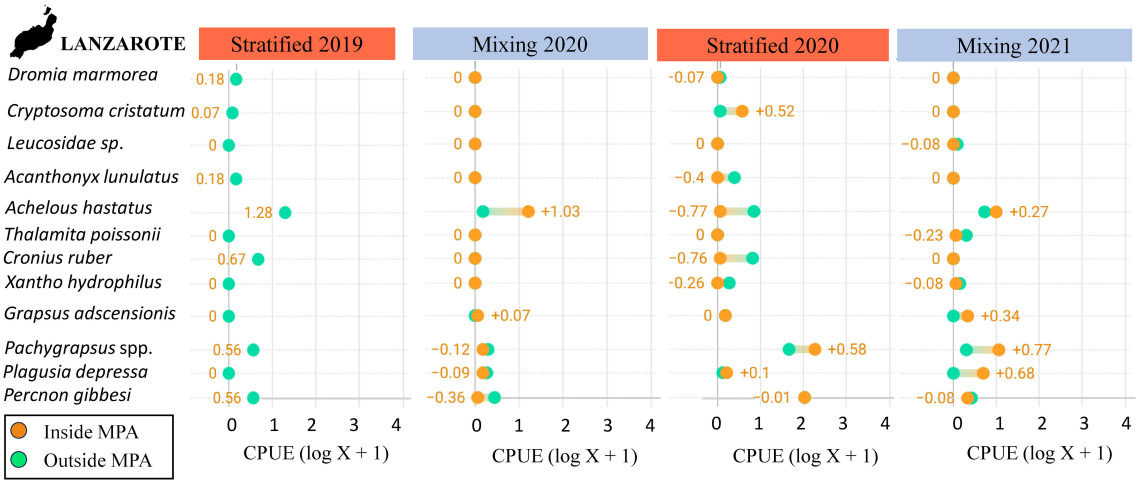

FIGURE 7
Mean abundance values, log (CPU +1), of each taxon within and outside the Marine Protected Area (MPA) for each sampling period in Lanzarote. Orange values are obtained subtracting the abundance within the MPA from the abundance outside the MPA.

et al., 2011; Stübner et al., 2016). In future investigations, it would be interesting to conduct weekly light trap samplings throughout an entire year to better understand the annual cycle of settlement larval stages.

In the present study, seasonal differences were driven by the dominance of *A. hastatus*, *P. gibessi*, and *C. ruber* during the stratified season. Interestingly, the tropical-subtropical species like *P. gibessi* and *C. ruber* were particularly abundant in El Hierro, where higher temperature occurs. Monthly samplings were conducted to assess the status and population structure of these species on Gran Canaria Island. Regarding *P. gibessi*, Guerra-Marrero et al. (2023) identified two primary reproductive seasons (March-April and August-September) based on the presence of ovigerous females. Similarly, for *C. ruber*, females with mature ovaries were observed consistently throughout the year, with a higher abundance noted from July to November, coinciding with the peak of ovigerous females (Triay-Portella et al.)[1]. These reproduction strategies are consistent with our observations of megalopa dynamics. Nevertheless, it is important to delve into the differing temporal distribution of *C. ruber* megalopae for each island. In El Hierro, we observed megalopae in both seasons, with a higher abundance during the stratified season, aligning with the reproduction pattern detailed by Triay-Portella et al[1]. However, in Lanzarote, no megalopae were encountered during the samplings conducted in the mixing season. The differences observed between the islands may suggest that during the colder season (mixing) when reproductive activity is reduced, the colder conditions of Lanzarote (more than 1°C colder than El Hierro) may not facilitate a proper reproduction for this subtropical species. Given that *C. ruber* is considered a non- indigenous species in the study region, its limited reproductive performance during certain times of the year could potentially reduce its expansion in the eastern islands, such as Lanzarote, which are more influenced by the cold waters originating from the NW Africa upwelling. It is well-established that temperature plays a pivotal role in driving spatial and temporal variations in the reproductive biology of crab species, as demonstrated in the case of *Portunus armatus* on the West coast of Australia (Johnston & Yeoh, 2021). However, as there are no documented instances of marine invertebrates displaying spatial phenological variations within the Canary Islands, it is important to approach this pattern with caution until further data become available.

4.3 Effect of marine protected area

The present study was also designed to test differences in megalopa abundance inside and outside the MPAs of "La Restinga-Mar de las Calmas" in El Hierro, and of "Isla de La Graciosa e Islotes del Norte" in Lanzarote. Interestingly, we found that species traditionally harvested from the intertidal zone for human consumption (*P. depressa*) or used as bait for recreational fishing (*Pachygrapsus* spp. and *P. gibessi*) (González et al., 2016) presented higher megalopa abundances inside the MPAs. Artisanal fisheries in the Canary Islands have benefited from more stable yields since the MPAs were established, compared to the overexploitation of most of demersal target fish species (Sanabria-Fernandez et al., 2019). Protection areas from fishing pressure not only has increased the fish biomass within the MPAs but also the densities of harvested intertidal invertebrates, such as limpets (López et al., 2012). Unfortunately, there are no data available to understand the protection effect on crustaceans in the Canary Islands, but we expect similar positive influence since it has been proved to be effective to increase the catches of portunid crabs inside MPAs of Thailand (Jones et al., 2017).

On the other hand, we found lower megalopa densities of the non-indigenous species *C. ruber* in the protected areas. Inside the MPAs various mechanisms can interplay to control the population densities of non-indigenous species within their boundaries. One such mechanism is the potential barrier created by the high indigenous species richness found within MPAs, which may deter the introduction and establishment of alien species (Levine & D'Antonio, 1999). Faunistic and botanic studies have described how the seascape recovers inside the MPAs of the Canary Islands, not only increasing the number of species but also producing a more balanced and better-structured ecosystem (Sangil et al., 2012b; Sanabria-Fernandez et al., 2019). A better-structured ecosystem, which allows more competitive native species, could be preventing the development of large populations of *C. ruber* within the MPA. Additionally, the restoration of top predator populations within MPAs can play a pivotal role in regulating the populations of certain non-indigenous species within these protected areas (Mumby et al., 2011). In this sense, there is already evidence of the top-down role of fish predators controlling the populations of a key herbivore, the sea urchin *Diadema africanum* (Clemente et al., 2009) in the Canary Islands. These authors observed that the presence of higher fish predator densities within MPAs led to an increase in post-settlement and post-recruitment mortality events among *D. africanum*. Therefore, it is plausible that top-down ecological processes, involving fish predation on megalopae, juveniles, and even adult crabs, are influencing the populations of the non-indigenous crab *C. ruber*. It is known that lower megalopa densities may indicate both small adult populations and lower larval survival rate (McLeod & Costello, 2017). Thus, the increased density of fish predators within the MPAs may explain the observed lower megalopa densities there. Consequently, our results might indicate that the invasiveness capability *C. ruber*, is reduced within the MPA. This finding has global relevance due to the scarcity of quantitative data to estimate the effect of protection on the densities of non-indigenous species (Giakoumi & Pey, 2017). In the future, it would be interesting to concurrently assess the size of adult populations alongside larval densities using light traps within and outside the MPAs to empirically test this hypothesis.

Data availability statement

The datasets presented in this study can be found in online repositories. The names of the repository/repositories and accession number(s) can be found in the article/Supplementary Material.

1 Triay-Portella, R., Martín, J. A., and Pajuelo, J. G. Reproductive features of the invasive crab Cronius ruber (Brachyura, Portunidae) on the Canary Islands (central eastern Atlantic). Spain. Reg. Stud. Mar. Sci. (Submitted to).

Ethics statement

The manuscript presents research on animals that do not require ethical approval for their study.

Author contributions

JL: Formal analysis, Visualization, Writing – original draft. EF: Data curation, Formal analysis, Investigation, Writing – review & editing. JC: Formal analysis, Investigation, Writing – original draft. CS: Investigation, Writing – review & editing. SM: Formal analysis, Investigation, Writing – review & editing. AR: Funding acquisition, Investigation, Project administration, Supervision, Writing – review & editing.

Funding

The author(s) declare financial support was received for the research, authorship, and/or publication of this article. This work was funded by the project "Seguimiento de especies y hábitats indicadores de cambio climático a largo plazo en el archipiélago canario", cofunded by Operational Program FEDER Canarias (2014-2010) and Gobierno de Canarias. Effrosyni Fatira was funded from the European Union's Horizon Europe research and innovation programme under the Marie Skłodowska-Curie grant agreement No 101090322 PLEASE. JL was supported by the "Beatriz Galindo" individual grant (BEAGAL 18/00172) from the Spanish Ministry of Science and Innovation. SM-B was funded by the Canarian Agency for Research, Innovation and Information Society of the Ministry of Economy, Industry and Competitiveness and by the European Social Fund (ESF) integrated operational program of the Canary Islands 2014-2020. Adriana Rodríguez was funded by the Viera and Clavijo Senior Excellence Programme of the University of La Laguna, financed by the Canary Islands Agency for Research, Innovation, and the Information Society.

Acknowledgments

We would like to thank the colleagues who took part in the sampling expeditions and/or with the sample processing at the lab: José Carlos Mendoza, David Martorell, Sandra Montañes and Daniel Álvarez Canali. We thank the Spanish Ministries of "Agriculture, Fisheries and Food" and "Ecological Transition and Demographic Challenge", and "Reservas Marinas de España" for processing and granting the necessary permissions for the field work. As well as, the staff directly involved in the management and vigilance of Marine Protected Areas (Zona Especial Canaria – ZEC, and Zonas de Especial Protección para las Aves – ZEPA). During the development of this study our dear friend and colleague Christoph D. Schubart tragically passed away, for this reason we would like to dedicate this work in fond memory of him.

Conflict of interest

The authors declare that the research was conducted in the absence of any commercial or financial relationships that could be construed as a potential conflict of interest.

Publisher's note

Supplementary material

The Supplementary Material for this article can be found online at: https://www.frontiersin.org/articles/10.3389/fmars.2024.1371782/full#supplementary-material

References

Anderson, M. J., Gorley, R. N., and Clarke, K. R. (2008). *PERMANOVA+ for PRIMER: Guide to Software and Statistical Methods* (Plymouth, UK: PRIMER-E).

Anger, K. (2006). Contributions of larval biology to crustacean research: a review. *Invertebr. Reprod. Dev.* 49, 175–205. doi: 10.1080/07924259.2006.9652207

Arístegui, J., Barton, E. D., Álvarez-Salgado, X. A., Santos, A. M. P., Figueiras, F. G., Kifani, S., et al. (2009). Sub-regional ecosystem variability in the Canary Current upwelling. *Prog. Oceanogr.* 83, 33–48. doi: 10.1016/j.pocean.2009.07.031

Arístegui, J., Hernández-León, S., Montero, M. F., and Gómez, M. (2001). The seasonal planktonic cycle in coastal waters of the Canary Islands. *Sci. Mar.* 65, 51–58. doi: 10.3989/scimar.2001.65s151

Barton, E. D., Arístegui, J., Tett, P., Canton, M., García-Braun, J., Hernández-León, S., et al. (1998). The transition zone of the Canary Current upwelling region. *Prog. Oceanogr.* 41, 455–504. doi: 10.1016/S0079-6611(98)00023-8

Bashevkin, S. M., Christy, J. H., and Morgan, S. G. (2020). Adaptive specialization and constraint in morphological defenses of planktonic larvae. *Funct. Ecol.* 34, 217–228. doi: 10.1111/1365-2435.13464

Brandão, M. C., Freire, A. S., and Burton, R. S. (2016). Estimating diversity of crabs (Decapoda: Brachyura) in a no-take marine protected area of the SW Atlantic coast through DNA barcoding of larvae. *Syst. Biodivers.* 14, 288–302. doi: 10.1080/14772000.2016.1140245

Brito, A., Falcón, J. M., Aguilar, N., and Pascual, P. (2001). "Fauna vertebrada marina," in *Naturaleza de las Islas Canarias: Ecología y, Conservación*. Eds. J. M. Fernández-Palacios and J. L. Martín-Esquivel (Turquesa, Santa Cruz de Tenerife), pp 219–pp 229.

Clarke, K. R., Gorley, R. N., Somerfield, P. J., and Warwick, R. M. (2014). *Change in marine communities: an approach to statistical analysis and interpretation. 3rd edition* (Plymouth: PRIMER-E).

Clavel-Henry, M., Solé, J., Bahamon, N., Carretón, M., and Company, J. B. (2021). Larval transport of *Aristeus antennatus* shrimp (Crustacea: Decapoda: Dendrobranchiata: Aristeidae) near the Palamós submarine canyon (NW Mediterranean Sea) linked to the North Balearic Front. *Prog. Oceanogr.* 192, 102515. doi: 10.1016/j.pocean.2021.102515

Clemente, S., Hernández, J. C., and Brito, A. (2009). Evidence of the top–down role of predators in structuring sublittoral rocky-reef communities in a Marine Protected Area and nearby areas of the Canary Islands. *ICES J. Mar. Sci.* 66, 64–71. doi: 10.1093/icesjms/fsn176

Couret, M., Landeira, J. M., Santana del Pino, Á., and Hernández-León, S. (2023a). A 50-year, (1971–2021) mesozooplankton biomass data collection in the Canary Current System: Base line, gaps, trends, and future prospect. *Prog. Oceanogr.* 216, 103073. doi: 10.1016/j.pocean.2023.103073

Couret, M., Landeira, J. M., Tuset, V. M., Sarmiento-Lezcano, A. N., Vélez-Belchí, P., and Hernández-León, S. (2023b). Mesozooplankton size structure in the Canary Current System. *Mar. Environ. Res.* 188, 105976. doi: 10.1016/j.marenvres.2023.105976

Crandall, K. A., and Fitzpatrick, J. F. J. (1996). Crayfish molecular systematics: using a combination of procedures to estimate phylogeny. *Syst. Biol.* 45, 1–26. doi: 10.1093/sysbio/45.1.1

Estoup, A. C. R. L., Largiader, C. R., Perrot, E., and Chourrout, D. (1996). Rapid one-tube DNA extraction for reliable PCR detection of fish polymorphic markers and transgenes. *Mol. Mar. Biol. Biotech.* 5, 295–298.

Félix-Hackradt, F. C., Hackradt, C. W., Treviño-Otón, J., Pérez-Ruzafa, A., and García-Charton, J. A. (2013). Temporal patterns of settlement, recruitment and post-settlement losses in a rocky reef fish assemblage in the South-Western Mediterranean Sea. *Mar. Biol.* 160, 2337–2352. doi: 10.1007/s00227-013-2228-2

Fowler, A. E., and McLay, C. L. (2013). Early stages of a new zealand invasion by charybdis japonica () (Brachyura: Portunidae) from asia: Population demography. *J. Crust. Biol.* 33, 224–234. doi: 10.1163/1937240X-00002127

García-Sanz, S., Navarro, P. G., Landeira, J. M., and Tuya, F. (2014). Colonization patterns of decapods into artificial collectors: seasonality between habitat patches. *J. Crustac. Biol.* 34, 431–441. doi: 10.1163/1937240X-00002242

Giakoumi, S., and Pey, A. (2017). Assessing the effects of marine protected areas on biological invasions: A global review. *Front. Mar. Sci.* 4. doi: 10.3389/fmars.2017.00049

González, J. A. (2016). Brachyuran crabs (Crustacea: Decapoda) from the Canary Islands (eastern Atlantic): checklist, zoogeographic considerations and conservation. *Sci. Mar.* 80, 89–102. doi: 10.3989/scimar.04350.10A

González, J. A. (2018). Checklists of Crustacea Decapoda from the Canary and Cape Verde Islands, with an assessment of Macaronesian and Cape Verde biogeographic marine ecoregions. *Zootaxa* 4413, 401–448. doi: 10.11646/zootaxa.4413.3.1

González, J. A., Triay-Portella, R., Escribano, A., and Cuesta, J. A. (2017). Northernmost record of the pantropical portunid crab *Cronius ruber* in the eastern Atlantic (Canary Islands): natural range extension or human-mediated introduction? *Sci. Mar.* 81, 81–89. doi: 10.3989/scimar.04551.17B

González-Delgado, S., López, C., Brito, A., and Clemente, S. (2018). Marine community effects of two colonial zoanthids in intertidal habitats of the Canary Islands. *Reg. Stud. Mar. Sci.* 23, 23–31. doi: 10.1016/j.rsma.2018.03.006

González-Gordillo, J., Dos Santos, A., and Rodríguez, A. (2001). Checklist and annotated bibliography of decapod crustacean larvae from the Southwestern European coast (Gibraltar Strait area). *Sci. Mar.* 65, 275–305. doi: 10.3989/scimar.2001.65n4

González-Gordillo, J. I., and Rodríguez, A. (2003). Comparative seasonal and spatial distribution of decapod larvae assemblages in three coastal zones off the south-western Iberian Peninsula. *Acta Oecol.* 24, S219–S233. doi: 10.1016/S1146-609X(03)00032-8

González-Ortegón, E., Berger, S., Encarnação, J., Chairi, H., Morais, P., Teodósio, M. A., et al. (2022). Free pass through the Pillars of Hercules? Genetic and historical insights into the recent expansion of the Atlantic blue crab Callinectes sapidus to the West and the East of the Strait of Gibraltar. *Front. Mar. Sci.* 9. doi: 10.3389/fmars.2022.918026

Guerra-Marrero, A., Bonino-Pérez, A., Espino-Ruano, A., Couce-Montero, L., Jiménez-Alvarado, D., and Castro, J. J. (2023). Life history parameters and fishing aspects of the alien nimble spray crab *percnon gibbesi* in a native area of the central-east atlantic. *Animals* 13, 1427. doi: 10.3390/ani13081427

Herrera, A., Landeira, J. M., Tuya, F., Packard, T., Espino, F., and Gómez, M. (2014). Seasonal variability of suprabenthic crustaceans associated with *Cymodocea nodosa* seagrass meadows off Gran Canaria (eastern Atlantic). *Cont. Shelf Res.* 88, 1–10. doi: 10.1016/j.csr.2014.06.014

Herter, H., and Eckert, G. L. (2008). Transport of Dungeness crab *Cancer magister* megalopae into Glacier Bay, Alaska. *Mar. Ecol. Prog. Ser.* 372, 181–194. doi: 10.3354/meps07667

Hjort, J. (1914). Fluctuations in the great fisheries of northern Europe viewed in light of biological research. *Rapp. P-V Réun. Cons. Int. Expl. Mer.* 20, 1–288.

Ingle, R. W. (1992). *Larval Stages of Northeastern Atlantic Crabs* (London: An Illustrated Key. Chapman & Hall). 363 pp.

Jeffs, A., Tolimieri, N., and Montgomery, J. C. (2003). Crabs on cue for the coast: The use of underwater sound for orientation by pelagic crab stages. *Mar. Freshw. Res.* 54, 841–845. doi: 10.1071/MF03007

Johnston, D. J., and Yeoh, D. E. (2021). Temperature drives spatial and temporal variation in the reproductive biology of the blue swimmer crab Portunus armatus A. Milne-Edwards 1861 (Decapoda: Brachyura: Portunidae). *J. Crustac. Biol.* 41, ruab032. doi: 10.1093/jcbiol/ruab032

Jones, E. V., Macintosh, D., Stead, S., and Gray, T. (2017). How effective are MPAs in conserving crab stocks? A comparison of fisheries and conservation objectives in three coastal MPAs in Thailand. *Ocean Coast. Manage.* 149, 186–197. doi: 10.1016/j.ocecoaman.2017.09.012

Kilpatrick, K. A., Podestá, G., Walsh, S., Williams, E., Halliwell, V., Szczodrak, M., et al. (2015). A decade of sea surface temperature from MODIS. *Remote Sens. Environ.* 165, 27–41. doi: 10.1016/j.rse.2015.04.023

Landeira, J. M., Brochier, T., Mason, E., Lozano-Soldevilla, F., Hernández-León, S., and Barton, E. D. (2017). Transport pathways of decapod larvae under intense mesoscale activity in the Canary-African coastal transition zone: implications for population connectivity. *Sci. Mar.* 81, 299–315. doi: 10.3989/scimar.2017.81n3

Landeira, J. M., and Lozano-Soldevilla, F. (2018). Seasonality of planktonic crustacean decapod larvae in the subtropical waters of Gran Canaria Island, NE Atlantic. *Sci. Mar.* 82, 119–134. doi: 10.3989/scimar.04683.08A

Landeira, J. M., Lozano-Soldevilla, F., and Hernández-León, S. (2013). Temporal and alongshore distribution of decapod larvae in the oceanic island of Gran Canaria (NW Africa). *J. Plankton Res.* 35, 309–322. doi: 10.1093/plankt/fbs089

Landeira, J. M., Lozano-soldevilla, F., Hernández-León, S., and Barton, E. D. (2009). Horizontal distribution of invertebrate larvae around the oceanic island of Gran Canaria: the effect of mesoscale variability. *Sci. Mar.* 73, 761–771. doi: 10.3989/scimar.2009.73n4

Landeira, J. M., Lozano-Soldevilla, F., Hernández-León, S., and Barton, E. D. (2010). Spatial variability of planktonic invertebrate larvae in the Canary Islands area. *J. Mar. Biol. Assoc. UK* 90, 1217–1225. doi: 10.1017/S0025315409990750

Landeira, J. M., Lozano-Soldevilla, F., and Barton, E. D. (2012). Mesoscale advection of upogebia pusilla larvae through an upwelling filament in the canaries coastal transition zone (CTZ). *Helgol. Mar. Res.* 66, 537–544. doi: 10.1007/s10152-011-0289-5

Lecaillon, G. (2004). The "C.A.R.E." (collect by artificial reef eco-friendly) system as a method of producing farmed marine animals for the aquarium market: An alternative solution to collection in the wild. *SPC Live Reef Fish Inf. Bull.* 12, 17–20.

Levine, J. M., and D'Antonio, C. M. (1999). Elton revisited: a review of evidence linking diversity and invasibility. *Oikos* 87, 15–26. doi: 10.2307/3546992

Lindley, J. A., Beaugrand, G., Luczak, C., Dewarumez, J.-M., and Kirby, R. R. (2010). Warm-water decapods and the trophic amplification of climate in the North Sea. *Biol. Lett.* 6, 773–776. doi: 10.1098/rsbl.2010.0394

López, C., Poladura, A., Hernández, J. C., Martín, L., Concepción, L., Sangil, C., et al. (2012). Contrasting effects of protection from harvesting in populations of two limpet species in a recently established marine protected area. *Sci. Mar.* 76, 799–807. doi: 10.3989/scimar.0.0n0

López, C., Poladura, A., Hernández, J. C., Martín, L., Concepción, L., Sangil, C., et al. (2012). Contrasting effects of protection from harvesting in populations of two limpet species in a recently established marine protected area. *Sci. Mar.* 74, 799–807. doi: 10.3989/scimar.03601.15

Mantelatto, F. L., Robles, R., Schubart, C. D., and Felder, D. L. (2009). "Molecular phylogeny of the genus Cronius Stimpson 1860, with reassignment of *C. tumidulus* and several American species of Portunus to the genus Achelous de Haan 1833(Brachyura: portunidae)," in *Decapod Crustacean Phylogenetics. Crustac*, vol. 18 . Eds. J. W. Martin, K. A. Crandall and D. L. Felder, 567–579.

Mantelatto, F. L., Terossi, M., Negri, M., Buranelli, R. C., Robles, R., Magalhães, T., et al. (2018). DNA sequence database as a tool to identify decapod crustaceans on the São Paulo coastline. *Mitochondrial DNA A DNA Mapp. Seq. Anal.* 29, 805–815. doi: 10.1080/24701394.2017.1365848

Marco-Herrero, E. (2015). *Aplicación de técnicas morfológicas y moleculares en la identificación de la megalopa de decápodos braquiuros de la Península Ibérica* (Universidad de Valencia). 143 pp.

Marco-Herrero, E., Cuesta, J. A., and González-Gordillo, J. I. (2021). DNA barcoding allows identifcation of undescribed crab megalopas from the open sea. *Sci. Rep.* 11, 1–19. doi: 10.1038/s41598-021-99486-4

Marco-Herrero, E., Drake, P., and Cuesta, J. A. (2018). Larval morphology and DNA barcodes as valuable tools in early detection of marine invaders: a new pea crab found in European waters. *J. Mar. Biol. Assoc.* 98, 1675–1683. doi: 10.1017/S0025315417000996

McLeod, L. E., and Costello, M. J. (2017). Light traps for sampling marine biodiversity. *Helgol. Mar. Res.* 71, 1–8. doi: 10.1186/s10152-017-0483-1

Miller, J. A., and Shanks, A. L. (2004). Ocean-estuary coupling in the Oregon upwelling region: Abundance and transport of juvenile fish and of crab megalopae. *Mar. Ecol. Prog. Ser.* 271, 267–279. doi: 10.3354/meps271267

Moreno-Borges, S., Mendoza, J. C., Martorell, D., Montañes, S., and Rodríguez, A. (2024). Spatio-temporal patterns in the inshore plankton community of the Canary Islands. In: R. Herrera, J. González, O. Ayza and L. Moro (eds). *Global Change in the Macaronesian Region*. Gobierno de Canarias and GESPLAN S.A.U.

Mumby, P. J., Harborne, A. R., and Brumbaugh, D. R. (2011). Grouper as a natural biocontrol of invasive lionfish. *PLoS One* 6, e21510. doi: 10.1371/journal.pone.0021510

Oliphant, A., and Thatje, S. (2021). Variable shrimp in variable environments: reproductive investment within *Palaemon varians*. *Hydrobiologia* 848, 469–484. doi: 10.1007/s10750-020-04455-z

Pan, M., Pierce, G. J., Cunningham, C. O., and Hay, S. J. (2011). Seasonal and interannual variation of decapod larval abundance from two coastal locations in Scotland, UK. *J. Mar. Biol. Assoc. UK* 91, 1443–1451. doi: 10.1017/S0025315411000191

Pires, R. F. T., Peliz, Á., and Pan, M. (2020). "There and back again" – How decapod megalopae find the way home: A modelling exercise for *Pachygrapsus marmoratus*. *Prog. Oceanogr.* 184, 102331. doi: 10.1016/j.pocean.2020.102331

Porter, S. S., Eckert, G. L., Byron, C. J., and Fisher, J. L. (2008). Comparison of light traps and plankton tows for sampling brachyuran crab larvae in an Alaskan fjord. *J. Crust. Biol.* 28, 175–179. doi: 10.1651/06-2818R.1

QGIS Development Team (2022). *QGIS Geographic Information System* (Open Source Geospatial Foundation). Available at: https://www.qgis.org/es/site/.

Reyns, N., and Sponaugle, S. (1999). Patterns and processes of brachyuran crab settlement to Caribbean coral reefs. *Mar. Ecol. Prog. Ser.* 185, 155–170. doi: 10.3354/meps185155

Sanabria-Fernandez, J. A., Alday, J. G., Lazzari, N., Riera, R., and Becerro, M. A. (2019). Marine protected areas are more effective but less reliable in protecting fish biomass than fish diversity. *Mar. pollut. Bull.* 143, 24–32. doi: 10.1016/j.marpolbul.2019.04.015

Sangil, C., Clemente, S., Martín-García, L., and Hernández, J. C. (2012b). No-take areas as an effective tool to restore urchin barrens on subtropical rocky reefs. *Estuar. Coast. Shelf Sci.* 112, 207–215. doi: 10.1016/j.ecss.2012.07.025

Sangil, C., Sansón, M., Afonso-Carrillo, J., Herrera, R., Rodríguez, A., Martín-García, L., et al. (2012a). Changes in subtidal assemblages in a scenario of warming: Proliferations of ephemeral benthic algae in the Canary Islands (eastern Atlantic Ocean). *Mar. Environ. Res.* 77, 120–128. doi: 10.1016/j.marenvres.2012.03.004

Sangrà, P., Auladell, M., Marrero-Díaz, A., Pelegrí, J. L., Fraile-Nuez, E., Rodríguez-Santana, A., et al. (2007). On the nature of oceanic eddies shed by the Island of Gran Canaria. *Deep-Sea Res. I* 54, 687–709. doi: 10.1016/j.dsr.2007.02.004

Schmoker, C., Arístegui, J., and Hernández-León, S. (2012). Planktonic biomass variability during a late winter bloom in the subtropical waters off the Canary Islands. *J. Mar. Syst.* 95, 24–31. doi: 10.1016/j.jmarsys.2012.01.008

Schubart, C. D. (2011). Reconstruction of phylogenetic relationship within Grapsidae (Crustacea: Brachyura) and comparison of trans-isthmian versus amphi-atlantic gene flow based on mtDNA. *Zool. Anz.* 250, 472–478. doi: 10.1016/j.jcz.2011.06.003

Schubart, C. D., Cuesta, J. A., and Felder, D. L. (2002). Glyptograpsidae, a new brachyuran family from Central America: larval and adult morphology, and a molecular phylogeny of the Grapsoidea. *J. Crust. Biol.* 22, 28–44. doi: 10.1163/20021975-99990206

Schubart, C. D., and Huber, M. G. J. (2006). Genetic comparisons of German populations of the stone crayfish, *Austropotamobius torrentium* (Crustacea: Astacidae). *Bull. Fr. pêche piscic.* 380–381, 1019–1028. doi: 10.1051/kmae:2006008

Schubart, C. D., and Reuschel, S. (2009). Proposal for a new classification of Portunoidea and Cancroidea (Brachyura: Heterotremata) based on two independent molecular phylogenies. *Crustacean issues: decapod crustacean Phylogenet.* 18, 533–549.

Sigurdsson, G. M., Morse, B., and Rochette, R. (2014). Light traps as a tool to sample pelagic larvae of American lobster (Homarus americanus). *J. Crustac. Biol.* 34, 182–188. doi: 10.1163/1937240X-00002219

Stübner, E. I., Søreide, J. E., Reigstad, M., Marquardt, M., and Blachowiak-Samolyk, K. (2016). Year-round meroplankton dynamics in high-Arctic Svalbard. *J. Plankton Res.* 38, 522–536. doi: 10.1093/plankt/fbv124

Torres, A. P., Dos Santos, A., Cuesta, J. A., Carbonell, A., Massutí, E., Alemany, F., et al. (2012). First record of *Palaemon macrodactylus* Rathbun 1902 (Decapoda, Palaemonidae) in the Western Mediterranean. *Mediterr. Mar. Sci.* 13, 278–282. doi: 10.1163/1568540041181466

Tuya, F., Boyra, A., Sánchez-Jerez, P., Barbera, C., and Haroun, R. (2004). Relationships between rocky-reef fish assemblages, the sea urchin Diadema antillarum and macroalgae throughout the Canarian Archipelago. *Mar. Ecol. Progr. Ser.* 278, 157–169. doi: 10.3354/meps278157

Whomersley, P., van der Molen, J., Holt, D., Trundle, C., Clark, S., and Fletcher, D. (2018). Modeling the dispersal of spiny lobster (*Palinurus elephas*) larvae: implications for future fisheries management and conservation measures. *Front. Mar. Sci.* 5. doi: 10.3389/fmars.2018.00058

frontiers | Frontiers in Marine Science

TYPE Brief Research Report
PUBLISHED 28 May 2024
DOI 10.3389/fmars.2024.1406753

OPEN ACCESS

EDITED BY
Kareen E. Schnabel,
National Institute of Water and Atmospheric Research (NIWA), New Zealand

REVIEWED BY
Jose Maria Landeira,
Instituto de Oceanografía y Cambio Global (IOCAG), Spain
Raül Triay-Portella,
University of Las Palmas de Gran Canaria, Spain

*CORRESPONDENCE
Ruma Chatterji
chattera@mail.uc.edu
John E. Layne
john.layne@uc.edu

RECEIVED 25 March 2024
ACCEPTED 16 May 2024
PUBLISHED 28 May 2024

CITATION
Chatterji R and Layne JE (2024) Spatiotemporal structure of foraging and path integration errors by fiddler crabs, *Leptuca pugilator*. *Front. Mar. Sci.* 11:1406753. doi: 10.3389/fmars.2024.1406753

Spatiotemporal structure of foraging and path integration errors by fiddler crabs, *Leptuca pugilator*

Ruma Chatterji* and John E. Layne*

Department of Biological Sciences, University of Cincinnati, Cincinnati, OH, United States

Path integration is the navigational process by which animals construct a memory of a previous location by continuously measuring and summing their movements to form a single home vector pointing to the starting location. It is intrinsically error prone, subject to random errors and, potentially, to systematic errors in either measurement or the summing algorithm. Both types of errors lead to an incorrect vector memory and thus to an error in homing. Because the errors are incurred when animals move, they are theoretically predictable from the movements. We analyzed the behavior of fiddler crabs (*Leptuca pugilator*) as they performed foraging excursions followed by homing with varying degrees of error. From video recordings we measured body orientations and locations and computed these spatiotemporal path characteristics: duration, distance, turns, bearing and arc sector. These were analyzed for their effect on, separately, the magnitude, and the direction, of crabs' homing error. The magnitude of the homing error was predicted by arc sector, Δbearing and path length, and several interactions. The direction of the homing error was predicted by interactions including arc sector x Δbearing, arc sector x turns, and Δbearing x turns. Covariance among these factors results in a path that traces a large arc while maintaining body orientation toward the burrow direction and leads to an error with the same clockwise/counterclockwise sign as the arc and the body turns. These results place *L. pugilator*'s path integration mechanism among others with known systematic errors.

KEYWORDS

navigation, path integration, fiddler crab, homing errors, home vector, systematic errors

Introduction

Spatial navigation is the integration of sensory information to orient and move from one place to another (Halliday and Slater, 1983; Schone, 1984; Papi, 1992). Many animals across a wide range of taxa use a spatial navigation strategy called path integration (Mittelstaedt and Mittelstaedt, 1980; Etienne and Jeffery, 2004). First postulated by Charles Darwin, the idea was that, like sailors' dead reckoning, animals could also use distance and

direction measurements to locate home from any point on their journey (Darwin, 1873). This was later formally defined by Mittelstaedt and Mittelstaedt (1980) as path integration whereby animals construct a memory of a previously visited location by measuring body rotations and translations and storing this information in memory (Mittelstaedt and Mittelstaedt, 1980). Each new movement is added to the existing vector to create a single, continuously updated memory-stored vector, called the home vector. This allows the animal a straight return home after a sinuous trip. It is a highly useful navigation mechanism as animals can explore new terrain, not requiring previous knowledge of the landscape and, in theory, travel distances without becoming lost. Path integration appears to be universal among animals that have a spatially restricted home or central reference point, including insects (von Frisch, 1967; Wehner and Wehner, 1986; Beugnon and Campan, 1989), arachnids (Mittelstaedt, 1985), crustaceans (Altevogt and Hagen, 1964; Hoffmann, 1984; Zeil, 1998; Layne et al., 2003a, 2003b; Cheng, 2012), birds (Mittelstaedt and Mittelstaedt, 1982; von Saint Paul, 1982; Wiltschko and Wiltschko, 1982), and mammals [(Mittelstaedt and Mittelstaedt, 1980); reviewed in (Etienne and Jeffery, 2004)], including humans (Loomis et al., 1993).

While obviously useful, path integration is also inherently error prone. Errors can arise in the accuracy with which directions and distances are measured, and in the precision of the algorithm for adding new vectors to the current home vector (Etienne et al., 2004). There inevitably will be random estimation errors, but also potentially systematic errors (Benhamou et al., 1990). Because both types of errors are incurred when animals move, they are theoretically predictable from those movements. In this study, we examined the homing errors made by a well-known path integrator, the Atlantic Sand Fiddler Crab, *Leptuca pugilator* (Bosc, 1802). These are central-place foragers that, at low tide, leave their burrows in the sand to go on short-range excursions to perform activities such as foraging and courtship (Crane, 1975; Zeil and Layne, 2002). They appear to do this using exclusively idiothetic (self-motion) cues (Layne et al., 2003b). The shapes of the crabs' paths during these excursions range from straight out-and-back to arcs subtending over 180° relative to the burrow. A unique aspect of these excursions is that the crabs tend to align their transverse body axis approximately with their burrow direction throughout, even if an object comes between them (Land and Layne, 1995; Zeil, 1998; Layne et al., 2003a). Though the body thus indicates a general notion of the home direction, it is often out of alignment to a significant degree. Crabs still accurately return home, so the home vector cannot be strictly identical to the body axis. Instead, the crabs know the amount by which their body is out of alignment, and monitor this angle constantly, and it is that which monitors this angle that forms the crabs' directional reference. It has been proposed that this directional reference is provided by the optokinetic system, and that the eyes better indicate the home vector direction than does the body axis (Chatterji and Layne, 2023). According to this theory, if the eyes are well stabilized the crab will maintain a more accurate home vector than if they are not, i.e., if the eyes "drift" then the home vector will also drift. Fiddler crabs have a robust optokinetic system that stabilizes the eyes against body rotations (Nalbach and Nalbach, 1987; Layne et al., 1997; Land, 2019), and movements that tax the optokinetic system are more likely to produce drift and thus errors in homing. A major portion of these errors may not be random but, rather, directionally biased according to the demands placed on the optokinetic system by the shape of the foraging path.

To test this idea that the structure of foraging paths can predict the type of errors they produce, we analyzed the spatiotemporal structure of fiddler crabs' foraging excursions. Specifically, we investigated the following path characteristics: length, duration, arc sector, change in crabs' bearing relative to the burrow, and body turns. We found that, not only can the presence and magnitude of homing errors be predicted, but the shape of the paths can predict the direction in which these errors occur.

Materials and methods

Experiments were conducted on the fiddler crab *Leptuca pugilator* at the University of Cincinnati, from fall of 2019 through spring of 2023 using animals imported from Beaufort, NC or purchased from livebrineshrimp.com (Oak Hill, FL, USA).

Laboratory setup and experimental design

The main tank was a 1.5-meter diameter stainless steel tank filled to ~25 cm with sand from North Carolina sandflats, a natural habitat of *L. pugilator*. A pseudo-tidal rhythm of brackish water created with Instant Ocean salt (salinity of 25 ppt as measured by a refractometer) was pumped in and out of the arena every ~6.2 hours, and the lab temperature was maintained at 26°C. To simulate circadian rhythms, a 12:12 hour day/night ratio was implemented. Fidder crabs were fed once every other day with crushed fish flakes (Tetra Cichlid Diet).

To track foraging excursions the left and right fronto-lateral tips of the carapace were marked with white reflective paint. Two to six painted animals were placed into the experimental arena, of which only one or two actively foraged at a time, while the others were underground. The arena consisted of a four-sided box (60 cm × 40 cm × 10 cm) constructed on top of the sand in the main tank, the walls of which were made of Sintra®. Vertical black and white stripes alternating with a spatial period of ~10 cm created visual contrast in the surround. Fiddler crabs were acclimated to the experimental arena for several hours, and acclimation was considered adequate when crabs exhibited natural behaviors such as making their own burrows, participating in courtship and burrow defense, and embarking on foraging excursions. Acclimated crabs making foraging excursions at pseudo low tide were continuously recorded with a Sony HDR-HC1 camcorder during both day and night (infrared nighttime illumination was achieved using the "night-shot" mode in the camera setting). Both sexes were used indiscriminately, with the exception of gravid females, and only adult fiddler crabs (with a minimum size of 1 cm carapace width) were used in this study.

Data analysis

Foraging excursions (n=70) were digitized using custom MATLAB code (Layne, 2023). Each excursion was clicked by hand at 10-frame intervals (three times per second). On every 10th frame the painted left and right fronto-lateral points of the carapace were clicked and the x-y data thus acquired were used to compute the path characteristics used to model homing error.

The section of the path within two body lengths of the burrow was trimmed to avoid computing spuriously large angles, and because crabs are often able to see the burrow entrance from that distance making path integration superfluous. The path characteristics used to model homing error were computed using the portion of the path between this (trimmed) departure from the burrow and the point at which the crabs clearly began homing. This homing point was identified by the cessation of feeding and a more-or-less straight journey of approximately the correct distance to the burrow and ending either at the burrow or in an abrupt, large-angle change in direction, the beginning of the search for the burrow entrance.

In order to compare spatial characteristics between natural paths all of them were resampled to a uniform step length. This was done by computing the center of the crab's carapace as the midpoint between the two clicked lateral points, and computing the cumulative distance traveled as the cumulative sum of the distances between successive center points. Plotting the body center x- and y-coordinates (ordinate) against cumulative distance traveled (abscissa), the latter of which increases monotonically, the body center x- and y-coordinates were resampled at regular distance intervals (0.05 body width) by linear interpolation. The length of the path was then recalculated from the new x-y coordinates, and this was always shorter than the original length due to the smoothing of digitizing noise. The resampling process was repeated until a new, re-calculated path length decreased less than 0.5 body width compared to path length from the previous resampling iteration.

Foraging paths were normalized to the clockwise direction. Because crabs venture away from their burrow by moving laterally, they face either clockwise or counterclockwise on a radius connecting them to their burrow entrance. Those facing counterclockwise had their paths flipped around the y-axis by multiplying their x-coordinates by -1 (with the burrow at x = 0, y = 0).

The body orientation of the crabs was computed using the original, non-resampled data, from the slope of the line connecting the two carapace points. It is an angle relative to a coordinate system established by the video frame (see Figure 1 inset). Body orientation was then subject to the same resampling procedure as body location (above). The path characteristic *Turns* is this vector of values differentiated (clockwise negative, counterclockwise positive) and summed.

The bearing of the crabs was computed using the resampled body center points, from the slope of the line connecting the body center with the burrow (see Figure 1 inset); like body orientation it is an angle in frame-based coordinates. The path characteristic Δ*Bearing* is this vector of values differentiated and summed, as with body *Turns*.

The path characteristic *Arc sector* is the angle subtending the counterclockwise-most to the clockwise-most bearing of the crabs' path, and is assigned a direction (clockwise negative, counterclockwise positive) according to which of these occurs earlier in the foraging excursion (see Figure 1).

We conducted a stepwise multiple linear regression analysis with interactions on the relationship between homing errors and the magnitudes and directions of path characteristics. To determine the overall significance of the multiple linear regression, an ANOVA test was conducted using a significance alpha value of 0.05. Data analysis was conducted using the Data Analysis ToolPak in Excel (Version 2402).

Results

We recorded 70 foraging excursions that ended with homing error magnitudes from 0° to ~55° (Figures 1, 2). From these we

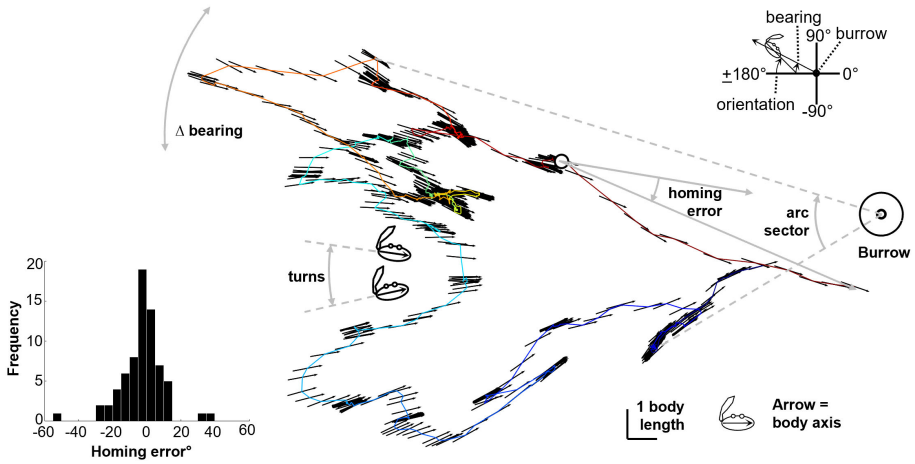

FIGURE 1
Example path illustrating the transverse body axis of the crab with the arrow pointing toward the 'homeward' side and defining the angular path characteristics. Top right inset: definition of "bearing" and "body orientation" angles. Bottom left inset: a histogram of the homing errors from the 70 foraging excursions. See Supplementary Material for video.

computed the following spatiotemporal characteristics: arc sector, Δbearing, turns, path length and path time. We created a multiple regression model of the relationship between the absolute magnitude of these characteristics and the absolute magnitude of the crabs' homing errors. This model showed that arc sector ($p<0.0001$), Δbearing ($p<0.0001$), and path length ($p=0.0002$) were all significant predictors of homing error magnitude. In addition, interactions between several characteristics had significant predictive effect: arc sector x Δbearing ($p=0.005$), arc sector x path time ($p=0.020$), Δbearing x turns ($p<0.0001$), Δbearing x path time ($p=0.044$), turns x path length ($p<0.0001$) (Figure 3A and Table 1).

We created a second multiple regression model to determine which (signed) spatiotemporal characteristics predicted the magnitude *and direction* of the crabs' homing error. For this, the homing error and those characteristics that are angular in nature all had a clockwise = negative, counterclockwise = positive convention. We found evidence of a systematic error, in that interactions between several characteristics had significant predictive effect: arc sector x Δbearing ($p=0.002$), arc sector x turns ($p=0.013$), Δbearing x turns ($p=0.049$), Δbearing x path length ($p=0.030$), and turns x time ($p<0.0001$) (Figure 3B and Table 1).

Discussion

In path integration animals measure their translations and rotations and continuously sum these to form a single memory-stored home vector (Mittelstaedt and Mittelstaedt, 1980). As with any biological mechanism path integration is not perfect, and is inherently error prone, especially if the sensory information used for the measurements is idiothetic (Benhamou et al., 1990), as is the case for the study species, *Leptuca pugilator* (Layne et al., 2003b). These errors can be random which is demonstrated by an arbitrary scatter in homing errors (Benhamou et al., 1990; Maurer and Séguinot, 1995; Seguinot et al., 1998). The errors can also be systematic in nature and can accrue in a directional pattern. Such errors can arise where there is a consistent under or overestimation of translation or rotations and are demonstrated by consistent homing error directions (Sommer and Wehner, 2004).

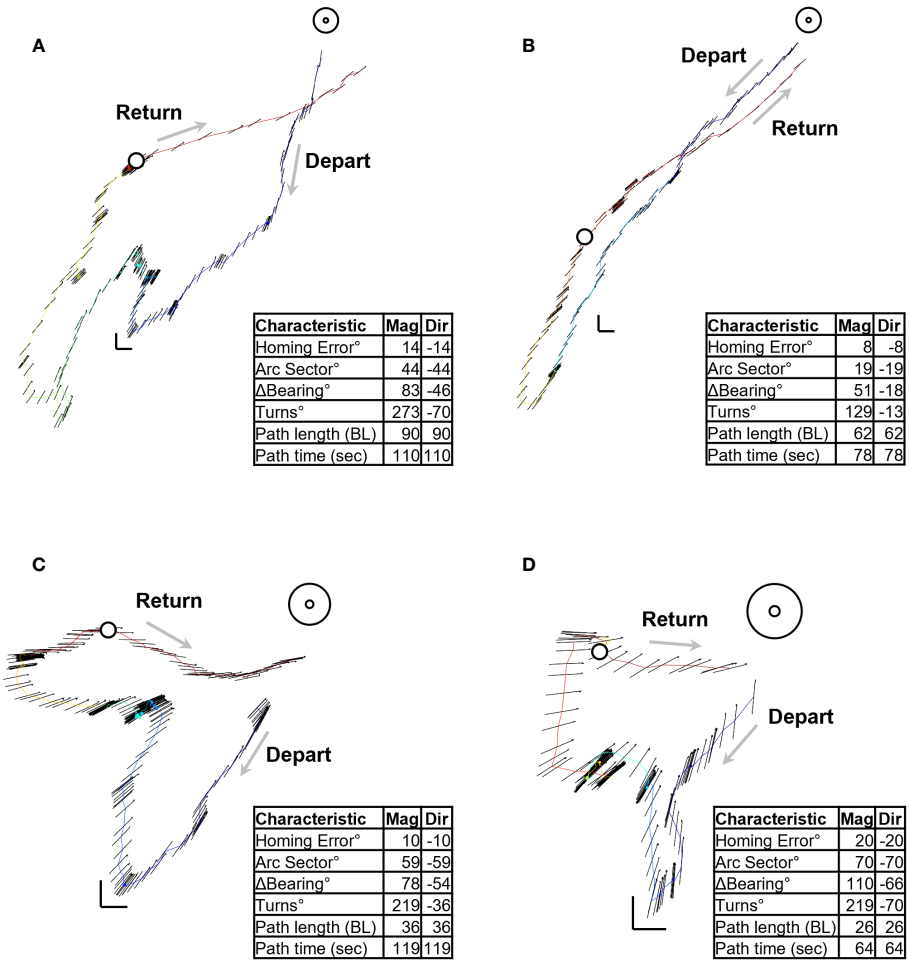

Characteristic	Mag	Dir
Homing Error°	14	-14
Arc Sector°	44	-44
ΔBearing°	83	-46
Turns°	273	-70
Path length (BL)	90	90
Path time (sec)	110	110

Characteristic	Mag	Dir
Homing Error°	8	-8
Arc Sector°	19	-19
ΔBearing°	51	-18
Turns°	129	-13
Path length (BL)	62	62
Path time (sec)	78	78

Characteristic	Mag	Dir
Homing Error°	10	-10
Arc Sector°	59	-59
ΔBearing°	78	-54
Turns°	219	-36
Path length (BL)	36	36
Path time (sec)	119	119

Characteristic	Mag	Dir
Homing Error°	20	-20
Arc Sector°	70	-70
ΔBearing°	110	-66
Turns°	219	-70
Path length (BL)	26	26
Path time (sec)	64	64

FIGURE 2
Four examples of digitized foraging excursions. Table in each panel **(A–D)** lists the magnitude and direction of the spatiotemporal characteristics. Open circle on each path indicates the beginning of the homeward journey. Color gradient indicates the direction of progress along the path, beginning with blue and ending in red.

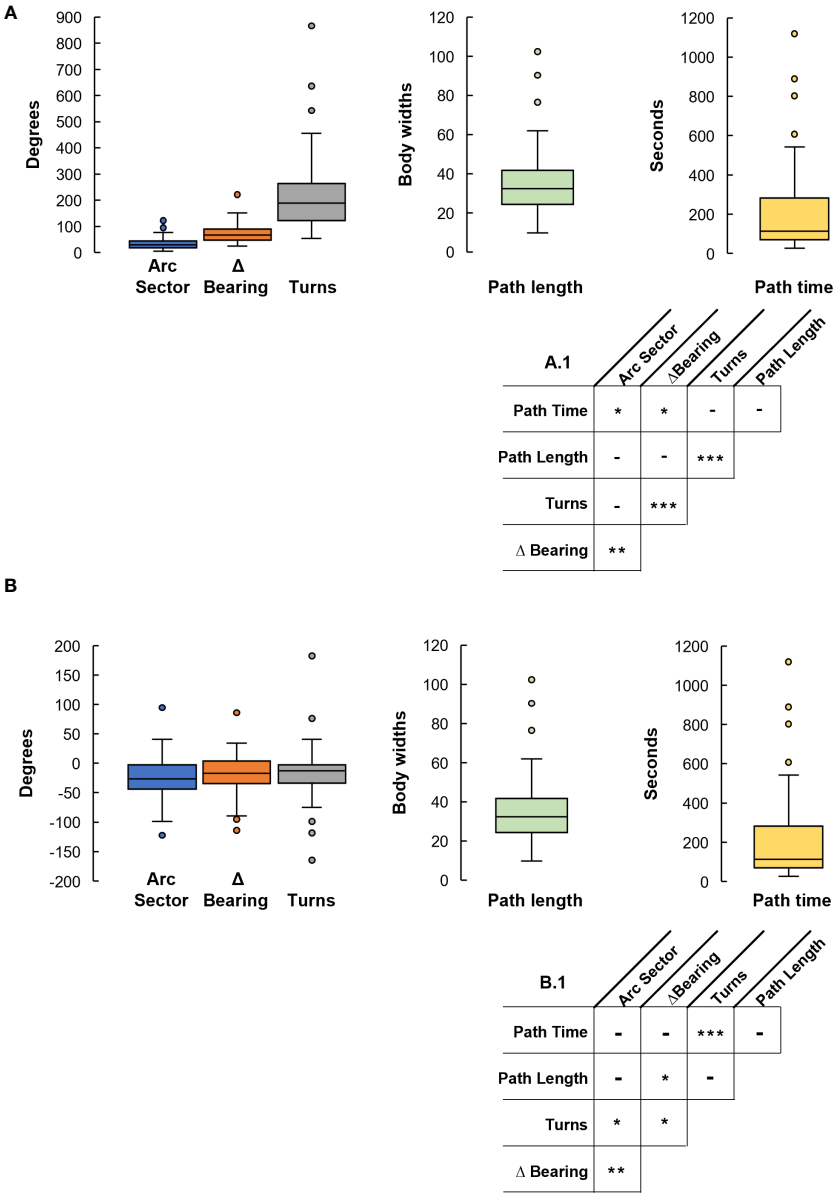

FIGURE 3
Results of the multiple regression analysis. **(A)** Box plots illustrating the magnitude of each spatiotemporal characteristic (n=70). **(A.1)** Interactions between the spatiotemporal magnitude characteristics. **(B)** Box plots of the signed spatiotemporal characteristics (n=70). **(B.1)** Interactions of the direction of the spatiotemporal characteristics. [* $p<0.05$; ** $p<0.01$; *** $p<0.001$].

In this study, we analyzed the natural foraging excursions of *L. pugilator* to determine the degree to which homing errors are random or systematic. Using the body locations and orientations of the crab, we analyzed a variety of path characteristics: arc sector, path length and duration, body turns and changes in the bearing of the animal relative to the burrow. These characteristics and associated body movements comprise the size and shape of the paths and they are causative of the errors that are produced. As such, the homing errors incurred can be predicted by the structure of the path.

We found evidence that homing errors incurred by *L. pugilator* during path integration are both random and systematic in nature. We first analyzed the relationship between the absolute magnitude of the above-mentioned path characteristics and the absolute magnitude of homing errors (which ranged from 0° to ~55°). Homing errors analyzed this way will include those arising from both random and systematic measurement errors. The results show a strong relationship between the magnitudes of the error and several path characteristics. For example, the longer the path and the larger the arc sector, the larger the homing error incurred. To determine what portion of these errors were specifically systematic we ran a second test, maintaining the signed direction of the path characteristics and homing errors, and this revealed several positive correlations. For example, there was a significant relationship between homing error and the interaction between arc sector and body turns. Thus, if the path consisted of a large, circumferential arc in the clockwise (negative, by our convention) direction, the

TABLE 1 Results of two multiple linear regression models (magnitude and direction): path characteristics as predictors of homing error.

	MAGNITUDE		DIRECTION	
	df	*Significance F*	*df*	*Significance F*
Regression	10	8E-08	10	2E-07
Residual	59		59	
Total	69		69	
	Coefficients	*P-value*	*Coefficients*	*P-value*
Intercept	-4.066	0.355	0.543	0.893
Arc Sector (deg)	0.694	0.000	0.146	0.062
ΔBearing(deg)	-0.417	0.000	-0.196	0.206
Turns (deg)	0.027	0.402	-0.129	0.274
Path length (body widths)	0.504	0.000	0.037	0.749
Path time (seconds)	-0.014	0.370	-0.003	0.608
Arc Sector x ΔBearing	-0.004	0.005	-0.005	0.002
Arc Sector x Path Time	-0.001	0.020	–	–
ΔBearing x Turns	0.001	0.000	-0.005	0.049
ΔBearing x Path Time	0.001	0.044	–	–
Turns x Path Length	-0.002	0.000	–	–
Arc Sector x Turns	–	–	0.008	0.013
ΔBearing x Path Length	–	–	0.006	0.030
Turns x Path time	–	–	0.001	0.000

homing error direction was also negative. Such errors generated in a direction-dependent way persist if clockwise and counterclockwise turns are not balanced (Müller and Wehner, 1988; Seguinot et al., 1993), as they are not when forming an arc.

This trend has been observed in other animals, such as in desert ants, where systematic errors generated during the outbound path resulted in a homing error that reflected the cumulative sum of the turn angles (Müller and Wehner, 1988). Systematic homing errors have also been observed from as early as 1957 in honeybees (Bisetzky, 1957) and are present in a wide range of taxa, from hamsters (Seguinot et al., 1993), spiders (Goerner, 1958), dogs and humans [(Seguinot et al., 1998); reviewed in (Etienne and Jeffery, 2004)]. The errors indicated in all these cases are strikingly similar in that they are all "inward", that is, they have the same sign as the cumulative turns in the path. This consistency throughout such a wide variety of taxa suggests that the algorithm for path integration has evolved in a similar manner among different groups (Etienne and Jeffery, 2004). Our results place *L. pugilator* among the disparate taxa exhibiting this type of systematic error, though very few of these have been examined for path-related sources of error. One exception is the desert ant (*Cataglyphis bicolor*), in which it has been demonstrated that cumulative turns and longer distances during foraging excursions predict error directions and wider search patterns, respectively, when returning home (Wehner and Wehner, 1986; Müller and Wehner, 1988; Merkle et al., 2006). Similarly, in humans, increasing distance (Stangl et al., 2020) and unbalanced turns account for systematic biases (Qi and Mou, 2023).

The systematic errors and their apparent path-related causes shown here are consistent with our theory of how this fiddler crab retains the direction of its home vector. While *L. pugilator* moves circumferentially around the burrow, the direction of home relative to its body orientation can be read out from, and is possibly maintained by, the neural-behavioral mechanism controlling eye stability, the optokinetic system (Chatterji and Layne, 2023). As this system rotates the eyes to counter body rotations, the horizontal eye-body angle becomes the basis of the crabs' directional reference for the home vector. If the optokinetic system functions efficiently, the only eye movements are saccadic updates of their orientation as the crab moves around an arc, and these are accounted for by the path integrator. However, if the eyes "drift" then the directional reference will also drift, thereby leading to an error in homing. The crabs' tendency to align their body with the burrow direction as they form an arc necessitates body rotations in one direction. This behavior places demands on the optokinetic system in a directionally biased way, and this can lead to directionally biased drift. One might even speculate that maintaining the eye-burrow relationship is the reason the crabs align with the burrow in the first place. Overall, our research shows that much of the error that *L. pugilator* incurs during path integration is systematic in nature and is consistent with the idea that their optokinetic system function ultimately determines the animals' homing success.

Data availability statement

The original contributions presented in the study are included in the article/Supplementary Material. Further inquiries can be directed to the corresponding authors.

Ethics statement

The manuscript presents research on animals that do not require ethical approval for their study.

Author contributions

RC: Conceptualization, Data curation, Formal analysis, Funding acquisition, Investigation, Methodology, Validation, Visualization, Writing – original draft, Writing – review & editing. JL: Conceptualization, Data curation, Formal analysis, Funding acquisition, Investigation, Methodology, Project administration, Resources, Software, Supervision, Validation, Visualization, Writing – original draft, Writing – review & editing.

Funding

The author(s) declare financial support was received for the research, authorship, and/or publication of this article. This research was supported by the University of Cincinnati-Wieman-Wendell-Benedict Research Award to RC.

Acknowledgments

We would like to thank Mildreth Diaz Perez, Prashanth Prabhakar, Joy Oakes, and Tyonna Mitchell for their assistance with data collection. We would also like to extend our gratitude to Matthew Hodanbosi, Stephanie Rollmann, and Dieter Vanderelst for their assistance and discussion on statistical analyses/presentation.

Conflict of interest

The authors declare that the research was conducted in the absence of any commercial or financial relationships that could be construed as a potential conflict of interest.

Publisher's note

Supplementary material

The Supplementary Material for this article can be found online at: https://www.frontiersin.org/articles/10.3389/fmars.2024.1406753/full#supplementary-material

References

Altevogt, R., and Hagen, H.-O. V. (1964). Über die orientierung von *uca tangeri* eydoux im freiland. *Z. für Morphologie und Ökologie der Tiere* 10, 636–656. doi: 10.1007/BF00407731

Benhamou, S., Sauvé, J.-P., and Bovet, P. (1990). Spatial memory in large scale movements: Efficiency and limitation of the egocentric coding process. *J. Theor. Biol.* 145, 1–12. doi: 10.1016/S0022-5193(05)80531-4

Beugnon, G., and Campan, R. (1989). Homing in the field cricket, *gryllus campestris*. *J. Insect Behav.* 2, 187–198. doi: 10.1007/BF01053291

Bisetzky, A. (1957). Zeitschrift fur vergleichende. *Physiologie* 40, 264–288. doi: 10.1007/BF00340571

Bosc, L. A. G. (1802). "Histoire naturelle des crustaces," in *Histoire naturelle de buffon*. Paris: R. R. Castel.

Chatterji, R., and Layne, J. E. (2023). Eye movement reflexes indicate the homing direction in the path-integrating fiddler crab, *uca pugilator*. *J. Mar. Sci. Eng.* 11. doi: 10.3390/jmse11091719

Cheng, K. (2012). ""Arthropod navigation ants, bees, crabs, spiders finding their way,"," in *The Oxford Handbook of Comparative Cognition* (New York, USA: Oxford University Press). doi: 10.1093/oxfordhb/9780195392661.013.0019

Crane, J. (1975). *Fiddler Crabs of the World: Ocypididae: Genus Uca* (Princeton, USA: Princeton University Press). doi: 10.1515/9781400867936

Darwin, C. (1873). Origin of certain instincts. *Nature* 7, 417–418. doi: 10.1038/007417a0

Etienne, A. S., and Jeffery, K. J. (2004). Path integration in mammals. *Hippocampus* 14, 180–192. doi: 10.1002/hipo.10173

Etienne, A. S., Maurer, R., Boulens, V., Levy, A., and Rowe, T. (2004). Resetting the path integrator: A basic condition for route-based navigation. *J. Exp. Biol.* 207, 1491–1508. doi: 10.1242/jeb.00906

Goerner, P. (1958). Die optische und kinästhetische Orientierung der Trichterspinne *Agelena labyrinthica*. *Z. für vergleichende Physiologie* 41, 111–153. doi: 10.1007/BF00345583

Halliday, T. R., and Slater, P. J. B. (Eds.) (1983). *Animal Behavior, Volume 1: Causes and Effects* (New York City, USA: Blackwell Science Ltd).

Hoffmann, G. (1984). Orientation behaviour of the desert woodlouse *Hemilepistus reaumuri*: Adaptations to ecological and physiological problems. *Symposium Zoological Soc. London* 53, 405–422. doi: 10.1007/BF00293211

Land, M. (2019). Eye movements in man and other animals. *Vision Res.* 162, 1–7. doi: 10.1016/j.visres.2019.06.004

Land, M., and Layne, J. (1995). The visual control of behaviour in fiddler crabs II. Tracking control systems in courtship and defence. *J. Comp. Physiol. A* 177, 91–103. doi: 10.1007/BF00243401

Layne, J. E. (2023). *Crab_manual_tracker*.

Layne, J. E., Barnes, W. J. P., and Duncan, L. M. J. (2003a). Mechanisms of homing in the fiddler crab *Uca rapax* 1. Spatial and temporal characteristics of a system of small-scale navigation. *J. Exp. Biol.* 206, 4413–4423. doi: 10.1242/jeb.00660

Layne, J. E., Barnes, W. J. P., and Duncan, L. M. J. (2003b). Mechanisms of homing in the fiddler crab *Uca rapax* 2. Information sources and frame of reference for a path integration system. *J. Exp. Biol.* 206, 4425–4442. doi: 10.1242/jeb.00661

Layne, J. E., Wicklein, M., Dodge, F. A., and Barlow, R. B. (1997). Prediction of maximum allowable retinal slip speed in the fiddler crab, *uca pugilator*. *Biol. Bull.* 193, 202–203. doi: 10.1086/BBLv193n2p202

Loomis, J. M., Klatzky, R. L., Golledge, R. G., Cicinelli, J. G., Pellegrino, J. W., and Fry, P. A. (1993). Nonvisual navigation by blind and sighted: Assessment of path integration ability. *J. Exp. Psychol. Gen.* 122, 73–91. doi: 10.1037/0096-3445.122.1.73

Maurer, R., and Séguinot, V. (1995). What is modelling for? a critical review of the models of path integration. *J. Theor. Biol.* 175, 457–475. doi: 10.1006/jtbi.1995.0154

Merkle, T., Knaden, M., and Wehner, R. (2006). Uncertainty about nest position influences systematic search strategies in desert ants. *J. Exp. Biol.* 209, 3545–3549. doi: 10.1242/jeb.02395

Mittelstaedt, H. (1985). "Analytical cybernetics of spider navigation," in *Neurobiology of Arachnids* (Springer Berlin Heidelberg, Berlin, Heidelberg), 298–316. doi: 10.1007/978-3-642-70348-5_15

Mittelstaedt, H., and Mittelstaedt, M.-L. (1982). "Homing by path integration," in *Avian navigation* (Springer-Verlag, Berlin), 290–297.

Mittelstaedt, M. L., and Mittelstaedt, H. (1980). Homing by path integration in a mammal. *Naturwissenschaften* 67, 566–567. doi: 10.1007/BF00450672

Müller, M., and Wehner, R. (1988). Path integration in desert ants, *cataglyphis fortis*. *Proc. Natl. Acad. Sci.* 85, 5287–5290. doi: 10.1073/pnas.85.14.5287

Nalbach, H.-O., and Nalbach, G. (1987). Distribution of optokinetic sensitivity over the eye of crabs: its relation to habitat and possible role in flow-field analysis. *J. Comp. Physiol. A* 160, 127–135. doi: 10.1007/BF00613448

Papi, F. (1992). *Animal Homing*. Ed. F. Papi (Chapman and Hall, London, United Kingdom: Springer). doi: 10.1007/978-94-011-1588-9

Qi, Y., and Mou, W. (2023). Sources of systematic errors in human path integration. *J. Exp. Psychol. Hum. Percept. Perform.* 49, 197–225. doi: 10.1037/xhp0001076

Schone, H. (1984). *Spatial Orientation: The Spatial Control of Behaviour in Animals and Man* (Princeton, USA: Princeton University Press). doi: 10.1515/9781400856848

Seguinot, V., Cattet, J., and Benhamou, S. (1998). Path integration in dogs. *Anim. Behav.* 55, 787–797. doi: 10.1006/anbe.1997.0662

Seguinot, V., Maurer, R., and Etienne, A. S. (1993). Dead reckoning in a small mammal: the evaluation of distance. *J. Comp. Physiol. A* 173, 103–113. doi: 10.1007/BF00209622

Sommer, S., and Wehner, R. (2004). The ant's estimation of distance travelled: Experiments with desert ants, *Cataglyphis fortis*. *J. Comp. Physiol. A Neuroethol Sens Neural Behav. Physiol.* 190, 1–6. doi: 10.1007/s00359-003-0465-4

Stangl, M., Kanitscheider, I., Riemer, M., Fiete, I., and Wolbers, T. (2020). Sources of path integration error in young and aging humans. *Nat. Commun.* 11. doi: 10.1038/s41467-020-15805-9

von Frisch, K. (1967). *The Dance Language and Orientation of Bees* (Cambridge, USA: Harvard University Press). doi: 10.4159/harvard.9780674418776

von Saint Paul, U. I. (1982). "Do geese use path integration for walking home?," in *Avian navigation*. (Berlin; Heidelberg; New York: Springer), 296–307.

Wehner, R., and Wehner, S. (1986). Path Integration in Desert Ants. Approaching a long-standing puzzle in insect navigation. *Ital. J. Zoology* 20, 309–331. doi: 10.1080/00269786

Wiltschko, W., and Wiltschko, R. (1982). "The role of outward journey information in the orientation of homing pigeons," in *Avian navigation*. 239–252. doi: 10.1007/978-3-642-68616-0_24

Zeil, J. (1998). Homing in fiddler crabs (*Uca lactea annulipes* and *Uca vomeris*: Ocypodidae). *J. Comp. Physiol. A* 183, 367–377. doi: 10.1007/s003590050263

Zeil, J., and Layne, J. (2002). "Path integration in fiddler crabs and its relation to habitat and social life," in *Crustacean Experimental Systems in Neurobiology* (Berlin, Heidelberg, New York: Springer Berlin Heidelberg), 227–246. doi: 10.1007/978-3-642-56092-7_13

frontiers | Frontiers in Marine Science

TYPE Original Research
PUBLISHED 10 June 2024
DOI 10.3389/fmars.2024.1389428

OPEN ACCESS

EDITED BY
Kareen E. Schnabel,
National Institute of Water and Atmospheric Research (NIWA), New Zealand

REVIEWED BY
Luzhen Chen,
Xiamen University, China
Charles Griffiths,
University of Cape Town, South Africa

*CORRESPONDENCE
Nasreen Peer
peer.nasreen@gmail.com

RECEIVED 22 February 2024
ACCEPTED 24 May 2024
PUBLISHED 10 June 2024

CITATION
Katharoyan C, Rajkaran A and Peer N (2024) Caught in transition: changes in brachyuran diversity following mangrove encroachment into saltmarshes at a southern distribution limit.
Front. Mar. Sci. 11:1389428.
doi: 10.3389/fmars.2024.1389428

Caught in transition: changes in brachyuran diversity following mangrove encroachment into saltmarshes at a southern distribution limit

Chaitanya Katharoyan[1], Anusha Rajkaran[2] and Nasreen Peer[1]*

[1]Department of Botany and Zoology, Stellenbosch University, Stellenbosch, South Africa, [2]Department for Biodiversity and Conservation Biology, University of the Western Cape, Bellville, South Africa

Mangroves are expanding polewards due to global change, often encroaching into adjacent temperate saltmarshes. In both vegetated ecosystems, brachyurans are responsible for ecological processes and functions such as nutrient cycling and sediment bioturbation. South African mangroves occur at a latitudinal limit and are establishing further south due to past planting events and global change, making these ideal study systems for the effects of mangrove expansion and encroachment. Here, we investigated the effect of mangrove encroachment on brachyuran community composition at two saltmarsh sites with planted mangrove stands of different ages. Transects were laid perpendicular to each estuary where three habitat types were demarcated (mangrove, ecotone, saltmarsh). Sediment samples were collected for analyses and quadrats were used to measure pneumatophore density, saltmarsh cover, and brachyuran abundance and diversity. We found that brachyuran community structure at each site has significantly changed over seven years, with two mangrove-associated fiddler crab species, *Tubuca urvillei* and *Paraleptuca chlorophthalmus*, now recorded at the younger planted site, indicating a new southern distributional limit. Community structure was also significantly different amongst habitat types ($p < 0.05$) with *Parasesarma catenatum* dominating saltmarshes while *Danielella edwardsii* was more prominent in mangroves. However, community composition did not differ significantly between the two (differently aged) sites ($p > 0.05$). Pneumatophore density had a proportional relationship with crab abundance, diversity and richness, while saltmarsh cover had an inversely proportional relationship with crab abundance, diversity and richness. It is likely that as mangroves continue to expand into saltmarshes, more mangrove-associated species will move into saltmarshes, potentially altering ecosystem processes in this unique habitat.

KEYWORDS

species distribution, ecotone, poleward expansion, brachyuran diversity, southern limit

1 Introduction

Globally, many faunal species are expanding or shifting their geographic range in response to climate change (Perry et al., 2005; Chen et al., 2011; Cannizzo et al., 2018, Loveless and Smee, 2019, Peer et al., 2018a; Pinsky et al., 2020; Adams et al., 2024). These faunal shifts are usually associated with shifts in foundation species, such as coral reefs, kelp forests, and terrestrial forests, responsible for structuring and shaping ecosystems (Walther, 2010; Cannizzo and Griffen, 2019). Species are expected to move polewards at a rate of 13 km per decade due to rising temperatures (Poloczanska et al., 2013). However, some faunal species move and expand into novel habitats at a faster rate than foundation species (Schweiger et al., 2008). This difference in the shifting rate between foundation species and their associated fauna may result in a species inhabiting a new ecosystem that it has not previously occupied (Schweiger et al., 2008) and could lead to cascading effects on both community structure and ecosystem function (Cannizzo et al., 2018; Muthukrishnan et al., 2020; Hensel et al., 2023). This range shift of both foundation and associated faunal species is expected to increase with ongoing climate change (Schweiger et al., 2008; Cannizzo et al., 2019). For example, mangrove encroachment into saltmarsh habitats can cause changes in both ecosystem-level processes and functions (Kelleway et al., 2017; Cavanaugh et al., 2019). This change in function is likely to affect the community structure of fish, invertebrates and other species inhabiting coastal vegetated ecosystems (Kelleway et al., 2017; Smee et al., 2017; Cavanaugh et al., 2019).

Mangrove-saltmarsh ecotones exist near mangrove latitudinal range limits across the world, in countries such as China (Liu et al., 2020), New Zealand (Lovelock et al., 2007), Australia (Eslami-Andargoli et al., 2009), Mexico (Comeaux et al., 2012), the United States (Osland et al., 2013) and South Africa (Adams et al., 2004; Raw et al., 2019). In South Africa, saltmarshes occur along the entire coastline (Adams, 2020), while mangroves occur along the east coast extending from Kosi Bay to Tyolomnqa (Raw et al., 2022). Mangroves are expanding their distribution to higher latitudes, due to the warming of estuarine and coastal waters and rising sea levels assisting propagule dispersion (Godoy and Lacerda, 2015; Raw et al., 2022). Where mangroves and saltmarsh habitats co-occur, mangroves have been encroaching into saltmarsh habitats, creating a mangrove-saltmarsh ecotone (Saintilan et al., 2014; Geldenhuys et al., 2016; Cavanaugh et al., 2019). Many mangrove-associated species reach their southernmost distributional range limit in South Africa (Peer et al., 2015). Ecotones occurring at these species range limits are sensitive to changes, making South African mangrove-saltmarsh ecotones ideal to study and predict future responses of macrofauna to global climate change (Saintilan et al., 2014; Raw et al., 2019).

Brachyurans (true crabs) tend to be the most dominant macrofauna, in terms of abundance and diversity, in mangroves and saltmarshes (Emmerson, 1994; Gutierrez, 2008; Vorsatz, 2009). The most abundant brachyuran superfamilies occurring in these two ecosystems are Ocypodoidea (mainly fiddler crabs) and Grapsoidea which are burrowing species (Nobbs, 2003). In mangroves, sesarmids and other Grapsoidae families can alter mangrove forest structure (Dahdouh-Guebas et al., 1997), facilitate nutrient recycling (Gao et al., 2024) and energy flow (Lee, 1998), while fiddler crabs (family: Ocypodidae) can alter both soil dynamics (Warren and Underwood, 1986) and primary productivity (Ólafsson and Ndaro, 1997). The herbivorous and detritivorous diets of these species are essential for mangrove ecosystem functioning, as these crabs consume mangrove leaf litter and organic materials on the mangrove floor (Dahdouh-Guebas et al., 1997). Both these groups consist of burrowing species, which aerate and oxygenate mangrove soil (Steinke et al., 1993), allowing movement of nutrients and water through soil influencing mangrove seedling development (Steinke et al., 1993) and altering physical structures in saltmarshes (Bertness, 1985; Taylor and Allanson, 1993).

Since the foundation species themselves (mangrove and saltmarsh vegetation) can influence crab assemblages, as mangroves move into saltmarshes, it is likely that their associated macrofauna, will also shift into this novel habitat (Cannizzo et al., 2018). While mangroves are characterized as woody shrubs and trees that grow in saline coastal habitats (Giri et al., 2011; Adams & Rajkaran, 2021), saltmarshes are characterized by a variety of halophytic shrubs, grasses and herbs (Adams, 2020). The mangroves provide a shaded habitat through canopy cover which allows crabs to maintain moderate internal temperatures and experience less evaporative losses compared to crabs in open clearings such as saltmarshes (Edney, 1961; Hogarth, 2015; Nobbs and Blamires, 2017). Mangroves also have dense pneumatophore mats which may influence the crab presence and abundance either positively through food availability, shelter or soil composition (Demopoulos and Smith, 2010) or negatively by acting as an obstruction for both feeding and burrowing (Sweetman et al., 2010; Leung, 2015; Freitas and Pagliosa, 2020). While in the saltmarshes, certain saltmarsh species are affiliated with mangrove-associated crabs (Luk and Zajac, 2013). For example, Bertness and Miller (1984) found that the fiddler crab *Minuca pugnax* uses the saltmarsh *Spartina alterniflora* (L.) in Barrington Rhode Island saltmarsh habitats to gain structural support for their burrows. However, a subsequent study found no significant evidence to support the idea that saltmarsh species support burrowing crabs (Nomann and Pennings, 1998). In South Africa, two species of fiddler crabs *Tubuca urvillei* and *Austruca occidentalis* were found in saltmarshes in the warm temperate Kariega Estuary, well beyond the mangrove latitudinal distribution limit, with the former being a dominant species at this habitat (Hodgson, 1987; Peer et al., 2016). Therefore, it is highly likely that the presence or absence of certain vegetation types (mangroves, saltmarshes or both) would influence the distribution of these burrowing species (Nobbs, 2003). Understanding the interaction between macrofauna and vegetation types is essential to understanding the ecological implications, especially with the expansion of mangroves into saltmarsh habitats amidst global climate change.

Although several studies have focused on mangrove encroachment into saltmarshes in South Africa (Adams et al., 2004; Saintilan et al., 2014; Hoppe-Speer et al., 2015; Adams et al., 2016; Geldenhuys et al., 2016; Whitfield et al., 2016, Raw et al., 2019; Adams and Rajkaran, 2021; Raw et al., 2023), very few studies focused on the impact of mangrove encroachment on

associated macrofauna (Vorsatz, 2009; Whitfield et al., 2016). South African mangroves provide insight into the climatic effect of mangrove expansion into saltmarshes (Adams and Rajkaran, 2021). The aim of this study is to understand the impact of mangrove encroachment into saltmarsh habitats on associated macrofauna. The objectives are therefore to, (i) record brachyuran abundance and diversity across the mangrove-saltmarsh gradient, (ii) compare brachyuran community structure over time and across two planted mangrove sites of different ages, and (iii) investigate the relationship between crab diversity, abundance and richness and vegetation structures. It was hypothesized that:

(i) Brachyuran community composition in mangroves would have changed over the last seven years when comparing data collected in 2016 (past data from Peer et al., 2018a) and 2023 (present).

(ii) There are more mangrove-associated species occurring at the older, more established mangrove site (Nahoon) compared to the younger mangrove site (Tyolomnqa).

(iii) Brachyuran community composition are different amongst all habitat types (mangrove, ecotone, saltmarsh).

(iv) Brachyuran abundance and diversity decreases with increasing saltmarsh cover and increases with increasing pneumatophore density.

2 Methods and materials

2.1 Study sites

The range expansion of mangrove forests further south along the South African east coast has been confounded by the planting of mangroves at two sites i.e. Nahoon and Tyolomnqa (Figures 1, 2A, B). Although some speculation exists as to the motivation for planting, it is known that the mangroves were planted by botanists to determine whether or not they would establish at higher latitudes, similar to areas around the world (Hoppe-Speer et al., 2015). The two planted sites were predominantly saltmarsh habitats prior to mangrove planting (Adams and Rajkaran, 2021). In Nahoon Estuary, *A. marina* was first planted in 1969 by Prof. Steinke (Steinke, 1972), followed by *Bruguiera gymnorrhiza* (L.) Lam. and *Rhizophora mucronata* Lam. planted by Carl Vernon a few years after (Hoppe-Speer et al., 2015). All three mangrove species are now well established at this site. In Tyolomnqa, *A. marina* was first planted in 1991 and has established in pockets along the estuary. The mangrove forest in Nahoon is relatively small, occupying less than 2 ha (Hoppe-Speer et al., 2015), while Tyolomnqa is less than 0.12 ha (Bolosha, 2016). Nahoon is a predominantly open estuary, while Tyolomnqa is a large temporarily closed estuary (Adams and Rajkaran, 2021), in which the warm Agulhas Current flows through. The rise in sea level and the flow of the Agulhas Current move mangrove propagules in a poleward direction, resulting in propagules being dispersed further south from these two planted sites, expanding latitudinally (Steinke and Ward, 2003; Raw et al., 2023). These two Eastern Cape sites were chosen as mangroves and saltmarshes co-exist here (Geldenhuys et al., 2016, Figure 2A, B) and to represent mangrove stands of different ages. Sites were sampled in summer (February) and winter (August) of 2023.

2.2 Field work and laboratory analysis

Two 20 m transects were placed perpendicular to the flow of the estuary. Along each transect, three 4 x 4 m quadrats were laid at each habitat type (mangrove, ecotone, saltmarsh) at 2 m, 10 m, and

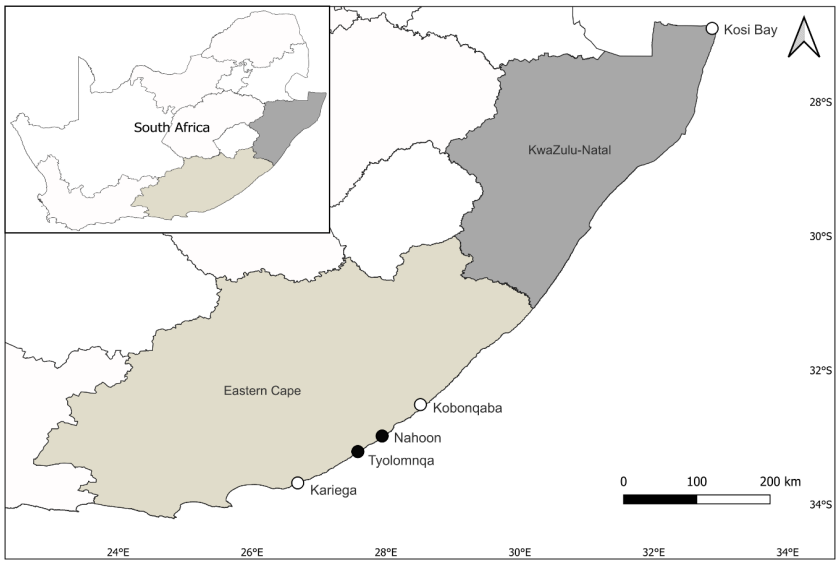

FIGURE 1
Map of South Africa, showing the two planted sites, Nahoon and Tyolomnqa, sampled in the Eastern Cape Province (represented by black dots) and other sites mentioned in this study (represented by white dots).

16 m (Figure 3). Within each 4 x 4 m quadrat, four 50 x 50 cm sub-quadrats were randomly placed where the density of pneumatophores, abundance and diversity of brachyurans, and percentage cover of each saltmarsh species was recorded. Individual trees and saplings were counted and height was measured using a tape measurer at each of the three 4 x 4 m quadrats at each habitat type. To determine sediment grain size (SGS), sediment moisture content (SMC %) and sediment organic matter (SOM %), three sediment samples (approximately 100 g each) were collected from each 4 x 4 m quadrat from each habitat type at both sites. Analyses of SGS, SMC and SOM were conducted in the laboratory following the protocol outlined in Adams and Human (2016). All data were recorded during low tide.

2.3 Statistical analysis

All statistical analyses were conducted using the statistical package R v 4.3.0 (R Core Team 2024) and PRIMER (Clarke and Gorley, 2006). Multivariate abundance data were square root transformed using the Bray-Curtis similarity index. A resemblance matrix was generated from the transformed data. The effects of site (Nahoon, Tyolomnqa), habitat type (mangrove, ecotone, saltmarsh), year (2016, 2023) and season (Feb, Aug) on brachyuran community composition were analyzed using a Permutational multivariate analysis of variance (PERMANOVA). Where significant differences were found amongst habitat types and years, a pairwise analysis was performed.

To determine if saltmarsh cover, pneumatophore density and mean burrow abundance were significantly different amongst habitat types, an analysis of variance (ANOVA) was performed for each with habitat and site as factors. To determine SGS, a ranking system was used according to the percentage composition with 1 = clay, 2 = clay/silt, 3 = silt, 4 = silt/sand and 5 = sand following protocol outlined in Peer et al. (2018b). Thereafter, an ANOVA was performed to determine if SGS, SMC and SOM significantly differed between site and habitat type nested within site. Where significant differences were found, a posthoc Tukey's HSD was performed. To determine the species contributions (similarities and dissimilarities) amongst sites and habitat types, a SIMPER analysis was performed on PRIMER using transformed data with a Bray Curtis similarity and a cut off low of 90%.

The species diversity (Shannon-Wiener diversity index), richness (total number of species) and evenness (Pielou's evenness) of brachyurans at each habitat type was calculated. To determine if pneumatophore density and saltmarsh cover drive brachyuran abundance, diversity and richness among sites and habitat types a 'manyglm' was performed. Thereafter, an 'anova' (p.uni = 'adjusted', nBoot = 1000) was used to determine the significance of predictors for overall abundance, diversity and richness of crabs, which included univariate tests nested within the multivariate model for each response variable (Wang et al., 2012; Peer et al., 2018b; Theron et al., 2022). For all analyses, the significance value was determined by α =0.05.

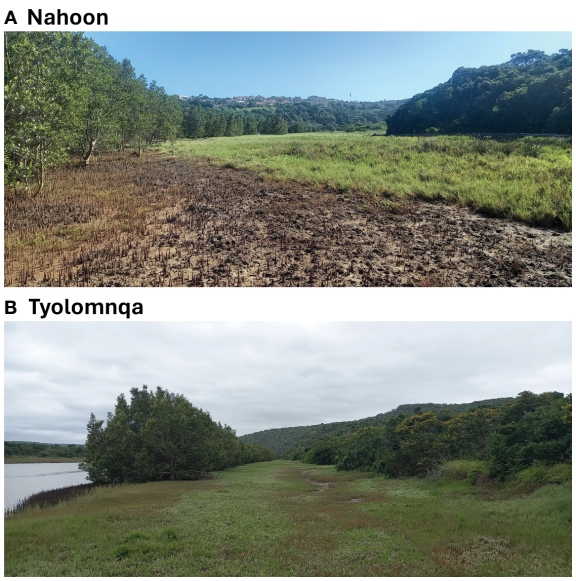

FIGURE 2
The two planted mangrove sites **(A)** Nahoon and **(B)** Tyolomnqa, showing each habitat type (mangrove, ecotone and saltmarsh). Mangroves occur on the left of the image, the ecotone in the middle and saltmarsh on the right. Images credited to Anusha Rajkaran.

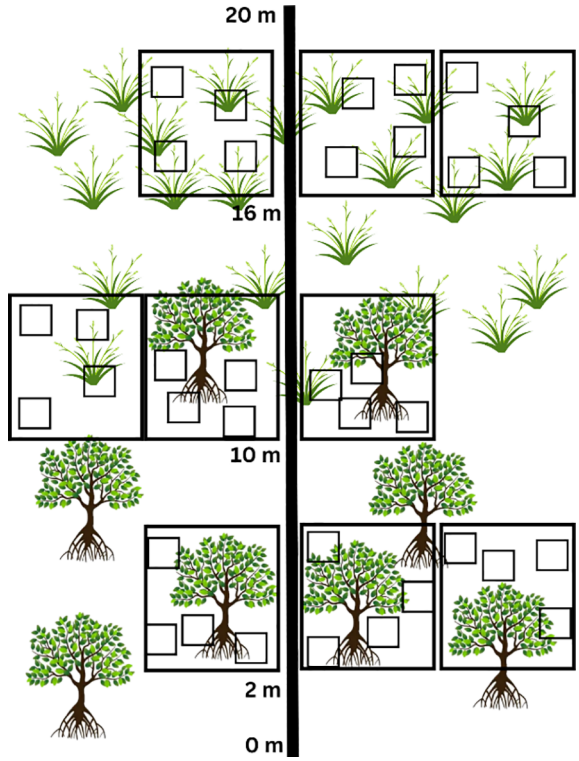

FIGURE 3
Depiction of sample design (Mitchell, 2010; Theron et al., 2022) for understanding mangrove encroachment into saltmarsh habitat. Two 20 m transects cut across saltmarsh habitats into mangrove habitats, where four 50 x 50 cm sub-quadrats were randomly placed within each of three 4 x 4 m quadrats.

10.3389/fmars.2024.1389428

3 Results

3.1 Brachyuran community structure over time

There was a significant change in brachyuran community structure in mangroves over the time (2016 vs 2023 data), at both Nahoon ($p = 0.001$, $t = 2.83$) and Tyolomnqa ($p = 0.002$, $t = 2.34$). Overall, 11 species of brachyurans were identified in both the planted mangroves (Table 1). The species richness decreased at Nahoon over the seven years from nine (2016) to seven (2023), while at Tyolomnqa species richness increased from four (2016) to five (2023). The crabs *Austruca occidentalis*, *Tubuca urvillei*, *Paraleptuca chlorophthalmus* and *Metograpsus messor* were observed in Nahoon (2016), however absent from this site in 2023.In Tyolomnqa the fiddler crabs *T. urvillei* and *P. chlorophthalmus* were absent in 2016 but were recorded for the first time at this site in 2023, explaining the change in species richness over time at both sites. The most abundant species at both sites (2016 and 2023) was *Danielella edwardsii* (Table 1) and the most common was also *Cyclograpsus punctatus* and *Parasersarma catenatum*. Four species, *Dotilla fenestrata*, *Neosarmatium africanum*, *C. eulimene* and *P. capensis* were absent from Tyolomnqa (2023) and only present in Nahoon, with three of these species (*D. fenestrata, N. africanum*, and *P. capensis*) all considered as mangrove-associated species. *Cristarma eulimene* and *Parasesarma capensis* occurred only at Nahoon (2023) at low average densities of one and four individuals per square meter, respectively.

TABLE 1 The mean abundance of brachyuran species in two planted mangrove estuaries, Nahoon and Tyolomnqa, in Eastern Cape, South Africa, comparing past (year 2016 - Peer et al., 2018a) and present (2023) data.

	Nahoon		Tyolomnqa	
Species	2016	2023	2016	2023
Grapsoidea—				
Cristarma eulimene Schubart & Ng, 2020	–	1 (2)	–	–
Cyclograpsus punctatus H. Milne Edwards 1837	1 (1)	2 (5)	1 (1)	7 (11)
Metopograpsus messor (Forsskål 1775)	5 (2)	–	–	–
Neosarmatium africanum (Ragionieri, Fratini and Schubart 2012)	4 (1)	3 (5)	2 (2)	–
Parasesarma capensis Fratini, Cannicci & Innocenti in Fratini, Cannicci, Porri & Innocenti, 2019	–	4 (23)	–	–
Parasesarma catenatum (Ortmann 1897)	6 (2)	7 (13)	8 (7)	7 (12)
Ocypodoidea—				
Austruca occidentalis (Naderloo, Schubart and Shih 2016)	11 (1)	–	–	–
Danielella edwardsii (MacLeay 1838)	10 (3)	100 (125)	71 (49)	24 (32)
Dotilla fenestrata Hilgendorf 1869	4 (1)	1 (4)	–	–
Paraleptuca chlorophthalmus (H. Milne Edwards 1837)	1 (1)	–	–	P
Tubuca urvillei (H. Milne Edwards 1852)	6 (2)	–	–	9 (13)
Species richness	9	7	4	5
Species diversity (H')	1.99	0.60	0.3	1.3
Species evenness (J')	0.90	0.31	0.35	0.80

The mean abundance is represented as average no. ind. m^{-2} (Standard Error) rounded off to the nearest whole number. Species richness, Shannon-Wiener diversity (H') and Pielou's evenness (J') is displayed for each mangrove site and year. P indicates the presence of a species where no quadrat data was available.

3.2 Brachyuran community structure between older and newer aged mangrove forests

Community structure was similar between older (Nahoon) and newer (Tyolomnqa) aged planted mangroves, with no significant difference found (Table 2). However, the effect of habitat type (nested within site) and the interaction between habitat type and season had a significant influence on brachyuran community structure (Table 2). Other factors that had a significant influence on brachyuran assemblages were season within habitat types.

3.3 Brachyuran community structure amongst habitat types

Species richness generally decreased from the mangroves to the saltmarsh habitats (Table 3). A few key crabs are shown in Figures 4A–F). *Parasesarma catenatum* was the only species to occur at all three habitat types at both sites. Whereas *Dotilla fenestrata* only occurred at the ecotone, and *Cristarma eulimene* and *Parasesarma capensis* only occurred at the mangroves in Nahoon. The species *Cyclograpsus punctatus*, *Daniellela edwardssi*, *P. catenatum* and *Tubuca urvillei* occurred at both the mangrove and ecotone habitats in Tyolomnqa. The only species that occurred in saltmarsh habitats were *Neosarmatium africanum* (Nahoon), *D. edwardsii* (Nahoon) and *P. catenatum* (both sites).

A pairwise comparison among three habitat types revealed that there is a significant difference in brachyuran assemblages between all habitat groups (Saltmarsh vs Ecotone, Saltmarsh vs Mangrove and Ecotone vs Mangrove) at both Nahoon and Tyolomnqa (Table 4). Habitat types also differed in sediment and vegetation characteristics that are presented in this section and Section 3.4.

There was an average dissimilarity in the abundance of crabs of 93.29% between saltmarshes and ecotones, 94.06% between saltmarshes and mangroves and 78.6% between mangroves and ecotones (Table 5). The crabs *Daniella edwardsii* and *Parasesarma catenatum* contributed the most towards the dissimilarities seen

10.3389/fmars.2024.1389428

TABLE 2 Results of PERMANOVA test for differences in brachyuran community structure between sites (fixed), habitat types (nested in site, fixed), season (fixed) and year (random).

Source	df	SS	MS	Pseudo-F	P(perm)
Site	1	7119.1	7119.1	0.80127	0.484
Year	1	7948	7948	2.3748	**0.007***
Season	1	21422	21422	2.3372	0.104
Habitat type (Site)	4	1.40E +05	34956	10.445	**0.001***
Site x Year	1	15426	15426	4.6093	**0.001***
Site x Season	1	9492.2	9492.2	1.0356	0.402
Habitat type (Site) x Season	4	36663	9165.8	2.7387	**0.001***
Residual	292	9.77E +05	3346.7		
Total	305	1.24E +06			

Significant values are in bold*.

between all habitat types, Saltmarsh vs Ecotone, Saltmarsh vs Mangrove and Mangrove vs Ecotone (Table 5). *Daniellela edwardsii* is more common and abundant in mangrove habitats compared to other habitat types (Table 4). Whereas *Parasesarma catenatum* occured at all habitat types, generally having the highest abundance in mangroves and lowest in saltmarshes, except for in Tyolomnqa where the ecotone has the highest abundance per square meter (Tables 4, 5). Mangroves had a higher average abundance of crab species followed by ecotone and saltmarsh groups.

Avicennia marina was the only mangrove species present along the 20 m transects at both sites and was confined to the mangrove and ecotone habitats (Table 6). The differences occurred between the ecotone and mangrove habitats at both sites in terms of mangrove tree density, height and adult:seedling ratios. Nahoon had the highest tree density in the mangrove habitats, with trees ranging between 4 – 530 cm in height and having an adult:seedling ratio of 1:1. While in Tyolomnqa, mangrove tree density was highest in mangrove habitats, with tree heights ranging from 3 – 661 cm, with an adult:seedling ratio of 1:30.

Regarding sediment characteristics, mangrove habitats had the highest sediment moisture content (%) and sediment organic matter (%) at both sites (Table 7). In Tyolomnqa, the ecotone habitat had the lowest SMC (%) and SOM (%), while in Nahoon, the ecotone had the lowest SMC (%) and the saltmarsh habitat had the lowest SOM (%). Mangroves generally consisted of clay and clay/silt, while the ecotone was generally clay/silt at Nahoon and silt/sand at Tyolomnqa. The sediment in the saltmarsh at Nahoon was silt while at Tyolomnqa, it was drier and sandier.

Sediment characteristics, such as sediment grain size, sediment organic moisture (%) and sediment moisture content (%) were significantly different amongst habitat types and site (ANOVA, $p < 0.01$), therefore the Tukey's HSD *post-hoc* test was conducted and the results for habitat type are presented in the Table 8. When comparing Mangroves vs Ecotone, only SMC and SOM differed significantly, however when comparing Saltmarsh vs Ecotone, only SGS was significantly different. When comparing the Mangrove vs Saltmarsh habitats, SGS and SOM differed significantly.

TABLE 3 Mean abundance of brachyuran species occurring at each of three habitat types (mangrove - MN, ecotone - ET, saltmarsh - SM) at both Nahoon and Tyolomnqa (for 2023), over a summer and winter sampling period.

	Nahoon			Tyolomnqa		
Species	MN	ET	SM	MN	ET	SM
Grapsoidea—						
Cristarma eulimene	1 (2)	–	–	–	–	–
Cyclograpsus punctatus	2 (5)	–	–	7 (11)	2 (9)	–
Neosamartium africanum	3 (5)	4 (6)	1 (3)	–	–	–
Parasesarma capensis	4 (23)	–	–	–	–	–
Parasesarma catenatum	7 (13)	7 (16)	3 (6)	7 (12)	10 (18)	1 (3)
Ocypodoidea—						
Daniellela edwardsii	100 (125)	43 (77)	1 (6)	24 (32)	5 (9)	–
Dotilla fenestrata	–	1 (5)	–	–	–	–
Tubuca urvillei	–	–	–	9 (13)	1 (1)	–
Species richness	6	4	3	4	4	1
Species diversity (H')	0.60	0.7	0.95	1.3	1.08	0
Species evenness (J')	0.31	0.51	0.86	0.80	0.78	–

The mean abundance is represented as average no. ind. m^{-2} (Standard Error) rounded off to the nearest whole number. Species richness, Shannon-Wiener diversity (H') and Pielou's evenness (J') is displayed for each habitat type within both sites.

3.4 Drivers of brachyuran abundance, diversity, and richness

Both Nahoon and Tyolomnqa were previously dominated by saltmarsh species. The three habitat types (mangrove, ecotone and saltmarsh) were chosen to make comparisons across established and transitional habitats. From the ANOVA, saltmarsh species composition was significantly different amongst habitat types ($p < 0.05$), however, a TukeyHSD posthoc test revealed that there was only a significant difference between mangrove and saltmarsh habitats at both sites ($p = 0.03$). In Nahoon, saltmarsh species composition differed between the saltmarsh and ecotone habitat types (Figure 5A), as *Juncus kraussii* Hochst. (< 2%) only occurred in the saltmarsh habitat and the buffalo grass, *Stenotaphrum secundatum* (H. Walter) Kuntze, had a higher coverage in the saltmarsh habitat (41.5%) than the ecotone habitat (0.02%). The Nahoon mangrove habitat had < 1% of *Sarcocornia* spp. present. In Tyolomnqa, saltmarsh species were similar between all three habitat types, with *Bassia diffusa* (Thunb.) Kuntze, dominating in saltmarsh and ecotone habitats. *Sarcocornia* spp. occurred in all three habitat

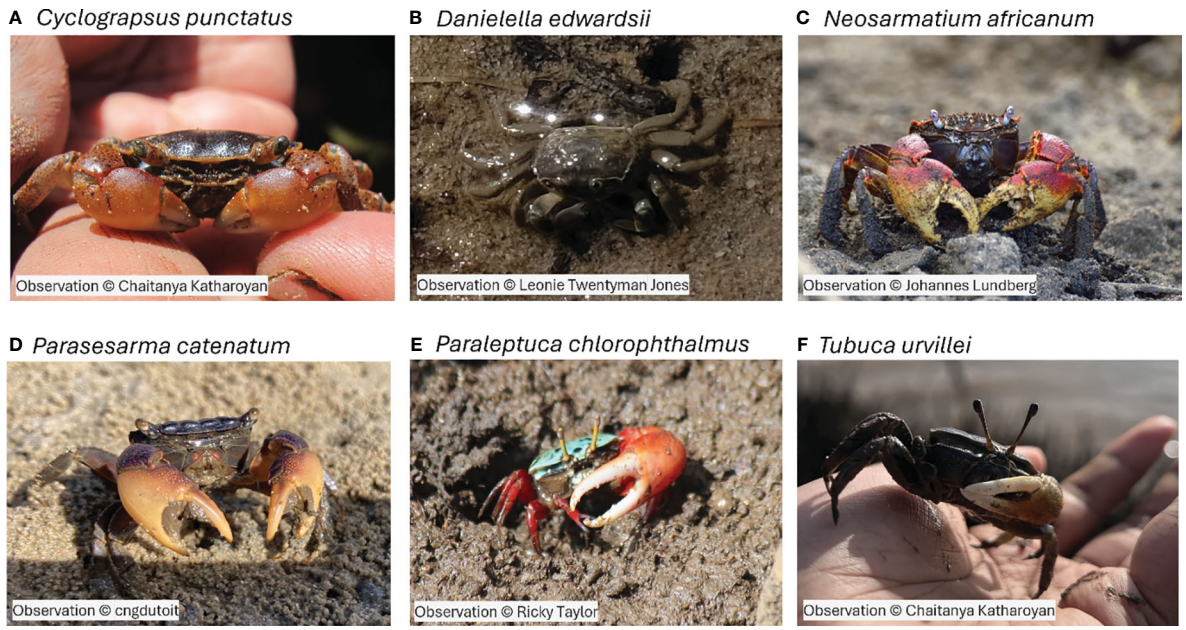

FIGURE 4
A few key crabs **(A–F)** that can be found at one or both planted sites (Nahoon and Tyolomnqa) amongst habitat types (mangrove, ecotone, saltmarsh). All photos are listed on iNaturalist.

TABLE 4 Pairwise comparison of brachyuran community structure among three habitat types (mangrove, ecotone, saltmarsh) at both study sites, Nahoon and Tyolomnqa, South Africa.

Habitat groups	Nahoon		Tyolomnqa	
	t	P(perm)	t	P(perm)
Saltmarsh vs Ecotone	2.2458	**0.001***	1.7375	**0.001***
Saltmarsh vs Mangrove	4.6699	**0.001***	4.3866	**0.001***
Ecotone vs Mangrove	2.5686	**0.001***	3.2892	**0.001***

Significant values are in bold*.

types in both sites (Figure 5A). In Nahoon, *Stenotaphrum secundatum* (H. Walter) Kuntze was more abundant in the saltmarsh habitat while *Limonium latifolium* (L.f.) Kuntze was more abundant in the ecotone.

Inversely, as expected, pneumatophore density (no. ind. m^{-2}) significantly decreased from mangroves to saltmarsh habitats at both estuaries (Figure 5B). In Tyolomnqa, pneumatophore density was highest in mangroves (358 (± 15 SE) ind. m^{-2}) and absent in saltmarsh habitats. In Nahoon, mangroves had the highest pneumatophore density of 199 (± 12 SE) ind. m^{-2} with the saltmarsh habitats having the lowest of 3 (± 2 SE) ind. m^{-2}.

There was a significant difference in mean burrow abundance amongst habitat types ($p = 0.003$). The mean burrow abundance generally decreased from mangroves into saltmarsh habitats (Figure 5C). As saltmarsh species cover increases, we see that burrow abundance decreases (Figures 5A, C) and as pneumatophore density increased, burrow abundance increased (Figures 5B, C).

Saltmarsh percentage cover and pneumatophore density appear to be significant drivers of brachyuran abundance (no. ind. m^{-2}), diversity (Shannon-Wiener index) and richness (Table 9). Saltmarsh cover was negatively correlated with brachyuran abundance ($r = -0.43$) and diversity ($r = -0.37$) while pneumatophore density was positively correlated with abundance ($r = 0.39$) and diversity ($r = 0.46$).

4 Discussion

Global climate change is resulting in coastal vegetation shifts, as mangroves expand polewards and into temperate saltmarsh habitats (Cavanaugh et al., 2014; Saintilan et al., 2014; Raw et al., 2022). In both mangroves and saltmarshes, brachyurans fulfil important functional roles, although geographic and vegetated structural differences can be a driver of macrofauna community structure variation. These shifts in vegetation types can have an impact on associated macrofaunal species by altering their behavior (Cannizzo and Griffen, 2016), morphology (Weiskopf et al., 2020) or causing range shifts (Lenoir and Svenning, 2015). In turn, a shift in fauna will influence the existing habitat type and ecosystem function. The effects of mangrove expansion in South Africa have rarely been studied in faunal assemblages (Vorsatz, 2009; Whitfield et al., 2016) and this paper is among the first to present insight into this phenomenon.

4.1 Differences in past and present brachyuran assemblages

There was a significant change in brachyuran community composition over the past seven years, supporting hypothesis 1.

10.3389/fmars.2024.1389428

TABLE 5 The average abundance and dissimilarities of crab species amongst habitat types (across both sites), with a cut of low of 90.00%.

Saltmarsh vs Ecotone				
Average dissimilarity = 93.29%				
	Saltmarsh	Ecotone		
Species	Abundance	Abundance	Dissimilarity	Contribution%
Daniellela edwardsii	0.13	2.62	39.3	42.12
Parasesarma catenatum	0.56	1.54	33.99	36.44
Neosamartium africanum	0.18	0.53	13.68	14.66
Saltmarsh vs Mangrove				
Average dissimilarity = 94.06%				
	Saltmarsh	Mangrove		
Species	Abundance	Abundance	Dissimilarity	Contribution%
Daniellela edwardsii	0.13	5.99	52.15	55.45
Parasesarma catenatum	0.56	1.59	14.85	15.78
Cyclograpsus punctatus	0	0.98	10.88	11.57
Tubuca urvillei	0	0.84	7.78	8.27
Ecotone vs Mangrove				
Average dissimilarity = 78.67%				
	Ecotone	Mangrove		
Species	Abundance	Abundance	Dissimilarity	Contribution%
Daniellela edwardsii	2.62	5.99	41.09	52.23
Parasesarma catenatum	1.54	1.59	14.17	18.02
Cyclograpsus punctatus	0.24	0.98	9.05	11.51
Tubuca urvillei	0.02	0.84	5.9	7.5
Neosamartium africanum	0.53	0.51	5.54	7.05

Our results are similar to Freitas et al. (2021) who also found that brachyuran community composition has changed over an eight-year monitoring period, in the Babitonga Bay mangrove ecosystem located along the southern Brazilian coast due to anthropogenic impacts. Other studies have found that brachyuran communities are also influenced by habitat modifications (Skilleter and Warren, 2000), environmental shifts in foundation species including poleward expansions (Kelleway et al., 2017; Peer et al., 2018a; Walker et al., 2021; Theron et al., 2022), biotic interactions such as competition for resources and predation (Cannicci et al., 2018; Freitas et al., 2021) or natural environmental fluctuations such as tides and salinity fluctuations (Lee, 1999; Macintosh et al., 2002; Peer et al., 2014). Over the past seven years, species richness decreased at Nahoon and increased years in Tyolomnqa. More notably, this includes the absence of the fiddler crabs from the Nahoon Estuary and the southward range shift of the fiddler crab *Tubuca urvillei* and *Paraleptuca chlorophthlamus* from its previous known distribution limit in Nahoon (Peer et al., 2018b; Theron et al., 2022) to Tyolomnqa. It is likely that more mangrove-associated species will move further south towards Tyolomnqa as climate change continues to influence poleward distribution.

TABLE 6 The mean mangrove tree density (no. ind. m^{-2} (Standard Error)), range of tree height (cm) and the adult to seedling ratios of *Avicennia marina* counted within three habitat types (Mangrove – MN, Ecotone – ET, Saltmarsh – SM) in both sampling sites.

	Nahoon			Tyolomnqa		
	MN	ET	SM	MN	ET	SM
Density	19.38 (0.5)	2.5 (0.08)	–	2.26 (0.4)	0.22 (0.15)	–
Height range (cm)	4 - 530	40 - 445	–	3 - 661	4 - 660	–
Adult: Seedling ratio	1:1	1:0.3	–	1:30	1:10	–

TABLE 7 The range of sediment moisture content (%) and sediment organic matter (%) and sediment grain size ranking from each of three habitat types (Mangrove – MN, Ecotone – ET, Saltmarsh – SM) at both sampling sites.

Sediment	Nahoon			Tyolomnqa		
	MN	ET	SM	MN	ET	SM
SMC (%)	19 - 58	20 - 41	26 - 53	13 - 28	7 - 20	7 - 24
SOM (%)	0.6 - 2.5	0.5 - 2.2	0.3 - 1.2	0.3 - 1.2	0.2 - 1	0.4 - 1.3
SGS (1–5)	1	2	3	2	4	5

Sediment ranking as follows (1 = clay, 2 = clay/silt, 3 = silt, 4 = silt/sand and 5 = sand). These data were collected only during the summer period at both sites.

TABLE 8 Results from Tukey's HSD *post-hoc* test, showing the significant differences in sediment grain size, sediment moisture content (%) and sediment organic matter (%) amongst habitat types across sites.

	Sediment grain size	Sediment moisture content	Sediment organic matter
Groups	P-value	P-value	P-value
Mangrove vs Ecotone	0.92	**< 0.01***	**< 0.05***
Saltmarsh vs Ecotone	**< 0.01***	0.09	0.99
Saltmarsh vs Mangrove	**< 0.01***	0.06	**< 0.05***

Significant differences are in bold*.

4.2 Differences between mangrove sites of different ages

Given that Nahoon was an older and more established planted mangrove site compared to Tyolomnqa (Hoppe-Speer et al., 2015), we expected community structure to differ between sites with more mangrove-associated species at Nahoon. However, brachyuran community structure was similar between these two sites supporting hypothesis 2. Ashton et al. (2003) observed that grapsoid crabs (mainly sesarmids) dominated in both high abundances and diversity at mature mangrove forests, whereas ocypodid crabs (such as fiddler crabs) were found at high abundances in younger mangrove forests. We found similar patterns to Ashton et al. (2003) as the fiddler crabs *T. urvillei* and *Paraleptuca chlorophtalmus* inhabited the younger mangrove site (Tyolomnqa), while only grapsoidcrabs (mainly sesarmids) inhabited the older site (Nahoon) (Table 1). Other studies also found this trend in both Malaysia and Thailand (Berry, 1972; Sasekumar, 1974; Macintosh, 1984).

4.3 Differences amongst habitat types

Brachyuran community structure differed between all habitat types at both sites supporting hypothesis 3. Factors such as vegetation and sediment characteristics could have resulted in the differences seen in community structure between habitat types. For instance, both grapsoids (mainly sesarmids) and ocypodids (fiddler crabs) are burrowing taxa and are thus influenced by both above- and below-ground vegetation structures (Nobbs, 2003; Walker et al., 2021). In terms of above-ground vegetation, mangrove adult trees provide shade through canopy cover which can drive high abundances of crabs (Peer et al., 2018b; Theron et al., 2022). Whereas the saltmarsh habitat is an open clearing with direct sunlight, which could be unfavourable for most mangrove crabs that have a physiological limitation to both high temperatures and high evaporation rates (Nobbs, 2003 and references therein). Our results show that brachyuran abundance and diversity significantly decrease with an increase in saltmarsh cover, which is supported by several other studies (Raposa et al., 2018; Wasson et al., 2019; Tyrrell et al., 2023), although van der Wal and Herman (2012) in the Netherlands, found that *Aster tripolium* and *Salicornia procumbens* saltmarsh species cover had no significant effect on macrofaunal diversity, structure or biomass; and Chen et al. (2022) found that crab burrows were more abundant in saltmarsh vegetation, with higher organic matter and water content, compared to unvegetated areas in the Doulong harbor of Yancheng intertidal flat in China.

In terms of pneumatophores, which form both above- and below-ground structures, mangrove quadrats had the highest pneumatophore density (Figure 5B) which drives the abundance, diversity and richness of brachyuran crabs. Our results correspond to other studies which find that macrofauna were more abundant and diverse with higher pneumatophore density (Virnstein, 1977; Walker et al., 2019; Freitas et al., 2021). On the other hand, saltmarsh vegetation has different root complexities (Bertness et al., 2014), that could inhibit and obstruct crabs from burrowing into the sediment (Wang et al., 2008). Roots of the buffalo grass *Stenotaphrum secundatum* are dense and deep (Busey, 2003) and had a high coverage in saltmarshes at Nahoon, likely reducing the available below-ground space for burrowing crabs. Whereas *Bassia diffusa* is a herb with fibrous taproots (Turki et al., 2008) occurring in saltmarshes and ecotones in Tyolomnqa, that likely obstruct burrowing crabs. The highly dense roots of saltmarshes usually stabilize and obstruct the sediment, making it difficult for brachyurans to burrow, as supported by the decrease in mean burrow abundance from mangroves to saltmarshes (Figure 5).

Studies have shown that crabs prefer soft substrates where sediment is easy to create connected tunnels in burrows (Flores et al., 2005; Bertness et al., 2014). The sediment grain size in saltmarshes was significantly different to mangroves and ecotones. Sediment grain size has been found to drive fiddler crab abundance (Peer et al., 2018b) and sesarmid crabs prefer soft clay substrates that occur in the mangroves (Nobbs, 2003). Contrary to Min et al. (2023) who found that crab burrow density decreases under canopy cover, we found that mean burrow abundance increases in mangrove areas where canopy cover is higher than in saltmarshes. Canopy cover can likely reduce predation risk (Nomann and Pennings, 1998) or increase soil moisture content (Nobbs, 2003; Kon et al., 2010). This is supported by our results which show that mangroves have a higher sediment moisture

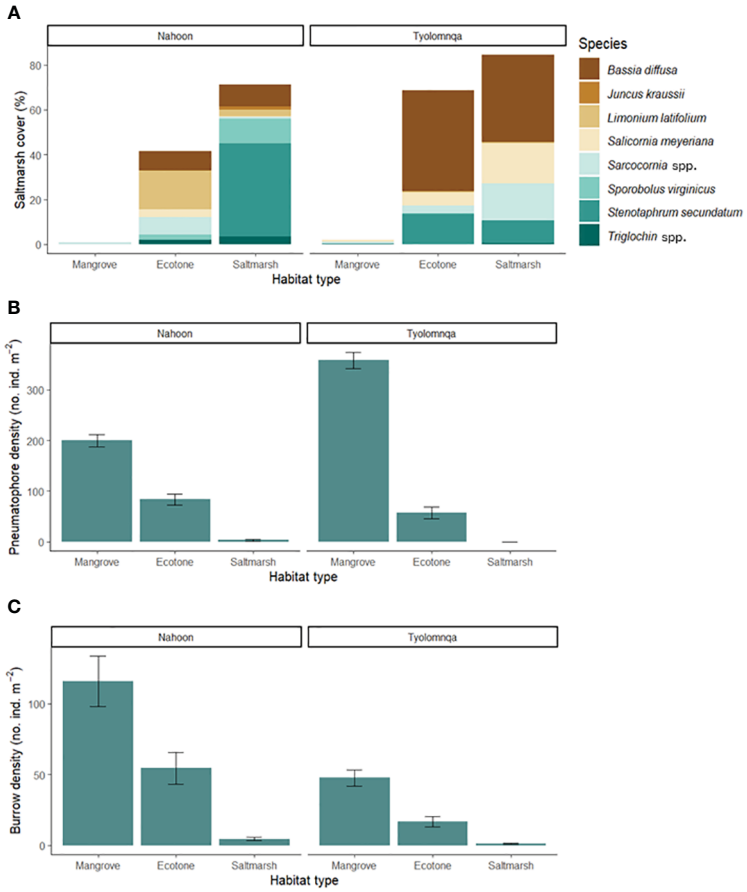

FIGURE 5
The composition and structure of the vegetation and crab burrows was characterised in 50 x 50 cm quadrats at each habitat type in both estuaries (Nahoon and Tyolomnqa) with **(A)** showing species composition of saltmarsh cover (%), **(B)** showing average (Standard Error) pneumatophore density (no. ind. m^{-2}) and **(C)** showing average (Standard Error) burrow density (no. ind. m^{-2}).

TABLE 9 Univariate generalised linear models for crab abundance, diversity and richness.

Univariate tests						
	Abundance (count)		Diversity		Richness	
	Dev	p	Dev	p	Dev	p
(Intercept)						
Root	53.296	**0.001***	33.72	**0.001***	92.346	**0.001***
Cover	35.917	**0.001***	7.637	**0.005***	26.388	**0.001***
Habitat	31.139	**0.001***	9.972	**0.008***	24.229	**0.001***
Site	29.893	**0.001***	0.003	0.953	0.877	0.508
Season	3.053	0.088	10.372	**0.004***	16.376	**0.001***

Model AIC score was 654.44. Proportion of deviance explained (Dev) and test significance values (p) are provided in bold*.

content (%) compared to the ecotones and saltmarshes which were much drier.

Lastly, the situation of mangroves and saltmarshes in relation to the adjacent estuary could also play a role in determining community structure, as mangroves in Nahoon and Tyolomnqa are situated adjacent to the estuarine water bodies and saltmarshes are situated further away. This results in more sesarmids occupying mangroves as they depend on water for respiration (Nobbs, 2003) and would thus require higher immersion rates. If mangrove associated species move into saltmarshes, it is likely that they can alter the ecosystem by either clearing saltmarsh species or changing the sediment composition. It is worth noting that many seedlings were recorded in both ecotones of Nahoon and Tyolomnqa, indicative of potential mangrove expansion into saltmarsh habitats. However, mangroves in Nahoon expanded in an open sandflat area rather than outcompeting saltmarsh species (Hoppe-Speer et al., 2015). Changes in the intertidal zone can favour saltmarshes over mangroves or vice versa (Whitfield et al., 2016).

4.4 Brachyuran ecology

The marsh crab, *Parasesarma catanatum*, was the only crab species that was common across all three habitats and both sites. This sesarmid crab is found at high densities in southern Cape estuaries within *Spartina* saltmarshes and is associated with

mangrove forests in Eastern Cape (Paula et al., 2003) as they consume both decomposed leaves of saltmarsh plants (Paterson & Whitfield, 1997; Bergamino and Richoux, 2015) and mangrove leaf litter (Lee, 1998). In Nahoon, aside from *P. catenatum*, *Neosarmatium africanum* and *Daniellela edwardsii* also occurred at all three habitat types. The red mangrove crab, *N. africanum* occurs in saltmarshes possibly because it can survive in drier areas (Dahdouh-Guebas et al., 1997) due to its semi-terrestrial air breathing trait (Lee, 1998). *Danielella edwardsii* is common in both mangroves and marshes, preferring wet, soft sand (Macnae, 1963). In Tyolomnqa, *D. edwardsii* was the dominant species. Although mangrove stands in Tyolomnqa are established, and despite the newly recorded presence of two fiddler crab species, the mangrove-associated macrofauna are still predominantly estuarine species that are known to occupy a range of different habitats (Peer et al., 2018b).

Fiddler crabs and grapsoids such as sesarmids differ in their burrowing and feeding activities (Warren and Underwood, 1986; Szura et al., 2017). Fiddler crabs create complex vertical burrows (Min et al., 2023) and are considered deposit feeders, consuming mainly microphytobenthos and plant and animal detritus (Dye and Lasiak, 1986), while sesarmids create simple and horizontal burrows (Min et al., 2023) and are considered herbivorous as they consume mangrove leaf litter (Micheli et al., 1991). The excessive burrowing and bioturbation from mangrove-associated fauna in saltmarshes can cause increased soil erosion and lower productivity of plants (Smith et al., 2013). Studies have shown that crabs such as *Parasesarma catenatum* and *Cyclograpsus punctatus* feed on the saltmarsh species in the genus *Spartina* (Alexander and Ewer, 1969; Smith and Tyrrell, 2012; Smith et al., 2013). If these species occur at high densities, they have the potential to weaken both above and below ground structures of saltmarsh causing a loss in plants and root decay (Coverdale et al., 2012). Whereas fiddler crabs could have positive effects on saltmarsh vegetation by oxygenating soil through bioturbation and enhancing sediment organic matter (Hughes et al., 2014).

5 Conclusion

Nahoon, the more established mangrove site, was dominated by mangrove-associated brachyuran species, while Tyolomnqa, the younger mangrove site, was still dominated by estuarine-associated crabs. Despite this, we present a new record of two fiddler crab species in Tyolomnqa, with one species occurring at a new southernmost limit. At both sites, mangrove-associated macrofauna do not occupy the saltmarsh habitat, however, with the expansion of mangroves into saltmarshes, it is possible that these species will start to move into saltmarsh habitats as reported in other studies (Whitfield et al., 2016; Cannizzo et al., 2018, 2019). Future studies should continue to monitor changes in brachyuran assemblages as mangroves continue to expand into saltmarsh habitats and investigate relationships between various saltmarsh species and mangrove-associated crabs.

Data availability statement

The raw data supporting the conclusions of this article will be made available by the authors, without undue reservation.

Author contributions

CK: Writing – original draft, Investigation, Formal analysis, Data curation, Conceptualization. AR: Writing – review & editing, Supervision, Resources, Methodology, Investigation, Funding acquisition, Conceptualization. NP: Writing – review & editing, Supervision, Resources, Project administration, Methodology, Investigation, Funding acquisition, Conceptualization.

Funding

The author(s) declare financial support was received for the research, authorship, and/or publication of this article. This work is based on the research supported by the National Research Foundation of South Africa through a Thuthuka Grant (Grant Reference TTK2204052094) and a Marine and Coastal Research Grant (Grant no. 136490). The authors acknowledge that opinions, findings and conclusions or recommendations expressed in this publication generated by the NRF supported research is that of the authors, and that the NRF accepts no liability whatsoever in this regard.

Acknowledgments

We are grateful to Emma Rossouw and Jake Mulvaney who assisted with data collection during field trips for this study. We would also like to thank Susana Fietz and Megan Mathese for use of their equipment during laboratory processing. A sampling permit was obtained from the Department of Forestry, Fisheries and the Environment of the Republic of South Africa (permit number Res2023–79).

Conflict of interest

The authors declare that the research was conducted in the absence of any commercial or financial relationships that could be construed as a potential conflict of interest.

Publisher's note

References

Adams, J. B. (2020). Salt marsh at the tip of Africa: Patterns, processes and changes in response to climate change. *Estuarine Coast. Shelf Sci.* 237, 106650. doi: 10.1016/j.ecss.2020.106650

Adams, J. B., Colloty, B. M., and Bate, G. C. (2004). The distribution and state of mangroves along the coast of Transkei, Eastern Cape Province, South Africa. *Wetlands Ecol. Manage.* 12, 531–541. doi: 10.1007/s11273-005-5165-0

Adams, D. H., Edwards, D. D., Schneider, J. E., and Searles, A. R. (2024). Range expansion and population shifts of estuarine fishes in a changing subtropical estuary. *Mar. Ecol. Prog. Ser.* 728, 221–238. doi: 10.3354/meps14314

Adams, J. B., and Human, L. R. D. (2016). Investigation into the mortality of mangroves at St. Lucia Estuary. *South Afr. J. Bot.* 107, 121–128. doi: 10.1016/j.sajb.2016.03.018

Adams, J. B., and Rajkaran, A. (2021). Changes in mangroves at their southernmost African distribution limit. *Estuarine Coast. Shelf Sci.* 248, 107158. doi: 10.1016/j.ecss.2020.107158

Adams, J. B., Veldkornet, D., and Tabot, P. (2016). Distribution of macrophyte species and habitats in South African estuaries. *South Afr. J. Bot.* 107, 5–11. doi: 10.1016/j.sajb.2016.08.001

Alexander, S. J., and Ewer, D. W. (1969). A comparative study of some aspects of the biology and ecology of *Sesarma catenata* and *Cyclograpsus punctatus* M.Edw., with additional observation on *Sesarma meinerti* De Man. *Zoologica Africana* 4, 1–35. doi: 10.1080/00445096.1969.11447364

Ashton, E. C., Hogarth, P. J., and Macintosh, D. J. (2003). A comparison of brachyuran crab community structure at four mangrove locations under different management systems along the Melaka Straits-Andaman Sea Coast of Malaysia and Thailand. *Estuaries* 26, 1461–1471. doi: 10.1007/BF02803654

Bergamino, L., and Richoux, N. B. (2015). Spatial and temporal changes in estuarine food web structure: differential contributions of marsh grass detritus. *Estuaries Coasts* 38, 367–382. doi: 10.1007/s12237-014-9814-5

Berry, A. J. (1972). The natural history of West Malaysian mangrove faunas. *Malayan Nat. J.* 25, 135–162. doi: 10.1136/jmg.9.1.135

Bertness, M. D. (1985). Fiddler crab regulation of *Spartina alterniflora* production on a New England salt marsh. *Ecology* 66, 1042–1055. doi: 10.2307/1940564

Bertness, M. D., Brisson, C. P., Bevil, M. C., and Crotty, S. M. (2014). Herbivory drives the spread of salt marsh die-off. *PloS One* 9, e92916. doi: 10.1371/journal.pone.0092916

Bertness, M. D., and Miller, T. (1984). The distribution and dynamics of *Uca pugnax* (Smith) burrows in a New England salt marsh. *J. Exp. Mar. Biol. Ecol.* 83, 211–237. doi: 10.1016/S0022-0981(84)80002-7

Bolosha, U. (2016). Revising the distribution of mangrove forests in South Africa and changes in growth of mangrove species along a latitudinal gradient (Masters dissertation, M. Sc. Thesis. Rhodes University, South Africa, 139.

Busey, P. (2003). *St. Augustine grass,* Stenotaphrum secundatum *(Walt.) Kuntze. Turfgrass biology, genetics, and breeding* (Hoboken, NJ: John Wiley & Sons), 309–329.

Cannicci, S., Fusi, M., Cimó, F., Dahdouh-Guebas, F., and Fratini, S. (2018). Interference competition as a key determinant for spatial distribution of mangrove crabs. *BMC Ecol.* 18, 1–12. doi: 10.1186/s12898-018-0164-1

Cannizzo, Z. J., Dixon, S. R., and Griffen, B. D. (2018). An anthropogenic habitat within a suboptimal colonized ecosystem provides improved conditions for a range-shifting species. *Ecol. Evol.* 8, 1521–1533. doi: 10.1002/ece3.3739

Cannizzo, Z. J., and Griffen, B. D. (2016). Changes in spatial behavior patterns by mangrove tree crabs following climate-induced range shift into novel habitat. *Anim. Behav.* 121, 79–86. doi: 10.1016/j.anbehav.2016.08.025

Cannizzo, Z. J., and Griffen, B. D. (2019). An artificial habitat facilitates a climate-mediated range expansion into a suboptimal novel ecosystem. *PloS One* 14, e0211638. doi: 10.1371/journal.pone.0211638

Cannizzo, Z. J., Nix, S. K., Whaling, I. C., and Griffen., B. D. (2019). Individual morphology and habitat structure alter social interactions in a range-shifting species. *Diversity* 11, no. doi: 10.3390/d11010006

Cavanaugh, K. C., Dangremond, E. M., Doughty, C. L., Williams, A. P., Parker, J. D., Hayes, M. A., et al. (2019). Climate-driven regime shifts in a mangrove–salt marsh ecotone over the past 250 years. *Proc. Natl. Acad. Sci.* 116, 21602–21608. doi: 10.1073/pnas.1902181116

Cavanaugh, K. C., Kellner, J. R., Forde, A. J., Gruner, D. S., Parker, J. D., Rodriguez, W., et al. (2014). Poleward expansion of mangroves is a threshold response to decreased frequency of extreme cold events. *Proc. Natl. Acad. Sci.* 111, 723–727. doi: 10.1073/pnas.1315800111

Chen, I. C., Hill, J. K., Ohlemüller, R., Roy, D. B., and Thomas, C. D. (2011). Rapid range shifts of species associated with high levels of climate warming. *Science* 333, 1024–1026. doi: 10.1126/science.1206432

Chen, X., Zhou, Z., He, Q., Zhang, H., Bouma, T., Gong, Z., et al. (2022). Role of abiotic drivers on crab burrow distribution in a saltmarsh wetland. *Front. Mar. Sci.* 9, 1040308. doi: 10.3389/fmars.2022.1040308

Clarke, K. R., and Gorley, R. N. (2009). PRIMER: Getting started with v6. PRIMER-E Ltd. Plymouth, United Kingdom.

Comeaux, R. S., Allison, M. A., and Bianchi, T. S. (2012). Mangrove expansion in the Gulf of Mexico with climate change: Implications for wetland health and resistance to rising sea levels. *Estuarine Coast. Shelf Sci.* 96, 81–95. doi: 10.1016/j.ecss.2011.10.003

Coverdale, T. C., Altieri, A. H., and Bertness, M. D. (2012). Belowground herbivory increases vulnerability of New England salt marshes to die-off. *Ecology* 93, 2085–2094. doi: 10.1890/12-0010.1

Dahdouh-Guebas, F., Verneirt, M., Tack, J. F., and Koedam, N. (1997). Food preferences of Neosarmatium meinerti de Man (Decapoda: Sesarminae) and its possible effect on the regeneration of mangroves. *Hydrobiologia* 347, 83–89. doi: 10.1023/A:1003015201186

Demopoulos, A. W., and Smith, C. R. (2010). Invasive mangroves alter macrofaunal community structure and facilitate opportunistic exotics. *Mar. Ecol. Prog. Ser.* 404, 51–67. doi: 10.3354/meps08483

Dye, A. H., and Lasiak, T. A. (1986). Microbenthos, meiobenthos and fiddler crabs: trophic interactions in a tropical mangrove sediment. *Mar. Ecol. Prog. Ser.* 32, 259–264. doi: 10.3354/meps032259

Edney, E. B. (1961). The water and heat relationships of fiddler crabs (*Uca* spp.). *Trans. R. Soc. South Afr.* 36, 71–91. doi: 10.1080/00359196109519035

Emmerson, W. D. (1994). Seasonal breeding cycles and sex ratios of eight species of crabs from Mgazana, a mangrove estuary in Transkei, southern Africa. *J. Crustacean Biol.* 14, 568–578. doi: 10.2307/1549002

Eslami-Andargoli, L., Dale, P. E. R., Sipe, N., and Chaseling, J. (2009). Mangrove expansion and rainfall patterns in Moreton Bay, southeast Queensland, Australia. *Estuarine Coast. Shelf Sci.* 85, 292–298. doi: 10.1016/j.ecss.2009.08.011

Flores, A. A., Abrantes, K. G., and Paula, J. (2005). Estimating abundance and spatial distribution patterns of the bubble crab *Dotilla fenestrata* (Crustacea: Brachyura). *Austral Ecol.* 30, 14–23. doi: 10.1111/j.1442-9993.2005.01409.x

Freitas, R. F., and Pagliosa, P. R. (2020). Mangrove benthic macrofauna: drivers of community structure and functional traits at multiple spatial scales. *Mar. Ecol. Prog. Ser.* 638, 25–38. doi: 10.3354/meps13260

Freitas, F. Jr., Pescinelli, R. A., Costa, R. C., Hilesheim, J. C., Dieh, F. L., and Branco, J. O. (2021). Brachyuran crab diversity across spatial and temporal scales in a mangrove ecosystem from the western Atlantic. *Regional Stud. Mar. Sci.* 43, 101703. doi: 10.1016/j.rsma.2021.101703

Gao, X., Gaitan-Espitia, J. D., and Lee, S. Y. (2024). Regulatory role of sesarmid crabs in nutrient dynamics and implications for the productivity of mangroves. *Estuarine Coast. Shelf Sci.* 298, 108655. doi: 10.1016/j.ecss.2024.108655

Geldenhuys, C., Cotiyane, P., and Rajkaran, A. (2016). Understanding the creek dynamics and environmental characteristics that determine the distribution of mangrove and salt marsh communities at Nahoon Estuary. *South Afr. J. Bot.* 107, 137–147. doi: 10.1016/j.sajb.2016.04.013

Giri, C., Ochieng, E., Tieszen, L. L., Zhu, Z., Singh, A., Loveland, T., et al. (2011). Status and distribution of mangrove forests of the world using earth observation satellite data. *Global Ecol. Biogeography* 20, 154–159. doi: 10.1111/j.1466-8238.2010.00584.x

Godoy, M. D., and Lacerda, L. D. D. (2015). Mangroves response to climate change: a review of recent findings on mangrove extension and distribution. *Anais da Academia Bras. Ciências* 87, 651–667. doi: 10.1590/0001-3765201520150055

Gutierrez, J. L. (2008). Crab influences on the export of plant detritus from salt marshes and mangroves: A review. In J. Chen and C. Guo (eds.), *Ecosystem Ecol. Res. Trends*, 327–344.

Hensel, M. J., Patrick, C. J., Orth, R. J., Wilcox, D. J., Dennison, W. C., Gurbisz, C., et al. (2023). Rise of Ruppia in Chesapeake Bay: Climate change–driven turnover of foundation species creates new threats and management opportunities. *Proc. Natl. Acad. Sci.* 120, e2220678120. doi: 10.1073/pnas.2220678120

Hodgson, A. N. (1987). Distribution and abundance of the macrobenthic fauna of the Kariega Estuary. *Afr. Zoology* 22, 153–162.

Hogarth, P. J. (2015). *The biology of mangroves and seagrasses* (Oxford, UK: Oxford University Press). doi: 10.1093/acprof:oso/9780198716549.001.0001

Hoppe-Speer, S. C., Adams, J. B., and Rajkaran, A. (2015). Mangrove expansion and population structure at a planted site, East London, South Africa. *South. Forests: J. For. Sci.* 77, 131–139. doi: 10.2989/20702620.2014.1001622

Hughes, A. R., Moore, A. F., and Piehler, M. F. (2014). Independent and interactive effects of two facilitators on their habitat-providing host plant, *Spartina alterniflora*. *Oikos* 123, 488–499. doi: 10.1111/j.1600-0706.2013.01035.x

Kelleway, J. J., Cavanaugh, K., Rogers, K., Feller, I. C., Ens, E., Doughty, C., et al. (2017). Review of the ecosystem service implications of mangrove encroachment into salt marshes. *Global Change Biol.* 23, 3967–3983. doi: 10.1111/gcb.13727

Kon, K., Kurokura, H., and Tongnunui, P. (2010). Effects of the physical structure of mangrove vegetation on a benthic faunal community. *J. Exp. Mar. Biol. Ecol.* 383, 171–180. doi: 10.1016/j.jembe.2009.11.015

Lee, S. Y. (1998). Ecological role of grapsid crabs in mangrove ecosystems: a review. *Mar. Freshw. Res.* 49, 335–343. doi: 10.1071/MF97179

Lee, S. Y. (1999). Tropical mangrove ecology: physical and biotic factors influencing ecosystem structure and function. *Aust. J. Ecol.* 24, 355–366. doi: 10.1046/j.1442-9993.1999.00984.x

Lenoir, J., and Svenning, J. C. (2015). Climate-related range shifts–a global multidimensional synthesis and new research directions. *Ecography* 38, 15–28. doi: 10.1111/ecog.00967

Leung, J. Y. (2015). Habitat heterogeneity determining the macrobenthic infaunal community in a mangrove swamp in South China: implication for plantation and plant invasion. *J. Coast. Res.* 31, 624–633. doi: 10.2112/JCOASTRES-D-13-00091.1

Liu, T., Liu, S., Wu, B., Xu, H., and Zhang, H. (2020). Increase of organic carbon burial response to mangrove expansion in the Nanliu River estuary, South China Sea. *Prog. Earth Planetary Sci.* 7, 1–9. doi: 10.1186/s40645-020-00387-3

Loveless, J. B., and Smee, D. L. (2019). Changes in arthropod communities as black mangroves *Avicennia germinans* expand into Gulf of Mexico salt marshes. *Arthropod-Plant Interact.* 13, 465–475. doi: 10.1007/s11829-018-9643-8

Lovelock, C. E., Feller, I. C., Ellis, J., Schwarz, A. M., Hancock, N., Nichols, P., et al. (2007). Mangrove growth in New Zealand estuaries: the role of nutrient enrichment at sites with contrasting rates of sedimentation. *Oecologia* 153, 633–641. doi: 10.1007/s00442-007-0750-y

Luk, Y. C., and Zajac, R. N. (2013). Spatial ecology of fiddler crabs, *Uca pugnax*, in southern New England salt marsh landscapes: potential habitat expansion in relation to salt marsh change. *Northeastern Nat.* 20, 255–274. doi: 10.1656/045.020.0213

Macintosh, D. J. (1984). *Ecology and productivity of Malaysian mangrove crab populations (Decapoda: Brachyura)*. Eds. E. Soepadmo and D. J. Rao A. N. & Macintosh (University of Malaya and UNESCO), 354–377. Proceedings of the Asean Symposium on Mangrove Environment – Research & Management. Chopmen Publishers: Singapore.

Macintosh, D. J., Ashton, E. C., and Havanon, S. (2002). Mangrove rehabilitation and intertidal biodiversity: a study in the Ranong mangrove ecosystem, Thailand. *Estuarine Coast. Shelf Sci.* 55, pp.331–pp.345. doi: 10.1006/ecss.2001.0896

Macnae, W. (1963). Mangrove swamps in South Africa. *J. Ecol.* 51, pp.1–pp25. doi: 10.2307/2257502

Micheli, F., Gherardi, F., and Vannini, M. (1991). Feeding and burrowing ecology of two East African mangrove crabs. *Mar. Biol.* 111, 247–254. doi: 10.1007/BF01319706

Min, W. W., Kandasamy, K., and Balakrishnan, B. (2023). Crab species-specific excavation and architecture of burrows in restored mangrove habitat. *J. Mar. Sci. Eng.* 11, 310. doi: 10.3390/jmse11020310

Mitchell, K. (2010). Quantitative analysis by the point-centered quarter method. arXiv preprint:1010.3303.

Muthukrishnan, R., Chiquillo, K. L., Cross, C., Fong, P., Kelley, T., Toline, C. A., et al. (2020). Little giants: a rapidly invading seagrass alters ecosystem functioning relative to native foundation species. *Mar. Biol.* 167, 1–15. doi: 10.1007/s00227-020-03689-8

Nobbs, M. (2003). Effects of vegetation differ among three species of fiddler crabs (Uca spp.). *J. Exp. Mar. Biol. Ecol.* 284, pp.41–pp.50. doi: 10.1016/S0022-0981(02)00488-4

Nobbs, M., and Blamires, S. J. (2017). Fiddler crab spatial distributions are influenced by physiological stressors independent of sympatric interactions. *J. Exp. Mar. Biol. Ecol.* 491, 19–26. doi: 10.1016/j.jembe.2017.03.007

Nomann, B. E., and Pennings, S. C. (1998). Fiddler crab–vegetation interactions in hypersaline habitats. *J. Exp. Mar. Biol. Ecol.* 225, 53–68. doi: 10.1016/S0022-0981(97)00209-8

Ólafsson, E., and Ndaro, S. G. (1997). Impact of the mangrove crabs *Uca annulipes* and *Dotilla fenestrata* on meiobenthos. *Mar. Ecol. Prog. Ser.* 158, 225–231. doi: 10.3354/meps158225

Osland, M. J., Enwright, N., Day, R. H., and Doyle, T. W. (2013). Winter climate change and coastal wetland foundation species: salt marshes vs. Mangrove forests in the southeastern United States. *Global Change Biol.* 19, 1482–1494. doi: 10.1111/gcb.12126

Paterson, A. W., and Whitfield, A. K. (1997). A stable carbon isotope study of the food-web in a freshwater-deprived South African estuary, with particular emphasis on the ichthyofauna. *Estuarine Coast. Shelf Sci.* 45, 705–715. doi: 10.1006/ecss.1997.0243

Paula, J., Dornelas, M., and Flores, A. A. V. (2003). Stratified settlement and moulting competency of brachyuran megalopae in Ponta Rasa mangrove swamp, Inhaca Island (Mozambique). *Estuarine Coast. Shelf Sci.* 56, 325–337. doi: 10.1016/S0272-7714(02)00165-8

Peer, N., Miranda, N. A. F., and Perissinotto, R. (2016). Suspended silt and salinity tolerances of the first zoeal stage of the fiddler crab Uca annulipes (Decapoda: Brachyura) and why marine connectivity is essential to the survival of the species. *African Journal of Marine Science* 38 (2), 161–169. doi: 10.2989/1814232X.2016.1169217

Peer, N., Miranda, N. A., and Perissinotto, R. (2015). A review of fiddler crabs (genus Uca Leach 1814) in South Africa. *Afr. Zoology* 50, 187–204. doi: 10.1080/15627020.2015.1055700

Peer, N., Perissinotto, R., Miranda, N. A. F., and Taylor, R. H. (2014). Temporal variations in the diversity of true crabs (Crustacea: Brachyura) in the St Lucia Estuary, South Africa. *Afr. Invertebrates* 55, 39–65. doi: 10.5733/afin.055.0103

Peer, N., Rajkaran, A., Miranda, N. A. F., Taylor, R. H., Newman, B., Porri, F., et al. (2018a). Latitudinal gradients and poleward expansion of mangrove ecosystems in South Africa: 50 years after Macnae's first assessment. *Afr. J. Mar. Sci.* 40, 101–120. doi: 10.2989/1814232X.2018.1466728

Peer, N., Rishworth, G. M., Miranda, N. A., and Perissinotto, R. (2018b). Biophysical drivers of fiddler crab species distribution at a latitudinal limit. *Estuarine Coast. Shelf Sci.* 208, 131–139. doi: 10.1016/j.ecss.2018.05.001

Perry, A. L., Low, P. J., Ellis, J. R., and Reynolds, J. D. (2005). Climate change and distribution shifts in marine fishes. *Science* 308, 1912–1915. doi: 10.1126/science.1111322

Pinsky, M. L., Selden, R. L., and Kitchel, Z. J. (2020). Climate-driven shifts in marine species ranges: Scaling from organisms to communities. *Annu. Rev. Mar. Sci.* 12, 153–179. doi: 10.1146/annurev-marine-010419-010916

Poloczanska, E. S., Brown, C. J., Sydeman, W. J., Kiessling, W., Schoeman, D. S., Moore, P. J., et al. (2013). Global imprint of climate change on marine life. *Nat. Climate Change* 3, 919–925. doi: 10.1038/nclimate1958

Raposa, K. B., McKinney, R. A., Wigand, C., Hollister, J. W., Lovall, C., Szura, K., et al. (2018). Top-down and bottom-up controls on southern New England salt marsh crab populations. *PeerJ* 6, e4876. doi: 10.7717/peerj.4876

Raw, J. L., Godbold, J. A., Van Niekerk, L., and Adams, J. B. (2019). Drivers of mangrove distribution at the high-energy, wave-dominated, southern African range limit. *Estuarine Coast. Shelf Sci.* 226, 106296. doi: 10.1016/j.ecss.2019.106296

Raw, J. L., van der Stocken, T., Carroll, D., Harris, L. R., Rajkaran, A., Van Niekerk, L., et al. (2022). Dispersal and coastal geomorphology limit potential for mangrove range expansion under climate change. *J. Ecol.* 111, 139–155. doi: 10.1111/1365-2745.14020

Raw, J. L., Van Niekerk, L., Chauke, O., Mbatha, H., Riddin, T., and Adams, J. B. (2023). Blue carbon sinks in South Africa and the need for restoration to enhance carbon sequestration. *Sci. Total Environ.* 859, 160142. doi: 10.1016/j.scitotenv.2022.160142

R Core Team. (2024). *R: A Language and Environment for Statistical Computing*. Vienna, Austria: R Foundation for Statistical Computing.

Saintilan, N., Wilson, N. C., Rogers, K., Rajkaran, A., and Krauss, K. W. (2014). Mangrove expansion and salt marsh decline at mangrove poleward limits. *Global Change Biol.* 20, 147–157. doi: 10.1111/gcb.12341

Sasekumar, A. (1974). The distribution of macrofauna on a Malayan mangrove shore. *J. Anim. Ecol.* 43, 51–69. doi: 10.2307/3157

Schweiger, O., Settele, J., Kudrna, O., Klotz, S., and Kühn, I. (2008). Climate change can cause spatial mismatch of trophically interacting species. *Ecology* 89, 3472–3479. doi: 10.1890/07-1748.1

Skilleter, G. A., and Warren, S. (2000). Effects of habitat modification in mangroves on the structure of mollusc and crab assemblages. *J. Exp. Mar. Biol. Ecol.* 244, 107–129. doi: 10.1016/S0022-0981(99)00133-1

Smee, D. L., Sanchez, J. A., Diskin, M., and Trettin, C. (2017). Mangrove expansion into salt marshes alters associated faunal communities. *Estuarine Coast. Shelf Sci.* 187, 306–313. doi: 10.1016/j.ecss.2017.02.005

Smith, S. M., and Tyrrell, M. C. (2012). Effects of mud fiddler crabs (Uca pugnax) on the recruitment of halophyte seedlings in salt marsh dieback areas of Cape Cod (Massachusetts, USA). *Ecol. Res.* 27, 233–237. doi: 10.1007/s11284-011-0886-4

Smith, S. M., Tyrrell, M. C., and Congretel, M. (2013). Palatability of salt marsh forbs and grasses to the purple marsh crab (*Sesarma reticulatum*) and the potential for re-vegetation of herbivory-induced salt marsh dieback areas in cape cod (Massachusetts, USA). *Wetlands Ecol. Manage.* 21, 263–275. doi: 10.1007/s11273-013-9298-2

Steinke, T. D. (1972). Further observations on the distribution of mangroves in the Eastern Cape Province. *Journal of South African Botany* 38, 165–178.

Steinke, T. D., Rajh, A., and Holland, A. J. (1993). The feeding behavior of the red mangrove crab Sesarma meinerti De Man 1887 (Crustacea: Decapoda: Grapsidae) and its effect on the degradation of mangrove leaf litter. *South Afr. J. Mar. Sci.* 13, 151–160. doi: 10.2989/025776193784287455

Steinke, T. D., and Ward, C. J. (2003). Use of plastic drift cards as indicators of possible dispersal of propagules of the mangrove Avicennia marina by ocean currents. *Afr. J. Mar. Sci.* 25, 169–176. doi: 10.2989/18142320309504007

Sweetman, A. K., Middelburg, J. J., Berle, A. M., Bernardino, A. F., Schander, C., Demopoulos, A. W. J., et al. (2010). Impacts of exotic mangrove forests and mangrove deforestation on carbon remineralization and ecosystem functioning in marine sediments. *Biogeosciences* 7, 2129–2145. doi: 10.5194/bg-7-2129-2010

Szura, K., Mckinney, R. A., Wigand, C., Oczkowski, A., Hanson, A., Gurak, J., et al. (2017). Burrowing and foraging activity of marsh crabs under different inundation regimes. *J. Exp. Mar. Biol. Ecol.* 486, 282–289. doi: 10.1016/j.jembe.2016.10.029

Taylor, D. I., and Allanson, B. R. (1993). Impacts of dense crab populations on carbon exchanges across the surface of a salt marsh. *Mar. Ecology-Progress Ser.* 101, 119–119. doi: 10.3354/meps101119

Theron, W., Peer, N., and Rajkaran, A. (2022). Effects of the mangrove forest environment and tree species characteristics on fiddler crab communities. *Mar. Freshw. Res.* 73, 1283–1296. doi: 10.1071/MF21309

Turki, Z., El-Shayeb, F., and Shehata, F. (2008). Taxonomic studies in the camphorosmeae (Chenopodiaceae) 1. Subtribe: kochiinae (Genera: bassia all., kochia roth and chenolea thunb.). *Acta Botanica Hungarica* 50, 181–201. doi: 10.1556/ABot.50.2008.1-2.14

Tyrrell, M. C., Courtney, S., Brown, E., and von Sperber, C. (2023). Burrowing crabs' influence on tidal marsh vegetation species composition and abundance in a temperate back-barrier marsh, Cape Cod, Massachusetts, USA. *J. Exp. Mar. Biol. Ecol.* 567, 151931. doi: 10.1016/j.jembe.2023.151931

van der Wal, D., and Herman, P. M. (2012). Ecosystem engineering effects of Aster tripolium and Salicornia procumbens salt marsh on macrofaunal community structure. *Estuaries Coasts* 35, 714–726. doi: 10.1007/s12237-011-9465-8

Virnstein, R. W. (1977). The importance of predation by crabs and fishes on benthic infauna in Chesapeake Bay. *Ecology* 6), 1199–1217. doi: 10.2307/1935076

Vorsatz, J. P. (2009). Ecological role of estuarine brachyuran crabs in mangrove and salt marsh estuaries, Eastern Cape, South Africa (Doctoral dissertation, PhD thesis. University of Port Elizabeth, South Africa.

Walker, J. E., Angelini, C., Safak, I., Altieri, A. H., and Osborne, T. Z. (2019). Effects of changing vegetation composition on community structure, ecosystem functioning, and predator–prey interactions at the saltmarsh-mangrove ecotone. *Diversity* 11, 208. doi: 10.3390/d11110208

Walker, J. B., Grosholz, E. D., and Long, J. D. (2021). Predicting burrowing crab impacts on salt marsh plants. *Ecosphere* 12, e03803. doi: 10.1002/ecs2.3803

Walther, G. R. (2010). Community and ecosystem responses to recent climate change. *Philos. Trans. R. Soc. B: Biol. Sci.* 365, pp.2019–2024. doi: 10.1098/rstb.2010.0021

Wang, Y. I., Naumann, U., Wright, S. T., and Warton, D. I. (2012). Mvabund–an R package for model-based analysis of multivariate abundance data. *Methods Ecol. Evol.* 3, pp.471–pp.474. doi: 10.1111/j.2041-210X.2012.00190.x

Wang, J. Q., Zhang, X. D., Nie, M., Fu, C. Z., Chen, J. K., and Li, B. (2008). Exotic *Spartina alterniflora* provides compatible habitats for native estuarine crab *Sesarma dehaani* in the Yangtze River estuary. *Ecol. Eng.* 34, pp.57–pp.64. doi: 10.1016/j.ecoleng.2008.05.015

Warren, J. H., and Underwood, A. J. (1986). Effects of burrowing crabs on the topography of mangrove swamps in New South Wales. *J. Exp. Mar. Biol. Ecol.* 102, pp.223–pp.235. doi: 10.1016/0022-0981(86)90178-4

Wasson, K., Raposa, K., Almeida, M., Beheshti, K., Crooks, J. A., Deck, A., et al. (2019). Pattern and scale: evaluating generalities in crab distributions and marsh dynamics from small plots to a national scale. *Ecology* 100, e02813. doi: 10.1002/ecy.2813

Weiskopf, S. R., Rubenstein, M. A., Crozier, L. G., Gaichas, S., Griffis, R., Halofsky, J. E., et al. (2020). Climate change effects on biodiversity, ecosystems, ecosystem services, and natural resource management in the United States. *Sci. Total Environ.* 733, 137782. doi: 10.1016/j.scitotenv.2020.137782

Whitfield, A. K., James, N. C., Lamberth, S. J., Adams, J. B., Perissinotto, R., Rajkaran, A., et al. (2016). The role of pioneers as indicators of biogeographic range expansion caused by global change in southern African coastal waters. *Estuarine Coast. Shelf Sci.* 172, 138–153. doi: 10.1016/j.ecss.2016.02.008

frontiers | Frontiers in Marine Science

TYPE Original Research
PUBLISHED 16 July 2024
DOI 10.3389/fmars.2024.1395000

OPEN ACCESS

EDITED BY
Kareen E. Schnabel,
National Institute of Water and Atmospheric Research (NIWA), New Zealand

REVIEWED BY
Ajit Kumar Mohanty,
Indira Gandhi Centre for Atomic Research (IGCAR), India
Hiroki Kise,
University of the Ryukyus, Japan

*CORRESPONDENCE
Emma Palacios Theil
emma.palaciostheil@biol.uni.lodz.pl

RECEIVED 02 March 2024
ACCEPTED 17 June 2024
PUBLISHED 16 July 2024

CITATION
Palacios Theil E and Błażewicz M (2024) Distribution of species in deep-sea biogeographic provinces and molecular phylogeny for the superfamily Neotanaoidea (Peracarida; Tanaidacea) indicate high levels of connectivity.
Front. Mar. Sci. 11:1395000.
doi: 10.3389/fmars.2024.1395000

Distribution of species in deep-sea biogeographic provinces and molecular phylogeny for the superfamily Neotanaoidea (Peracarida; Tanaidacea) indicate high levels of connectivity

Emma Palacios Theil* and Magdalena Błażewicz

Department of Invertebrate Zoology and Hydrobiology, Faculty of Biology and Environmental Protection, University of Lodz, Łódź, Poland

Here we analyze available recorded occurrences for species of Neotanaoidea, a deep-sea peracarid superfamily, in the frame of biogeographic bathyal, abyssal, and hadal provinces. In addition, we provide the first phylogeny based on molecular data for this group. Despite the existence of large knowledge gaps, the observed patterns reveal levels of connectivity across biogeographic provinces, oceans, and depths higher than initially expected for a superfamily consisting of relatively small deep-sea benthic invertebrates without a pelagic larval stage, and therefore hypothetically low mobility capabilities. We have detected neotanaid species with closely related populations across the Pacific Ocean or able to overpass a geographical barrier as significant as the Mid-Atlantic Ridge. Additionally, the molecular analyses expose the need for a taxonomic review of the four genera within Neotanaoidea. A search for better suited morphological and possibly ecological characters as diagnostic traits for genera and species should be undertaken, aiming at a better definition of the existing taxa and the description of new ones.

KEYWORDS

abyssal, bathyal, benthic crustacean, direct development, hadal, marine biodiversity, sexual dimorphism, small invertebrate

1 Introduction

Neotanaidae Lang, 1956 is a deep-water family within Tanaidacea, represented by species with most charismatic males. They grow up larger than most tanaidaceans [although with some exceptions (e.g. Kudinova-Pasternak, 1975)], and are therefore considered the giants of this order (Gardiner, 1975; Larsen, 2005; Błażewicz-Paszkowycz et al., 2012), even when they are relatively small if compared to other invertebrates. They

are distinguished by an exceedingly marked sexual dimorphism (Wolff, 1956; Gardiner, 1975) in addition to a set of unique morphological characteristics revealed by the females (Wi et al., 2015). Neotanaids lack eyes and the thoracic or spinning glands found in other tanaidaceans, they have antennules with seven or eight articles and antennae with nine, a mandible with strong and heavily calcified molars, well-developed maxillae with multiple specialized setae, an ischium is present in the chelipeds (although small and incomplete), and they count five pairs of pereopods, all of similar unspecialized "walking" type with a coxa present in all of them (e.g., Kakui et al., 2011 or Larsen et al., 2015, Figure 1A).

Despite them being found in all oceans at depths starting at 223 m (*Neotanais antarcticus* Kussakin 1967, www.obis.org, last visited 02 Feb 2024), neotanaids are not as often collected from the oceanic floor as other tanaidaceans and much is still unknown about their distribution patterns, life history, or behavior. They form a relatively diverse family represented currently by a total of 51 species, distributed among four genera: *Neotanais* Beddard, 1886, *Herpotanais* Wolff, 1956, *Carololangia* Gardiner, 1975, and *Venusticrus* Gardiner, 1975. That means that, out of the 36 extant tanaidacean families currently recognized, neotanaids hold place 16 regarding the number of species. Of the four genera, *Neotanais*, which was described as one of the first tanaidaceans ever, is the genus with the largest number of species. It covers 44 of the 51 species in the family. *Herpotanais* and *Venusticrus* include two and four species respectively, whereas *Carololangia* remains to this date a monotypic genus (Figure 1). In addition to the number of species and genera, the taxonomical classification of the entire family has been updated as well. It has transitioned along history from been originally grouped together with all other tanaidaceans in one family within the isopods, to being currently placed as a single family within Neotanaoidea, one of three superfamilies in the suborder Tanaidomorpha (Kakui et al., 2011).

The genus *Neotanais*, originally placed in the family Tanaidae, at that time part of the order Isopoda, was erected by Beddard (1886a). The same year, Norman and Stebbing (1886) described three species, assigned to the genus *Alaotanais* (Norman and Stebbing, 1886), and placed them within Tanaidae as well. They considered Isopoda to be a subclass rather than an order though, indicating a lack of consensus for higher taxonomic ranks in the group back then. Genus *Alaotanais* was later synonymized with *Neotanais*, since *Neotanais serratispinosus*, one of the three species described by Norman and Stebbing (1886), was declared a junior synonym of *N. americanus*, the first species introduced by Beddard (Gardiner, 1975). In 1895, Tanaidacea appeared on a publication for the first time as a name with the rank of order (Hansen, 1895). Later, Hansen (1913) reported on the Danish Ingolf Expedition, which explored Greenland, Iceland, and the Faroe Islands waters, and recorded the collection of two neotanaid species,

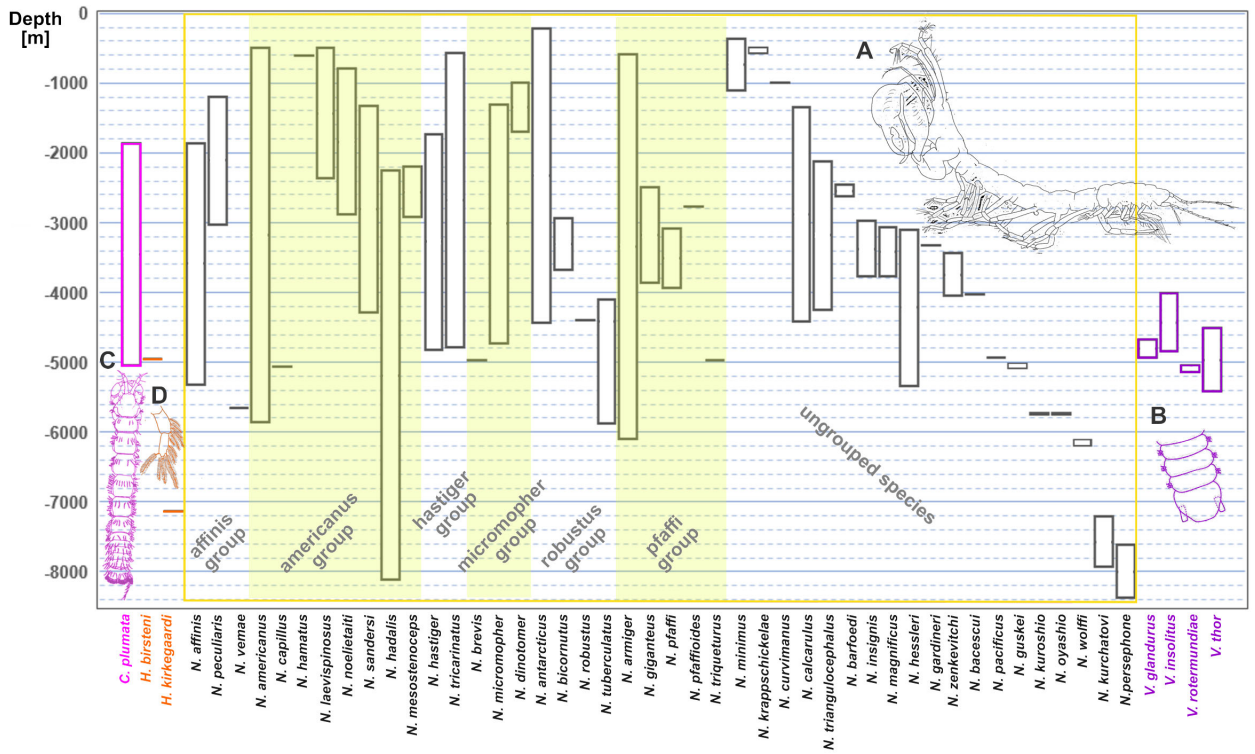

FIGURE 1
Depth ranges for the currently accepted 51 species and 4 genera of the family Neotanaidae. The text colour of the species names groups them into the four genera: *Carololangia*, *Herpotanais*, *Neotanais*, and *Venusticrus*. Golden shades separate the genus *Neotanais* into the six "Gardiner groups" (Gardiner, 1975). **(A)** Male of a species of *Neotatanis* from the Sea of Okhotsk. **(B)** Part of the pleotelson of *V. thor*, redrawn from [Araújo-Silva et al. (2015), (fig. 5K)], to show the ventral attachment of the uropods, characteristic for the genus. **(C)** *Carololangia plumata*, only species of its genus, redrawn from [Gardiner (1975): (fig. 74, as *C. mirabunda*)], and **(D)** pleopod of *Herpotanais kirkegaardi*, with one ramus only, characteristic of the genus, redrawn from [Gardiner (1975): (fig. 88)].

one of them previously undescribed. Nevertheless, Hansen did not yet deem necessary to establish a new family for the genus. That happened only after Lang studied details in antennules, antennae, and mouth parts of a few *Neotanais* species (Lang, 1956). He recognized the similarities and differences to other tanaidaceans and proposed a new system for the order, dividing it into five families (two of them new) separated in two suborders, based on the morphology of cephalothorax appendages, the number of oostegites in the marsupium, and the genital cones in males. Neotanaidae was accepted as a distinct group, at an intermediary position between what were at the time the families Apseudidae, Tanaidae and Paratanaidae. The particular placement of neotanaids among them, however, varied depending on the weight attributed by the different authors to the chosen set of morphological characters (Lauterbach, 1970; Gardiner, 1975; Sieg, 1980a; Sieg, 1984). Eventually, Sieg (1980b) found the differences between families larger than previously considered and replaced Lang's two-suborder system with a classification consisting of four suborders, one of them being Neotanaidomorpha, elevating thus the rank for neotanaids. A revision of fossil tanaidaceans led to the addition of a fifth, extinct, superfamily (Schram et al., 1986). Suborder Neotanaidomorpha, however, suffered no change, until the taxonomic relationships within the order Tanaidacea were analyzed using molecular methods (Kakui et al., 2011). These phylogenetic analyses revealed that the relationships between some of the previously established suborders are closer than suggested by their ranks. These associations were supported by morphological characters as well, which warranted an amendment of the previous five-suborder classification. The classification established by Kakui et al. (2011) for extant tanaidaceans divides the group into two suborders, Apseudomorpha and Tanaidomorpha, which encompass apseudids, tanaids, paratanaids and neotanaids, accepted currently as superfamilies. Neotanaids are placed within suborder Tanaidomorpha as a superfamily composed of a single family. Some claim the suborder rank is still under debate (Larsen et al., 2015), nevertheless the two-suborder classification system for extant species is accepted as the current valid system at the World Register of Marine Species (WoRMS, http://www.marinespecies.org, last visited 02 Feb 2024). According to the most updated classification, Neotanaoidea is the only of the four superfamilies within Tanaidacea composed solely of deep-sea species. This makes it an important key for resolving the puzzle of colonization, diversity, and evolution of invertebrates in the ocean depths.

The genera within Neotanaidae can be distinguished by morphological characters, including the shape and size of pereopods and uropods, together with their setation or spines, the number of pleopod rami, the geometry of the pleoteson, or the number of articles for the antennae (Figure 1).

Gardiner (1975) established a key for the genera, although Araújo-Silva et al. (2015) provided a re-diagnosis for *Venusticrus* when describing *V. thor* and reassigning *Neotanais rotermundiae* Gardiner, 1975 to this genus as well. On the other hand, Larsen (1999) produced a key for the 30 species for which the female was known, out of the 37 species described at the time. The differences between species can be subtle and elusive. Rather than by a particular character, most species are identified by a combination, or a set of morphological features. Furthermore, identification can be challenging due to marked sexual dimorphism, differences among developmental (ontogenetic) stages, and the fact that deep-sea collections are usually low in numbers and in many cases one of the sexes or some stages remain unknown. Neotanaid species, similar to other deep-sea tanaidacenas, are usually described based on the female, since they are more common, and for more than a dozen the males are unknown. However, the opposite is true for *N. magnificus* Kudinova-Pasternak, 1972 and *N. mesostenoceps* Gardiner, 1975. They were described on the basis of a male specimen and the females remain unknown. In some cases, not all developmental stages are known either. The most notable example is *N. hessleri* Gardiner, 1975, known only from two mancas. These facts deliver additional compelling arguments for an integrative approach when tackling the study of the biodiversity, taxonomy, and ecology of the group, for which molecular data will be necessary. However, DNA fragments are available so far only for two of the 51 neotanaid species (GenBank, www.ncbi.nlm.nih.gov/genbank/, last visited 2 Feb 2024). Furthermore, only one of them, *Venusticrus thor* Araújo-Silva and Larsen, 2015, has been identified to specific level. The second taxon for which DNA sequences are available was simply identified as *Neotanais* sp. Additionally, one transcriptome is available for a taxon identified as *Neotanais* cf. *kuroshio*, included in a study on the silk proteins of tanaidaceans (Kakui et al., 2021).

Here we initiate an integrative-approach study of the singular deep-sea superfamily Neotanaoidea. Initially we analyze available records for occurrences of neotanaids worldwide to compare their distribution among bathyal and hadal oceanic biogeographic provinces. In addition, we are building the first molecular phylogeny for neotanaids, using material collected relatively recently and preserved in a way that allows for nucleic acids extraction and sequencing, in order to scope the magnitude of genetic diversity and connectivity across oceanic regions and ocean depths.

2 Materials and methods

In future mentions the following abbreviations will be used for DNA fragments: *COI* and *H3* for the mitochondrial cytochrome c oxidase subunit I and the nuclear histone subunit 3 genes respectively, and *16s*, *18s*, and *28s* for the mitochondrial *16s rRNA*, and the nuclear *18s* and *28s rRNA* genes.

For the sampling campaigns from which the sequenceable material was obtained we will use in figures and tables the following abbreviations:

AleB: AleutBio, in 2022, aboard the RV Sonne along the Aleutian Trench, led by the Senckenberg Gesellschaft für Naturforschung, Germany.

Div3: Diva3, in 2009, latitudinal gradients of deep-sea biodiversity in the Atlantic, aboard the RV Meteor, German Centre of Marine Biodiversity (DZMB).

IceA: IceAge, Icelandic marine animals: genetics and ecology, in 2011, aboard the RV Meteor, German Centre of Marine Biodiversity (DZMB).

JPIO: JPI Oceans Ecological Aspects of Deep-Sea Mining, in 2015, aboard the RV Sonne at the Mn-nodule belt in the Clarion-Clipperton Zone (CCZ), Joint Programming Initiative Healthy and Productive Seas and Oceans.

KaD: KanaDeep, in 2019 aboard L'Atalante, off New Caledonia, French National Museum of Natural History (MNHN) and Research Institute for Development (IRD).

KuB: KuramBio, Kuril-Kamchatka Biodiversity studies, in 2012 and 2016, aboard the RV Sonne, German Ministry for Science and Education (BMBF) and Russian Scientific Foundation.

Saya: MEIO1-Saya, Monaco Explorations Indian Ocean Expedition, Saya de Malha ecosystem, in 2022 aboard the SA Agulhas.

SoB: SokhoBio, Sea of Okhost expedition, in 2015, aboard the Akademik M.A. Lavrentyev, German Ministry for Science and Education (BMBF) and Russian Scientific Foundation.

VT: Vema-TRANSIT, in Dec 2014 – Jan 2015, aboard the RV Sonne, in the Vema Fracture are and the Puerto Rican Trench, GEOMAR Helmholtz-Zentrum für Ozeanforschung, Germany.

The abbreviations used for sampling gear are:

AGT: Agassiz Trawl.

BC: box corer.

EBS: epibenthic sledge.

2.1 Analyses of the geographical and depth distributions for neotanaids

Data on occurrences for geographical distribution and depth for neotanaids were downloaded from OBIS (Ocean Biodiversity Information System, obis.org, March 2023). We checked for duplicates, updated the list with the most recently described species, and completed the information, when possible, with records from the literature. Most records correspond to the original species descriptions, and nearly half of the species have been reported only for the type location. Other entries can be traced back to digitally available museum collections, such as those for the natural history museums in London or the Smithsonian Institution in Washington DC. The information shown reflects only the occurrences for taxa identified to species level (Figures 2, 3). Out of the 635 records, about 70 occurrences correspond to unidentified neotanaids, simply identified as "*Neotanais* sp." or "Neotanaidae". Although only records from digitalized collections and published occurrences were available to us, the available data shed some light on the known geographical and depth distribution for members of the family.

The distribution of neotanaid records was evaluated in the frame of the biogeographic provinces proposed by Watling et al. (2013) for the ocean floor. In order to do that, two layers with biogeographic provinces, kindly provided by Les Watling, were mapped together with the layer containing the occurrences for neotanaids and analyzed using QGIS 3.22.14 (newer versions available at http://qgis.org, last checked 31 Jan 2024). When defining these biogeographic provinces, Watling et al. (2013) excluded from their analyses regions within economic exclusive zones (EEZs) by discarding bathymetric data from layers above 800 m depth. For the evaluation of the neotanaid occurrences studied here it means that only 15 points could not be assigned to one of the provinces as described by Watling. Nevertheless, most of them belong to locations within the Gulf of Mexico or off Antarctica, and all of them could be manually assigned to a region. The layers provided did not include hadal provinces, since for these Watling et al. (2013) adopted the ones proposed by Belyaev (1989). For our case in particular, this had very little impact on the analyses of species among provinces again, since only 18 of the records were located in hadal zones, most of which could be easily attributed to well-known deep-sea trenches.

2.2 Molecular data

A collection of more than 320 neotanaid samples from all over the world were available to us at the University of Lodz, gathered from sampling campaigns carried out in the last 15 years, or from museum loans. The samples were visually examined and for every project they were roughly divided into morphogroups, for which sequencing attempts were made, targeting both mitochondrial (*16s*, *COI*) and nuclear markers (*18s*, *28s*, *H3*). Tentative identifications of the specimens to species were made, however, are not included here. Additional morphological studies, beyond the scope of the current work, are ongoing, aiming at refining valid diagnostic characters and apomorphies to characterize potential new genera, and in some cases, when the available number of specimens allows, including morphometrics and species delimitation analyses, in order to distinguish members of species complexes. For the purposes of the present work, specimens used for molecular studies are identified to the level of genus, and given numeric identifications in combination with a code assigning them to the corresponding sampling campaign. Two of the analyzed specimens were loaned from the Victoria Museum in Melbourne, Australia, and are labelled "aus". When necessary, also haplotypes are properly identified. This will make it possible to track the specimens used in this study, if future investigations should so require (Table 1; Figure 4; Supplementary Figures S1–S4). Genomic DNA was extracted using the Sherlock AX kit for DNA purification (A&A Biotechnology, Gdynia, Poland), following the instructions indicated for fresh tissue, although adding a step to re-hydrate the tissue in sterile water, before the lysis step. If the specimens were small (up to 1-2 mm), the whole animal was used in the extractions, but if the specimen was large enough and both chelipeds were available, one of them was dissected and used in the extraction. In some cases, if parts of the specimen were already damaged or detached, they were used for the DNA extraction instead. When possible, the specimens or the parts used in the extractions were recovered after the lysis step for future potential morphological analyses. The isolation protocol was slightly modified to increase the yield of extracted DNA: after the washing steps, when mixing

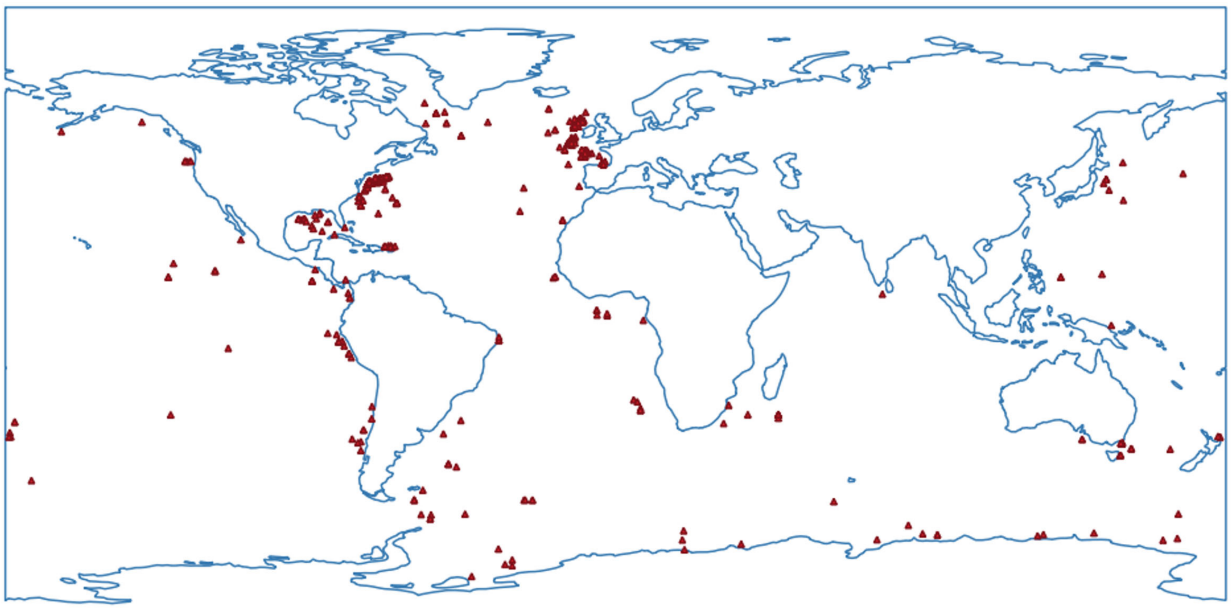

FIGURE 2
Map of the available occurrences for samples of Neotanaidae identified to the level of species, obtained from the Ocean Biodiversity Information System (www.obis.org) and curated to eliminate duplicates, and to add data from recent species descriptions and digitally available museum collections.

the filtrates with DNA with the isopropanol solution, instead of continuing right away with the next step, the mix was incubated at -20°C for a few hours (usually overnight). The DNA was resuspended in the TE buffer provided with the kit.

Polymerase chain reactions (PCRs) were performed following the recommendations of the polymerase's manufacturer (DreamTaqTM Green DNA polymerase, Thermo-Fisher Scientific, Waltham, MA, USA, and AccuStart II PCR SuperMix, QuantaBio, Beverly, MA, USA). The fragments targeted were the mitochondrial *COI* and *16s*, as well as the nuclear *18s*, *28s* and *H3* genes. For *COI* we used primers LCOI-1490 and HCOI-2198 (Folmer et al., 1994), and their degenerated forms designed by Astrin and Stüben (2008) (LCOI1490-JJ and HCOI2198-JJ), and by Lobo et al. (2013) (LoboF1 and LoboR1). For *16s* we used primers Ft_amp and Rt2_amp, designed for amphipods (Lörz et al., 2018), but that have proven successful also for their use with neotanaids. Some fragments for *18s*, *28s*, and *H3* could be obtained using primers 18s 4F and 18s 2R (Pitz and Sierwald, 2010) or SSU_F04 and SSU_R22 (Blaxter et al., 1998), 28sA and 28sB (Taylor et al., 1999), and Hex3AF and Hex3AR (Svenson and Whiting, 2004) respectively. The PCR conditions for amplifying *COI* and *28s* sequences followed the protocol indicated by Hou et al. (2007) for

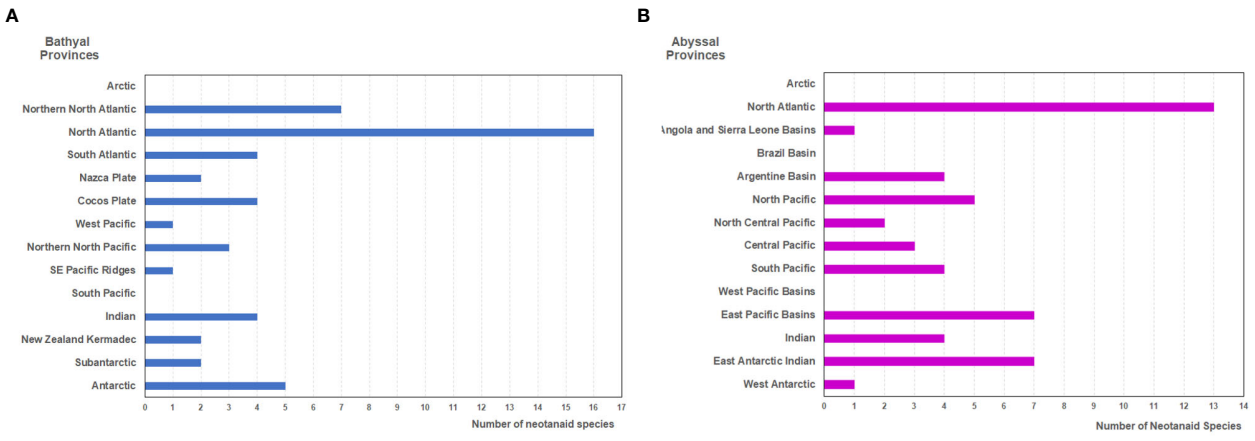

FIGURE 3
Number of neotanaid species in the biogeographic provinces of the deep ocean floor (as proposed by Watling et al., 2013) for **(A)** bathyal, and **(B)** hadal provinces.

TABLE 1 Specimens used for the phylogenetic analyses of the superfamily Neotanaoidea.

taxon	station	coordinates	depth [m]	gear	GenBank accession numbers		
					COI	16s	H3
***Neotanais* sp. 1 AleB HT1**	8-69	52.37; -167.03	4544 – 4608	EBS	PP977046	PP976932	PP977425
***Neotanais* sp. 1 AleB HT2**	2-20	54.56; -171.57	3649 – 3651	EBS	PP977048	PP976935	PP977426
***Neotanais* sp. 1 AleB HT3**	2-20	54.56; -171.57	3649 – 3651	EBS	PP977047	PP976933	–
***Neotanais* sp. 1 SoB HT1**	11-6	45.59; 146.41	3206	EBS	PP977050	PP976934	PP977428
***Neotanais* sp. 1 SoB HT2**	4-10	47.20; 149.61	3366	EBS	PP977049	PP976959	PP977427
***Neotanais* sp. 2 Div3**	534-1	-36.01; -49.03	4607	EBS	PP977051	PP976936	–
***Neotanais* sp. 3 VT**	13-4	19.78; -67.10	8329 – 8317	EBS	PP977054	PP976940	PP977430
***Neotanais* sp. 4 SoB**	9-9	46.26; 152.05	3580	AGT	PP977053	PP976939	–
***Neotanais* sp. 5 IceA**	1172-1	67.57; -6.92	2457	EBS	PP977052	PP976938	PP977429
***Neotanais* sp. 6 IceA**	1069-1	62.99; -28.09	1588 – 1626	EBS	PP977045	PP976937	–
***Neotanais* sp. 7 AleB**	7-63	51.37; -168.94	6556	BC	PP977041	PP976949	PP977423
***Neotanais* sp. 8 KuB**	2-9	46.91; 154.50	4830 – 4863	EBS	PP977040	PP976948	–
***Neotanais* sp. 9 JPIO**	20	11.00; -117.14	4144 – 4093	EBS	PP977043	PP976947	PP977424
***Neotanais* sp. 10 KuB**	7-9	43.09; 153.03	5216 – 5223	EBS	PP977042	PP976946	–
***Neotanais* sp. 11 Div3**	636-1	29.32; -28.63	4338	EBS	PP977044	PP976945	–
***Neotanais* sp. 12 JPIO**	197	18.81; -128.38	4805	EBS	PP977055	–	PP977431
***Neotanais* sp. 13 KaD**	EB5082	-24.49; 168.73	2376 – 2376	EBS	PP977032	PP976953	PP977419
***Neotanais* sp. 14 IceA**	1057-1	61.64; -31.36	2504 – 2531	EBS	PP977031	PP976952	PP977418
***Neotanais* sp. 15 aus HT1**		-41.63; 149.33	4022 – 4052		PP977029	PP976950	–
***Neotanais* sp. 15 aus HT2**		-32.09; 153.25	1741 – 2115		PP977030	PP976951	PP977417
***Neotanais* sp. 16 KaD**	EB5076	-23.88; 170.02	3674 – 3676	EBS	PP977039	PP976944	–
***Neotanais* sp. 17 Saya**	CP5412	-9.75; 60.8	1441 – 1396		PP977038	PP976943	–
***Neotanais* sp. 18 IceA**	1010-1	62.55; -20.40	1384 – 1389	EBS	PP977037	PP976942	–
***Venusticrus* sp. Div3**	593-1	-3.95; -28.09	5190		PP977028	PP976941	PP977416
***Venusticrus* sp. VT HT1**	12-6	19.82; -66.76	8340 – 8336	EBS	PP977034	PP976955	PP977421
***Venusticrus* sp. VT HT2**	6-7	10.36; -36.93	5102 – 5079	EBS	PP977033	PP976954	PP977420
***Venusticrus thor* JPIO**	118	13.87; -123.25	4511	EBS	PP977036	PP976957	PP977422
***Venusticrus thor* KuB**	1-10	43.97; 157.4	5423 – 5429	EBS	PP977035	PP976956	–
Apseudomorphan OutGr (*Carpoapseudes varindex*)	SoB 5-3	48.62; 150.05	1700	BC	PP977541	PP976958	PP977415

Taxa are identified to the level of genus, to species for Venusticrus thor, the only neotanaid species with genetic data previously available on GenBank. For tracking down of the corresponding specimens, the abbreviation of the corresponding sampling campaign or museum lending the material (see Material and Methods) is added. When necessary, the haplotypes are identified with the abbreviation HT and assigning them a number.

COI. The settings for *16s* and *H3* fragments included an initial 5 min activation at 95°C, followed by 36 cycles of 30 s at 95°C, 60 s at 48°C, 60 s at 72°C, and a final 5 min extension at 72°C. The PCR conditions for *18s* were similar to those for *16s*, but with an annealing temperature of 54°C and an extension time of 120 s. A 2-µl aliquot of the PCR product was visualized in a Midori Green-stained (Nippon Genetics) 1.5% -agarose gel to verify its quality and length and consequently 5 µl of PCR products were cleaned using a combination of 0.1 µl Exonuclease I (0.1 µl) and 1 µl Fast Polar-BAP Thermosensitive Alkaline Phosphatase (EURx Sp.z o.o., Gdansk, Poland), diluted with 1.9 µl water for reactions following a standard protocol including 15 min incubation at 37°C and 15 min inactivation at 85°C. The cleaned PCR products with the appropriate primers were sent for sequencing at Macrogen Europe (Amsterdam, Netherlands). The obtained sequences were assembled and manually edited, when necessary, with Geneious Prime® 2023.2.1 (Biomatters Ltd., Boston, MA, USA). To reduce the chances of including pseudogenes or contaminated fragments in

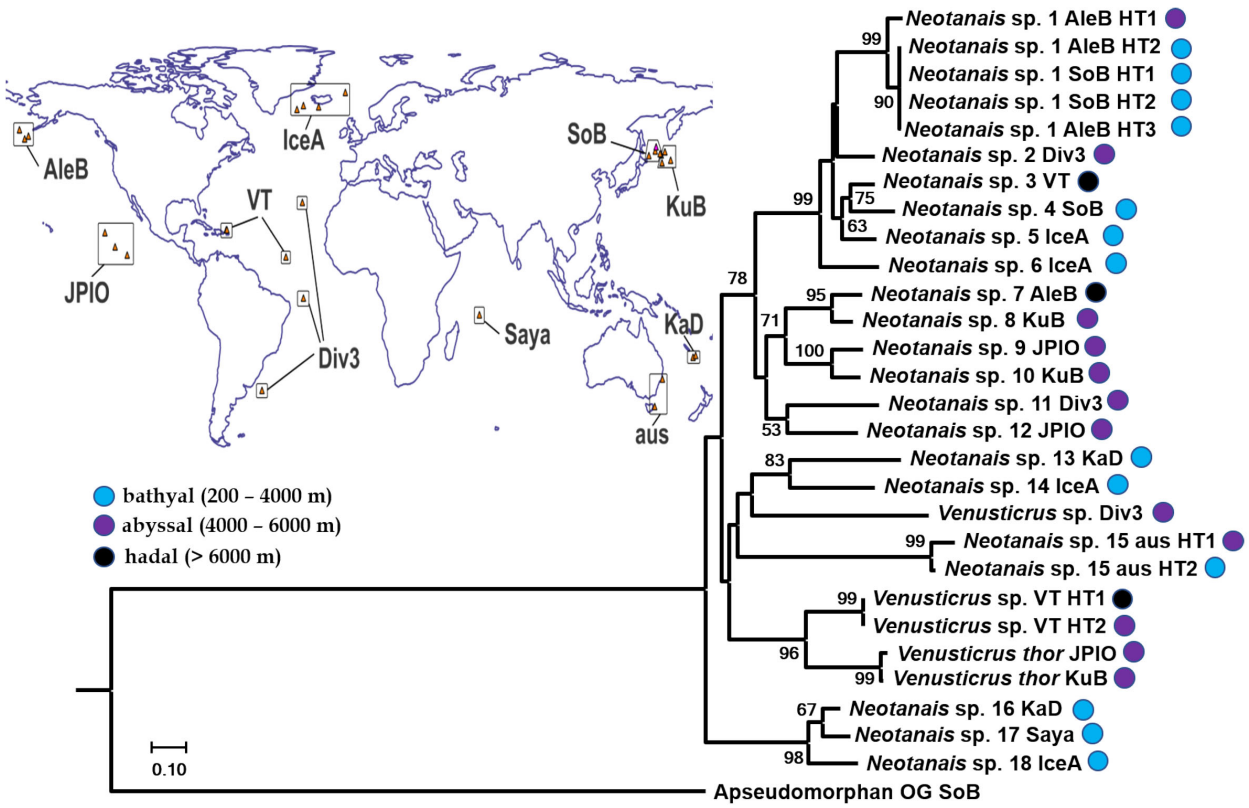

FIGURE 4
Phylogeny of Neotanaoidea (best tree) inferred from Maximum Likelihood analysis (RAxML) of concatenated 1360 bp long sequences including fragments of the mitochondrial *COI* (656 bp) and *16S* (375 bp), and the nuclear *H3* (329 bp) genes. Bootstrap values (5000 bp with bootstopping) are shown when higher than 50%. Taxa are identified to the level of genus, to species for *Venusticrus thor*, the only neotanaid species with genetic data previously available on GenBank. For tracking down of the corresponding specimens, the abbreviation of the corresponding sampling campaign or museum lending the material (see Material and Methods) is added. When necessary, the haplotypes are identified with the abbreviation HT and assigning them a number. Locations for the sampling campaigns are indicated on the included world map.

the analyses, the obtained sequences were compared with those available on GenBank using the BLASTn suite (Basic Local Alignment Search Tool, Altschul et al. 1990). Preliminary alignments for the *16s*, *COI* and *H3* sequences were assembled, including the apseudomorphan *Carpoapseudes varindex* Bamber, 2007 as an outgroup, and subsequently concatenated into one final alignment with BioEdit 7.1.3.0 (Hall, 1999). An additional concatenated alignment was built with the two mitochondrial genes. The number of sequences successfully obtained for the other two nuclear genes, *18s* and *28s*, was very low, and were therefore not included in the concatenated alignment. Nevertheless, the combinations of *16s*, *COI* and *H3*, and of *16s* and *COI*, have shown enough resolution for the identification of neotanaids to specific level, with the possibility for further studies on the relationships among neotanaids in the future, when more sequences will be available for comparison and additional taxa can be included in the analyses.

Prior to the concatenation, the *16s* alignment was tested for accuracy with MUSCLE (Multiple Sequence Comparison by Log-Expectation; Edgar, 2004) using the online tool made available by the European Bioinformatics Institute (www.ebi.ac.uk, last visited 29th Jan 2024). Poorly aligned positions were identified with Gblocks v. 0.91b (Castresana, 2000) using the online tool on http://www.phylogeny.fr/index.cgi (Dereeper et al., 2008, last visited 29th Jan 2024) allowing all three categories for choosing a less stringent selection. This was not necessary for the *COI* or the *H3* alignments, as the alignments had no gaps.

The resulting concatenated alignment had a total sequence length of 1357 bp, for which 656 bp corresponded to *COI*, 375 bp to *16s* and 329 bp to *H3*. This alignment, the concatenated alignment of both mitochondrial genes, as well as the alignments for the individual genes were submitted to the Cyberinfrastructure for Phylogenetic Research (CIPRES) web portal (www.phylo.org, last visited 19th Nov 2023) for Model test of the individual gene alignments (jModelTest2 on XSEDE, Darriba et al., 2012) and Randomized Accelerated Maximum Likelihood (RAxML) analyses (Stamatakis et al., 2008) using the RAxML-NG tool with 5000 bootstraps, although using autoMRE with a cutoff of 0.3 for bootstopping, choosing the "All-in-One" option, indicating the outgroup and the partition. The best models resulting from the model tests, and subsequently indicated in the partition, were HKY +I+G for *COI*, TIM2+G for *16s* and K80+I+G for *H3*. The resulting trees from the RAxML analyses were visualized and analyzed with Mega 11.0.11 (Tamura et al., 2021). The obtained tree files were

edited with Microsoft PowerPoint (Microsoft Office 2019) and Corel Photo-Paint (Home & Student 2018, v. 20.0.0.633). The fragments resulting from these Sanger sequencing efforts have been accessioned to GenBank (Table 1). The corresponding sequences will be updated in a near future in order to add the identification of the specimens to species, once associated morphological and morphometric studies, discussed in upcoming papers, make it possible. Furthermore, the studied specimens will be deposited at a museum, the Senckenberg Museum in Germany for samples associated with German projects or the National Museum of Natural History in France for samples from projects funded by French and Monegasque agencies, where they will be properly catalogued and linked accordingly to their GenBank accession numbers.

In addition to the phylogenetic analyses, genetic distances were calculated for the *COI* sequences. The fragments were trimmed to the length of the shortest sequence (507 bp) and the genetic distances were obtained using DNADIST version 3.5c (copyright 1986-1993 by Joseph Felsenstein and the University of Washington) on BioEdit 7.1.3.0 (Hall, 1999).

3 Results

3.1 Biogeographic patterns

The map (Figure 2) shows the world distribution of the current records for neotanaid samples. We have counted a total of 565 individual occurrences for neotanaid samples identified to species. Of these occurrences, 410 are located in the North Atlantic.

Mapping the occurrences for neotanaid species together with the layers provided by Watling et al. (2013) with the bathyal and abyssal biogeographic provinces for the deep-sea floor allowed us to assign a province to a large majority of our records. Of the 565 individual records, only 36 did not match any of these bathyal or abyssal biogeographic provinces. These 36 records correspond for the most part to locations where neotanaids were collected from waters 6156 m deep or more (18 occurrences) and from waters 676 m deep or less (15 occurrences). The records from the deepest waters represent collections resulting from the exploration of deep-sea trenches (Puerto Rican trench 11 records, Kermadec Trench three records, South Sandwich Trench two records, Mariana Trench one record, all deeper than 7150 m) and from the North Pacific, off Honshu, Japan (one record). The occurrences from shallower waters were recorded in the Gulf of Mexico (six records), the Antarctic (four records), off the coast of Pernambuco, Recife (three records), the straits of Florida (one record) and off Valentia, southwest of Ireland (one record). In addition, three occurrences did not fall into any of biogeographic provinces as described by Watling et al. (2013), although their depths were within the bathyal or the abyssal range: one location off the Falkland Islands at -1105 m, one off Antarctica at -2920 m, and one location west of Nicaragua at -3777 – -3950 m.

Neotanaids have been recorded in all but in two of the 14 bathyal biogeographic provinces (Figure 3A). Figure 3 shows the number of neotanaid species present in each of these provinces. The North Atlantic is, with 16 species, the province that hosts the most species, followed by far by the Northern North Atlantic, where seven neotanaid species are present. In a bathyal province usually two to five species can be found. In the West Pacific province and the south east Pacific ridges, on the other hand, only one neotanaid taxon is present, whereas in the Arctic and the South Pacific provinces, no neotanaid has been recorded.

The distribution of neotanaid species among the 14 abyssal biogeographic provinces (Figure 3B) shows to some extent a similar picture. The North Atlantic province displays again the highest diversity in terms of number of neotanaid species. Whereas the highest number for neotanaid species present in an abyssal province is four or five, the North Atlantic hosts 13 species. It is followed in numbers by the East Pacific Basins with seven. For the abyssal provinces, the Antarctic is divided into East Antarctic Indian and West Antarctic. While the East Antarctic Indian province shows also a high diversity with seven neotanaid species, only one can be found in the West Antarctic. Similar as for bathyal provinces, in the case of the abyssal biogeographic provinces, no neotanaid is reported for the Arctic. Neither for the Brazil or the West Pacific Basins could any collection occurrences be found.

When considering the distribution of neotanaids among the biogeographic provinces, we observed that most species have been found in only one province, no matter if deep-bathyal, abyssal, hadal, or shallower than 800 m (Figure 5). Of the 51 known species, 24 have been reported in only one province, while only six species have been reported for five or more provinces. The most widespread neotanaid species in terms of their presence in a variety of biogeographic provinces are *Neotanais americanus* and *Neotanais armiger* Wolff, 1956. They are present in eight provinces, when adding together their distribution considering depth as well as coordinates.

3.2 Phylogenetics

A total of 69 neotanaid specimens were considered for DNA extraction. When available, adults were used, although in some cases juvenile mancas were subjected to molecular analyses for the purpose of confirming identification, or to extend the geographical coverage of the study. In 13 cases out of these 69 DNA extractions no DNA fragment could be successfully obtained. The most successful were PCRs targeting *16s*, for which high-quality fragments were obtained for 44 specimens, followed by *COI* with 39 fragments, and *H3* with 30 fragments. For *18s* and *28s* only 13 and 19 high-quality sequences respectively were obtained. In the final alignments, only sequences representing unique haplotypes were included. In addition, only those sequences were taken into account for which at least two of the three genes were available, so that robust comparisons between the different alignments were possible. That resulted in a final number of 28 sequences included in the alignments for *COI*, 27 sequences for *16s*, and 16 sequences for *H3* (Table 1).

Of these 28 studied specimens, five were identified as belonging to the genus *Venusticrus* and all others to *Neotanais*. No representatives of *Herpotanais* were available to us, and, although

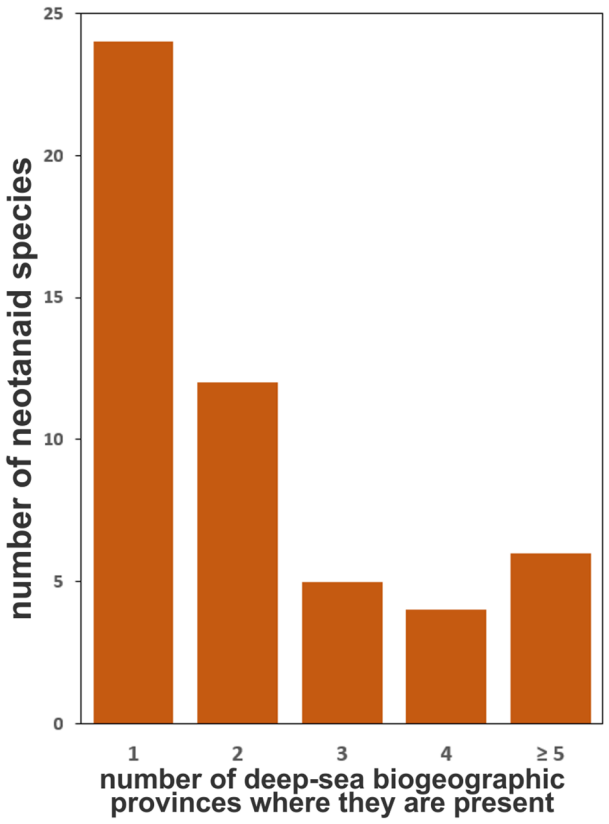

FIGURE 5
Number of the 51 current neotanaid species that are present in one or two biogeographic provinces of the deep ocean floor (as proposed by Watling et al., 2003) and number of species that are more widespread (present in 3, 4, or more provinces).

we had access to catalogued samples of *Carololangia plumata* (Kudinova-Pasternak, 1975) from the Natural History Museum in London and the National Museum of Natural History in Paris, several PCR attempts failed and no quality molecular data could be produced for this species. After comparison of the obtained sequences with the publicly available fragments on GenBank, two of the specimens could be identified as *Venusticrus thor*, which was in agreement with the tentative morphological identification.

None of the five phylogenies built, based on the analyses with the two different combinations of genes (concatenation of *COI*, *16s* and *H3*, Figure 4, and concatenation of *COI* and *16s*, Supplementary Figure S1) or on the alignments of the individual genes (Supplementary Figures S2–S4 for *COI*, *16s*, and *H3* in that order), resulted in either of the two represented genera showing as monophyletic. In the case of *Venusticrus*, of the three included species only two, *Venusticrus thor* and *Venusticrus* species from the North Atlantic, grouped together as a highly supported clade (no support in the *COI* phylogeny, Supplementary Figure S2), whereas the *Venusticrus* sp. from the Atlantic tropical area, just south of the Equator, is included in clades with *Neotanais* species, although never with any relevant support values. Regarding the genus *Neotanais*, the included specimens grouped into up to five well supported clades, the largest one including *Neotanais* sp. 1–6, always with very high support values (94% or higher), followed in size by a clade formed by *Neotanais* sp. 7 – 10, although this one with lower support values (no higher than 72%). *Neotanais* sp. 11 and *Neotanais* sp. 12 always grouped together, but with low support (no higher than 58%), same for *Neotanais* sp. 13 and *Neotanais* sp. 14, in this case with relatively high support values (as high as 86%). Additionally, *Neotanais* sp. 16–18 built also a highly supported clade. On the other hand, *Neotanais* sp. 15, represented by two specimens loaned from the Museum Victoria in Melbourne, Australia, was never included in a highly supported clade grouping it to any other neotanaid species included in the analyses.

The two phylogenies based on the two concatenated alignments, one including only the mitochondrial genes and the other one analyzing additionally the available *H3* fragments, were very similar, showing the same major clade formation, and differing mainly in the support values and the genetic distances. In general, the built clades showed slightly better support in the phylogeny based on all three genes than when dropping *H3*. The same tendency is observed when comparing to the phylogeny based on *COI* only: similar clades were built, although with, once again, slightly lower support values. In some cases, the internal clade formation of the major six clades changed to a small extent. However, for most instances, those internal clades showed low support values. Likewise, the phylogeny based on *16s* only, showed a similar main clade formation. In this case, however, some more obvious differences were observed. Unlike in the previous tree, in the *16s* phylogeny *Neotanais* sp. 7-8 and *Neotanais* sp. 9-10 did not group together into a well-supported clade, but split instead into the two internal clades, both with high support values. Additionally, and since no *16s* fragment was available for *Neotanais* sp. 12, the corresponding clade formation with *Neotanais* sp. 11 resolved in the other phylogenies could not be analyzed here. The phylogeny built based on *H3* only revealed a low resolution power for this gene. Only three clades grouping different species together showed support values higher than 50%, the highest been for a clade formed by the two north Atlantic species of *Venusticrus*.

3.3 Phylogenetics within biogeographic and bathymetric frames

When examining the phylogenies built within a biogeographic frame, of the six well-supported clades observed, only one brings together species from one single ocean, namely the clade composed of *Neotanais* sp. 7–10, all from the Pacific, but that fit into three different biogeographic provinces according to Watling et al. (2013) distribution. *Neotanais* sp. 7 was collected at the Aleutian Trench from more than 6500 m deep, *Neotanais* sp. 8 and 10 in the abyssal North Pacific, and *Neotanais* sp. 9 in the abyssal Central Pacific provinces. All other five highly supported clades combining different neotanaid species are grouping together specimens from distant regions, including species from different oceans.

Regarding the depths from where the specimens were collected, of the six highly supported main clades only two are formed of species from only one depth zone: the clade with only two species, *Neotanais* sp. 11 and 12, encompasses only abyssal specimens, and the clade formed of the three bathyal species *Neotanais* sp. 16–18.

On the other hand, in the clade assembling species *Neotanais* sp. 1–6, we find the two extremes of *Neotanais* sp. 6, collected during an epibenthic sled tow starting at a depth of 1588 m and finishing at 1626 m, grouped together with *Neotanais* sp. 3, collected from waters deeper than 8300 m at the Puerto Rican Trench.

Table 2 shows the genetic distances for the 507 bp-long *COI* fragments between all 29 specimens included in the phylogenetic analyses (28 neotanaids and one apseudomorphan outgroup). The largest genetic distance between neotanaid specimens corresponds to that between *Neotanais* sp. 14 from Icelandic waters (IceA) and *Neotanais* sp. 1 haplotypes collected in the North Pacific, off Alaska (AleB), and in the Sea of Okhotsk (SoB) with 0.347, whereas the smallest genetic distances shown correspond to those between haplotypes of what are here considered specimens of the same species, *Venustricus thor* collected in the Kuril-Kamchatka Trench (KuB) and the Clarion-Clipperton Zone (JPIO) with 0.047, *Neotanais* sp. 1 haplotypes (AleutB and SoB), values between 0.00 and 0.087, *Venusticrus* sp. collected in the North Atlantic (VT), from the Puerto Rican Trench and the Vema Fracture with 0.002, and the two specimens from the Museum Victoria in Melbourne, with 0.0806. The smallest genetic distance observed for neotanaid specimens considered here as belonging to different species is 0.117, the distance between *Neotanais* sp. 9 (JPIO) and *Neotanais* sp. 10 (KuB).

4 Discussion and conclusions

4.1 Discovering neotanaid species

The family Neotanaidae Lang, 1956 presents a great opportunity to illustrate the exploration of the deep-sea and the study of its biodiversity. The first species of the group, *Neotanais americanus* Beddard, 1886, was collected in 1873 and 1876 during the historical HSM Challenger expeditions off American Atlantic coasts (Beddard, 1886a, b). Its description was based on only two specimens, two 6-mm long males, one of which was collected SE of New York, and the other off Río de la Plata. That publication was followed shortly after by the report of two more species, *N. hastiger* Norman and Stebbing, 1886 and *N. laevispinosus* Norman and Stebbing, 1886, originally described as members of the genus *Alaotanais*, now a junior synonym for *Neotanais* Beddard, 1886. Both species were collected 1869 and 1875 from Northeast Atlantic waters during British Expeditions aboard the HSM Valorous and the HSM Porcupine (Norman and Stebbing, 1886). After this promising start, however, for the next seven decades only one more neotanaid, *Neotanais giganteus* Hansen, 1913, was described (Hansen, 1913). Six more species were reported after a 43-years gap from the previous description (Wolff, 1956), as a result of the study of the collections from the Danish Galathea Expedition (1950–1952). Since then, however, a slow but steady trickling income of new species are being added to the family, found not only in the Atlantic Ocean but around the world, due to the increasing number of oceanic expeditions and the exploration of the deep-sea accelerating in the second half of the last century (e.g. Koslow, 2007; Thaler and Amon, 2019). The steepest increase in the number of neotanaid species up to this date took place in the 1970s, when Kudinova-Pasternak studied material collected mostly, although not exclusively, during Soviet expeditions in a variety of oceanic regions, including North Pacific bathyal provinces, the Pacific and South Atlantic abyssal zones, and specimens from the newly discovered deepest trenches and Antarctic waters (Kudinova-Pasternak, 1970; 1972; Kudinova-Pasternak 1973a; b; 1975; 1978). In addition, Gardiner published in 1975 a major revision of the family Neotanaidae, as part of his studying material collected in the 1960s aboard ships of the Woods Hole Oceanographic Institution. Gardiner (1975) erected two new neotanaid genera as well, bringing it to the current number of four. Despite the amount of information contributed up to this point, many questions on the taxonomy, systematics and ecology of the group remained open.

It was not until the beginning of this century that a new update in the study of neotanaids and their diversity was tackled. Larsen studied the deep-sea tanaids from the Gulf of Mexico, what led, among other results, to the publication of an extensive monograph on the biology, ecology and taxonomy of deep-sea tanaids (Larsen, 2005). These four authors together, Wolff, Gardiner, Kudinova-Pasternak and Larsen, are responsible for the description of two-thirds of the known 51 neotanaid species to date (Figure 1).

Here we have been able to detect at least 21 species, based mainly on molecular data, combined with morphological examinations for a limited number of specimens. The majority of them belong to already known species. Nevertheless, a few probably represent complexes of species that are similar morphologically, but separated due to ecological or biogeographic factors, such as dispersal abilities, currents, or other physical barriers. Establishing the extent of such separations will require studies including more specimens, to allow for species delimitation analyses, morphometrics, or ecological modelling. In some cases, the number of required specimens are readily available to us, whereas for other species, further sampling would be necessary. (See below, under 4.4. Genetic diversity and connectivity for neotanaids, for additional discussion points on the matter).

4.2 Ecology of neotanaids

Similarly to many deep-sea taxa, ecological information on individual neotanaid species is scarce, as many of them are collected from benthic and epibenthic dredge and sled or box core samples, mostly in low numbers, and therefore with little possibility to record information on habitat, lifestyle, feeding habits or social and reproductive behavior. Their small size limits the number of collecting devices that can be deployed. It also imposes a very restrictive approach when it comes to material handling and preservation. Therefore, most ecological data had to be inferred from morphological characteristics (e.g. the development of walking or swimming appendages, the absence of glands for the building of tubes, or the shape, size, or setation of mouth appendages) and from indirect observations, such as gut contents. Their lack of eyes clears any doubt of this family radiating in the deep-sea. So far, no neotanaid has been reported from depths above 200 m (Gardiner, 1975; Figure 1), not even in polar regions, possibly

TABLE 2 Genetic distances matrix for *COI* sequences (507 bp) for the specimens included in this study.

		1	2	3	4	5	6	7	8	9	10	11	12	13	14	15	16	17	18	19	20	21	22	23	24	25	26	27	28	29
***Neotanais* sp. 1 AleB HT1**	**1**	0.000																												
***Neotanais* sp. 1 AleB HT2**	**2**	0.085	0.000																											
***Neotanais* sp. 1 AleB HT3**	**3**	0.087	0.008	0.000																										
***Neotanais* sp. 1 SoB HT1**	**4**	0.083	0.006	0.010	0.000																									
***Neotanais* sp. 1 SoB HT2**	**5**	0.083	0.006	0.010	0.000	0.000																								
***Neotanais* sp. 2 Div3**	**6**	0.178	0.169	0.169	0.169	0.169	0.000																							
***Neotanais* sp. 3 VT**	**7**	0.176	0.198	0.198	0.198	0.198	0.134	0.000																						
***Neotanais* sp. 4 SoB**	**8**	0.208	0.230	0.227	0.230	0.230	0.175	0.169	0.000																					
***Neotanais* sp. 5 IceA**	**9**	0.167	0.194	0.194	0.194	0.194	0.145	0.164	0.170	0.000																				
***Neotanais* sp. 6 IceA**	**10**	0.214	0.237	0.239	0.242	0.242	0.188	0.193	0.206	0.192	0.000																			
***Neotanais* sp. 7 AleB**	**11**	0.272	0.282	0.285	0.277	0.277	0.234	0.228	0.270	0.230	0.265	0.000																		
***Neotanais* sp. 8 KuB**	**12**	0.272	0.274	0.276	0.274	0.274	0.238	0.234	0.252	0.252	0.248	0.119	0.000																	
***Neotanais* sp. 9 JPIO**	**13**	0.283	0.302	0.301	0.305	0.305	0.274	0.232	0.252	0.250	0.251	0.230	0.217	0.000																
***Neotanais* sp. 10 KuB**	**14**	0.270	0.289	0.294	0.286	0.286	0.252	0.228	0.246	0.237	0.250	0.192	0.188	0.117	0.000															
***Neotanais* sp. 11 Div3**	**15**	0.308	0.314	0.314	0.321	0.321	0.260	0.271	0.293	0.257	0.243	0.235	0.227	0.213	0.236	0.000														
***Neotanais* sp. 12 JPIO**	**16**	0.269	0.292	0.295	0.292	0.292	0.233	0.227	0.238	0.214	0.249	0.210	0.208	0.235	0.225	0.198	0.000													
***Neotanais* sp. 13 KaD**	**17**	0.272	0.278	0.278	0.275	0.275	0.225	0.268	0.264	0.246	0.260	0.247	0.229	0.244	0.250	0.215	0.224	0.000												
***Neotanais* sp. 14 IceA**	**18**	0.292	0.288	0.285	0.285	0.285	0.253	0.275	0.287	0.280	0.261	0.247	0.248	0.278	0.284	0.246	0.270	0.245	0.000											
***Neotanais* sp. 15 Div3**	**19**	0.277	0.302	0.300	0.300	0.300	0.254	0.266	0.240	0.278	0.272	0.263	0.243	0.282	0.265	0.261	0.251	0.202	0.257	0.000										
***Neotanais* sp. 16 aus HT1**	**20**	0.323	0.308	0.311	0.314	0.314	0.292	0.304	0.284	0.312	0.310	0.278	0.301	0.273	0.267	0.330	0.288	0.311	0.313	0.316	0.000									
***Neotanais* sp. 16 aus HT2**	**21**	0.294	0.306	0.303	0.306	0.306	0.260	0.285	0.252	0.266	0.294	0.245	0.268	0.265	0.258	0.291	0.260	0.296	0.287	0.296	0.081	0.000								
***Neotanais* sp. 17 KaD**	**22**	0.331	0.347	0.344	0.347	0.347	0.314	0.287	0.319	0.329	0.319	0.283	0.278	0.273	0.272	0.307	0.306	0.270	0.281	0.261	0.321	0.330	0.000							
***Neotanais* sp. 18 Saya**	**23**	0.327	0.342	0.339	0.345	0.345	0.300	0.324	0.312	0.315	0.307	0.294	0.286	0.288	0.302	0.287	0.293	0.249	0.309	0.285	0.327	0.328	0.109	0.000						
***Neotanais* sp. 19 IceA**	**24**	0.321	0.339	0.343	0.342	0.342	0.317	0.327	0.277	0.320	0.293	0.299	0.269	0.295	0.312	0.275	0.290	0.236	0.286	0.246	0.333	0.299	0.163	0.166	0.000					
***Venusticrus thor* JPIO**	**25**	0.309	0.321	0.318	0.321	0.321	0.290	0.294	0.283	0.276	0.301	0.277	0.258	0.279	0.259	0.291	0.288	0.227	0.268	0.250	0.318	0.290	0.301	0.306	0.304	0.000				
***Venusticrus thor* KuB**	**26**	0.299	0.317	0.320	0.317	0.317	0.290	0.284	0.290	0.286	0.282	0.248	0.245	0.259	0.264	0.272	0.264	0.213	0.265	0.239	0.310	0.275	0.305	0.303	0.295	0.047	0.000			
***Venusticrus* sp. VT HT1**	**27**	0.299	0.321	0.321	0.321	0.321	0.248	0.253	0.265	0.260	0.280	0.229	0.207	0.246	0.231	0.215	0.187	0.219	0.260	0.236	0.311	0.274	0.267	0.263	0.276	0.228	0.208	0.000		
***Venusticrus* sp. VT HT2**	**28**	0.299	0.321	0.321	0.321	0.321	0.248	0.256	0.268	0.263	0.280	0.229	0.207	0.246	0.231	0.212	0.190	0.219	0.260	0.237	0.312	0.274	0.267	0.263	0.276	0.229	0.209	0.002	0.000	
Apseudomorphan OG SoB	**29**	0.514	0.522	0.519	0.518	0.518	0.561	0.578	0.522	0.561	0.503	0.520	0.498	0.503	0.537	0.526	0.525	0.495	0.459	0.472	0.488	0.495	0.504	0.522	0.463	0.503	0.524	0.510	0.509	0.000

(See Material and Methods for details on geographic origin).

10.3389/fmars.2024.1395000

ruling out a depth distribution associated with water temperature rather than with depth. Whether or not the distribution of neotanaids is subjected to polar emergence should be investigated once sufficient data on depth, salinity, and temperature for the collection stations can be assembled. On the other end of the depth range, *Neotanais hadalis* Wolff, 1956 was described based on four specimens collected from a depth of 8210 m at the Kermadec Trench, northeast of New Zealand, whereas *N. persephone* Messing, 1977 was collected from the Puerto Rican Trench from 8381 m deep waters. These are two of the deepest records for neotanaids up to date. A few other species have been collected from waters deeper than 7000 m, however, most commonly occurrences for neotanaids are found at depths 1000–5000 m (Figure 1). Nevertheless, it should be pointed out that this might not reflect the actual depth distribution for the group, but rather indicate the allocation of sampling efforts for deep-sea expeditions.

4.3 Biogeographic distribution of neotanaids

The distribution of the occurrences for neotanaids, with an overwhelming majority located in the North Atlantic, reveals the strong asymmetry in the historic exploration of deep-sea biodiversity (Figures 2, 3). Many of these North Atlantic samples can be traced back to the activity of the Woods Hole Oceanographic Institution and the British Natural History Museum, where some of the efforts toward the study of the deep-sea were promoted with periodical transects and repeated cruises for the collections and study of material in relatively close areas off their respective coasts. It is even possible to find some of these locations labelled as "permanent station", quotation marks included, beautifully hand-written on the pages of the paper catalogue for the crustacean collection of the British Museum of Natural History (e.g. https://data.nhm.ac.uk/media/738536fd-9ec3-426a-b477-09ef60ed1a57) Natural History Museum (2014). The North Atlantic biogeographic provinces, both bathyal and abyssal, host much larger numbers of neotanaid species than any other province, even when some other regions are better known as biodiversity hotspots (Costello et al., 2022). One could almost say that some oceanic regions seem to have been forgotten. The complete lack of records for neotanaids from the Arctic Ocean, or the extremely low numbers of occurrences in the South Atlantic are puzzling, indicating how perhaps more remote or hard-to-access locations remain unexplored. Since scientific exploration and knowledge go hand in hand with technological advance and economic progress, we would expect that additional regions will gain more attention in the future, especially if accompanied by an increase in international collaboration in scientific projects. Most likely, when other oceanic areas are explored to the same extent as the North Atlantic has historically been studied, the levels of biodiversity for the deep-sea will increase exponentially, probably not only for neotanaids, but for marine fauna in general.

Therefore, looking into the known distribution of neotanaids from the perspective of the individual species and how widespread they are, needs to be done with care. The examined records show that of the 51 neotanaid species, 24 can be found in only one biogeographic province (Figure 5). It is necessary to remember, however, that many of them are still known only from the type collection. According to the available records, 27 have been so far reported only in the original species description and for 15 of them only a single collection station was indicated. The study of deep-sea fauna remains in the discovery phase (e.g. Webb et al., 2010; Paulus, 2021), with large gaps and scarce data for marine invertebrates (Tittensor et al., 2010), and many deep-sea species remain undescribed (Ramírez-Llodra et al., 2010). It could be suspected that at such a young stage in the study of deep-sea fauna there will be a correlation between the number of times a taxon has been reported and the amount of time for how long that species has been known. Nevertheless, the data do not offer an unequivocal answer regarding such hypothesis. For *Neotanais americanus*, the species described the longest ago, there are relatively many occurrences (50). However, for *N. giganteus*, described already in 1913, we have only 10 records. Whether the differences among the occurrences for neotanaid species can be explained through sample bias, or if they reflect to some extent the differences in their levels of rarity and endemism, will require a deeper knowledge on their ecology and life strategies, in addition to exploring a larger portion of the sea floor than what has been covered so far. Sampling effort, method of collections chosen in deep-sea expeditions, and definitely pure chance most likely play a part in the numbers and current known distribution for neotanaid species. The number of records for the species were also plotted against the number of biogeographic provinces in which they are present (Figure 6). The chances of a species being found in more than one region should increase if that species is recorded more often. The plot on Figure 6 shows that tendency, although there are some outliers. *Neotanais giganteus* and *N. hadalis* have been reported only 11 times each, but at locations that span over five and seven biogeographic provinces respectively. Moreover, their distributions extend across two oceans (Atlantic, Indian) for *N. giganteus* and three oceans (Atlantic, Antarctic, Indian) for *N. hadalis*. One of the other most widespread species, *N. antarcticus*, is, with only 12 records, present in six provinces. These are, however, all located within the Antarctic Ocean or

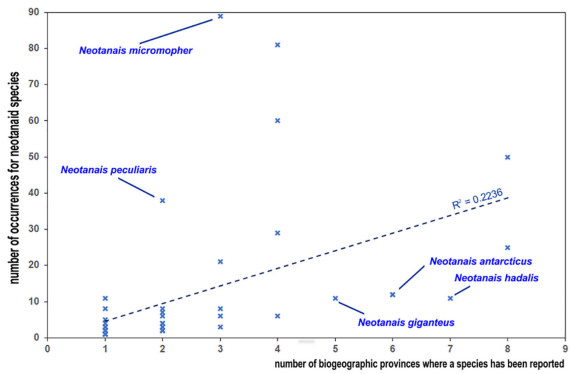

FIGURE 6
Plot of the relationship between the number of records for species and how widespread they are according to the number of biogeographic provinces where they have been recorded.

adjacent regions (Subantartic, Falklands). The data for *Carololangia plumata* include 12 records distributed across six biogeographic provinces located in three oceans (Atlantic, Antarctic, Indian). However, cases in the opposite direction can also be observed, for which species with a relatively high number of occurrences show a more limited distribution: *Neotanais micromopher*, the neotanaid with the most occurrences reported (89), is present in three biogeographic provinces, all of them in the Atlantic Ocean. Similarly, *N. peculiaris*, has been reported 38 times, but always from the bathyal North Atlantic (37 records) and the bathyal Northern North Atlantic (one record only) provinces.

Additional data and studies are necessary to separate sampling artifacts from evolutionary and ecological factors that can help us explain neotanaid biodiversity and distribution. One of those factors will be certainly depth. The number of provinces in which a neotanaid species is present will depend to some extent on its depth range and whether or not it is capable of occupying habitats in different zones. The depth ranges for neotanaids (Figure 1) show a rather large variability, with some species displaying a range restricted to the bathyal zone, but others having a very wide range, reaching from the upper-bathyal into the abyssal zones, some even into hadal depths. The two species with a widest depth range are *N. armiger*, with depths records from 600 to 6100 m depth, and *N. hadalis*, with records between 2270 and 8120 m. Such wide depth ranges and widespread distributions are unusual for marine fauna with limited dispersal abilities, as is the case for neotanaids with their lifestyle of brooding and walking benthic organisms. Further studies of already existing as well as of new collections will most probably lead to the description of new species, as some of those wide ranges and distributions could be explained by the fact that they might not be a single species, but rather a species complex of cryptic species, morphologically similar in appearance but with different physiological and ecological characters. In order to reveal these potential cryptic species, specimens with similar morphologies, but from different depths need to be included in species delimitation analyses. Ideally, these should be complemented with morphometric studies. Of special interests are the species whose depth ranges span over both, bathyal and abyssal depths. A high species turnover characterizes the transition between bathyal and abyssal fauna, related to a physiological bottleneck that requires adaptation for species to adapt to higher hydrostatic pressure (Brown and Thatje, 2014). These adaptations have been associated with the ability of membrane-folding proteins to withstand the increasing loss of membrane fluidity with increasing hydrostatic pressure past that threshold (Yancey, 2020) and including specimens from both sides of that potential physiological barrier could help detect if these adaptations translate into the formation of complexes of different species separated by depth.

The discovery of such species complexes would lead to the establishment of yet-to-be described genera as well, due to both, the placement of known species into currently undescribed taxa and because of the description of genera for newly discovered species. Gardiner (1975) established already six subgroups for 23 species of *Neotanais* based on morphological similarities among the members of each group. Some of the species described since then show characters matching features corresponding to one of these groups (Larsen and Hansknecht, 2003; Wi et al., 2014; Wi et al., 2015). These groups are indicated on Figure 1 with an intercalated shade-light pattern superimposed on the species of genus *Neotanais* (yellow rectangle) labelled with their corresponding names, and to the right of these groups, the remaining ungrouped 26 species, in ordered of their depth range, from shallowest, *N. minimus*, to deepest, *N. persephone*. The features characterizing some of these groups have potential as diagnostic characters for possible undescribed genera. For example, the species in the *micromopher* group are distinguished by having rectangular wider-than-long pereonites 4-6, a very short pleotelson fused to pleonite 5, long, slender, ventral cheliped carpal setae, and, for the males, slender and not sharply bent chelipedal carpi (Gardiner, 1975). However, for other groups it could be problematic. For instance, the *americanus* group, is, in Gardiner's own words "noted for a lack of distinctive morphologic features compared to other groups" (Gardiner, 1975; page 43). Something similar can be observed when looking into the depth ranges within the groups. In some groups, for example the *americanus* group, the depth ranges are quite similar for all the species, but in others, such as the *hadalis* group or the *robustus* group, there is little consistency. On the same note, the depth ranges for species within *Herpotanais* and *Venusticrus*, especially the latter, display rather similar values, indicating that this ecological character could represent further support for the morphological characters defining genera in Neotanaidae.

Additional study of these groups should reveal if such characteristics can support their elevation to genus rank. This task will be facilitated by the implementation of an integrative approach, taking advantage of morphology, physiology, ecology, and molecular data.

4.4 Genetic diversity and connectivity for neotanaids

The phylogenies built for Neotanaidae were somewhat limited in their coverage, since they only included two of the four current genera and 21 species, while there are 51 recognized species in the family. The specimens included in the phylogenetic analyses were divided into species based on a combination of criteria, including tentative morphological identifications, biogeographic distances, or the results of the molecular analyses themselves. Some of those divisions might change in the future, when more specimens are available for further research, such as species delimitation analyses, and when ongoing morphological studies can be completed. These will allow us to establish further taxonomic assignments, discern which ones are valid species, or which rather represent species complexes, in addition to detecting new species as well as potential synonymies. For example, the genetic distance between the two haplotypes of *Neotanais* sp. 15, from the southeast coasts of Australia (Table 2), indicates that despite their morphological and geographic similarities, they might belong into different species. Another interesting study case is offered by *Neotanais* sp. 1, collected in the North Pacific in both, eastern and western areas. This species belongs to the *N. americanus-sandersi-laevispinosus*

complex, three taxa already pointed out as "sibling species" by Gardiner (1975) and whose further investigation could result in them been appointed as populations of the same species, segregated by geographic distance or possibly depth. Neotanaids are usually collected in very low numbers, which hinders population studies. In this case, however, we are fortunate to have access to material from several locations in the North Pacific, allowing for our upcoming study on the genetic connectivity of populations of this species across the region.

Despite the limited coverage of the phylogenetic analyses, we can conclude that the generic assignments within Neotanaidae is in need of a thorough revision. This was not unexpected for genus *Neotanais*, historically the first genus, including 44 species, a large majority of neotanaids. Nevertheless, this is striking for the second genus included in the analyses, genus *Venusticrus*. There are four recognized species within that genus and it has recently been the subject of a revision, including a re-diagnosis of its morphological characters, the main diagnostic trait being a uropod ventrally attached to the telson (Figure 1B), as opposed to laterally or dorsally, as in other neotanaids. We were able to include three species of *Venusticrus* in our alignments, and in none of the phylogenies these three species formed a monophyletic clade. One of the specimens, labelled here *Venusticrus* sp. Div3 and that probably belongs to *V. glandurus* Gardiner, 1975, the type species of the genus, was never part of a well-supported clade with any of the other species included. Morphological re-examinations will be necessary to re-evaluate which characters can represent true diagnostic features, and what weights should be attributed to them for the purpose of assigning taxonomic identities, at generic, as well at specific levels. Furthermore, additional molecular analyses should be undertaken, in an effort to increase the number of taxa included at all levels, population, species and genus, to achieve better resolution and robustness in the analyses.

The increase in the studied specimens should also aim at providing a better picture of the connectivity of neotanaids across biogeographic regions and oceans. Our molecular analyses indicate that the evolutionary processes shaping the diversity and biogeography of neotanaid species might not be as confined as initially assumed, considering the frame of a small deep-sea benthic invertebrate with, in theory, limited dispersal abilities. Our observations reveal that, at least some, neotanaid species are able to travel relatively long distances. As an example, specimens from the Aleutian Trench in the eastern East Pacific are closely related to what seem to be conspecific populations from the Sea of Okhotsk, in the western North Pacific (Figure 4, *Neotanais* sp. 1). A similar case can be made for samples found in the North Atlantic, where two specimens, one collected east of the Mid-Atlantic Ridge, east of the Vema fracture, and another one from the Puerto Rican Trench, display nearly identical haplotypes (Figure 4, *Venusticrus* VT). In the latter case, the high genetic connectivity of the populations takes place not only across large distances, overpassing a hypothetically substantial geographical barrier, but also along a wide depth gradient, as one of the samples was collected from as deep as 8340 m and the other one from about 5100 m. Such high connectivity across large distances is not observed in other deep-sea tanaidaceans. For instance, Jakiel et al. (2019) observed spatial structure of the species of family Pseudotanaidae collected in different regions of the Clarion-Cliperton Fracture Zone (CCFZ), in correlation with geographical barriers, such as fractures and seamount chains crossing the CCFZ and separating the sampled areas. Similarly, diversity studies with other peracarids also in the CCFZ, namely deep-sea isopods, showed that, although a large proportion of species have rather restricted distributions, some could be found in areas as far from each other as 5000 km (Kaiser et al., 2023 and references therein). Nevertheless, some deep-sea isopods are known to be good swimmers, and display different types of swimming behavior (see for ex. Marshall and Diebel, 1995). In fact, distribution patterns in abyssal isopods have been linked to the locomotion abilities of adult stages for four families (Brix et al., 2020). Whether or not the findings on neotanaid connectivity across biogeographic provinces and depths, can be linked as well to behavioral or physiological patterns can only be determined once enough information on their ecology is available.

From our survey of what is known so far about the distribution and biogeography of neotanaid species, together with a first phylogeny based on molecular data for the family, we have been able to gather new insights on the diversity and genetic connectivity patterns of the group. Nevertheless, we also have opened new questions that can only be adequately answered after assembling new data. Much of the sea-floor remains unexplored, with big gaps for some large and important regions. The search for scientific knowledge is motivated mostly by short- to mid-term commercial interests, and the deep-sea is no exception. The deep-sea floor is screened for economically valuable resources and new ways of gaining power, and the study of biodiversity is often simply the means to justify such enterprises or the result of a need to find an urgent solution for a problem, generated by our ways of exploiting natural resources in unsustainable ways. Many times the search for long-term effects of our actions on natural ecosystems or for a big-picture understanding of natural processes is neglected. The records or occurrences and the available samples for neotanaids are biased towards the northern hemisphere, in addition to areas that have been historically considered of economic or strategical interest. Only if we close the existing large knowledge gaps, will we be able to develop a clear picture of the processes that shape marine biodiversity and only then will we have the ability to properly protect marine ecosystems.

Data availability statement

The genetic data produced for this study have been made publicly available by accessioning them to GenBank, with the accession numbers indicated in Table 1.

Ethics statement

This study was conducted in accordance with local legislations and insitutional requirements, as part of a project approved by Poland National Science Centre. For the collection of specimens appropriate permits were issued.

Author contributions

EPT: Conceptualization, Data curation, Formal analysis, Investigation, Methodology, Software, Validation, Visualization, Writing – original draft, Writing – review & editing. MB: Funding acquisition, Project administration, Resources, Software, Supervision, Validation, Writing – review & editing.

Funding

The author(s) declare financial support was received for the research, authorship, and/or publication of this article. Major support was provided under Polish Nacional Science Centre grant BIOPASS: BIOdiversity PAtternS and Scale: the case of peracarid Crustacea from south–eastern Australia (OPUS 2018/31/B/NZ8/03198), in addition to financial support by the Dean's office of the Faculty of Biology and Environmental Protection of the University of Lodz. Frontiers has granted this paper a discount of 10% on the total invoice fee.

Acknowledgments

We would like to thank the organizing committee of the 10th International Crustacean Congress and the Crustacean Society for making such an interesting and successful meeting possible, as well as Rachael Peart and Kareen Schnabel for creating this opportunity for us to share our findings, offering their abilities, professionalism, and time as the editors of this special issue. We want to thank also the masters, nautical officers, and all crew members of the research vessels Sonne (AleutBio2022, JPIO2015, KuramBio2012 and 2016), Meteor (Diva3-2019, IceAge2011), L'Atalante (KanaDeep2019), SA Agulhas (MEIO1-Saya-2022), and Akademik M.A. Lavrentyev (SokhoBio2015), as well as the science parties involved in these expeditions for their support collecting samples. We would like to acknowledge as well the efforts of the curators of the invertebrate collections of the Natural History Museum in London, the National Museum of Natural History in Paris, the Museum Victoria in Melbourne, and the Senckenbeg Museum in Frankfurt, and their assistance with attaining further material. We would like to appreciate also the help of two rewires, whose comments and suggestions proved useful for improving the quality of the manuscript. Additionally, we need to thank our colleagues and friends in the Polarna lab at the University of Lodz for their help and support along the way, whether facilitating the sorting and preservation of material, the adjustment of PCR protocols, or the edition of text and figures, among others.

Conflict of interest

The authors declare that the research was conducted in the absence of any commercial or financial relationships that could be construed as a potential conflict of interest.

The authors declare that one of them (MB) was an editorial board member of Frontiers at the time of submission. This had no impact on the peer review process and the final decision.

Publisher's note

Supplementary material

The Supplementary Material for this article can be found online at: https://www.frontiersin.org/articles/10.3389/fmars.2024.1395000/full#supplementary-material

SUPPLEMENTARY FIGURE 1
Phylogeny of Neotanaoidea (best tree) inferred from Maximum Likelihood analysis (RAxML) of concatenated 1031 bp long sequences including fragments of the mitochondrial *COI* (656 bp) and *16S* (375 bp) genes. Bootstrap values (5000 bp with bootstopping) are shown when higher than 50%. Taxa are identified to the level of genus, to species for *Venusticrus thor*, the only neotanaid species with genetic data previously available on GenBank. For tracking down of the corresponding specimens, the abbreviation of the corresponding sampling campaign or museum lending the material (see Material and Methods) is added. When necessary, the haplotypes are identified with the abbreviation HT and assigning them a number.

SUPPLEMENTARY FIGURE 2
Phylogeny of Neotanaoidea (best tree) inferred from Maximum Likelihood analysis (RAxML) of 656 bp long sequences of the mitochondrial *COI* gene. Bootstrap values (5000 bp with bootstopping) are shown when higher than 50%. Taxa are identified to the level of genus, to species for *Venusticrus thor*, the only neotanaid species with genetic data previously available on GenBank. For tracking down of the corresponding specimens, the abbreviation of the corresponding sampling campaign or museum lending the material (see Material and Methods) is added. When necessary, the haplotypes are identified with the abbreviation HT and assigning them a number.

SUPPLEMENTARY FIGURE 3
Phylogeny of Neotanaoidea (best tree) inferred from Maximum Likelihood analysis (RAxML) of concatenated 375 bp long sequences of the mitochondrial *16S* gene. Bootstrap values (5000 bp with bootstopping) are shown when higher than 50%. Taxa are identified to the level of genus, to species for *Venusticrus thor*, the only neotanaid species with genetic data previously available on GenBank. For tracking down of the corresponding specimens, the abbreviation of the corresponding sampling campaign or museum lending the material (see Material and Methods) is added. When necessary, the haplotypes are identified with the abbreviation HT and assigning them a number.

SUPPLEMENTARY FIGURE 4
Phylogeny of Neotanaoidea (best tree) inferred from Maximum Likelihood analysis (RAxML) of concatenated 329 bp long sequences including fragments of the nuclear *H3* gene. Bootstrap values (5000 bp with bootstopping) are shown when higher than 50%. Taxa are identified to the level of genus, to species for *Venusticrus thor*, the only neotanaid species with genetic data previously available on GenBank. For tracking down of the corresponding specimens, the abbreviation of the corresponding sampling campaign or museum lending the material (see Material and Methods) is added. When necessary, the haplotypes are identified with the abbreviation HT and assigning them a number.

References

Altschul, S. F., Gish, W., Miller, W., Myers, E. W., and Lipman, D. J. (1990). Basic local alignment search tool. *J. Mol. Biol.* 215, 403–410. doi: 10.1016/S0022-2836(05)80360-2

Araújo-Silva, C. L., Froufe, E., and Larsen, K. (2015). Two new species of family Neotanaidae (Peracarida: Tanaidacea) from the Antarctic and Mid-Pacific Oceans. *Zootaxa* 4018, 535–552. doi: 10.11646/zootaxa.4018.4.3

Astrin, J. J., and Stüben, P. (2008). Phylogeny in cryptic weevils: molecules, morphology and new genera of western Palaearctic Cryotorhynchinae (Coleoptera: Curculionidae). *Inv. Syst.* 22, 503–522. doi: 10.1071/IS07057

Beddard, F. E. (1886a). Preliminary notice of the Isopoda collected during the voyage of H.M.S. 'Challenger.' - Part III. *Proc. Sci. Meetings Zoological Soc. London* 1886, 97–122.

Beddard, F. E. (1886b). "Report on the Isopoda collected by H.M.S. Challenger during the years 1873-76. Second part," in *Zoology. Report on the Scientific Results of the Voyage of H.M.S. Challenger During the Years 1873–76 Under the Command of Captain George S. Nares, R.N., F.R.S. and the Late Captain Frank Tourle Thomson, R.N. Wyville Thomson, C. and J. Murray (series eds.)*, vol. 17 . Ed. J. Murray (Neill and Company, Edinburgh), 1–178. Plates I–XXV, 1 chart.

Belyaev, G. M. (1989). *Deep Sea Ocean Trenches and their Fauna* (Moscow: Nauka), 255. in Russian, translation courtesy of Scripps Institution of Oceanography Library.

Błażewicz-Paszkowycz, M., Bamber, R. N., and Anderson, G. (2012). Diversity of Tanaidacea (Crustacea: Peracarida) in the World's Oceans – How far have we come? *PloS One* 7, e33068. doi: 10.1371/journal.pone.0033068

Blaxter, M. L., De Ley., P., Garey, J. R., Liu, L. X., Scheldeman, P., Vierstraete, A., et al. (1998). A molecular evolutionary framework for the phylum Nematoda. *Nature* 392, 71–75. doi: 10.1038/32160

Brix, S., Osborn, K. J., Kaiser, S., Truskey, S. B., Schnurr, S. M., Brenke, N., et al. (2020). Adult life strategy affects distribution patterns in abyssal isopods – implications for conservation in Pacific nodule areas. *Biogeosciences* 17, 6163–6184. doi: 10.5194/bg-17-6163-2020

Brown, A., and Thatje, S. (2014). Explaining bathymetric diversity patterns in marine benthic invertebrates and demersal fishes: physiological contributions to adaptation of life at depth. *Biol. Rev.* 89, 406–426. doi: 10.1111/brv.12061

Castresana, J. (2000). Selection of conserved blocks from multiple alignments for their use in phylogenetic analysis. *Mol. Biol. Evol.* 17, 540-552. doi: 10.1093/oxfordjournals.molbev.a026334

Costello, M. J., Vale, M. M., Kiessling, W., Maharaj, S., Price, J., and Talukdar, G. H. (2022). "Cross-chapter paper 1: biodiversity hotspots," in *Climate Change 2022: Impacts, Adaptation and Vulnerability. Contribution of Working Group II to the Sixth Assessment Report of the Intergovernmental Panel on Climate Change*. Eds. H.-O. Pörtner, D. C. Roberts, M. Tignor, E. S. Poloczanska, K. Mintenbeck, A. Alegría, M. Craig, S. Langsdorf, S. Löschke, V. Möller, A. Okem and B. Rama (Cambridge University Press, Cambridge, UK and New York, NY, USA), 2123–2161. doi: 10.1017/9781009325844.018

Darriba, D., Taboada, G. L., Doallo, R., and Posada, D. (2012). jModelTest 2: more models, new heuristics and parallel computing. *Nat. Methods* 9, 772. doi: 10.1038/nmeth.2109

Dereeper, A, Guignon, V, Blanc, G, Audic, S, Buffet, S, Chevenet, F, et al. (2008). Phylogeny.fr: robust phylogenetic analysis for the non-specialist. *Nucleic Acids Res.* 36, W465-9. doi: 10.1093/nar/gkn180

Edgar, R.C. (2004). MUSCLE: multiple sequence alignment with high accuracy and high throughput. *Nucleic Acids Res.* 32, 1792–1797. doi: 10.1093/nar/gkh340

Folmer, O., Black, M., Hoeh, W., Lutz, R., and Vrijenhoek, R. (1994). DNA primers for amplification of mitochondrial cytochrome c oxidase subunit I from diverse metazoan invertebrates. *Mol Mar. Biol. Biotech.* 3, 294–299.

Gardiner, L. F. (1975). The systematics, postmarsupial development, and ecology of the deep-sea family Neotanaidae (Crustacea: Tanaidacea). *Smithsonian Contributions to Zoology* 170, 1–265. doi: 10.5479/si.00810282.170

Hall, T. A. (1999). BioEdit: a user-friendly biological sequence alignment editor and analysis program for Windows 95/98/NT. *Nucleic Acids Symp. Ser.* 41, 95–98.

Hansen, H. J. (1895). "Isopoden, Cumaceen u. Stomatopoden der Plankton-Expedition," in *Ergebnisse der Plankton-Expedition der Humboldt-Stiftung. Bd. II G.c* (Kiel, Germany: Lipsius & Tischer). Hensen, V. doi: 10.5962/bhl.title.10413

Hansen, H. J. (1913). *Crustacea Malacostraca II. Danish Ingolf-Expedition*. Available online at: https://www.biodiversitylibrary.org/item/40413 (Accessed 11th Jan 2024).

Hou, Z., Fu, J., and Li, S. (2007). A molecular phylogeny of the genus *Gammarus* (Crustacea: Amphipoda) based on mitochondrial and nuclear gene sequences. *Mol. Phylogenet. Evol.* 45, 596–611. doi: 10.1016/j.ympev.2007.06.006

Jakiel, A., Palero, F., and Błażewicz, M. (2019). Deep ocean seascape and Pseudotanaidae (Crustacea: Tanaidacea) diversity at the Clarion-Clipperton Fracture Zone. *Sci. Rep.* 9, 17305. doi: 10.1038/s41598-019-51434-z

Kaiser, S., Christodoulou, M., Janssen, A., Kihara, T. C., Mohrbeck, I., Pasotti, F., et al. (2023). Diversity, distribution and composition of abyssal benthic Isopoda in a region proposed for deep–seafloor mining of polymetallic nodules: a synthesis. *Mar. Biodivers.* 53, 30. doi: 10.1007/s12526-023-01335-2

Kakui, K., Fleming, J. F., Mori, M., Fujiwara, J., and Arakawa, K. (2021). Comprehensive transcriptome sequencing of Tanaidacea with proteomic evidences for their silk. *Genome Bio. Evol.* 13. doi: 10.1093/gbe/evab281

Kakui, K., Katoh, T., Hiruta, S. F., Kobayashi, N., and Kajihara, H. (2011). Molecular systematics of Tanaidacea (Crustacea: Peracarida) based on 18S sequence data, with an amendment of suborder/superfamily-level classification. *Zoological Sci.* 28, 749–757. doi: 10.2108/zsj.28.749

Koslow, T. (2007). *The Silent Deep: The Discovery, Ecology and Conservation of the Deep Sea* (Sydney: UNSW Press), 270.

Kudinova-Pasternak, R. K. (1970). Tanaidacea of the Kuril-Kamchatka trench. *Trudy Instituta Okeanologii, Akademiya Nauk SSSR* 86, 341–381.

Kudinova-Pasternak, R. K. (1972). New species of the genus *Neotanais* (Crustacea, Tanaidacea). *N. magnificus* n. sp. from the Antarctic. *Complex Res. Nat. Ocean (Moscow)* 3, 259–263.

Kudinova-Pasternak, R. K. (1973a). New species of the genus *Herpotanais* Wolff 1956 of the deep-sea family Neotanaidae (Crustacea: Tanaidacea) from the Pacific. *Complex Res. Nat. Ocean (Moscow)* 4, 189–193.

Kudinova-Pasternak, R. K. (1973b). Tanaidacea (Crustacea, Malacostraca) collected on the R/V "Vitajz" in regions of the Aleutian Trench and Alaska. *Trudy Instituta Okeanologii, Akademiya Nauk* 91. 141–168.

Kudinova-Pasternak, R. K. (1975). Tanaidacea (Crustacea, malacostraca) from the atlantic sector of antarctic and subantartic. *Trudy Instituta Okeanologii, Akademiya Nauk SSSR* 103. 194–229.

Kudinova-Pasternak, R. K. (1978). Tanaidacea (Crustacea, Malacostraca) from the deep-sea trenches of the western part of the Pacific. *Trudy Instituta Okeanologii, Akademiya Nauk SSSR* 108. 115–135.

Lang, K. (1956). Neotanaidae nov. fam., with some remarks on the phylogeny of the Tanaidacea. *Arkiv för Zoologi Uppsala 2.* 9, 469–475.

Larsen, K. (1999). Deep-sea tanaidaceans (Crustacea: Peracarida) from the Albatross cruises 1885-86 with keys to the suborder Neotanaidomorpha. *J. Natural History* 33, 1107–1132. doi: 10.1080/002229399299969

Larsen, K. (2005). "Deep-see tanaidacea (Peracarida) from the gulf of Mexico," in *Crustacean Monographs*, vol. 5. (Brill, Leiden, Boston).

Larsen, K., Guţu, M., and Sieg, J. (2015). "Order Tanaidacea Dana, 184," in *Treatise on zoology – anatomy, taxonomy, biology. The Crustacea. Chapter 59*. Eds. J. C. von Vaupel Klein, M. Charmantier-Daures and F. R. Schram (Brill, Leiden, Boston), 249–329.

Larsen, K., and Hansknecht, T. (2003). Three new species of the deep-sea genus *Neotanais* Beddard (Crustacea: Peracarida). *J. Natural History* 37, 2787–2806. doi: 10.1080/0022293021000007390

Lauterbach, K.-E. (1970). Der Cephalothorax von *Tanais cavoliniid* Milne Edwards (Crustacea—Malacostraca). Ein Beitrag zur vergleichenden Anatomie und Phylogenie der Tanaidacea. *Zoologische Jahrbücher Abteilung Anatomie und Ontogenie der Tiere* 87, 94–204.

Lobo, J., Costa, P. M., Teixeira, M. A., Ferreira, M. S. G., Costa, M. H., and Costa, F. O. (2013). Enhanced primers for amplification of DNA barcodes from a broad range of marine metazoans. *BMC Ecol.* 13, 34. doi: 10.1186/1472-6785-13-34

Lörz, A.-N., Tandberg, A. H. S., Willassen, E., and Driskell, A. (2018). Rhachotropis (Eusiroidea, Amphipoda) from the North East Atlantic. *Zookeys* 731, 75–101. doi: 10.3897/zookeys.731.19814

Marshall, N., and Diebel, C. (1995). 'Deep-sea spiders' that walk through the water. *J. Exp. Biol.* 198, 1371–1379. doi: 10.1242/jeb.198.6.1371

Natural History Museum. (2014). *Specimens (from Collection specimens) [Data set resource]* (London, UK: Natural History Museum). Available at: https://data.nhm.ac.uk/dataset/collection-specimens/resource/05ff2255-c38a-40c9-b657-4ccb55ab2feb.

Norman, A. M., and Stebbing, T. R. R. (1886). On the crustacea of the 'Lighting', 'Porcupine' and 'Valorous' Expeditions. *Trans. Zoological Soc. London* 12, 77–141. doi: 10.1111/j.1096-3642.1886.tb00008.x

Paulus, E. (2021). Shedding light on deep-sea biodiversity – A highly vulnerable habitat in the face of anthropogenic change. *Front. Mar. Sci.* 8. doi: 10.3389/fmars.2021.667048

Pitz, K. M., and Sierwald, P. (2010). Phylogeny of the millipede order Spirobolida (Arthropoda: Diplopoda: Helminthomorpha). *Cladistics* 26, 497–525. doi: 10.1111/j.1096-0031.2009.00303.x

Ramírez-Llodra, E., Brandt, A., Danovero, R., De Mol, B., Escobar, E., German, C. R., et al. (2010). Deep, diverse and definitely different: unique attributes of the world's largest ecosystem. *Biogeoscienes* 7, 2851–2899. doi: 10.5194/bg-7-2851-2010

Schram, F. R., Sieg, J., and Malzahn, E. (1986). Fossil tanaidacea. *Trans. San Diego Soc. Natural History* 21, 127–144.

Sieg, J. (1980a). Taxonomische monographie der tanaidae dana 1849 (Crustacea: tanaidacea). *Abh Senckenb. Natforsch. Ges.* 537, 1–267.

Sieg, J. (1980b). Sind die Dikonophora eine polyphyletische Gruppe? *Zoologischer Anzeiger* 205, 401–416.

Sieg, J. (1984). Neuere Erkenntnisse zum natürlichen System der Tanaidacea. *Eine phylogenetische Studie. Zoologica* 136, 1–132.

Stamatakis, A., Hoover, P., and Rougemont, J. (2008). A fast bootstraping algorithm for the RAxML web-servers. *Syst. Biol.* 57, 758–771. doi: 10.1080/10635150802429642

Svenson, G. J., and Whiting, F. M. (2004). Phylogeny of Mantodea based on molecular data: evolution of a charismatic predator. *Syst. Entomol.* 29, 359–370. doi: 10.1111/j.0307-6970.2004.00240.x

Tamura, K., Stecher, G., and Kumar, S. (2021). MEGA11: Molecular Evolutionary Genetics Analysis versión 11. *Mol. Biol. Evol.* 38, 3022–3027. doi: 10.1093/molbev/msab120

Taylor, D. J., Crease, T. J., and Brown, W. M. (1999). Phylogenetic evidence for a single long-lived clade of crustacean cyclic parthenogens and its implications for the evolution of sex. *Proc. R. Soc Lond. B (1999)* 266, 791–797. doi: 10.1098/rspb.1999.0707

Thaler, A. D., and Amon, D. (2019). 262 Voyages Beneath the Sea: A global assessment of macro- and megafaunal biodiversity and research effort at deep-sea hydrothermal vents. *Peer J.* 7, e7397. doi: 10.7717/peerj.7397

Tittensor, D., Mora, C., Jetz, W., Lotze, H. K., Ricard, D., Vanden Berghe, E., et al. (2010). Global patterns and predictors of marine biodiversity across taxa. *Nature* 466, 1098–1101. doi: 10.1038/nature09329

Watling, L., Guinotte, J., Clark, M. R., and Smith, C. R. (2013). A proposed biogeography of the deep ocean floor. *Prog. Oceanography* 111, 91–112. doi: 10.1016/j.pocean.2012.11.003

Webb, T. J., Vanden Berghe, E., and O'Dor, R. (2010). Biodiversity's big wet secret: The global distribution of marine biological records reveals chronic under-exploration of the deep pelagic ocean. *PloS One* 5, e10223. doi: 10.1371/journal.pone.0010223

Wi, J. H., Suh, H. L., and Yu, O. H. (2014). Two new species of the deep-sea genus *Neotanais* Beddard, 1886 (Tanaidacea: Neotanaididae) from the eastern central Pacific. *J. Crustacean Biol.* 34, 875–885. doi: 10.1163/1937240X-00002274

Wi, J. H., Suh, H. L., and Yu, O. H. (2015). Description of two new species of *Neotanais* Beddard, 1886 (Crustacea, Tanaidacea) from KODOS area. *Zootaxa* 39, 244–256. doi: 10.11646/zootaxa.3926.2.5

Wolff, T. (1956). Isopoda from depths exceeding 6000 m. *Galathea Rep.* 2, 85–157.

Yancey, P. H. (2020). Cellular responses in marine animals to hydrostatic pressure. *J. Exp. Zool.* 2020, 1–23. doi: 10.1002/jez.2354

frontiers | Frontiers in Marine Science

TYPE Original Research
PUBLISHED 17 July 2024
DOI 10.3389/fmars.2024.1392758

OPEN ACCESS

EDITED BY
Kareen E. Schnabel,
National Institute of Water and Atmospheric Research (NIWA), New Zealand

REVIEWED BY
Ajit Kumar Mohanty,
Indira Gandhi Centre for Atomic Research (IGCAR), India
Gustavo Lovrich,
CONICET Centro Austral de Investigaciones Científicas (CADIC), Argentina

*CORRESPONDENCE
Madeleine Hamamé
mhamame@ciep.cl

RECEIVED 28 February 2024
ACCEPTED 26 June 2024
PUBLISHED 17 July 2024

CITATION
Hamamé M, Aedo G, Ortiz P, Olguín A and Pardo LM (2024) Biological and fishery indicators for the small-scale marble crab fishery in Northern Patagonia: recommendations for improving a monitoring program and stock assessment of a data-limited fishery.
Front. Mar. Sci. 11:1392758.
doi: 10.3389/fmars.2024.1392758

Biological and fishery indicators for the small-scale marble crab fishery in Northern Patagonia: recommendations for improving a monitoring program and stock assessment of a data-limited fishery

Madeleine Hamamé[1]*, Gustavo Aedo[1,2], Paula Ortiz[1], Andrés Olguín[3] and Luis Miguel Pardo[4,5]

[1]Centro de Investigación en Ecosistemas de la Patagonia (CIEP), Coyhaique, Chile, [2]Programa de Doctorado en Ciencias con Mención en Manejo de Recursos Acuáticos Renovables (MaReA), Departamento de Oceanografía, Universidad de Concepción, Concepción, Chile, [3]Departamento de Pesquerías, Instituto de Fomento Pesquero, Valparaíso, Chile, [4]Instituto de Ciencias Marinas y Limnológicas, Laboratorio Costero Calfuco, Facultad de Ciencias, Universidad Austral de Chile, Valdivia, Chile, [5]Centros de Investigación en Áreas Prioritarias (FONDAP): Investigación Dinámica de Ecosistemas Marinos de Altas Latitudes, (IDEAL), Universidad Austral de Chile, Valdivia, Chile

Small-scale fisheries have been typically data-limited despite their economic importance for local communities. This is especially true in zones where fishing operations occur in remote areas under harsh weather conditions. Crab fishery in Chile is exclusively artisanal, and marble crab (*Metacarcinus edwardsii*) has the highest landing records. This species is found in most parts of the coast of Chile, but it is mainly caught in the south of the country (including Patagonia). Fishery management is data-limited, and monitoring has not established the spatial and temporal variability baseline necessary to determine its exploitation status. This fishery is currently evaluated annually under a scheme based on reporting biological and fishery information, primarily from the landing ports and secondarily from fishing grounds. In the present study, we collected data from fishing grounds on board artisanal fishing vessels around 45°S during an annual cycle to establish indicators based on catch per unit effort (above and below minimum legal size), size, sex ratio, and the relationship between weight and size. Our results showed that fishery and biological indicators respond more to seasonal patterns than to expected spatial heterogeneity related to different fishing grounds: proportional stock density (lowest in winter), sex ratio (biased toward males in winter), retained catch (highest in autumn), and released catch (highest in winter), while the average size of the largest 10% of the sample only showed differences between males and females. Additionally, released catch varied according to soak time, which indicates the effectiveness of escape rings incorporated in the traps. These results lead to recommendations related to the current monitoring program, which should include the selection of a limited

10.3389/fmars.2024.1392758

number of fishing grounds standardized by season and the incorporation of information related to soak time and the presence of escape rings. Finally, this study highlights the importance of on-board scientific monitoring for any fisheries, even those of small scale.

KEYWORDS

M. edwardsii, monitoring, data-limited fishery, North Patagonia, small-scale fishery

1 Introduction

Since 2013, Chilean fisheries have been regulated by a legislative framework [General Law of Fisheries and Aquaculture (LGPA)] that establishes the maximum sustainable yield (MSY) as the main management objective (Tsikliras and Froese, 2018). This requires the implementation of stock assessment models, based on long-term abundance data and life-history parameters, which allow the estimation of biological reference points (BRPs) (Collie and Gislason, 2001; Morgan et al., 2014). In Chile, there are currently 44 stocks formally declared as fisheries, 27 of which have BRPs (Subpesca, 2022), a low percentage, considering that *ca*. 150 species of fish, crustaceans, mollusks, and other resources are reported in the national landing statistics. This implies that at least 70% of the species that landed in the country lack estimations of MSY, stock abundance, or fishery parameters.

Most of these data-limited fisheries are identified in the category of small-scale fisheries (SSFs) (Béné, 2006). In the Aysén Region, southern Chile (43°38′–49°16′S), only SSFs are allowed in the so-called "inner sea" since the marine ecosystem is restricted to narrow channels and fjords. Over the years, several fishing grounds have been established, maintaining mainly demersal and benthic fisheries that are the main sustenance for local economies. In this region, latitudinal and longitudinal productivity gradients are the result of a marked seasonal pattern associated with solar radiation, freshwater discharge, and precipitation (Aracena et al., 2011; Montero et al., 2011), creating different oceanographic conditions that influence species distribution and their behavioral patterns on a small scale. Therefore, any monitoring strategy should consider the possible effects of this spatial and temporal heterogeneity.

The marble crab, *Metacarcinus edwardsii* (Bell, 1835), is an SSF concentrated mainly in southern Chile (from 36°6′ to 45°3′S), with average annual landings of 4,300 t in the last 10 years (Sernapesca, 2022). The official records of marble crab landings in the Aysén Region date back to 1976 and have been increasing since 1991, being a persistent artisanal fishery for over 30 years. This region contributed on average 20% of this species' landings (an average of 800 t in the last 10 years; Sernapesca, 2022), and 83% of local fishers have licenses to catch this species. This fishery is monitored annually under a scheme that records biological and fishery information, mainly from the landing ports (Olguín and Mora, 2022) since data collection from fishing grounds is difficult and costly. The remoteness of fishing grounds, typically requiring 8 to 48 hours of sailing from the main port, along with harsh weather conditions prevailing for most of the year, represent the primary obstacles to monitoring efforts. Under this context, the government monitoring program estimates total landings (in biomass), size structure, and sex ratio (Olguín and Mora, 2022). However, it lacks estimations for crucial fishery indicators such as effort, catch, and other operational variables like soak time, which necessitate direct collection from fishing operations. This data limitation does not allow the detection of spatial and temporal changes in biological and fishery indicators, and hence, the status of the fishery has not been established. As a result, the regulation of this fishery is restricted only to fishing licenses, gear requirements, minimum legal size, and the prohibition of harvesting of ovigerous females. So far, no regulations on fishing effort or total allowable catch have been implemented.

The main objective of this study was to determine the seasonal and spatial trends of the biological and fishery indicators of *M. edwardsii* in its southernmost fishing grounds, the Aysén Region. The results will allow for recommendations on improving the current monitoring program.

2 Materials and methods

2.1 Study area

The study was carried out in northern Chilean Patagonia, in an area located around 45°20′S and 73°40′W (Figure 1). The marine ecosystem in this region is influenced by a main channel called Moraleda, which separates the archipelago to the west from the continental coast to the east. Fjords, channels, and numerous islands characterize this "inner sea". Water exchange from the open ocean, glacial inputs, light regime, and freshwater discharge varied over latitudinal and longitudinal gradients, presenting a strong seasonal cycle that determines hydrographic conditions and hence productivity patterns (Aracena et al., 2011; Montero et al., 2011). Near the southern extreme of the Moraleda Channel, there is a shallow sill (60 m deep), called the "Meninea Constriction", which partially isolates the southern part of the

10.3389/fmars.2024.1392758

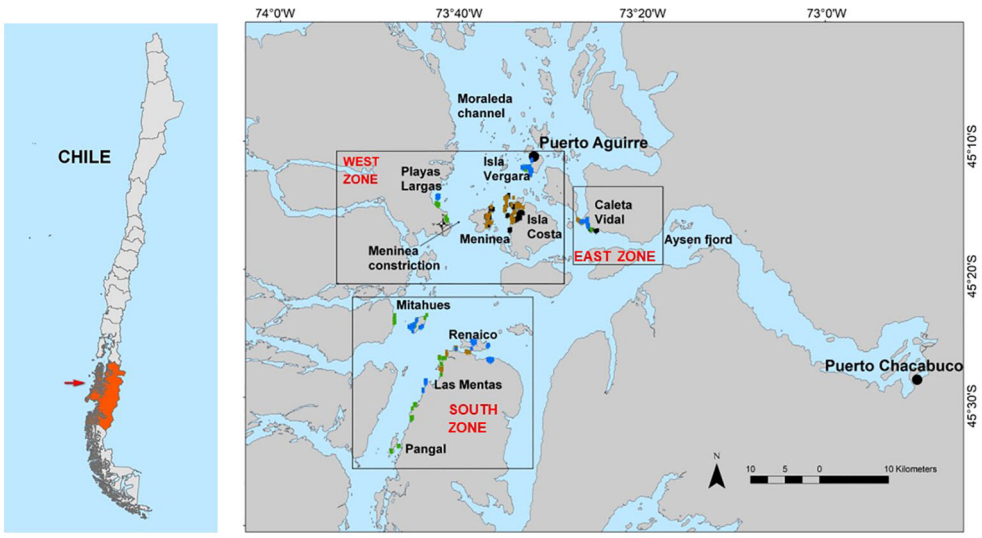

FIGURE 1
Study area; red squares show the main marble crab fishing grounds, south of Puerto Aguirre cove (45°10′S–45°30′W). Colors indicate the location of the fishing traps during autumn (brown), winter (black), spring (green), and summer (blue).

Moraleda Channel and Aysén Fjord from the open ocean. The sill constrains circulation, forming two basins (North and South); the southern basin is warmer, less saline, and more oxygenated than the northern one (Silva et al., 1995, Silva et al., 2000). The northern basin in its western part is influenced by water masses from the Moraleda Channel, i.e., estuarine waters on the surface, modified subantarctic waters as an intermediate water mass, and, in deeper zones, equatorial subsurface waters. In the east, the basin is influenced by waters from the Aysén Fjord. Two water masses are present during the year at the mouth of this fjord, varying their depth according to the season. At the mouth of the fjord, salty estuarine water (21–31 psu) dominates the upper 40 m of the water column, becoming deeper in winter (approximately 100 m). Below this water mass, modified subantarctic water mass dominates at different depths depending on the season (Guzman, 2004).

The study area was selected since it is the main regional fishing ground associated with marble crab (*M. edwardsii*). Fishers and their families reside near the fishing grounds, with travel times ranging from 10 min to several hours of navigation. Extraction occurs year-round, except for a summer break, typically from mid-December until early March, following commercial agreements with buyers.

In this context, 10 fishing grounds were sampled, with efforts to cover all seasons through an annual cycle. Zones were grouped considering oceanographic conditions associated with the Meninea Constriction and the influence of the Aysén Fjord; in this sense, the study areas were divided into the west (n = 4), east (n = 1), and south zones (n = 5, see polygons in Figure 1).

2.2 Sampling

In the study area, the fishery was monitored in the three zones based on seasonal surveys (Table 1). Due to weather conditions, the southern zone could not be sampled during the winter season. Sampling was planned daily according to fishers' activities since the assessment was made on board fishing boats using their traps as the sample unit. Traps are the only fishing gear legally allowed for crabs (Subpesca, 2013). Traps used by the fishers were truncated cone-shaped (Nasa type) and composed of three metal rings, one in the bottom, another in the middle, and a third upper ring to which a plastic entrance tunnel is attached; the diameter of the entrance varied between 25 and 35 cm (Figure 2). Most traps had escape rings with a diameter approximately of 8 cm. Traps were individually set on the seabed at a distance greater than 50 m between them. Therefore, it is assumed that there is no overlap between the effective fishing areas (Aedo and Arancibia, 2003). For each trap, the catch was recorded by the number of individuals, categorized into retained [carapace width (CW), ≥120 mm] and released (CW < 120 mm) [following the minimum legal size (MLS)

TABLE 1 Seasonal sampling in the different fishing zones, Aysén Region.

Season	Sampling date	Fishing grounds
Autumn	March 24 until April 3, 2018	East: Caleta Vidal West: Isla Costa, Isla Meninea South: Las Mentas, Renaico
Winter	June 21–24, 2018 August 13–19, 2018	East: Caleta Vidal West: Isla Costa, Isla Meninea South: no data
Spring	November 26 until December 6, 2018	East: Caleta Vidal West: Isla Vergara, Playas Largas South: Mitahues, Las Mentas
Summer	March 14–23, 2019	East: Caleta Vidal West: Isla Vergara, Playas Largas South: Mitahues, Pangal, Renaico

10.3389/fmars.2024.1392758

FIGURE 2
Boats and fishing gear commonly used by fishers to catch marble crabs in Aysén Region.

of extraction, established in 120-mm CW; D. Ext. No. 9 of 1990 establishes MLS)]. This procedure allowed the estimation of catch per unit effort (CPUE) in a number of individuals. During each fishing trip, three or four traps were randomly selected to collect enough individuals (between 25 and 281 individuals per trap) to allow biological sampling, registering crab size, weight, and sex (Table 2).

2.3 Data analysis

Since 80% of the traps used in the extraction of marble crab have lateral escape rings, soak time could have influenced escape rates and hence CPUE. Consequently, the effect of soak time on released and retained CPUE was analyzed separately.

TABLE 2 Number of traps analyzed as a function of soak time.

Season/ zone	Soak time (days)				
	1	2	3	4	31
Autumn	**64**	**35**	-	**22**	-
West	–	31	–	22	–
East	37	–	–	–	–
South	27	4	–	–	–
Winter	**90**	**12**	**40**	**1**	-
West	71	12	40	1	–
East	19	–	–	–	–
South	-	-	–	–	–
Spring	**96**	**42**	-	**13**	**5**
West	53	17	–	–	–
East	–	–	–	13	–
South	43	25	–	–	5
Summer	**152**	**37**	**23**	-	-
West	15	37	23	–	–
East	29	–	–	–	–
South	108	–	–	–	–
Total	**402**	**126**	**66**	**36**	**5**

Bold numbers indicate the sum of traps analyzed per season.

Seasonal and zone effects were analyzed based on five indicators: i) released and retained CPUE, ii) proportional stock density (PSD), iii) largest 10% of the sample (Lmax), iv) sex ratio, and v) length–weight relationship. PSD relates the number of individuals in a specific size class to the total number of individuals collected. The limit size adopted for the estimation of PSD was the MLS, and therefore, PSD estimates the percentage of individuals whose size exceeds this MLS. This indicator had been proposed by Froesse (2004), describing it as "let them spawn" since it is a measure of the percentage of mature specimens in the catch and hence can show trends of the status of a fishery. Data were also explored considering the average size of the largest 10% of the sample (Lmax) and selected as a measure that is less affected by environmental effects and recruitment variability (Miethe et al., 2016). Sex ratio was estimated as the proportion of the number of males in each trap to the total number of individuals (females + males) and was estimated using only individuals over MLS. Therefore, a sex ratio greater than 0.5 indicates an increased number of males compared to females. Length–weight relationship was calculated using the following formula:$TW = aCW^b$, where TW is body wet weight of crab in g, CW is carapace width in mm, and "a" and "b" are intercept and slope of equation, respectively. The length–weight relationship was transformed into a linear model by taking the natural logarithms of both sides of the equation (Patil and Patil, 2012), making the errors additive, and stabilizing the variances in the model. To test the isometric growth hypothesis ($b = 3$), a t-test was used:$t = \frac{b - b_0}{SE_b}$, where $\hat{b}$,SE_b and df (degrees of freedom, df = n − 2) are from the linear regression, and b_0 is the specified value in the H_0 (Maity, 2018). To compare the slopes of the regressions, first, the coefficients of the slope were estimated using the nlme package (Pinheiro et al., 2018), and then the slopes were compared using least square means (lsmeans; Lenth, 2016).

Non-parametric ANOVA with permutations (using the function aovp from lmPerm package; Wheeler and Torchiano, 2016) was used to search for differences in CPUE (released and retained) among fishing zones and seasons since the data were not normally distributed (Kolmogorov–Smirnov test, $p < 0.05$) and presented heterogeneity of variance (Levene's test, $p < 0.05$). *Post-hoc* tests were performed using permutations pairwise comparisons (rcompanion package; Mangiafico, 2019). ANOVA test was used,

with Tukey's test as *post-hoc* analyses, for Lmax, PSD, and soak time since they presented a normal distribution and homogeneity of variance. A generalized linear model (GLM) test, assuming a quasi-binomial distribution of errors, was used to assess the sex ratio discrepancy between zones and seasons (Wilson and Hardy, 2002).

All calculations and analyses were conducted in the R programming environment (R Core Team, 2023).

3 Results

3.1 Fishing operation

The number of traps varied between boats from 26 and up to 37, depending on whether they had davits or not. A boat without a davit works with fewer traps compared to a larger boat with a davit that operates with two fishers and more traps. During the field trips, it was noticed that under good weather conditions and sufficient bait availability, fishers went daily through all their traps. In these cases, the soak time was typically 1 day. However, in instances of adverse weather conditions or limited bait availability, the soak time could extend beyond this period. The maximum soak time recorded was 31 days. Throughout the study period, all traps employed the same bait, consisting of 3 to 4 kg of Chilean mussels (*Mytilus chilensis*).

3.2 CPUE and soak time

The seasonal surveys between autumn 2018 and summer 2019 resulted in 632 independent and validated records associated with catch per unit effort (CPUE). The soak time of these traps varied between 1 day (n = 402), 2 days (n = 126), 3 days (n = 63), 4 days (n = 36), and 31 days (n = 5).

Retained catch (CPUE ≥ 120 mm) did not show significant differences between 1 and 2 days, nor between 3 and 4 days of soak time (Figure 3A; Tukey's test, $p < 0.001$). However, significant differences were detected at soak times of 1–2 days compared to 3–4 days (Tukey's test; $p < 0.001$). The catch retained with 31 days of soak time was significantly different only from that recorded with 3–4 days (Tukey's test; $p < 0.05$).

Released catch revealed significant differences at soak times of 1 and 2 days and 2 and 3 days (Figure 3B; Tukey's test; $p < 0.001$). For all other possible comparisons, no significant differences were found (Tukey's test; $p > 0.05$).

The influence of soak time on retained and released catch enabled the selection of the most suitable datasets for analyzing spatial (fishing zones) and temporal (seasons) factors concerning various biological and fishery indicators. The analysis for retained CPUE and sex ratio considered catches with 1 and 2 days of soak time (n = 528). In contrast, released CPUE and most other biological indicators were analyzed only with 1 day of soak time (n = 402, Table 2). For the analysis of the length–weight relationship, the information corresponding to all soak times was considered (n = 632) since the relationship between both metric variables is not affected by the rates of entry and escape to the trap.

3.3 Retained catch

For retained catch (considering 1 and 2 days of soak time), the highest size frequencies were between 120- and 130-mm CW (51%) even though maximum sizes reached 190-mm CW.

Seasonal variability was evident across all zones (Figure 4A). In the eastern zone, the retained catch during autumn (average 53 ± SE 2) was higher than in winter (average 41 ± SE 4) and summer (average 43 ± SE 4) (pairwise permutation test; $p < 0.05$). Conversely, in the southern zone, there were no significant differences between autumn and summer (average 34 ± SE 2 and average 37 ± SE 2, respectively) (pairwise permutation test; $p > 0.1$). Additionally, in both seasons, the retained catch was higher than in spring (average 24 ± SE 2) (pairwise permutation test; $p < 0.001$). In the western zone, retained catch in autumn (average 47 ± SE 4) and winter (average 50 ± SE 2) was similar (pairwise permutation test; $p > 0.05$), being higher in both seasons compared to summer (average 38 ± SE 2) and spring (average 26 ± SE 1)

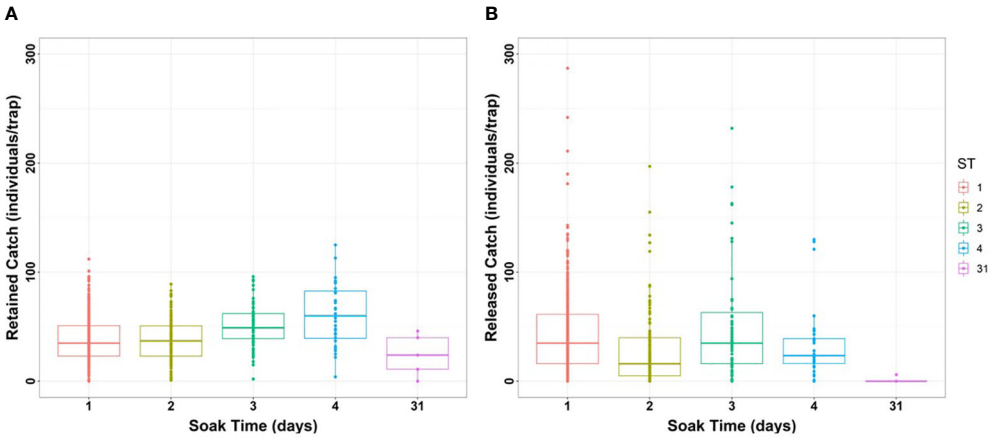

FIGURE 3
(A) Retained and **(B)** released catch (individuals/trap) of marble crab as a function of soak time (days).

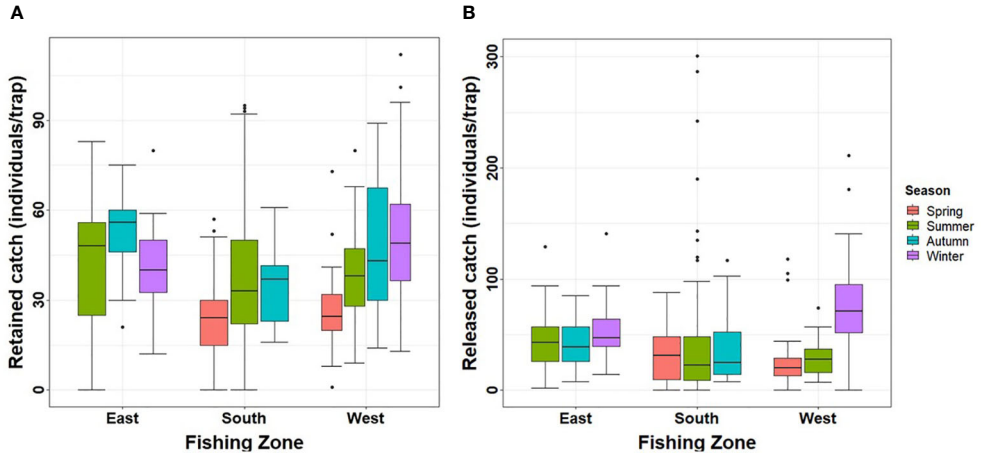

FIGURE 4
(A) Retained catch and **(B)** released catch (individuals/trap) estimated in three fishing zones during an annual cycle in Aysén Region.

(pairwise permutation test; $p < 0.001$). Retained catch in spring was the lowest of all seasons. Data for all zones were available only for summer and autumn; in summer, no differences were found between zones (aovp test; $p > 0.1$), but in autumn, the retained catch was lower in the south (average 34 ± SE 2) compared to the east (average 53 ± SE 2) and west zones (average 47 ± SE 4) (pairwise permutation test; $p < 0.001$). Retained catch in these latter zones was similar, presenting no significant differences (pairwise permutation test; $p > 0.1$).

3.4 Released catch

For total released catch (considering 1 day of soak time), the highest size frequencies were found between 109- and 119-mm CW (72%), but individuals as small as 54-mm CW were retained in the traps. The only zone exhibiting seasonal variation in released catch was the west (Figure 4B), with winter showing higher values (average 77 ± SE 4) compared to the other seasons, namely, spring and summer (pairwise permutation test; $p < 0.01$). Data for all zones were available only for summer. When analyzing this season, no significant differences in the released catch were found between zones (pairwise permutation test; $p > 0.05$).

3.5 Proportional stock density and Lmax

PSD (as a percentage of crabs ≥ MLS) could not be estimated for all seasons in the zones because the data considered only 1 day of soak time. However, in the east and west zones, PSD was minimal in winter, increasing toward spring and summer to a maximum in

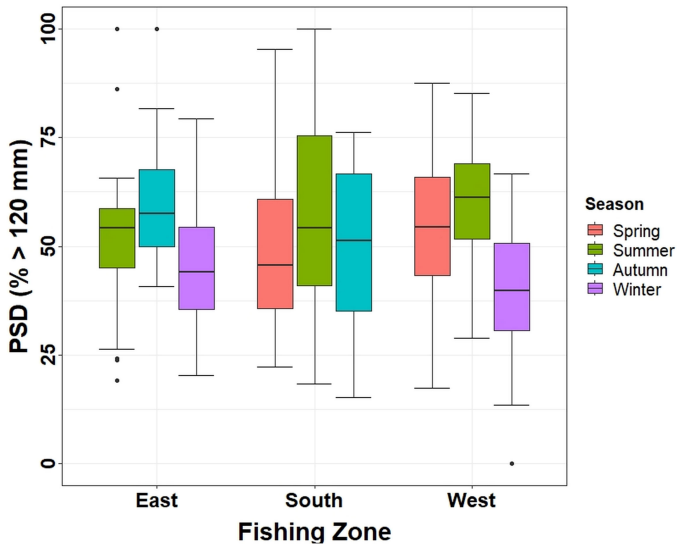

FIGURE 5
PSD (expressed as average percentage of individuals over 120 mm) estimated in the three fishing zones during an annual cycle in Aysén Region. PSD, proportional stock density.

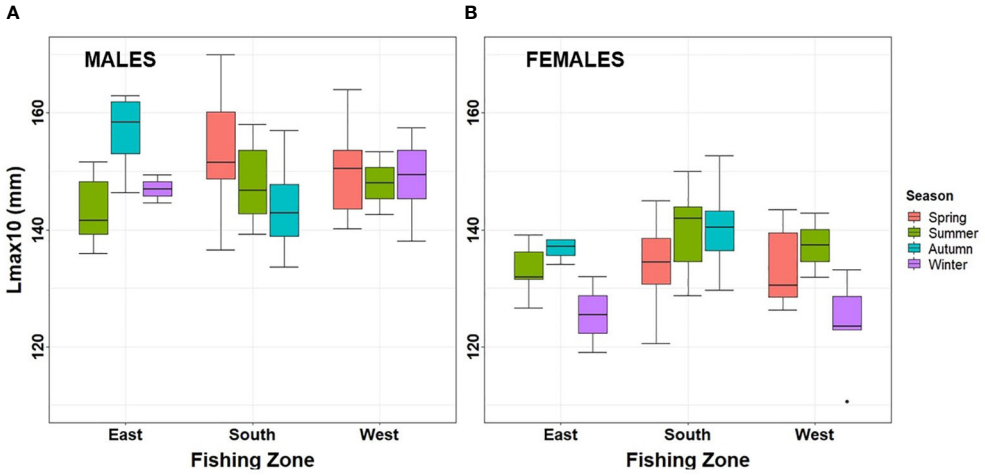

FIGURE 6
Lmax of **(A)** males and **(B)** females estimated in the three fishing zones during an annual cycle in Aysén Region. Lmax, largest 10% of the sample.

autumn (Figure 5). In the eastern zone, PSD in autumn was higher (average 60 ± SE 3) than in summer (average 52 ± SE 3; pairwise permutation test, $p < 0.05$) and winter (average 44 ± SE 3; pairwise permutation test, $p < 0.001$). In the western zone, PSD could not be estimated in autumn, but spring (average 54 ± SE 2) and summer (average 59 ± SE 4) presented a higher PSD compared to winter (average 40 ± SE 2; pairwise permutation test, $p < 0.001$). Conversely, in the south, no significant differences were found between seasons (ANOVA test; $p > 0.1$), although winter could not be sampled. In summer (where all zones were sampled), no significant differences were found (ANOVA test; $p > 0.1$).

Lmax (top 10%) were similar between seasons in the same zone (ANOVA test; $p > 0.1$) and were also similar in summer when all zones could be sampled (ANOVA test; $p > 0.1$). Lmax varied on average between 136- and 147-mm CW, having a minimum value of 110-mm CW and a maximum of 170-mm CW. Lmax were different between sexes (ANOVA test; $p < 0.001$), as males were larger (average 149 ± SE 1) compared to females (average 135 ± SE 1) (Figures 6A, B).

3.6 Sex ratio

The sex ratio was analyzed based on individuals exceeding the MLS using both 1 and 2 days of soak time. For most seasons and zones, males dominated this fraction of the stock (Figure 7). Generally, males were predominant during winter (average 0.84 ± SE 0.05) compared to the other seasons. In contrast, in autumn in the west and south zones, females dominated the catch (average 0.34 ± SE 0.08), being statistically different from spring and summer in the south (GLM test; $p < 0.05$; Supplementary Material; Table S1) and spring and winter in the west (GLM test; $p < 0.05$). In summer and autumn when there were enough data to compare all zones, no significant differences were found during summer between zones (GLM test; $p > 0.1$), but in autumn, significant differences were found between the east zone (average 0.59 ± SE 0.03) and the south and west zones (GLM test; $p < 0.05$; Supplementary Material; Table S1).

3.7 Length–weight relationship

The sample sizes for the length–weight relationship varied between 591 and 2,033 individuals for the spatial analysis (zones) and between 515 and 1,361 individuals for the temporal analysis (seasons). For each sex in the different fishing zones and seasons, after the log transformation of data, the adjustment of the length–weight relationship was significant (Student's t-test; $p < 0.05$) (Supplementary data, Tables S2 and S3). In terms of growth type, slope b was significantly higher than 3 in males and statistically less than 3 in females, indicating positive and negative allometric growth, respectively (Student's t-test; $p < 0.05$) (Supplementary data, Tables S2 and S3). The comparison between the slopes of the regressions determined a significant effect of the zone (ANOVA test; $p < 0.01$) and season (ANOVA test; $p < 0.001$) only in the case of males, but not for females (in both factors: ANOVA test; $p > 0.05$). The slope b of males collected in the eastern zone was statistically lower than the estimated for the western (Tukey's test; $p < 0.05$) and southern zones (Tukey's test; $p < 0.01$). In addition, the slope b of males collected in spring was statistically higher than the estimated for autumn (Tukey's test; $p < 0.001$), winter (Tukey's test; $p < 0.001$), and summer (Tukey's test; $p < 0.01$).

4 Discussion

Our study is the first to collect data on the marble crab in the main fishing grounds of Northern Patagonia through a design implemented on board artisanal vessels during an annual cycle. Although we encountered sampling limitations since in some fishing zones data could not be obtained across seasons, most estimated indicators presented seasonal variability, and some

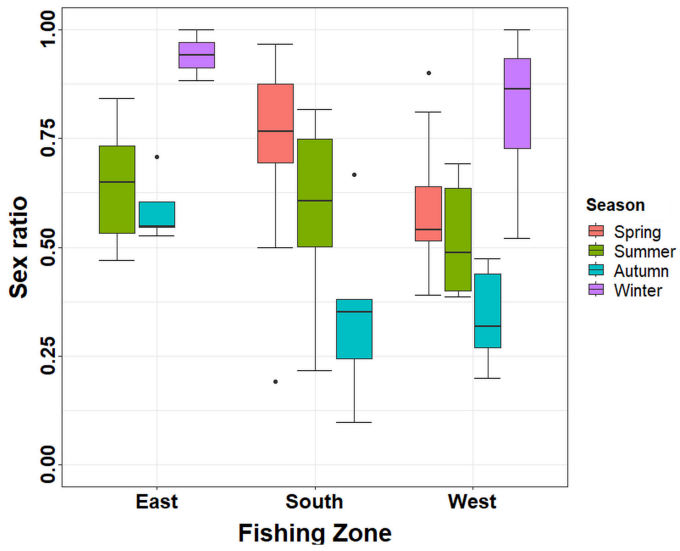

FIGURE 7
Sex ratio (expressed as average with standard error) of individuals over 120-mm CW estimated in the three fishing zones during an annual cycle in Aysén Region. CW, carapace width.

patterns could be identified along the zones. For all zones, retained CPUE was higher during autumn compared to other seasons. In contrast, in spring, retained CPUE was the lowest. This seasonal variability could be associated with the reproductive cycle of the studied species. In autumn, trap efficiency could be enhanced by higher foraging activity related to increased energetic demand preceding spawning in females and gonadal recovery after mating in males (Pardo et al., 2013, 2015, 2020). In contrast, low retained CPUE in spring could be associated with an intensive mating period described for this species from the end of spring/beginning of summer (Pardo et al., 2013, 2016). It has been observed during this phase that male and female crabs reduce their feeding response (Skinner and Hill, 1987; Kennelly and Watkins, 1994). Other non-exclusive factors could be seasonal bathymetric migrations, described for this species in lower latitudes (Pardo et al., 2020), and stock depletion through the year (Bez et al., 2006) since the fishing period usually ends in spring.

Released CPUE was seasonal only in the western fishing zone, with the highest catch recorded during winter. Under the assumption that the catch per trap is proportional to the abundance and availability for both juveniles and adults, at least at short soak times (i.e., 1 day), an increase in the capture of individuals classified as pre-fishery recruits (dominated by individuals between sizes of 104 and 119 mm) could be associated with migratory movements (Pardo et al., 2020). In crabs, movement patterns have been mostly associated with changes in habitat use, search for refuge sites, and reproductive migration events (Hines et al., 1995; Muñoz et al., 2006; Curtis and McGaw, 2008). However, these hypotheses should be explored since in the eastern zone, no seasonal changes were observed in the released catch.

Other fishery indicators (PSD, Lmax, and sex ratio) showed seasonal variability. The main trend was associated with a lower proportion of stock catches in winter, principally by large males. This tendency was found in the east and west zones. The lack of seasonal variability in the southern zone could be explained by sampling difficulties in winter. The higher proportion of males found in winter could be explained by catch bias by sex, considering that during this period most females are carrying embryos. Since it had been demonstrated that their foraging activity is reduced during this stage (Howard, 1982), they are not easily drawn to the trap.

Our results showed that catches of crabs ≥120-mm CW were biased toward males in most of the seasons and zones. The sex ratio could get as high as 11 males per female, averaging between 2 and 3 males per female. Although the optimal sex ratio is unclear, the skewed ratio toward males and the presence of large males indicate that fishing is not adversely affecting these reproductive traits. In our study, males could be on average 14 mm larger than females, which is consistent with results found in areas of low fishing intensity (Pardo et al., 2017). Sexual dimorphism was evident not only in size but also in the relationship between size and weight. Females exhibited negative allometry, whereas males showed positive allometry, as previously described for this species (Pool et al., 1998; Olguín and Mora, 2022; Daza et al., 2023). Considering that females mate after molting, previous studies have found they preferentially mate with larger males due to the need for a pre- and post-copulatory embrace to ensure survival (Pardo et al., 2018). This mating process may also be favored by the greater weight growth in males compared to females (Waiho et al., 2015). In our study, higher weight in spring for males compared to other seasons agrees with this: during the mating period (i.e., spring), males could shift their energy investment toward growth (Sumer et al., 2013) to protect females.

Fishery stock monitoring based on the recording of variables on board artisanal vessels allows the establishment of indicators that compare the exploited (legal) and unexploited (non-legal) fractions,

which in the case of the marble crab fishery corresponds to individuals below and above the minimum legal size of extraction (MLS ≥ 120 mm CW). For example, median PSD varied mostly between 40% and 60% for different fishing zones and seasons. This level of detailed fishing information provides higher resolution fishing information compared to solely monitoring retained catch from landing ports (Olguín and Mora, 2019).

Our results showed that soak time differences between traps are key to a correct estimation and, hence, comparison of biological and fishery indicators. Especially in zones where the presence of escape rings is a common practice among fishers (as in the Aysén Region), favoring after 1 day of soak time, the escape of small individuals through this mechanism. These results agreed with field observations since we could verify that bait decreases its effectiveness when soak time exceeds 1 day, causing small individuals to leave the traps through the escape rings. Literature also indicates that the capture of small individuals decreases with escape rings (Rosa-Pacheco and Ramírez-Rodríguez, 1996; Aguilar and Pizarro, 2006; Arana et al., 2011). From the operational point of view, this benefits not only the fishers hauling traps by hand (i.e., decreasing the weight of each trap) but also the juveniles since handling may affect survival. This ultimately highlights the importance of incorporating escape rings as a mandatory administrative measure.

5 Conclusions

Our results showed that the variability of fishery and biological indicators responds more to seasonal patterns than to expected heterogeneity across fishing grounds. These results allowed us to make monitoring recommendations for crab fisheries.

- Monitoring should be based on a representative and easily accessible number of fishing zones that could be monitored over time.
- Design should be oriented on annual seasonality that allows coupling between catch indicators (CPUE), size, and reproductive parameters.
- Biological and fishery indicators should be estimated with data from 1 or 2 days of soak time since the catch is affected by this variable.
- Trap design for capturing crabs must incorporate escape rings to reduce the catchability of small individuals. This not only has operational advantages but also improves the survival of non-commercial individuals.
- Monitoring on board artisanal vessels allows georeferencing with a high spatial resolution, giving an opportunity to evaluate the exploitation status of marble crabs at the scale of fishing zones (e.g., data-limited and index-based).

In conclusion, these results allow us to develop improved monitoring recommendations for this fishery in Northern Patagonia. Specifically, monitoring could be based on a more limited number of fishing grounds but should be standardized by season, soak time, and presence/absence of escape rings. Moreover, the correlation between indicator temporal variability with the reproductive cycle of this species highlights the necessity for monitoring its possible seasonal variations in parallel.

Data availability statement

The original contributions presented in the study are included in the article/Supplementary Material. Further inquiries can be directed to the corresponding author.

Ethics statement

Ethical approval was not required for the study involving animals in accordance with the local legislation and institutional requirements because during the study we did not sacrifice the animals, all individuals were return immediately after being weighed and measured to their marine environment trying to ensure their maximum survival.

Author contributions

MH: Conceptualization, Data curation, Formal analysis, Funding acquisition, Investigation, Methodology, Project administration, Resources, Software, Supervision, Validation, Visualization, Writing – original draft, Writing – review & editing. GA: Conceptualization, Data curation, Investigation, Methodology, Software, Validation, Visualization, Writing – original draft, Writing – review & editing. PO: Funding acquisition, Investigation, Methodology, Project administration, Validation, Writing – review & editing. AO: Conceptualization, Validation, Writing – review & editing. LP: Conceptualization, Investigation, Methodology, Validation, Visualization, Writing – original draft, Writing – review & editing.

Funding

The author(s) declare financial support was received for the research, authorship, and/or publication of this article. This research was funded by CORFO through grant BPCR 75810 “Línea base biológica-pesquera del recurso Jaiba marmola: insumos para su manejo sustentable en la Región de Aysén”. Partial funding was available through Programa Regional ANID R20F0002.

Acknowledgments

The authors would like to thank Brian Reid for the English revision of the manuscript and Nahuelquin and Legue families and Adan Mansilla for allowing us to go with them on their fishing trips and to collect samples. Luis Miguel Pardo thanks to FONDAP IDEAL 15150003.

Conflict of interest

The authors declare that the research was conducted in the absence of any commercial or financial relationships that could be construed as a potential conflict of interest.

Publisher's note

All claims expressed in this article are solely those of the authors and do not necessarily represent those of their affiliated organizations, or those of the publisher, the editors and the reviewers. Any product that may be evaluated in this article, or claim that may be made by its manufacturer, is not guaranteed or endorsed by the publisher.

Supplementary material

The Supplementary Material for this article can be found online at: https://www.frontiersin.org/articles/10.3389/fmars.2024.1392758/full#supplementary-material

References

Aedo, G., and Arancibia, H. (2003). Estimating the attraction area and the effective fishing area for Chilean lemon crab (*Cancer porteri*) using traps. *Fisheries Res.* 60, 267–272. doi: 10.1016/S0165-7836(02)00177-7

Aguilar, M., and Pizarro, P. (2006). Empleo de ventanas de escape en trampas para la captura de jaiba peluda (*Cancer setosus*) en Iquique. *Chile. Investigaciones Marinas Valparaíso* 34, 63–70. doi: 10.4067/S0717-71782006000200007

Aracena, C., Lange, C. B., Iriarte, J. L., Rebolledo, L., and Pantoja, S. (2011). Latitudinal patterns of export production recorded in surface sediments of the Chilean Patagonian fjords (41–55°S) as a response to water column productivity. *Continental Shelf Res.* 31, 340–355. doi: 10.1016/j.csr.2010.08.008

Arana, P., Orellana, J. C., and De Caso, A. (2011). Escape vents and trap selectivity in the fishery for the Juan Fernández rock lobster (*Jasus frontalis*), Chile. *Fisheries Res.* 110, 1–9. doi: 10.1016/j.fishres.2011.03.021

Bell, T. (1835). Observations on the genus Cancer of Dr. Leach (Platycarcinos Latr.), with descriptions of three new species. *Proceedings of the Zoological Society of London* 1835, 86–88.

Bez, N., De Oliveira, E., and Duhamel, G. (2006). Repetitive fishing, local depletion, and fishing efficiencies in the Kerguelen Islands fisheries. *ICES J. Mar. Sci.* 63, 532–542. doi: 10.1016/j.icesjms.2005.10.005

Béné, C. (2006). *Small-scale fisheries: assessing their contribution to rural livelihoods in developing countries. FAO Fisheries Circular No. 1008* (Rome: FAO), 46.

Collie, J. S., and Gislason, H. (2001). Biological reference points for fish stocks in a multispecies context. *Can. J. Fisheries Aquat. Sci.* 58, 2167–2176. doi: 10.1139/cjfas-58-11-2167

Curtis, D. L., and McGaw, I. J. (2008). A year in the life of a Dungeness crab: methodology for determining microhabitat conditions experienced by large decapod crustaceans in estuaries. *J. Zoology* 274, 375–385. doi: 10.1111/j.1469-7998.2007.00397.x

Daza, E., Olguín, A., Almonacid, E., Mora, P., and Pacheco, H. (2023). Programa de Seguimiento de las Principales Pesquerías Nacionales, año 2022: Pesquerías: Crustáceos Bentónicos. *Informe Final IFOP-Ministerio Economía*, 391.

Froese, R. (2004). Keep it simple: three indicators to deal with overfishing. *Fish Fisheries* 5, 86–91. doi: 10.1111/j.1467-2979.2004.00144.x

Guzman, D. (2004). "Caracterización hidrográfica, oceanográfica y balance de nitrógeno y fosforo del fiordo Aysén. Tesis para obtener el grado de magister en oceanografía," in *Facultad de recursos naturales* (Pontificia Universidad Católica de Valparaíso, Valparaíso. Chile).

Hines, A. H., Wolcott, T. G., González-Gurriarán, E., González-Escalante, J. L., and Freire, J. (1995). Movement patterns and migrations in crabs: telemetry of juvenile and adult behavior in *Callinectes sapidus* and *Maja squinado*. *J. Mar. Biol. Assoc. United Kingdom* 75, 27–42. doi: 10.1017/S0025315400015174

Howard, A. E. (1982). The distribution and behaviour of ovigerous edible crabs (Cancer pagurus), and consequent sampling bias. *J. duConseil Int. pour l'Exploration la Mer* 40, 259–261. doi: 10.1093/icesjms/40.3.259

Kennelly, S. J., and Watkins, D. (1994). Fecundity and reproductive period, and their relationship to catch rates of spanner crabs, *Ranina ranina*, off the east coast of Australia. *J. Crustacean Biol.* 14, 146–150. doi: 10.1163/193724094X00533

Lenth, R. V. (2016). Least-squares means: the R package lsmeans. *J. Stat. Software* 69, 1–33. doi: 10.18637/jss.v069.i01

Maity, R. (2018). *Statistical methods in hydrology and hydroclimatology*. (Singapure: Springer), 444. doi: 10.1007/978-981-10-8779-0

Mangiafico, S. (2019). *Functions to support extension education program evaluation* (R Package 'rcompanion' Version 2.1.1). Available online at: https://rcompanion.org/handbook/G_14.html.

Miethe, T., Dobby, H., and McLay, A. (2016). The use of indicators for shellfish stocks and fisheries: A literature review. *Scottish Mar. Freshw. Sci.* 7, 78. doi: 10.7489/1764-1

Montero, P., Daneri, G., González, H. E., Iriarte, J. L., Tapia, F. J., Lizárraga, L., et al. (2011). Seasonal variability of primary production in a fjord ecosystem of the Chilean Patagonia: implications for the transfer of carbon within pelagic food webs. *Continental Shelf Res.* 31, 202–215. doi: 10.1016/j.csr.2010.09.003

Morgan, M. J., Shelton, P. A., and Rideout, R. M. (2014). An evaluation of fishing mortality reference points under varying levels of population productivity in three Atlantic cod (*Gadus morhua*) stocks. *ICES J. Mar. Sci.* 71, 1407–1416. doi: 10.1093/icesjms/fsu092

Muñoz, C., Pardo, L. M., Henriquez, L., and Palma, A. (2006). Variaciones temporales en la composición y abundancia de cuatro especies de *Cancer* (Decapoda: Brachyura: Cancridae) capturadas con trampas en bahía San Vicente, Concepción (Chile central). *Investigaciones Marinas Valparaíso* 34, 9–21. doi: 10.4067/S0717-71782006000200002

Olguín, A., and Mora, P. (2019). "Seguimiento General de Pesquerías: Crustáceos Bentónicos: Jaibas y Centolla X y XI Regione," in *IFOP, Ministerio de economía* Fomento y Turismo, Valparaíso, Chile, vol. 149.

Olguín, A., and Mora, P. (2022). "Seguimiento General de Pesquerías: Crustáceos Bentónicos: Jaibas y Centolla, Región de Los Lagos y Región de Aysén. 2021," in *IFOP, Ministerio de economía* Fomento y Turismo, Valparaíso, Chile, vol. 171.

Pardo, L. M., Riveros, M., Chaparro, O., and Pretterebner, K. (2018). . Ejaculate allocation in brachyura: what do males of *Metacarcinusedwardsii* respond to? *Aquat. Biol.* 27, 25–33. doi: 10.3354/ab00693

Pardo, L. M., Riveros, M., Fuentes, J. P., and Lopez-Greco, L. (2013). Functional morphology of the seminal receptacle in the crab *Metacarcinus edwardsii*. *Invertebrate Biol.* 132, 386–393. doi: 10.1111/ivb.12038

Pardo, L. M., Riveros, M. P., Fuentes, J., Pinochet, R., Cárdenas, C., and Sainte-Marie, B. (2017). High fishing intensity reduces females' sperm reserve and brood fecundity in a eubrachyuran crab subject to sex- and size-biased harvest. *ICES J. Mar. Sci.* 74, 2459–2469. doi: 10.1093/icesjms/fsx077

Pardo, L. M., Riveros, M. P., Fuentes, J. P., Rojas-Hernandez, N., and Veliz, D. (2016). An effective sperm competition avoidance strategy in crabs drives genetic monogamy despite evidence of polyandry. *Behav. Ecol. Sociobiology* 70: 1, 73–81. doi: 10.1007/s00265-015-2026-6

Pardo, L. M., Rosas, Y., Fuentes, J. P., Riveros, M. P., and Chaparro, R. C. (2015). Fishery induces sperm depletion and reduction in male reproductive potential for crab species under male-biased harvest strategy. *PloS One* 10, e0115525. doi: 10.1371/journal.pone.0115525

Pardo, L. M., Rubilar, P. R., and Fuentes, J. P. (2020). North Patagonian estuaries appear to function as nursery habitats for marble crab (*Metacarcinus edwardsii*). *Regional Stud. Mar. Science.* 36, 101315. doi: 10.1016/j.rsma.2020.101315

Patil, K. M., and Patil, M. U. (2012). Length-weight relationship and condition factor of freshwater crab *Barytelphusagurini* (Decapoda, Brachyura). *J. Exp. Sci.* 3, 13–15. doi: 10.3170/ajas.5.1.14902

Pinheiro, J., Bates, D., DebRoy, S., and Sarkar, D. (2018). *R Development Core Team; nlme: Linear and Nonlinear Mixed Effects Models. Rpackage version 3.1-137*. Available online at: http://CRAN.R-project.org/package=nlme.

Pool, H., Montenegro, C., Canales, C., Barahona, N., and Vicencio, C. (1998). "Análisis de la Pesquería de jaibas en la X Región," in *proyecto FIP*, vol. 76. , 96–35.

R Core Team (2023). *R: A language and environment for statistical computing* (Vienna: R Foundation for Statistical Computing). Available at: https://www.R-project.org.

Rosa-Pacheco, R. D. L., and Ramírez-Rodríguez, M. (1996). Escape vents in traps for the fishery of the California spiny lobster, *Panulirus interruptus*, in Baja California Sur, Mexico. *Cienc. Mar. Baja Calif. Mexico* 22, 235–243. doi: 10.7773/cm.v22i2.849

Sernapesca (2022).Anuario Estadístico de pesca 2010-2022. Ministerio de Economía, Fomento y Reconstrucción. Sección Desembarques artesanales y Acuicultura. In: *Servicio Nacional de Pesca y Acuicultura*. Available online at: www.sernapesca.cl (Accessed September 10, 2023).

Silva, N., Guzmán, D., and Valdenegro, A. (2000). "Aysén sound, Chile," in *Estuarine system of the South American region: carbon, nitrogen and phosphorus fluxes. LOICZ*

Reports and Studies 15, Texel. Eds. S. V. Smith, V. Dupra, J. I. M. Crossland and C. J. Crossland (The Netherlands), 55–64.

Silva, N., Siervers, H., and Prado., R. (1995). Características oceanográficas y una proposición de circulación para algunos canales australes de Chile (41° 20'S, 46° 40'S). *Rev. Biología Marina* 30, 207–254.

Skinner, D. G., and Hill, B. J. (1987). Feeding and reproductive behaviour and their effect on catchability of the spanner crab *Ranina ranina*. *Mar. Biol.* 94, 211–218. doi: 10.1007/BF00392933

Subpesca (2013). "Nómina nacional de pesquerías artesanales. Res. Ext. N° 3115, nov 2013," in *Ministerio de Economía, Fomento y Turismo*, Valparaíso, Chile.

Subpesca (2022).Estado de situación de las principales pesquerías Chilenas. Año 2020. In: *Departamento de Pesquerías. División de Administración Pesquera* (Chile: Valparaíso). Available online at: https://www.subpesca.cl/portal/618/w3-article-117812.html (Accessed October 4, 2023).

Sumer, C., Teksam, I., Karatas, H., Beyhan, T., and Aydin, C. M. (2013). Growth and reproduction biology of the blue crab, *callinectes sapidus* rathbun 1896, in the beymelek lagoon (Southwestern coast of Turkey). *Turkish J. Fisheries Aquat. Sci.* 13, 675–684. doi: 10.4194/1303-2712-v13_4_13

Tsikliras, A. C., and Froese, R. (2018). *Maximum sustainable yield. 2nd ed*. Ed. B. Fath (Amsterdam, Holanda: Elsevier), 1–20.

Waiho, K., Mustaqim, M., Fazhan, H., Wan Norfaizza, W. I., Megat, F. H., and Ikhwanuddin, M. (2015). Mating behaviour of the orange mud crab, *Scylla olivacea*: The effect of sex ratio and stocking density on mating success. *Aquaculture Rep.* 2, 50–57. doi: 10.1016/j.aqrep.2015.08.004

Wilson, K., and Hardy, I. C. W. (2002). *Sex ratios concepts and research methods* (Cambridge University Press Print), 48–92. doi: 10.1017/CBO9780511542053.004

Wheeler, B., and Torchiano, M. (2016). *lmPerm: permutation tests for linear models, version: 2.1.0*. https://CRAN.R-project.org/package=lmPerm.

frontiers | Frontiers in Marine Science

TYPE Original Research
PUBLISHED 03 September 2024
DOI 10.3389/fmars.2024.1457051

OPEN ACCESS

EDITED BY
Sabrina Lo Brutto,
University of Palermo, Italy

REVIEWED BY
Sara Ignoto,
University of Milan, Italy
Lena Hartebrodt,
The University of Auckland, New Zealand

*CORRESPONDENCE
Rachael A. Peart
rachael.peart@niwa.co.nz

RECEIVED 30 June 2024
ACCEPTED 23 July 2024
PUBLISHED 03 September 2024

CITATION
Peart RA and Schnabel KE (2024) A new species of *Pentaceration* (Paramunnidae, Isopoda, Crustacea) from the Otago region of Aotearoa New Zealand.
Front. Mar. Sci. 11:1457051.
doi: 10.3389/fmars.2024.1457051

A new species of *Pentaceration* (Paramunnidae, Isopoda, Crustacea) from the Otago region of Aotearoa New Zealand

Rachael A. Peart* and Kareen E. Schnabel

Biodiversity and Biosecurity, Oceans Centre, National Institute of Water and Atmospheric Research, Wellington, New Zealand

A new paramunnid species, *Pentaceration forkandbrewer* sp. nov., is described from Otago, Aotearoa New Zealand (Otago region). The majority of specimens examined were collected during a "Ports of Otago" survey carried out by the National Institute of Water and Atmospheric Research Ltd., Christchurch. *Pentaceration forkandbrewer* sp. nov. can be identified by the following characters: by the lack of dorsal protuberances, the reduced mid-head spine and the flattened, and calcified pereon with serrated margins. All the pereonites end in a point and are reasonably broad. *Pentaceration forkandbrewer* sp. nov. is most similar to the Australian species *P. serrata* and the Argentinian species *P. pleonarietis*. The new species is described, and an adapted key to the *Pentaceration* species of Aotearoa New Zealand is provided.

LSIDurn: lsid:zoobank.org:pub:138FAF76-3721-408F-AE39-C3F88F295E38.

KEYWORDS

Isopoda, *Pentaceration*, New Zealand, Paramunnidae, species

1 Introduction

Pentaceration Just, 2009 is a species-rich genus in the family Paramunnidae (Vanhöffen, 1914) containing 23 species, including this current new species. It is the most species rich genus in the family and primarily has a Gondwanan distribution (Just, 2009, 2011; Kaiser and Marner, 2012), with all but one species recorded from Australian and Aotearoa New Zealand waters. This genus generally occurs from shallow, coastal waters to depths of approximately 5,500 m. This is a large genus established by Just in 2009. In that paper, the genus was established along with two new species. This was followed up by a large 2011 monograph by Just describing another 18 species from Australia and New Zealand. Subsequent work has included one new species from New Zealand (Kaiser and Marner, 2012) and one species from Argentina (Doti, 2017).

In New Zealand waters, there are seven species including the species described here. These are *Pentaceration bifficlyro* Kaiser and Marner, 2012, *P. curvicornis* Just, 2011,

P. dentifera Just, 2011, *P. epipedos* Just, 2011, *P. forkandbrewer* sp. nov., *P. novaezealandia* Just, 2011, and *P. setosa* Just, 2011, with an eighth species on the edge of New Zealand's Exclusive Economic Zone, *P. kermadecia* Just, 2011.

Pentaceration species are often distinctive in appearance and sometimes extremely sculptured. There appears to be two main groups of species within this genus: those with a row of dorsal projections and those who are smooth dorsally. Here, we describe a new species of *Pentaceration* from the Otago coast of the South Island of New Zealand, collected from shallow water. This new species is compared to both the New Zealand fauna and the global *Pentaceration* fauna in general. A key to the New Zealand species of *Pentaceration* is also provided.

2 Materials and methods

The material was obtained from a series of collections for an environmental assessment of the impact of dredging over time conducted every three years in the Otago port region (Seaward et al., 2021). The specimens were identified as being new to science through the use of Just, (2009, 2011) and Kaiser and Marner (2012).

Dorsal illustrations were conducted of specimens in glycerine. The female holotype and one male paratype were dissected and the appendages fixed in glycerine. Pencil drawings were made using a Zeiss Axioskop 2 compound microscope with a camera lucida. These drawings were inked using pens and drawing film, scanned and plates were arranged using a Wacom Intuos 4 drawing board using Adobe Photoshop CS software. In addition, scanning electron microscope (SEM) pictures were taken of a paratype female and a paratype male to examine micro-structural features. Assessment of length:width ratios and the terminology follows methods proposed by Just and Wilson (2004, 2006) and Just (2009); the length provided for specimens under examined material is given as total body length in mm taken. Additionally, lateral pereonite spine length is measured from the point, where pereonites diverge from each other, to the distal tip. Furthermore, the length of distal projection of the pleotelson is measured from the insertion of the uropods to the posterior tip. The terminology of the setation follows Riehl and Brandt (2010).

The type materials, including those used for SEM images, are deposited at the National Institute of Water and Atmospheric Research Ltd. (NIWA), Wellington (New Zealand) (NIWA173287 – 90).

Abbreviations used in text and figures include the following: A1, antennula; A2, antenna; Mx1, maxilla; Mx2, maxillula; Mxp, maxilliped; MdR, right mandible; Op, operculum; PI–VII, pereopods I–VII; Plp1–5, pleopods 1–5; Urp, uropods; NIWA, National Institute of Water and Atmospheric Research Ltd.

3 Results

3.1 Genus composition

3.1.1 Composition

Order ISOPODA Latreille, 1817

Suborder ASELLOTA Latreille, 1802

Paramunnidae Vanhöffen, 1914

Pentaceration Just, 2009

Synonyms: *Janirella*? sp. Gamō, 1987: 44

Type species: *Pentaceration bassiana* Just, 2009, by original designation.

Species composition. *P. bassiana* Just, 2009, *P. bifficlyro* Kaiser and Marner, 2012, *P. bifida*, Just, 2011, *P. bovicornis* Just, 2011, *P. curvicornis* Just, 2011, *P. denticornis* Just, 2011, *P. dentifera* Just, 2011, *P. epipedos* Just, 2011, *P. globopleonis* Just, 2011, *P. kermadecia* Just, 2011, *P. lancifera* Just, 2011, *P. magna* Just, 2011, *P. megalomos* Just, 2011, *P. novaezealandia* Just, 2011, *P. omalos* Just, 2011, *P. pleonarietis* Doti, 2017, *P. rihothalassa* Just, 2011, *P. serrata* Just, 2011, *P. setosa* Just, 2011, *P. simplex* Just, 2011, *P. spinosissima* Just, 2009, *P. tasmaniensis* Just, 2011.

3.1.2 Genus distribution

South-East Australia, Arafura Sea, Kermadec Trench, New Zealand, and associated sub-Antarctic islands; Argentine Sea, South-West Atlantic. 7–5340 m.

3.1.3 Genus diagnosis

(After Just, 2009). Head frontal margin between antennulae with 1 median forward pointing spine and 2 lateral spines pointing forward and outward at ~60° angle to the head midline. Eyestalks elongate, spine-like, or distally rounded, with or without ommatidia. Coxae not visible in dorsal view. Pereonites with lateral spines of varying length, pereonite 1 often rounded laterally; width of pereonite 4 reduced compared with 3 and 5. Pleotelson lateral margins serrate. Mandible palp present, stubby with bean-shaped article 3, molar process triturative, distally flared. Pereopod I carpus with 2 straight robust setae on posterior margin; propodus with robust and simple setae on margin opposing carpus. Uropods inserted dorsally just inside pleotelson margin, uniramous or biramous, protopod recessed, exopod distinctly developed, vestigial, or absent.

3.1.4 Genus remarks

Due to the high morphological diversity in this genus, there have been numerous comments and discussions regarding the possibility of splitting the genus based on apparent apomorphies. These include: presence/absence of a middorsal spine on pereonites 1 – 7: present in *P. spinosissima*, *P. denticornis*, *P. curvicornis*, *P. lancifera*, *P. omalos* and *P. magna* and absent in the other species (Just, 2011); the state of presence/vestigial/absence of the uropod exopod: obviously present – *P. bifficlyro* and *P. magna*; vestigial/reduced – *P. bassiana, P. bovicornis, P. kermadecia, P. rihothalassa, P. spinosissima* or absent – all remaining) (Kaiser and Marner, 2012); and the shape of the pleotelson: lateral margins diverging with distolateral corners hooked inwards – *P. rihothalassa, P. bassiana*; possessing an elongated distal projection – *P. bifficlyro, P. denticornis, P. lancifera, P. omalos*, and *P. spinosissima* (Doti, 2017); two anterolateral processes curved backwards – *P. pleonarietis*; possessing a short distal projection – all remaining (Doti, 2017). It is evident by the variety and distribution of states that no clear set of characters can divide the genus.

3.2 Proposed species

3.2.1 New species

Pentaceration forkandbrewer sp. nov.

LSIDurn:lsid:zoobank.org:act:4CD66AE8–25D7–490C-BCAA-5A37D434F36B

Figures 1–5

3.2.2 Material examined

Holotype, female, 1.0 mm, NIWA 173287, station AB C4, Blueskin Bay, Otago, 45°39.044736′ S 170°48.873858′ E, 25 m, collectors: NIWA.

Paratypes: male, 1.5 mm, NIWA 173288, female, 1.5 mm, NIWA173289 (SEM), male, 1.0 mm, NIWA173289 (SEM), same collection data as holotype.

Additional material examined. 1 female (1.5 mm), 1 male (1.0 mm), 1 juvenile (0.5 mm), NIWA173290, same collection data as holotype.

3.2.3 Etymology

The name *forkandbrewer* is derived from the craft beer brewery "The Fork and Brewer" in Wellington New Zealand. During the Tenth International Crustacean Congress held in Wellington May 2023, a 'most crustiest craft beer' competition was run by the conference organisers, the various beers were judged by the delegates of the conference and the general public with the reward being the naming of a species after the brewery. Fork and Brewer won with an interesting stout beer. The species name is used as a noun in apposition.

3.2.4 Diagnosis

Head, cephalothorax without functional eyes; frontal margin mid-spine broad and rounded with small acute point, lateral spines narrower and longer from head than anterior projection, sinuous in shape, curving anteriorly ending in an acute point. Lateral spines diverging at approximately 115°, all three projections with denticulate margins, stronger on the anterior margins. Eyestalks shorter than the lateral margins of pereonite 1, pointing almost laterally (~10°), distally rounded, without ommatidia. Pereonites 1–7 without mid-dorsal projections; pereonites 1–7 laterally pointed and projecting, pereonite 4 shorter than all the others, pereonite 7 angled posteriorly; lateral margins of all pereonites denticulate. Pleotelson roughly triangular, no hooked projection; lateral margins denticulate; apex rounded or subacute.

Antenna article 3 slender but slightly rounded. Pleotelson subtriangular, with numerous lateral denticles; distal projection reduced, length less than half pleotelson length. Operculum ovoid, with several (14) setae medially. Uropods uniramous inserting dorsolaterally in cuticle fold of the pleotelson, tipped with 4 setae each.

3.2.5 Description

Based on holotype female, 1.0 mm, NIWA 173287.

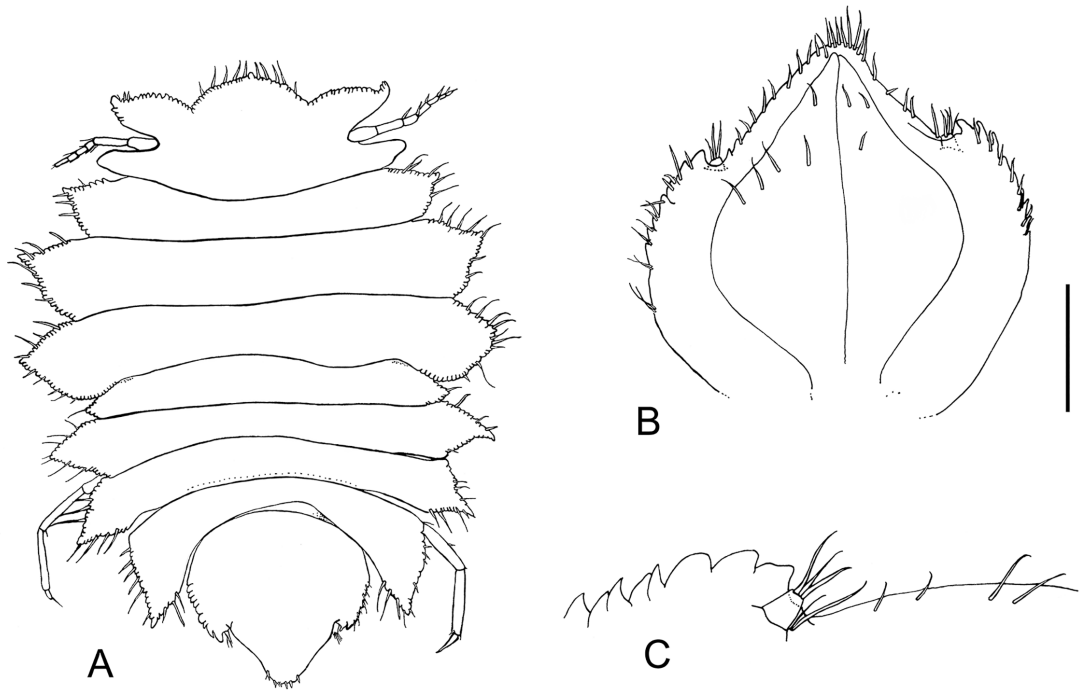

FIGURE 1
Pentaceration forkandbrewer sp. nov., holotype, female, NIWA 173287, 1.0 mm, Otago, New Zealand. **(A)** Habitus-dorsal. **(B)** Pleotelson, ventral view. **(C)** Close-up of uropod, ventral view. Scale represents 0.1 mm.

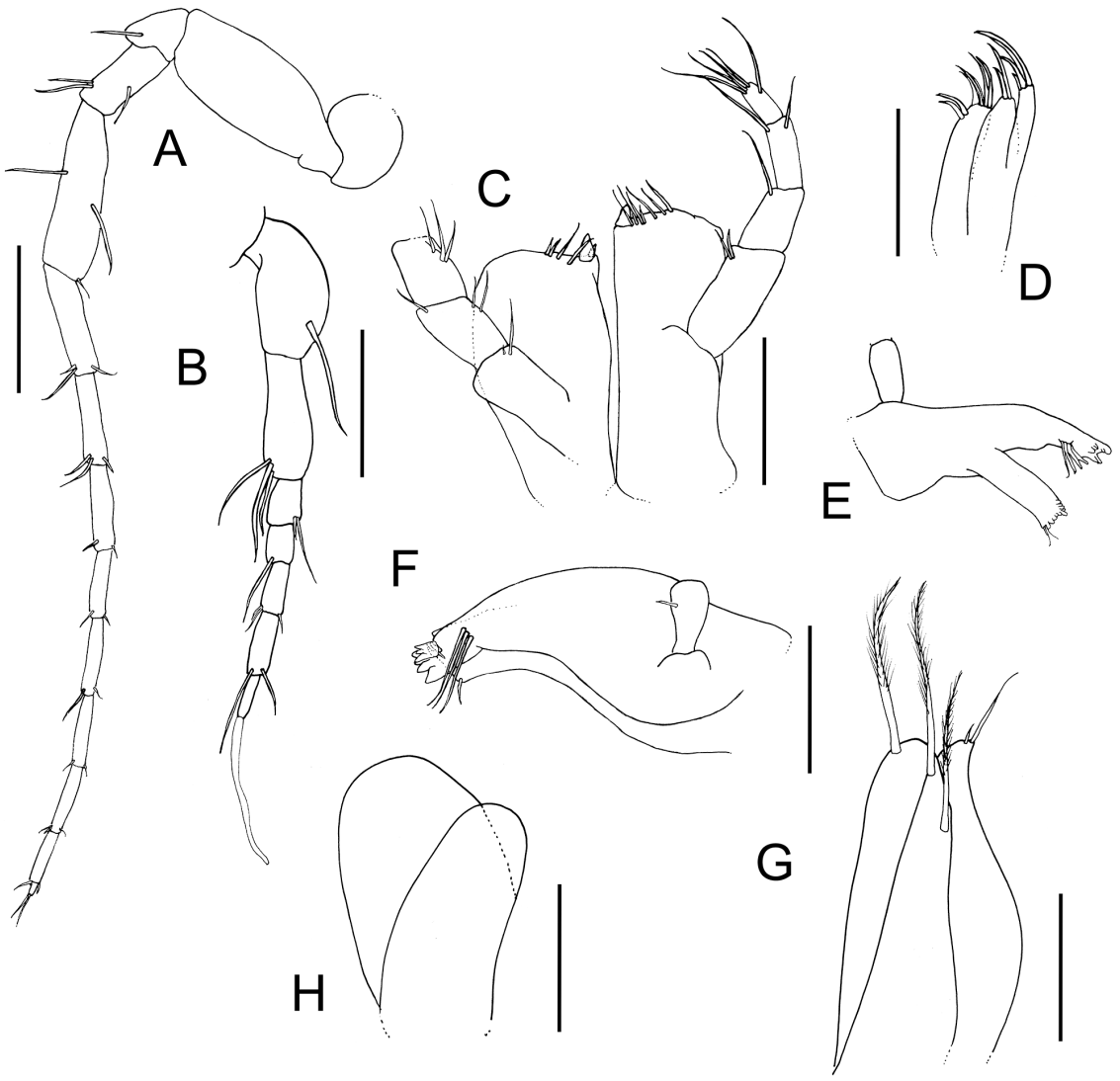

FIGURE 2
Pentaceration forkandbrewer sp. nov., holotype, female, NIWA 173287, 1.0 mm, Otago, New Zealand. **(A)** Antenna. **(B)** Antennula. **(C)** Maxillipeds, ventral view. **(D)** Left Maxillula. **(E)** Left mandible. **(F)** Right mandible. **(G)** Pleopod 3. **(H)** Pleopod 5. Scales represent 0.1 mm.

Head and body: body dorsoventrally flattened, ovoid almost rounded, width 0.61 times length, widest between pereonites 2 and 3; pereonites 1–7 length ratio: 1: 1.6: 1.4: 1.2: 0.9: 0.8: 0.85; pereonite 1 – 7 lateral margins broad, ending in an acute tooth/process, with denticles of varying size and intermittent setae; pereonites 2–6 with acute lateral spines; lateral spines of pereonite 3 and 7 longest, though pereonite 7 curved and directed posteriorly; pereonite 4 by far the shortest. Pleotelson oval, with numerous lateral denticles; length just under one-third body length; distal projection short and broad, length less than half pleotelson length.

Cephalothorax: Head length 0.3 × width; length approximately 0.15 × body length, no mid-dorsal spines. Eyestalks length approximately 2 × width, smooth without denticles, lateral projections and mid-cephalic projection with several lateral denticles and few small, simple setae in between; insertion of eyestalks approximately 0.4 from posterior margin and 0.5 from anterior margin; eyestalk length 1.7 × mid-cephalic spine length, about 0.3 cephalothorax width; lateral spine length 0.4 cephalothorax width, 2 × mid-cephalic spine length.

Pereonites 1–7 lateral margins sinuous and distinctly projecting; all pereonites marginally denticulate; coxae not visible in dorsal view. Pereonites 2–3 lateral spines diverging from each other at around 108°.

Antennula: length 0.17 × body length, with 7 articles; first article twice as long as wide, with 1 long simple seta subdistally; second article long and slender, 0.82 × length of article 1, about 2.5 × longer than wide, with 3 simple setae of equal size distally; third article slightly longer than fourth (1.15 ×) and about 0.37 × article 2, fourth article about 0.3 × of article 2 length; article 4 with 1 short simple seta distally; article 5 about 0.43 × length of article 2, 2.5× longer than wide, with 2 simple setae distally; article 6 1.3 × length of article 5, with 2 long, simple setae distally; article 7 0.7 × article 6 and with 1 aesthetasc and 1 tiny simple seta terminally.

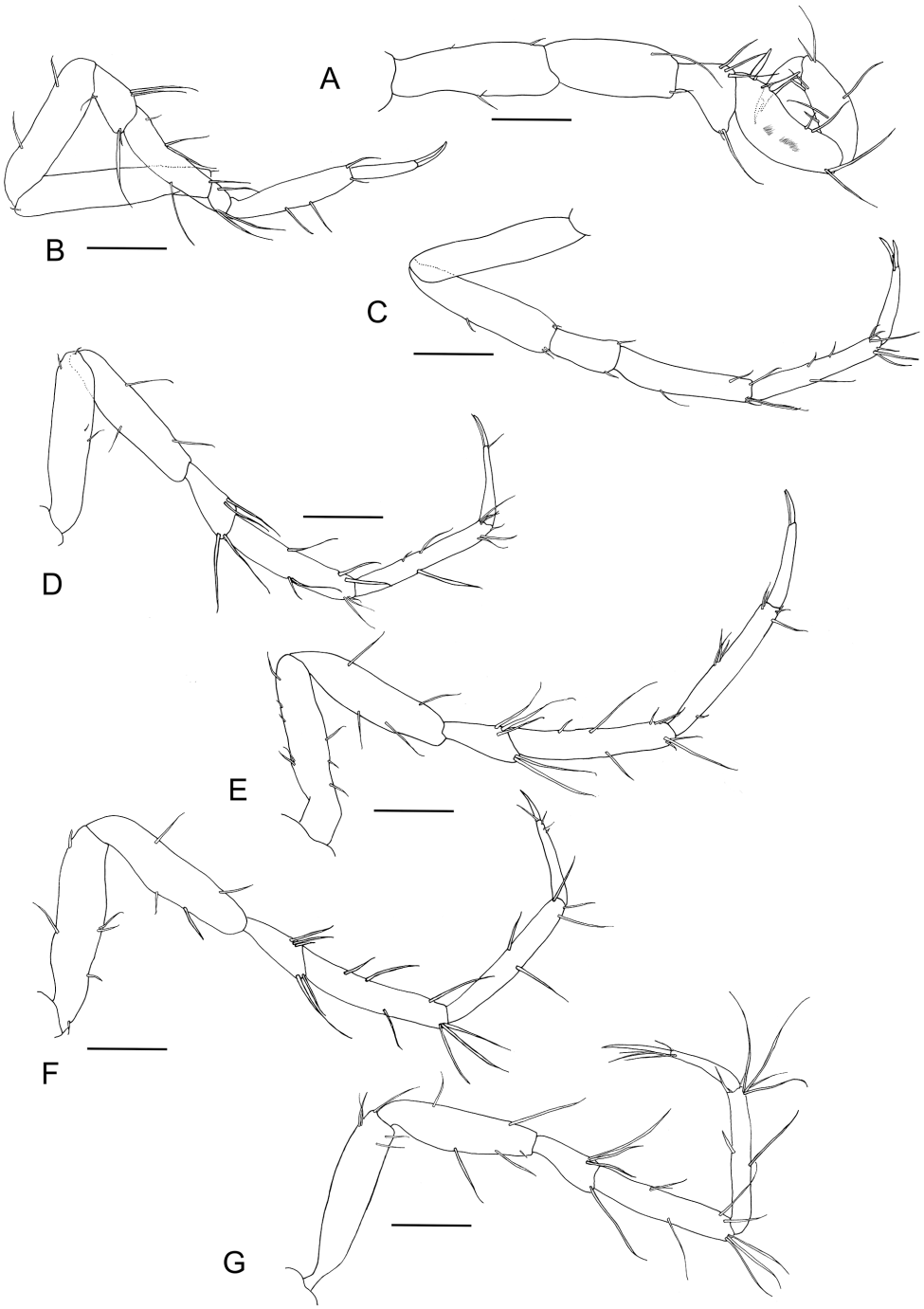

FIGURE 3
Pentaceration forkandbrewer sp. nov., holotype, female, NIWA 173287, 1.0 mm, Otago, New Zealand. **(A)** Pereopod I. **(B)** Pereopod II. **(C)** Pereopod III. **(D)** Pereopod IV. **(E)** Pereopod V. **(F)** Pereopod VI. **(G)** Pereopod VII. Scales represent 0.1 mm.

Antenna: length approximately 0.4 × body length, with 6 peduncular and 9 flagellar articles (peduncular article 1 broken off); peduncular article 3 long and slightly expanded, 2.6 × longer than wide, without setae; peduncular article 4 short and subtriangular, length 0.2 × of article 2, as long as wide, with 1 simple seta; peduncular article 5 medium length and slender 1.8 × article 4, 2.4 × longer than wide, with 3 lateral setae; peduncular article 6 long and slightly expanded, length 2.0 × article 5, 3.75 × longer than wide, with 2 long slender setae laterally, and one small seta distally; flagellar article 1 slightly longer than article 2 (1.15 ×), together about as long as peduncular article 3, each with 3 simple setae distally; flagellum articles 3 and 4, and 5 and 6 of similar length, gradually getting shorter than flagellum article 1, each with 1–3 simple setae distally; flagellum articles 7–9 length decreasing distally; flagellum article 7 somewhat shorter than article 6, with 3 short simple setae; flagellum article 8 with 4 simple setae distally;

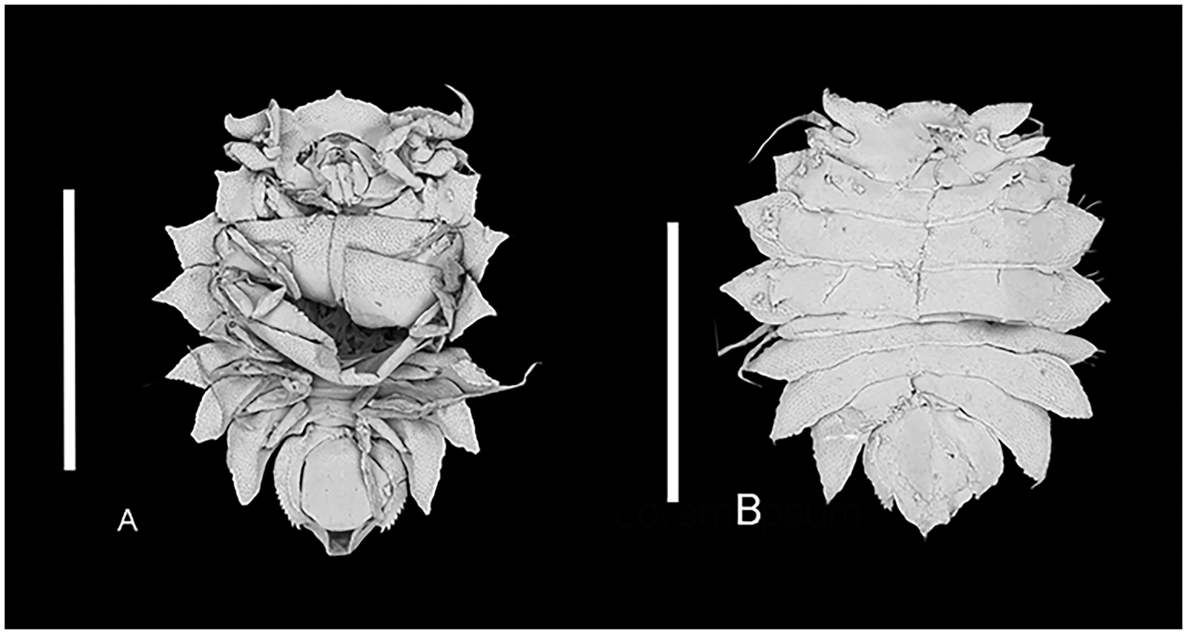

FIGURE 4
Pentacertion forkandbrewer sp. nov. **(A)** Paratype, female, NIWA 173289, 1.5 mm. Otago. Ventral view (SEM). **(B)** Paratype, male, NIWA 173289, 1.5 mm, dorsal view (SEM). Scales represent 1.0 mm.

flagellum article 9 short, about 0.25 × article 8 with 2 long, slender setae terminally.

Maxillula: outer endite with 10 strong spine-like setae distally, with small slender setae on outer margin; inner endite slender; width about half outer endite width; length 1.2 × outer endite length, with 3 robust setae and 2 slender simple setae distally.

Maxilla: lateral endite slightly shorter than inner endite; lateral and medial endite each with 3 long, strong setae terminally; inner (medial) margin and ventral surface of inner endite with several setae of varying size, with 7 setae distally.

Mandible: palp on both mandibles broken to one article; incisor process with 5 teeth, lacinia mobilis with 2 cusps; setal row with 4 long robust setae, distal one dentate, dentation and robustness of setae decreasing proximally; molar process elongated and cylindrical, with several teeth and few simple setae distally.

Maxilliped: left and right maxilliped connected by 2 retinacula; epipod smooth, twice as long as wide, reaching mid-length of palpal article 3, outer lateral margin weakly convex, inner margin slightly curved; palpal article 1 short, as long as wide; palpal article 2 1.4 × as long as article 1 length, longer than wide, with 1 short and 1 long robust setae on inner margin; palpal article 3 slightly shorter (0.88 ×) than article 4, length 1.6 × article 1 length, with 8 strong, long setae medially and laterally; palpal article 4 as long as article 3 and article 5, article 4 2.5 × longer than wide, with 3 long, slender setae; palpal article 5 about 1.56 × as long as article 1, with 3 slender simple setae terminally; endite reaching midlength of palpal article 3, with 2 feathered three-lobed fan setae distally, with several simple setae of varying size on posterior margin and 1 plumose seta medially.

Pereopod I: more robust than pereopods 2–7; basis 3.0 × longer than wide, with 2 small slender setae on posterior margin and one small slender seta on the anterior margin; ischium length 0.88 × basis length, 2.3 × longer than wide; with 1 long slender simple seta on the posterior margin; merus length 0.45 × ischium length, flask/triangular shaped, as wide as long (at the widest point), with 1 long and 1 small slender simple seta on the disto-anterior margin, and with 3 long slender simple setae on posterior and distal margin; carpus curved, rectangular shape, anterior margin convex and posterior margin concave, length 2.0 × merus length, about 2.4 × as long as wide; with 2 long slender setae on the distal anterior margin, with 2 long, robust setae on the proximal half of the posterior margin and 2 long slender simple setae on the distal half of the posterior margin; propodus length 0.8 × carpus length, 2.6 × longer than wide; with 1 long slender simple seta on anterior margin, with 2 long, slender setae distally, with 2 small robust setae and 4 slender simple setae on the posterior margin; dactylus 0.8 × propodus length, 4.6 × as long as wide, without setae, unguis about half the length of dactylus, ventral claw about half length of unguis.

Pereopod II: basis 5.1 × longer than wide, with 2 short simple setae on posterior margin; ischium length 0.75 × basis length, 3.6 × longer than wide; with 2 simple setae on posterior margin; merus length 0.36 × ischium length, 1.5 × longer than wide; with 1 long simple seta on anterior margin and 2 slender simple setae, one long, one short distally, 2 long setae on the distal part of the posterior margin; carpus length 2.2 × merus length, 4.4 × longer than wide; with 1 long slender seta on anterior margin and 2 long slender setae distally, with 4 long setae and 1 short simple seta on posterior margin; propodus length 0.9 × carpus length, 4.6 × longer than wide; with 2 long, slender simple setae on posterior margin, and 1 small seta distally, with 1 long seta on anterior-distal margin; dactylus 0.8 × propodus length, about 7.5 × times as long as wide.

Pereopod III: basis 5.0 × longer than wide, without setae on margins; ischium length 0.95 × basis length, 3.9 × longer than wide;

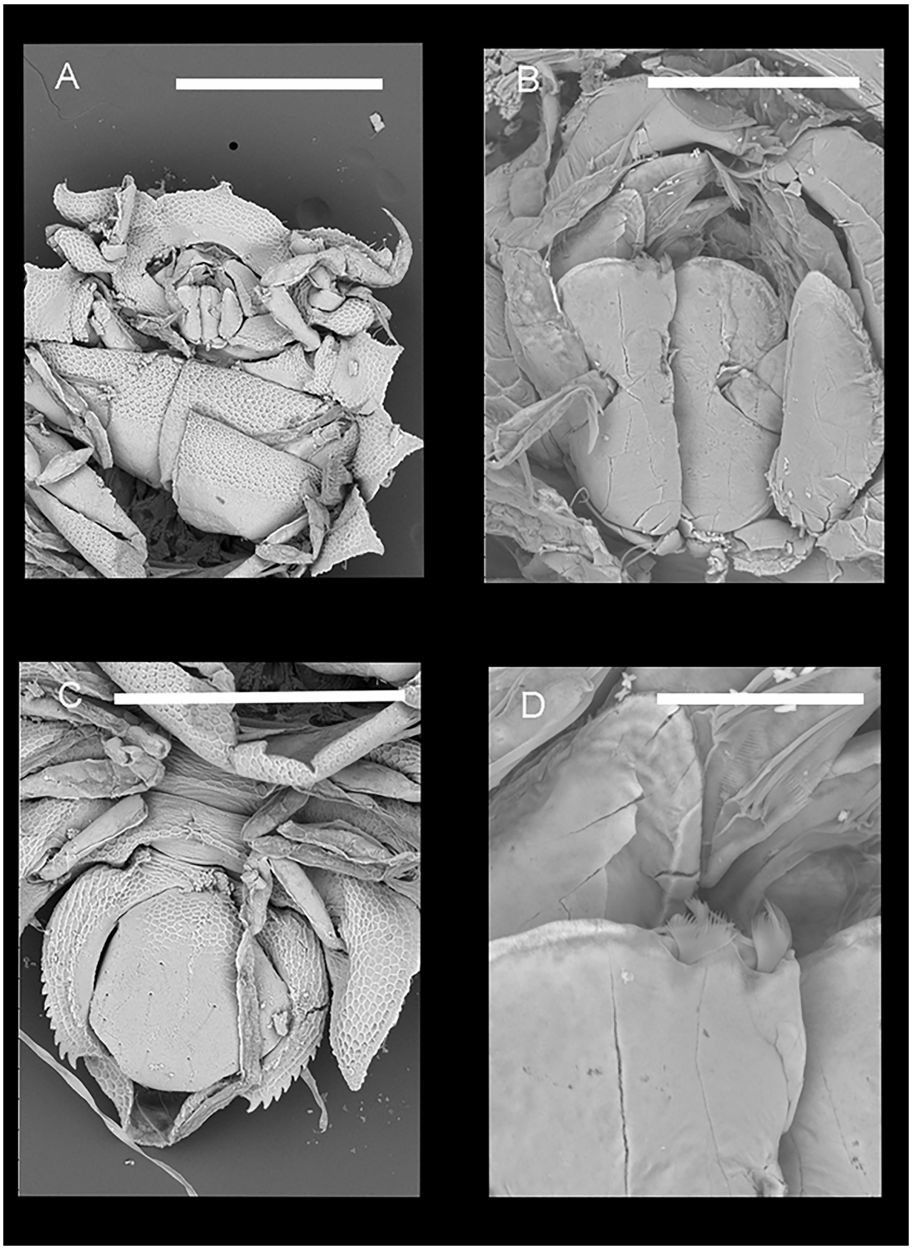

FIGURE 5
Pentaceration forkandbrewer sp. nov. **(A)** Paratype, female, NIWA173289, head and anterior body, ventral view (SEM). Scale represents 0.5 mm. **(B)** Paratype, female, NIWA173289, ventral close-up of maxilliped (SEM). Scale represents 0.1 mm. **(C)** Paratype, female, NIWA173289, pleotelson (SEM). Scale represents 0.5 mm. **(D)** Paratype, female, NIWA173289, close-up of feathered setae on the maxilliped (SEM). Scale represents 0.03 mm.

with 1 simple seta on anterior margin and 2 simple setae on each side of the distal corner; merus length 0.4 × ischium length, about 2.1 × longer than wide, with 1 simple seta on disto-anterior margin, with 2 simple setae on posterior-distal corner; carpus length 2.0 × merus length, 4.8 × longer than wide; with 1 slender seta on anterior margin and 3 simple setae on anterodistal corner, with 1 simple seta on posterior margin and 1 simple seta on postero-distal corner, propodus approximately the same length as carpus length, 6.5 × longer than wide; with 4 long, slender simple setae on anterior margin, and 5 slender setae on posterior margin, dactylus 0.5 × propodus length, about 5.25 × longer than wide; with 1 long, slender seta between unguis and ventral claw; unguis about 0.4 × dactylus length, ventral claw about as long as unguis.

Pereopod IV: basis 4.3 × longer than wide, with 2 short simple setae on anterior margin and 2 small simple setae on the postero-distal corner; ischium 0.9 × basis length, 4.5 × longer than wide; with 2 long simple setae on anterior margin and 1 simple seta on posterior margin; merus length 0.43 × ischium length, about 1.9 × longer than wide; with 2 simple setae on antero-distal corner, with 2 long, slender setae on postero-distal corner, carpus length 2 × merus length, 4.4 × longer than wide; with 3 slender setae of varying size on anterior margin, and 3 simple slender setae on antero-distal

corner with 3 long simple setae on posterior margin; propodus same length as carpus, 8.1 × longer than wide; with 4 slender simple setae on anterior margin, with 2 slender setae on posterior margin with 3 slender simple setae distally; dactylus 0.53 × propodus length, about 6.1 × longer than wide; with 1 short, simple seta on disto-anterior margin; unguis 0.4 × dactylus length, ventral claw very thin and slightly longer than unguis.

Pereopod V: basis 4.8 × longer than wide, with 3 short simple setae on anterior margin and 5 simple setae on posterior margin; ischium length 0.85 × basis length, 4.1 × longer than wide; with 2 long simple setae on each of the margins; merus length 0.4 × ischium length, about 1.9 × longer than wide; with 2 long simple setae on disto-anterior margin, with 3 long simple setae on postero-distal corner; carpus length 2.3 × merus length, 5.6 × longer than wide; with 4 slender setae of varying size on anterior margin, with 4 simple setae on posterior margin; propodus length as long as carpus length, 6.3 × longer than wide; with 3 long, slender simple setae on anterior margin, with 6 slender setae on posterior margin; dactylus 0.5 × propodus length, about 5.3 × longer than wide, without setae; unguis 0.4 × dactylus length, ventral claw same length as unguis.

Pereopod VI: basis 3.6 × longer than wide, with 3 simple long setae on anterior margin and 3 simple setae on posterior margin; ischium length nearly as long as basis length, 4.1 × longer than wide; with 2 simple setae on anterior margin and 2 long simple setae on the posterior margin; merus length 0.4 × ischium length, about 2.3 × longer than wide; with 2 simple setae on disto-anterior margin, with 2 simple setae on disto-posterior margin; carpus length 2.2 × merus length, 5.2 × longer than wide; with 4 long, slender setae on anterior margin, and 3 long simple setae on posterior margin; propodus length about as long as carpus length, about 5.3 × longer than wide; with 1 slender simple seta on anterior margin, with 3 simple setae of varying size distally, with 3 simple setae on posterior margin; dactylus 0.5 × propodus length, about 6 × longer than wide; with 2 simple setae medially; unguis about 0.44 × dactylus length, ventral claw slightly shorter than unguis.

Pereopod VII: basis 4.8 × longer than wide, with 2 short simple setae on anterior margin and 3 long slender setae on posterior margin; ischium length 0.84 × basis length, 3.7 × longer than wide; with 2 simple setae on anterior margin and 2 simple long setae on posterior margin; merus length 0.4 × ischium length, 2.4 × longer than wide; with 1 long simple seta on disto-anterior margin, with 3 simple setae on postero-distal margin; carpus length 2.2 × merus length, 5.3 × longer than wide; with 1 simple seta on anterior margin, with 4 setae distally, and 3 simple setae on posterior margin; propodus length 0.95 × carpus length, 7.6 × longer than wide; with 5 long, slender simple setae on anterior margin and 3 slender setae on posterior margin; dactylus 0.56 × propodus length, 6.1 × longer than wide; with 3 slender setae distally; unguis 0.9 × dactylus length, ventral claw about 0.8 × unguis.

Pleopod 2 (operculum): ovoid almost diamond-shape, width 0.73 × length, ventral surface alveolarly structured, with 6 simple medial setae.

Pleopod 3: endopod width 0.5 ×length, with 3 long plumose setae distally. Exopod with 1 long, slender seta distally.

Pleopod 4: large, oval, width 0.7 × length, no setae.

Pleopod 5: small oval lobe, width 0.6 times length.

Uropods: (drawn in situ, holotype female) uniramous, inserting postero-laterally in non-protruding cuticle fold, with 4 long simple setae distally.

Male (based on paratype, NIWA 173288). Head lateral projections almost straight. Pereon broader. Pleotelson as broad as long.

3.2.6 Distribution

Known from the east coast of Aotearoa New Zealand, 20 – 30 m.

4 Discussion

Paramunnidae species, especially those from the genus *Pentaceration*, appear to show a particular Australasian phylogenetic radiation (Just, 2011). This newly recorded species adds to the New Zealand fauna and is distinctive from all the other *Pentaceration* species recorded due to the lack of mid-dorsal spines, the shape of the pereonites (all extending to form acute points), the serrations on all the margins of the cephalothorax, pereon and pleotelson, the conservative shape of the pleotelson, and the reduced size of the anterior projection on the head.

Pentaceration forkandbrewer sp. nov. is superficially similar to *P. pleonarietis* due to the strongly serrated margins of the head, pereonites and pleotelson. However, there are significant differences, primarily the shape of the pleotelson. The pleotelson lateral margins of the new species are evenly convex reaching to small subacute tip whereas *P. pleonarietis* has the pleotelson with two posteriorly curved antero-lateral processes. Additionally, the new species has pereonites 5 – 7 a similar size to pereonites 1–4, also subtriangular with serrated margins whereas, *P. pleonarietis* has pereonites 5 – 7 reduced and rounded. The new species also has superficial similarities to *P. serrata* from Australian waters. The similarities include the serrated margins of all the pereonites and the shape and size of the pleotelson. The main differences include the size and shape of the central head projection (rounded with small tooth in *P. forkandbrewer* sp. nov., but acute and elongate in *P. serrata*) and the shape of the lateral projections of the head (sinuous in the new species and straight and acute in *P. serrata*), and the shape of the pereonite 1 projections (extended and acute in the new species and broadly rounded in *P. serrata*).

Within the New Zealand *Pentaceration* species, the new species has the closest affinity to *P. dentifera*. This is a species that also has strongly serrated/denticulated margins of the head, pereonites and pleotelson. The new species differs from *P. dentifera* by having serrated/denticulated margins on pereonites 4 and 7, the anterior head spine is broadly rounded and not hugely extended, pereonite 1 is subtriangular not broadly subquadrate and blunt eyestalks and no obvious eyes.

The depth distribution as shown in Just (2011) shows that the majority of species occur between 150 – 1000 m depth. This makes the new species one of four that occur in shallower than 50 m depth. The species were recorded from relatively shallow environs with fine sand and mud. Interesting, samples from a similar environment of sediment and depth but off Hawkes Bay (North Island, New Zealand) were also examined from another project and very similar (most likely the same species) specimens were seen (Leduc et al. 2024).

5 Key for New Zealand *Pentaceration*

1. Head spines broad, pereonites 1 – 7 shape broad triangular… ***P. forkandbrewer* sp. nov.**

- Head spines and pereonite shape acute, narrow triangular… 2

2. Pereon with middorsal row of slender upright spines; pleotelson posteriorly extended into long spine… 3

- Pereon dorsum without spines or at most with low, broad spines; pleotelson posteriorly triangular, pointed or rounded… 4

3. Pereonites 1–7 with single row of mid-dorsal spines; uropods uniramous; distal projection of pleotelson about half length of pleotelson… ***P. curvicornis*** Just, 2011.

- Pereonites 1–7 with two rows of smaller mid-lateral spines in addition to prominent mid-dorsal spines, uropods biramous; length of distal projection of pleotelson slightly longer than pleotelson length… ***P. bifficlyro*** Kaiser and Marner, 2012.

4. Each pereonites with single broad, conical middorsal spine; uropods inserted in low cuticle tubes rimmed with pointed denticles… ***P. kermadecia*** Just, 2011.

- Pereon dorsally smooth; uropod insertion not flanked by distinct denticles… 5

5. Head spines and pereonite lateral spines fringed with dense rows of equal-sized denticles; eyestalks apex blunt, with a few small ocelli, barely overreaching pereonite 1 lateral margin… ***P. dentifera*** Just, 2011.

- Head spines and pereonite lateral spines without regular marginal denticles, or with tiny denticles not in regular rows, or with some large, irregularly placed denticles… 6

6. Body strongly flattened; pereonite 1 lateral margins with mid spines; pereonite 2 lateral spines slender, unadorned… ***P. epipedos*** Just, 2011.

- Body ordinarily vaulted; pereonite 1 lateral margin without spines… 7

7. Pereonite 1 lateral margin convex, broadest at posterior corner, with irregular denticles; pereonites 2 and 3 lateral spines with dentate lobe in proximal half of posterior margin; eyestalks not reaching widest point of pereonite 1… ***P. novaezealandia*** Just, 2011.

- Pereonite 1 lateral margin truncate, with irregular denticles; pereonites 2 and 3 lateral spines with anterior and posterior dentate lobes at base; eyestalks overreaching pereonite 1 with about 0.25 their length; head and body spines with numerous short, curled setae along margins … ***P. setosa*** Just, 2011.

6 Conclusion

This newly recorded species, *Pentaceration forkandbrewer* sp. nov., is added to the shallow-water Australasian paramunnid fauna. The asellotes are abundant in abyssal basin and inshore sediments and this new species adds to this vital fauna, which contributes to the transfer of carbon through the water column.

Data availability statement

The datasets presented in this study can be found in online repositories. The names of the repository/repositories and accession number(s) can be found in the article/supplementary material.

Ethics statement

Ethical approval was not required for the study involving animals in accordance with the local legislation and institutional requirements because the study used retrospectively collected specimens.

Author contributions

RP: Conceptualization, Data curation, Formal analysis, Investigation, Methodology, Software, Visualization, Writing – original draft, Writing – review & editing. KS: Data curation, Writing – review & editing.

Funding

The author(s) declare financial support was received for the research, authorship, and/or publication of this article. RP and KS were funded by NIWA under Coasts and Oceans Research Programme 2 Marine Biological Resources: discovery and definition of the marine biota of New Zealand (2023–20242 SCI).

Acknowledgments

We are grateful to the staff of the NIWA Invertebrate Collection for their tireless work, especially Amelia Connell for registering the material. We thank Kimberley Seaward for collecting and providing the material. We also thank the two reviewers for their efforts in making this a more complete and better paper.

Conflict of interest

The authors declare that the research was conducted in the absence of any commercial or financial relationships that could be construed as a potential conflict of interest.

Publisher's note

References

Doti, B. L. (2017). Three new paramunnids (Isopoda: Asellota: Paramunnidae) from the Argentine Sea, South-west Atlantic. *J. Mar. Biol. Assoc. United Kingdom* 97, 1695–1709. doi: 10.1017/S0025315416001016

Gamō, S. (1987). "Systematic studies on the bathyal benthic small crustaceans in the Flores Sea," in Preliminary Report on the Hakuho Maru Cruise KH-*85–1*. Japan: Ocean Research Institute: University of Tokyo 44–45.

Just, J. (2009). *Pentaceration*, an unusual new genus of Paramunnidae from Australia (Isopoda, Asellota). *Zootaxa* 2134, 36–48. doi: 10.11646/zootaxa.2134.1

Just, J. (2011). Remarkable Australasian marine diversity: 18 new species in Pentaceration Just 2009 (Crustacea, Isopoda, Paramunnidae). *Zootaxa* 2813, 1–54. doi: 10.11646/zootaxa.2813.1

Just, J., and Wilson, G. D. (2004). Revision of the *paramunna* complex (Isopoda: asellota: paramunnidae). *Invertebrate Systematics* 18, 377–466. doi: 10.1071/IS03027

Just, J., and Wilson, G. D. (2006). Revision of southern hemisphere *austronanus* hodgson 1910 with two new genera and five new species of Paramunnidae (Crustacea: Isopoda: Asellota). *Zootaxa* 1111, 21–58. doi: 10.11646/zootaxa.1111.1

Kaiser, S., and Marner, M. (2012). A new species of Pentaceration Just 2009 (Isopoda, asellota, paramunnidae) from the challenger plateau, New Zealand (Tasman sea). *Zoosystematics Evol.* 88, 171–184. doi: 10.1002/zoos.v88.2

Latreille, P. A.. (1802-1805). Histoire Naturelle, Générale et Particulière des Crustacés et des Insectes. Familles naturelles des genre. *Ouvrage faisant suite à l'Histoire Naturelle générale et particulière, composée par Leclerc de Buffon, et rédigée par C.S. Sonnini, membre de plusieurs Sociétés savantes*. de L'imprimerie de F. Dufart, Paris. 14 vols.:413 pp.

Latreille, P. A. (1817). Les Crustacés, les Arachnides, et les Insectes. In: [G. L. C. F. D.] Cuvier *Le Règne Animal, Distribué d'après son Organisation, pour Servrir de Base a l'Histoire Naturelle des Animaux et d'Introduction a l'Anatomie Comparée*.Volume 3:i-xxix+1-653. Paris: Deterville [Dated 1817, published 2 December 1816 fide Roux, 1976].

Leduc, D., Collins, C., Gall, M., Lundquist, C., Macdonald, H., Mackay, K., et al. (2024). Cyclone impacts on fisheries. *New Z. Aquat. Environ. Biodiversity Rep. No. 326*., 167.

Riehl, T., and Brandt, A. (2010). Descriptions of two new species in the genus Macrostylis Sars 1864 (Isopoda, Asellota, Macrostylidae) from the Weddell Sea (Southern Ocean), with a synonymisation of the genus *Desmostylis* Brandt 1992 with *Macrostylis*. *Zookeys* 57), 9. doi: 10.3897/zookeys.57.310

Seaward, K., Stead, J., Page, M., Olsen, L., Miller, A., Peart, R., et al. (2021). "Project next generation monitoring 2020," in *Prepared for Port Otago Ltd.* NIWA Client Report *2021062CH*, NIWA Client Report, 39.

Vanhöffen, E.. (1914). *Die Isopoden der deutschen Südpolar-Expedition 1901-1903*. Deutsche Südpolar-Expedition, Zoologie. 15, 447–598.

frontiers | Frontiers in Marine Science

TYPE Original Research
PUBLISHED 10 September 2024
DOI 10.3389/fmars.2024.1412024

OPEN ACCESS

EDITED BY
Les Watling,
University of Hawaii at Manoa, United States

REVIEWED BY
William Santana,
Regional University of Cariri, Brazil
Ajit Kumar Mohanty,
Indira Gandhi Centre for Atomic Research (IGCAR), India

*CORRESPONDENCE
Kareen E. Schnabel
Kareen.Schnabel@niwa.co.nz

RECEIVED 04 April 2024
ACCEPTED 05 August 2024
PUBLISHED 10 September 2024

CITATION
Schnabel KE and Peart RA (2024) First record of the family Callianopsidae (Decapoda: Axiidea) and a new species of *Vulcanocalliax* from the Hikurangi Margin off Aotearoa New Zealand, with a key to species of Callianopsidae.
Front. Mar. Sci. 11:1412024.
doi: 10.3389/fmars.2024.1412024

First record of the family Callianopsidae (Decapoda: Axiidea) and a new species of *Vulcanocalliax* from the Hikurangi Margin off Aotearoa New Zealand, with a key to species of Callianopsidae

Kareen E. Schnabel* and Rachael A. Peart

Marine Biodiversity, National Institute of Water and Atmospheric Research, Wellington, New Zealand

Introduction: The Aotearoa New Zealand ghost shrimp of the infraorders Axiidea and Gebiidea have never been comprehensively reviewed, with recent work uncovering a diverse regional fauna representing eight of the 14 known families.

Methods: Using standard morphological and DNA sequencing tools, the family Callianopsidae is, for the first time, recorded off New Zealand, represented by a new species of *Vulcanocalliax*.

Results: The new species was found near hydrocarbon seeps on the Hikurangi Margin, on the eastern New Zealand continental slope, and is only the second species now known in this genus. The single congener, *V. arutyunovi*, is only known from a mud volcano in the Gulf of Cádiz, off the Iberian Peninsula. *Vulcanocalliax* sp. nov. was formerly reported as an unnamed host of a new endemic New Zealand rhizocephalan barnacle *Parthenopea australis* and is here formally described as *Vulcanocalliax beervana* sp. nov.

Discussion: The new species differs, e.g., in the shape of the anterior carapace margin (convexly rounded and without elevated postantennal shoulder present in *V. arutyunovi*), the ocular peduncle having a convex anterolateral margin (compared to a straight margin), and the uropodal exopod has a dorsomedian ridge, lacking the elevated anterior portion that is distinct in *V. arutyunovi*. This brings the number of described New Zealand ghost shrimp species to 18. A key to all known Callianopsidae is provided.

ZOOBANK: LSID urn:lsid:zoobank.org:pub:4EDE6CE1-B644-4FFB-94CA-C8725A7549DD.

KEYWORDS

ghost shrimp, integrative taxonomy, Crustacea, 16S rRNA, southwestern Pacific

Introduction

The small group of ghost shrimp in the family Callianopsidae Manning and Felder, 1991 currently recognizes six recent species (DecaNet eds., 2024, accessed 1 August 2024). Originally described as a subfamily Callianopsinae in a new family Ctenochelidae by Manning and Felder (1991), it was designated to accommodate a single species *Callianopsis goniophthalma* (Rathbun, 1902); Sakai (2011) subsequently places it in the new family Callianopsidae.

As the other members in the broader group commonly referred to as ghost shrimp that, for example, include the abundant and diverse coastal callianassids, they are pale in life color and inhabit burrows that the animals build into soft sediments [see references in the work of Poore and Ahyong (2023)]. The ghost shrimp taxonomy and systematics have recently undergone substantial reviews with many new genera derived from a combined molecular-morphology phylogeny (Poore et al., 2019; Robles et al., 2020), and there was convincing support for the validity of the family Callianopsidae as a basal group of the "callianassoid" family tree. The term "Callianassoidea" commonly refers to a group of families of ghost shrimp of "Callianassidae and related families"; however, Poore et al. (2019) questioned this superfamily as some of their proposed diagnostic morphological characters overlap with other axiidean families that are not included in this term. Nevertheless, Robles et al. (2020), who include Gary Poore as an author, continued to use the term and pointed out that it formed a monophyletic and well-supported clade within the axiidean phylogeny. The study by Robles et al. (2020) supported close evolutionary relationships between the families Callianopsidae and the Eucalliacidae (Manning and Felder, 1991) at the base of this clade. These two taxa share the broadly expanded maxilliped 3 dactylus that bears a dense field of setae on a truncate margin (typically for the other ghost shrimp, the dactylus is narrow and digitate) and between the Callianopsidae and the Ctenochelidae that share a simple uropodal exopod, i.e., without an elevated dorsal plate (compared to the dorsal plate presenting as a triangular thickening with a distal row of stiff setae that is typical for other ghost shrimp like the Callianassidae or Callichiridae).

Three genera are recognized in the Calllianopsidae: *Callianopsis* de Saint Laurent, 1973 with four species being the most speciose, with a fragmented distribution in all major oceans and reported from shelf to slope depths (~300–700 m); *Bathycalliax* Sakai and Türkay, 1999 containing the single species *B. geomar* Sakai and Türkay, 1999 known only from the northeastern Pacific at around 630-m depth and representing the first record of a ghost shrimp potentially associated with a deep-water cold seep; and *Vulcanocalliax* Dworschak and Cunha, 2007 for a single species *V. arutyunovi* Dworschak and Cunha, 2007, the second record of a ghost shrimp from chemoautotrophic communities, described from a mud volcano in the Gulf of Cádiz off Spain, and the deepest record for this family with just over 1,300-m depth. Lörz et al. (2008) reported an undescribed species of *Vulcanocalliax* as the host of an undescribed species of kentrogonid rhizocephalan, subsequently described by Lützen et al. (2009) as *Parthenopea australis* from a single specimen collected during the 2006 RENEWZ voyage sampling cold seep communities along the east coast of Aotearoa New Zealand (Baco et al., 2010). Here, the new species of *Vulcanocalliax* is formally described; its distribution remains restricted to two samples collected during the RENEWZ voyage between 650- and 808-m depth (Figure 1). Samples have only been acquired through sediment samplers (grab and multi corer), indicating that more typical gear used to collect epibenthic fauna is insufficient to sample burrowing benthic infauna. This new species represents the first and only callianopsid known from the New Zealand region and is named with our gratitude to Ryan McArthur, the manager of the biggest New Zealand beer festival Beervana, who has contributed to the success of the 10th International Crustacean Congress held in Wellington in 2023.

Material and methods

Sample collections

Specimens were collected from two locations during the 2006 RENEWZ voyage conducted by the R/V *Tangaroa* (Stations TAN0616/13 and TAN0616/35) and using the van Veen grab and multicorer (Figure 1). Specimens were extracted from the sediment on board and preserved in 80% ethanol.

Morphological examination

Specimens were examined using a Leica MZ 9.5 stereomicroscope. Size is expressed as carapace length (cl.), including rostrum, in mm. The description covers the holotype female of the new species, with comments on variation on the males and juvenile covered in the Remarks section below. Material examined is deposited in the National Institute of Water and Atmospheric Research Invertebrate Collection, Wellington (NIWA).

DNA sequencing for molecular taxonomy

Total genomic DNA was extracted from a single pleopod from the last three pairs of the specimen using a QIAamp DNA Micro Kit (Qiagen, Hilden, Germany) according to the manufacturer's instructions. The extracted DNA was eluted in 100 µL of sterile distilled H_2O (RNase (Ribonuclease) free), quantified by 1.5% agarose gel electrophoresis and using N60 NanoPhotometer (Implen, Munich, Germany). Then, the total genomic DNA solution was sent to Berry Genomics Co., Ltd (Beijing, China) for library preparation and whole-genome sequencing. Paired-end libraries were constructed with an insert size of 300 base pairs (bp) and sequenced (2 × 150 bp) on the Illumina NovaSeq 6000 platform, and approximately 6 Gb of raw data were produced. Trimmomatic v 0.39 (Bolger et al., 2014) was used to remove adaptors and low-quality reads. Spades v 3.15.4 (Bankevich et al., 2012) was applied with multiple k-mer strategies to assemble the reads into contigs. Contigs containing mitochondrial ribosomal RNA sequences were identified using BLAST+ v 2.12.0 (Camacho et al., 2009) and checked by mapping to corresponding reference sequences using Unipro UGENE v. 42.0 (Rose et al., 2019). The 16S rRNA

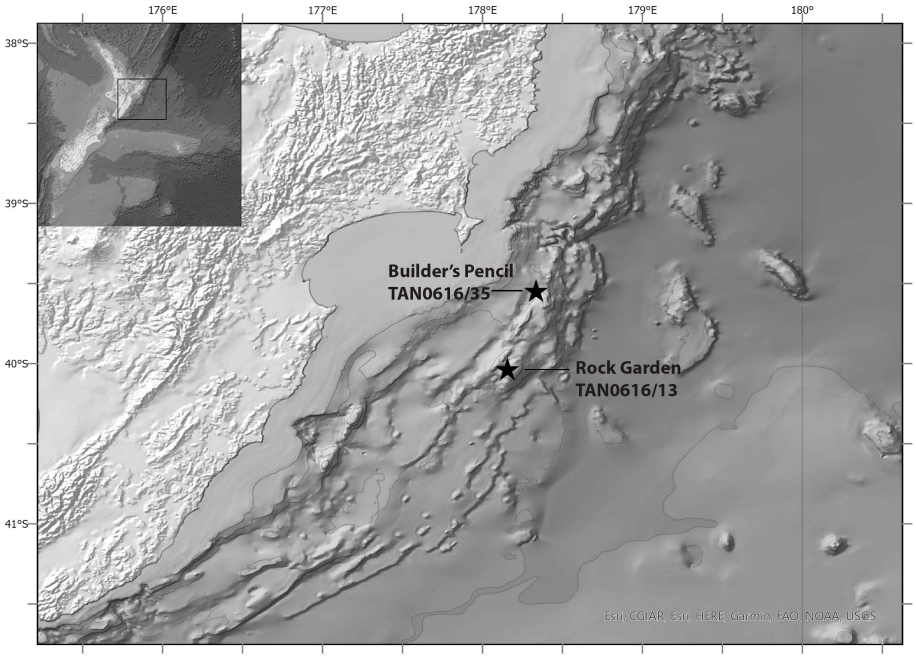

FIGURE 1
Map of the Aotearoa New Zealand region (inset) and the Hikurangi Margin off the east coast of the North Island. The black stars indicate the sampling locations of the specimens of *Vulcanocalliax beervana* sp. nov., in the vicinity of the two cold seep sites known as "Builder's Pencil" and "Rock Garden" sampled during the 2006 RENEWZ voyage (Baco et al., 2010).

sequence was extracted for the purposes of this study and was aligned with reference sequences available on GenBank using Geneious (v 2021.1.1) (http://www.geneious.com; Kearse et al., 2012). The default Clustal Omega alignment function parameters were applied to calculate the percentage identity and patristic distance matrix (Tamura-Nei distance mode, neighbor-joining tree build method, outgroup not specified). The sequences for the paratype of the new species (NIWA 69439) are deposited on GenBank under accession numbers: PQ137440.

Results

Family Callianopsidae Manning and Felder, 1991

Genus *Vulcanocalliax* Dworschak and Cunha, 2007

Vulcanocalliax Dworschak and Cunha, 2007: 37—Sakai (2011): 350–351—Poore et al. (2019): 102—Robles et al. (2020): phylogeny.

Diagnosis: Carapace, longitudinal carina absent; cardiac sulci absent. Rostrum obsolete or obtusely triangular, flat, not reaching cornea. Pleonite 1 with anterolateral lobe, not overlapping with posterolateral lobe of carapace; pleonite 6 without prominent lateral projections. Maxilliped 2 with arthrobranch. Maxilliped 3 exopod absent or rudimentary. Epipods present on maxilliped 3 through P4. Minor cheliped merus with one to two small proximal teeth on lower margin. Male pleopod 2 with appendix interna, appendix masculina absent *[adjusted from the work of* Poore and Ahyong (2023)*]*.

Type species: *Vulcanocalliax arutyunovi* (Dworschak and Cunha, 2007).

Remarks: The family Callianopsidae contains two hitherto monotypic genera *Bathycalliax* Sakai and Türkay, 1999 and *Vulcanocalliax* Dworschak and Cunha, 2007, in addition to *Callianopsis* de Saint Laurent, 1973 that currently contains four recent and nine fossil species (DecaNet eds., 2024, accessed 1 August 2024). *Callianopsis* is easily distinguished from the others by the presence of a dorsal carina on the rostrum (versus carina absent in the other two genera) and pleomere 6 with prominent lateral projections (versus absent in the other two genera). *Vulcanocalliax* differs from *Bathycalliax* in the absence of cardiac sulci and the male pleopod is reduced, not flagellate as in *Bathycalliax*. The presence (*Bathycalliax geomar*) or absence (*Vulcanocalliax arutyunovi*) of an exopod of maxilliped 3 cannot be considered diagnostic at a generic level with the finding of a rudimentary exopod in the new species of *Vulcanocalliax* (see below). The presence of an anterolateral lobe of the first abdominal somite is present in both species of *Vulcanocalliax* and appears present in *Bathycalliax geomar* (Sakai and Türkay, 1999: fig. 1), but it remains to be confirmed across other callianopsids. Dworschak and Cunha (2007) proposed this character as unique to *Vulcanocalliax* and argued that it is not homologous to the anterolateral projection in other axiidean families.

Table 1 provides the comparative branchial formula for callianopsids. Shared diagnostic characters are provided by the epipods present on the maxillipeds and the first three pereiopods in *Bathycalliax* and *Vulcanocalliax*; epipods are only present on maxilliped 1 and rudimentary on maxilliped 2 in *Callianopsis anovalis* Lin et al., 2007. The two *Vulcanocalliax* species, furthermore, share an arthrobranch on maxilliped 2, which is absent in both *Bathycalliax* and *Callianopsis*.

TABLE 1 Comparative branchial formula for select Callianopsidae: *Callianopsis anovalis* Lin et al., 2007, *Bathycalliax geomar* Sakai and Türkay, 1999, *Vulcanocalliax arutyunovi* Dworschak and Cunha, 2007, and *Vulcanocalliax beervana* sp. nov. (r, rudimentary).

	Maxillipeds			Pereopods				
	1	2	3	1	2	3	4	5
Callianopsis anovalis Lin et al., 2007								
Arthrobranch	—	—	2	2	2	2	2	—
Podobranch	—	r	—	—	—	—	—	—
Epipods	1	r	—	—	—	—	—	—
Exopods	1	1	—	—	—	—	—	—
Bathycalliax geomar Sakai and Türkay, 1999								
Arthrobranch	—	—	2	2	2	2	2	—
Podobranch	—	1	—	—	—	—	—	—
Epipods	1	1	1	1	1	1	r	—
Exopods	1	1	r	—	—	—	—	—
Vulcanocalliax arutyonovi Dworschak and Cunha, 2007								
Arthrobranch	—	1	2	2	2	2	2	—
Podobranch	—	—	—	—	—	—	—	—
Epipods	1	1	1	1	1	1	r	—
Exopods	1	1	—	—	—	—	—	—
Vulcanocalliax beervana sp. nov.								
Arthrobranch	—	1	2	2	2	2	2	—
Podobranch	—	1	—	—	—	—	—	—
Epipods	1	1	1	1	1	1	r	—
Exopods	1	1	r	—	—	—	—	—

***Vulcanocalliax beervana* sp. nov.**

(Figures 2–4)

ZOOBANK LSID urn:lsid:zoobank.org:act:3F10DC90-F860-4BD9-A46B-B570735A2551

Type material: Holotype: female (9.5 mm), R/V *Tangaroa* Stn. TAN0616/13, Rock Garden, 40.0328 S, 178.1563 E, 650 m, van Veen Grab, 04 Nov 2006 (NIWA 29413).

Paratypes: 3 males (6.0, 5.8, and 5.3 mm), same as holotype (NIWA 69439).

1 juvenile (4.1 mm), R/V *Tangaroa* Stn. TAN0616/35, Builder's Pencil, 39.5437 S, 178.3348 E, 808 m, Multicorer, 06 Nov 2006 (NIWA 29414).

Diagnosis: Carapace anterior margin convexly rounded on either side of rostrum, not elevated behind second antenna. Ocular peduncle distolateral margin convex. Uropodal exopod with dorsomedian ridge, anterior portion of exopod smooth, not elevated. Maxilliped 2 with podobranch. Maxilliped 3 with rudimentary exopod.

Etymology: Named after New Zealand's annual beer festival Beervana, with our gratitude for the organizer Ryan McArthur who supported the 10th International Crustacean Congress in Wellington 2023. Used as noun in apposition.

Description of female holotype (additional specimens noted where aspects of holotype are missing): Dorsally, carapace slightly longer than abdominal somites 1 and 2 combined. Frontal margin of carapace with narrow triangular acute rostrum, postorbital margin smoothly descending (prominences absent); rostrum extending to 0.3 times the visible length of eyestalks in dorsal view, ventrally setose. Lateral projections of carapace setose dorsally. Carapace lacking distinct dorsal oval and dorsal carina. A single median pit dorsally halfway between rostrum and distinct cervical groove, one pair of smaller pits anterior to cervical groove. Indistinct cardiac prominence bearing median pit in posterior quarter of carapace. Transverse sutures absent. Linea thalassinica well-defined, parallel to midline of carapace. Lateral surface of carapace finely tuberculate, ventral margin with short setae.

Eyestalks dorsally flattened and depressed, slightly convex ventrally, keeled laterally, in dorsal view reaching beyond basal antennal article; mesial surfaces flattened so eyestalks abut closely at midline over entire length; distolateral margin convexly rounded, not pigmented.

Antennular peduncle shorter than antennal peduncle, barely reaching base of antennal article 4; basal article with long setae dorsally near distal end; second article 0.65 times length of basal article with few dorsal setae near distal end; third article about 1.9 times length of second, with ventrolateral row of long, ventrally directed setae continued onto ventral ramus of flagellum; rami of flagellum about equal length; dorsal ramus with few short setae, subterminal articles of dorsal ramus thicker than those of ventral rami, distal 4 rami bearing dense line of ventral aesthetascs.

Antennal peduncle 1.8 times length of antennular peduncle; basal article with ventrolaterally produced excretory pore; second article with deep, diagonal ventrolateral furrow, distally with field of long setae below ventrolateral suture; small, rounded, articulated dorsal scale at joint proximal to third article; third article elongate, same length as fourth or combined length of first two; fourth article narrower than third; flagellum missing (nearly twice length of cl. in paratypes NIWA 69439).

Mandible with large, terminally setose, 3-segmented palp, third article of palp terminally rounded; incisor process thin, regular row of small teeth on cutting margin, mesial surface with lip giving rise to molar process proximal to incisor process.

First maxilla with narrow endopodal palp, terminal article deflected proximally at articulation; proximal endite setose on slightly concave margin, terminally with field of thick simple setae; distal endite elongate, terminally truncate and armed with stiff simple setae.

Second maxilla with endopod narrowed distally, basal and coxal endites each longitudinally subdivided; exopod forming large, broad scaphognathite, lacking very long setae on posterior lobe.

First maxilliped with endopod reduced; proximal endite triangular; distal endite elongate, lateral surface and all margins heavily setose, mesial surface concave; exopod without transverse suture; distal part broadened, with long marginal setation at its mesial end, proximal part with field of mesially directed setae near mesial end; epipod large, broad, anterior end tapered, angular.

Second maxilliped with long endopod; merus straight, mesial surface concave, slightly thicker in proximal half than in distal,

FIGURE 2
Vulcanocalliax beervana sp. nov.: Holotype female (NIWA 29413; cl., 9.5 mm); left, dorsal habitus; right, lateral habitus.

flexor margin with dense fringe of long, close-set setae; carpus short; propodus weakly arcuate, length 1.6 times width, about one-third length of merus; dactylus short, less than half-length of propodus, densely setose; exopod as long as endopodal merus and carpus combined, fringed marginally by long setae; epipod small, leaf-shaped; podobranch long, lancet-shaped; single arthrobranch small.

Third maxilliped with rudimentary exopod; endopod robust, with long dense setation on mesial margin; endopodal ischium subrectangular, 1.5 times as long as broad, proximomesial lip rounded, mesial surface with medial longitudinally oriented elevation bearing well-defined curved row of 18 sharp teeth; merus oval, slightly shorter than wide, mesial surface with setose elevation proximally and distally; carpus subtriangular, with setose lobe on flexor margin; propodus large, subrectangular, about as long as broad; dactylus 1.3 times as long as broad, ovate distally, fringed with very dense field of close-set, stiff, serrated setae.

Branchial formula (Table 1) includes exopods, epipods, and a podobranch as described for the first, second, and third maxillipeds above; branchiae limited to single arthrobranch on second maxilliped, pair of arthrobranchs on third maxilliped, and pair of arthrobranchs on each of the first through fourth pereopods. Epipods are present on all maxillipeds and pereopods 1–3.

Chelipeds strongly calcified, unequal. Left (major) cheliped larger; coxa with strong, posteriorly curved spine posteriomesially, simple epipod laterally; ischium slender, nearly as long as merus, extensor margin proximally concave, flexor margin with row of small spines, distalmost largest, length about 2.5 times distal breadth; merus stout, length about 1.6 times breadth at midlength, extensor margin curved, flexor margin with row of spines along proximal three-fourth; carpus broad, broadest distally, flexor margin arcuate and keeled, ventrodistally round, with small granule at corner, dorsal margin straight; propodus heavy, length (including fixed finger) about 1.6 times width, mesial surface of palm smooth; dorsal and ventral propodal margins slightly curved, tufts of setae on inner face above ventral margin, absent below dorsal margin; fixed finger thick, prehensile margin armed with low tooth at about mid-length, proximally with denticles, terminating in rounded tip; excavated below the prehensile margin on mesial face; dactylus heavy, curved, line of several setose punctae on mesial side of dorsal margin, cutting edge sinusoidal, smooth, tip strongly curved.

Minor cheliped (right); coxa with strong, posteriorly curved spine posteriomesially, simple epipod laterally; ischium slender, extensor margin slightly concave, flexor margin with spines increasing in size distally, length about 2.5 times distal breadth; merus stout, length about 1.8 times breadth at midlength, extensor and flexor margins evenly convex, flexor margin with two spines proximally; carpus broad, broadest distally, flexor margin arcuate and keeled, distoventrally rounded, extensor margin straight; propodus less heavy than major cheliped, length (including fixed finger) about 1.9 times width, mesial surface of palm smooth bar a few setose punctae; dorsal propodal margin straight, ventral margin slightly curved, tufts of setae on outer face below dorsal margin and above ventral margin; fixed finger narrows to slender tip, directed straight forward, prehensile margin with few tiny corneous teeth proximally, gently concave; dactylus narrow, longer than fixed finger and distinctly crossing fixed finger, nearly straight, line of several setose punctae on dorsal margin, cutting edge with few tiny corneous teeth.

Second pereopod chelate, most of flexor margins of ischium and merus lined with evenly spaced long setae, similar setae restricted primarily to distal patches on flexor margin in carpus, flexor margin of propodus densely setose, long proximally, progressively more reduced in length and stiffened distally; prehensile margins of both fingers corneous, finely microserrate along straight edge over most of length; dorsal margin of dactylus straight, with patches of stiff, arched setae becoming increasingly reduced in length.

Third pereopod ischium short, one-quarter length of merus; merus length about three times breadth, with several tufts of setae; carpus subtriangular, forming distal lobe on flexor margin, distal width about 0.7 times mid-length, flexor margin terminally with field of long arched setae; propodus extensor margin convex, flexor margin sub-rectangular in shape, 0.75 times as broad as long, lateral surfaces with fields of setae, long setae on margins; dactylus tear-shaped, length about 1.8 times width, terminating in narrow, straight tip, setose on margins, lateral face crossed by fields of short setae.

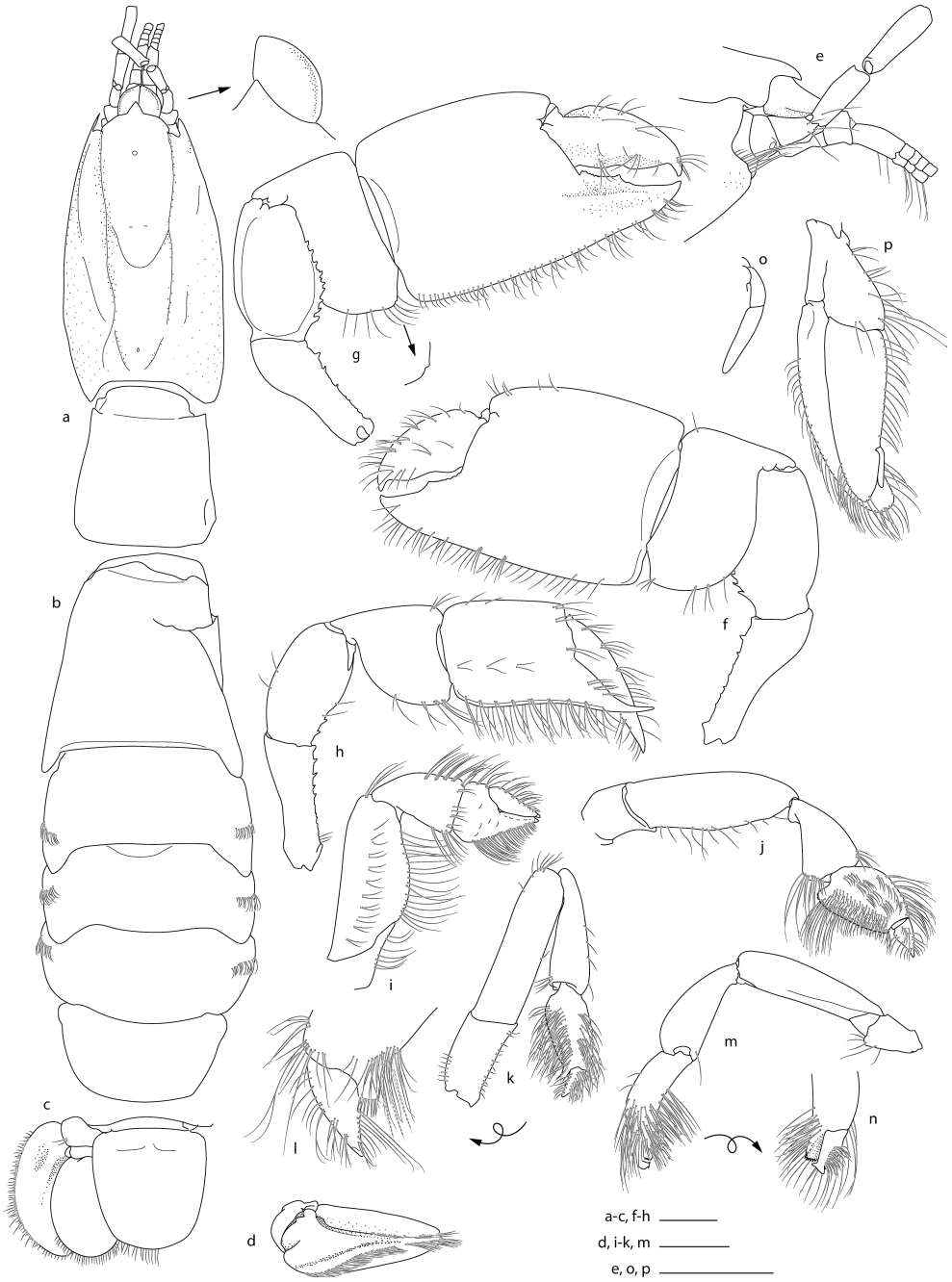

FIGURE 3
Vulcanocalliax beervana sp. nov.: Holotype female (NIWA 29413; cl., 9.5 mm); **(A)** carapace, abdominal somite 1, dorsal view with detail of rostrum and right eye; **(B)** abdominal somites 2–6, dorsal view; **(C)** telson, left urosome, dorsal view; **(D)** left uropodal endopod and exopod, lateral view; **(E)** anterior carapace, eyestalk, antennule, antenna, lateral view; **(F)** major (left) cheliped, lateral face; **(G)** major cheliped, mesial face; **(H)** minor (right) cheliped, lateral face; **(I)** pereopod 2; **(J)** pereopod 3; **(K)** pereopod 4; **(L)** pereopod 4 distal propodus and dactylus inside view; **(M)** pereopod 5; **(N)** pereopod 5 detail of distal propodus and dactylus, oblique inside view; **(O)** pleopod 1; **(P)** pleopod 2. Scale bars, 2 mm.

Fourth pereopod semichelate, ventrodistal corner of propodus expanded, with spiniform setae along tip of finger, single strong serrate spiniform seta at base; dense fields of setae on lateral surface of both propodus and drop-shaped dactylus proximally field of thick, serrate setae near articulation with dactylus.

Fifth pereopod chelate, opposable surfaces of propodus and minute dactylus excavate, terminally rounded with marginal spiniform setae; dactylus forming beak-like chela, with distodorsal spine, obscured by dense fields of simple and serrate setae on distal half of propodus and surface of dactylus.

Abdomen long, unarmed; dorsal length ratio (along midline) of first to sixth abdominal somites: 1.0: 1.29: 0.79: 0.84: 0.89: 0.76. First somite slightly narrowed anteriorly, pleuron not expanded laterally or ventrally, rounded. Second somite with straight anterior margin, posterior margin expanded posterolaterally, ventral and posterior margin bearing sparse setae. Third to fifth somites each

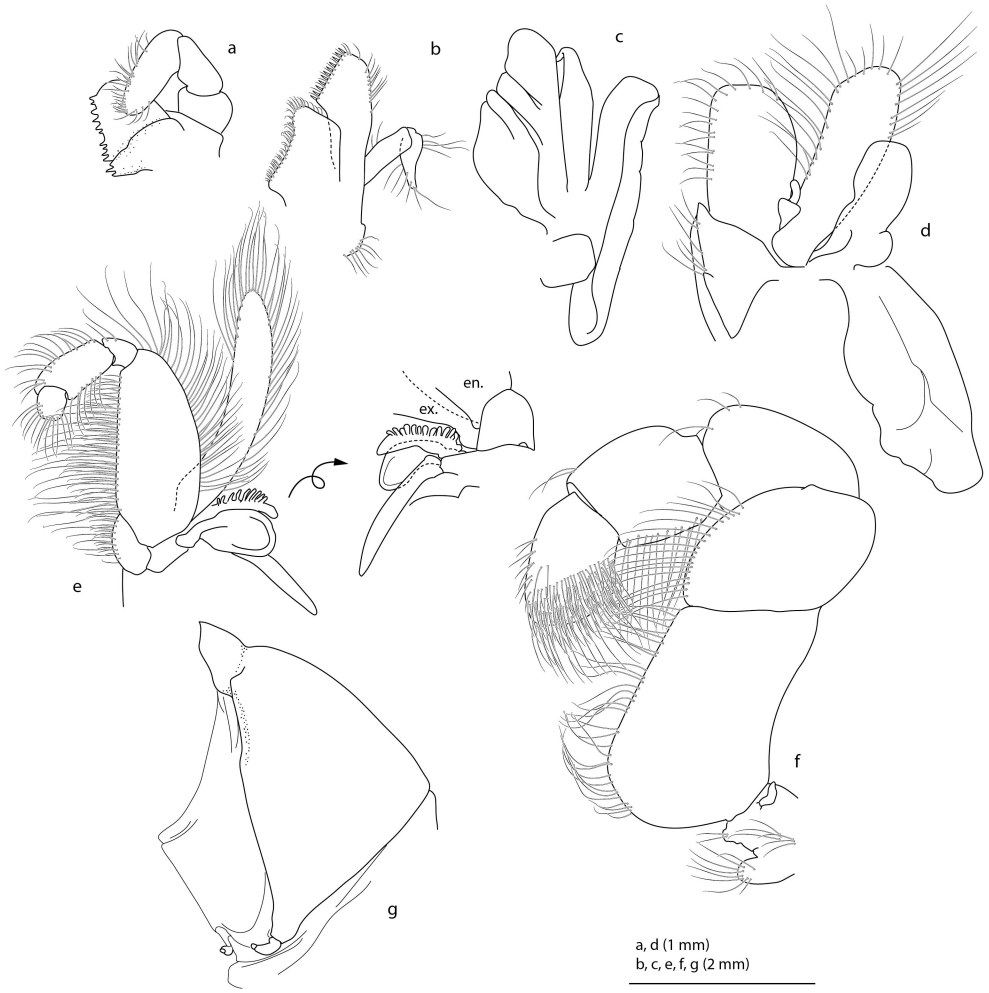

FIGURE 4
Vulcanocalliax beervana sp. nov.: Holotype female (NIWA 29413; cl., 9.5 mm); **(B)** first maxilla; **(C)** second maxilla; **(E)** second maxilliped with detail of proximal portion of endopod (en.) and exopod (ex.) and branchiae; **(F)** maxilliped 3. Paratype male (NIWA 69439; cl., 6. 0 mm); **(A)** mandible, excluding paragnaths; **(D)** first maxilliped; **(G)** first pleomere with paired reduced pleopods. Scale bars: **(A, D)** 2 mm and **(B, C, E–G)** 1 mm.

distinctly shorter than second somite, posterior margins expanded posterolaterally; pleura each with pairs of crescent-shaped setal tufts midlaterally, and simple setae on posteroventral margin. Sixth somite trapezoid in dorsal view, narrowed posteriorly, ventral margin of pleonite with short setae, posterior margin with tuft of long setae on each side.

Telson about as long as broad, broadest proximally, narrowing distally, posterolateral margin rounded, with few short simple setae, dorsally smooth and convex, with few simple long setae.

Uropod with endopod oval, 1.4 times as long as broad, slightly overreaching telson, posterolateral and posterior margins with few simple setae, dorsal surface convex and smooth, without longitudinal carina; exopod oval, about 1.7 times as long as broad, anterior portion smooth, not elevated, longitudinal carina developed dorsally, lateral margin with fringe of short, spiniform setae and simple setae, posterodistal margin of exopod with few simple setae.

First female pleopod uniramous, composed of two articles, total length less than half (0.37) that of second pleopod; proximal article half as long as distal article, straight; terminal article straight.

Second female pleopod biramous, with appendix interna; dense setation largely restricted to distal lobe of basipod, lateral margin of exopod, and mesial margin of endopod; bearing small appendix interna with cincinnuli.

Third to fifth pleopod pairs forming large, posteriorly cupped fans when cross-linked by hooked setae of appendices internae on opposed margins of endopods; endopod of each triangular. Appendices internae stubby, movably articulated to mesial margin of endopod.

Remarks on male and juvenile form: The remaining material is comprised of three small males (NIWA 69439) that may not be fully developed yet. The largest specimen has gonopores on coxa of the fifth pereopod, indistinct in the smaller specimens, in all specimens the first pleopods are vestigial and simple (Figure 4G). The smallest specimen (NIWA 29414) is considered a juvenile as it does not have any discernible gonopores or pleopods 1 developed. The body and appendages of these specimens are generally similar to that of the female holotype with the minor exceptions as follows: antennal article three is slightly shorter than (not same length as)

the fourth article (largest male; cl., 6.90 mm; NIWA 69439); there are both a right and a left detached major cheliped retained in the sample of three males (NIWA 69439); and cheliped merus is slightly longer at 1.70–1.75 length-width (compared to 1.6), as is the propodus (1.66–1.70 for males and 1.6 for holotype female). Proportions of abdominal segments differ slightly with ranges of segments 1 to 6 presented as 1: 1.26–1.54: 0.67–0.92: 0.59–0.75: 0.74–0.92: 0.8–1.0.

Color: Not documented but probably pale in life color as typical for the family.

Distribution: Known only from the Hikurangi Margin, east of the North Island of Aotearoa New Zealand, 650–808 m (Figure 1).

Remarks: *Vulcanocalliax beervana* sp. nov. is morphologically and genetically similar to *V. arutyunovi*, but some distinct morphological differences are apparent: the anterior carapace margin without the rostrum is distinctly convex in *V. beervana*, lacking the elevated postantennal shoulder present in *V. arutyunovi*; the anterolateral shape of the eye stalk is convexly rounded in *V. beervana* but acutely angled with a straight margin in *V. arutyunovi*; the second maxilliped has a long podobranch in *V. beervana*, which is absent in *V. arutyunovi*; the third maxilliped is furnished with a rudimentary exopod in *V. beervana*, which is absent in *V. arutyunovi*; the shape of the chelipeds differ, e.g., the flexor margin of the ischium is concave in *V. beervana* but straight in *V. arutyunovi*; the ventrodistal corner of the carpus is rounded in *V. beervana* but subacute in *V. arutyunovi*; the cutting edge of the fixed finger of both the major and minor chelipeds are lacking prominent triangular teeth in *V. beervana*, which are present in *V. arutyunovi*; and the dorsal surface of the uropodal exopod differ with only a simple longitudinal ridge near the midline in *V. beervana*, whereas *V. arutyunovi* has an exopod with a proximal elevation and no median ridge.

In the latter shape of the telson, uropods, and chelipeds and the presence of a rudimentary epipod on maxilliped 3, *V. beervana* is more similar to *Bathycalliax geomar* from the eastern Pacific, but the new species lacks cardiac sulci of the carapace (present in *B. geomar*) and has an arthrobranch on maxilliped 2 (absent in *B. geomar*) and the eyestalks are anterolaterally convex (subtriangular in *B. geomar*). The first male pleopod is uniquely flagellate in *B. geomar*, whereas, in both *V. arutyunovi* and *V. beervana*, the first pleopods are vestigial; however, only small males are available for both species of *Vulcanocalliax* and the adult form of the first male pleopod might yet be unknown.

Vulcanocalliax beervana sp. nov. was collected during a 2006 voyage that explored hydrocarbon seeps along the Hikurangi Margin off New Zealand's east coast. Neither station where this new ghost shrimp was collected (TAN0616/13 and 35) were in the immediate vicinity of observed chemoautotrophic fauna or seepage flares detected in echograms (Greinert et al., 2010: Baco et al., 2010). Organisms collected in the same grab sample (TAN0616/13) and deposited in the NIWA Invertebrate Collection and database included non-chemoautotrophic fauna such as corals (stylasterid, primnoid, and a small solitary hard coral); therefore, *V. beervana* does not appear to be associated with the chemoherms and their local biological communities dominated by *Calyptogena* clams. Whereas diffuse seepage occurs along many areas along the Hikurangi Margin, neither of the grabs or multicorers nearer the known seeps sampled any further ghost shrimps. Considering that both relatives *V. arutyunovi* and *Bathycalliax geomar* were collected in the vicinity of seeps (Gulf of Cádiz at around 1330 m and off Oregon at 627 m, respectively), it appears that this group of species are at least tolerant of the environmental conditions present around areas of hydrocarbon seeps.

The single holotype of the kentrogonid rhizocephalan *Parthenopea australis* described by Lützen et al. (2009) remains the only specimen for this species. It was found as a parasite of one specimen of *Vulcanocalliax* sp. nov. collected at the same station (TAN0616/13) as the female holotype of *V. beervana*. Unfortunately, the host specimen cannot be located, but it almost certainly belongs to the same species described here.

Molecular taxonomy

The multi-gene analysis presented for 123 species of Callianassidae and related families by Robles et al. (2020) included sequences for the holotype of *Vulcanocalliax arutyunovi* (NHMW 21927) and resolved the two representatives of the family Callianopsidae (*V. arutyunovi* and *Callianopsis goniophthalma*) as a basal family of the remaining "callianassoid" families with high nodal support.

Only a 16S sequence could be generated for the new species *V. beervana* for comparative purposes (kindly provided by Qi Kou, Chinese Academy of Sciences, GenBank accession number PQ137440, with a partial 328-bp fragment generated for NIWA 69439 (paratype) aligning with GenBank sequence EU874919 for *V. arutyunovi*, with 80.55% sequence identity (Table 2). Out of 328 bp, 64 bp differ, including five insertions for *V. beervana* sp. nov. Sequences for the nearest proposed relative *Bathycalliax geomar* are so far not available; the only other callianopsid voucher available is provided by *Callianopsis goniophthamla* [MN237708, deposited by Robles et al. (2020)] that aligns with a sequence similarity of 76.596% and 75.445% for *V. arutyunovi* and *V. beervana* sp. nov., respectively. All other sequences for a range of Ctenochelidae, Eucalliacidae, and Callianassidae representatives included in the Robles et al. (2020) phylogeny resolve with higher sequence divergences (Table 2).

Discussion

Vulcanocalliax beervana sp. nov. is the first and only species of the family Callianopsidae recorded in New Zealand, the wider southwestern Pacific region and the southern hemisphere. Other callianopsid species are known from the northeastern Atlantic (*V. arutyunovi* and *Callianopsis mauritana*), the Bay of Bengal in the Indian Ocean (*C. coecigena*), the eastern Pacific from Alaska to Mexico (*C. goniophthalma* and *Bathycalliax geomar*), and Taiwan in the northwestern Pacific (*C. anovalis*) (Sakai, 2011). A key to the currently known callianopsid species is provided below.

Webber et al. (2010) provided a first summary of the New Zealand axiidean ghost and sponge shrimp fauna, which have since

TABLE 2 Pairwise percentage genetic distances for aligned partial 16S rRNA gene (328 bp) between *Vulcanocalliax beervana* sp. nov. and published GenBank sequences for a selection of families and species previously presented by Robles et al. (2009, 2020).

Family	Taxon	PQ137440	EU874919	MN237708	MN237676	MN237850	MN237662	MN237848	MN237763	EU882926	EU874925
Callianopsidae	*Vulcanocalliax beervana* sp. nov. (PQ137440)	—									
Callianopsidae	*Vulcanocalliax arutyunovi* (EU874919)	80.547	—								
Callianopsidae	*Callianopsis goniophthalma* (MN237708)	75.455	76.596	—							
Ctenochelidae	*Ctenocheloides almeidai* (MN237676)	70.000	71.818	71.733	—						
Ctenochelidae	*Gourretia* sp. ULLZ 9707 (MN237850)	70.303	71.818	74.772	77.204	—					
Ctenochelidae	*Ctenocheles balssi* (MN237662)	74.503	75.497	76.744	76.412	85.284	—				
Ctenochelidae	*Dawsonius* aff. *latispina* (MN237848)	72.424	73.333	76.292	78.116	79.205	79.933	—			
Eucalliacidae	*Calliaxina novaebritanniae* (MN237763)	72.205	73.414	68.182	74.164	72.340	73.667	73.556	—		
Eucalliacidae	*Eucalliaxiopsis jonesi* (EU882926)	70.181	72.892	74.320	75.152	72.205	74.917	75.529	73.414	—	
Callianassidae	*Callianassa aqabaensis* (EU874925)	68.882	67.976	67.879	70.303	71.212	71.761	73.636	69.091	71.084	—

10.3389/fmars.2024.1412024

expanded to 14 species with descriptions of a callianassid by Schnabel et al. (2023b) and a challichirid by Poore et al. (2022). Current efforts continue to, for the first time, comprehensively inventory the Zealand Axiidea, with a number remaining to be formally described (Schnabel et al., 2023a).

Key to Callianopsidae Manning and Felder, 1991

1. Pleomere 6 with prominent lateral projections; carapace with longitudinal carina running from rostrum; epipods absent on pereopods ***Callianopsis*** **(four species) (2)**.

- Pleomere 6 without prominent lateral projections; rostrum dorsally smooth, without longitudinal carina; epipods present on maxilliped 3 to pereopod 4 **(5)**.

2. Lateral spines or spine-like projections on abdominal pleura 2–6 ***Callianopsis caecigena*** (Alcock and Anderson, 1894).

- Abdominal pleura 2–4 laterally and ventrally unarmed, distoventral or lateral projections present on pleura 5 and/or 6 **(3)**.

3. Abdominal pleuron 5 unarmed, ventral projection only on the sixth pleuron ***Callianopsis mauritana*** (Sakai et al., 2015).

- Abdominal pleura 5 and 6 with acute ventral projections **(4)**.

4. Dorsal oval on carapace absent; abdominal tergite 1 distinctly notched anteriorly; maxilliped 2 exopod simple, not flagellate ***Callianopsis anovalis*** Lin et al., 2007.

- Dorsal oval on carapace present; abdominal tergite 1 straight anteriorly; maxilliped 2 exopod distally flagellate ***Callianopsis goniophthalma*** (Rathbun, 1902).

5. Two cardiac sulci present; minor cheliped merus with more than two proximal spines on flexor margin; maxilliped 2 without arthrobranch; male pleopod 1 distally flagellate ***Bathycalliax geomar*** **(monotypic genus)**.

- Cardiac sulci absent; minor cheliped merus with two proximal spines on flexor margin; maxilliped 2 with arthrobranch; male pleopod 1 vestigial ***Vulcanocalliax*** **(two species) (6)**.

6. Carapace anterior margin concave lateral to rostrum, produced behind second antenna; ocular peduncle anterolateral margin subtriangular, straight; uropodal exopod thickened anterodorsally (strongly curved, descending to distal margin) ***Vulcanocalliax arutyunovi*** Dworschak and Cunha, 2007.

- Carapace anterior margin convexly rounded on either side of rostrum, round behind second antenna; ocular peduncle anterolateral margin convex; uropodal exopod with dorsomedian ridge, anterior portion of exopod smooth, not elevated ***Vulcanocalliax beervava*** **sp. nov.**

Data availability statement

The original contributions presented in the study are publicly available. This data can be found here: NCBI GenBank, accession number PQ137440 (https://www.ncbi.nlm.nih.gov/nuccore/PQ137440.1/). Vulcanocalliax beervana Schnabel & Peart, 2024 is registered with ZooBank under (https://zoobank.org/NomenclaturalActs/3f10dc90-f860-4bd9-a46b-b570735a2551).

Ethics statement

Ethical approval was not required for the study involving animals in accordance with the local legislation and institutional requirements because we used preserved animals deposited in a natural history collection.

Author contributions

KS: Writing – original draft. RP: Writing – review & editing.

Funding

The author(s) declare financial support was received for the research, authorship, and/or publication of this article. KS and RP were funded by NIWA under Coasts and Oceans Research Programme 2 Marine Biological Resources: discovery and definition of the marine biota of New Zealand (2023–2024 SCI).

Acknowledgments

We are grateful to the staff of the NIWA Invertebrate Collection for their tireless work. We thank Qi Kou (Institute of Oceanology, Chinese Academy of Sciences, Qingdao, China) for sequence data for the new species and Gary Poore (Museums Victoria, Melbourne, Australia) for guidance on comparative morphology of callianassoid shrimp. Specimens were collected by the voyage TAN0616 – RENEWZ I/NEW ZEEPS, the first component of the project 'Exploration of Chemosynthetic Habitats of the New Zealand Region, funded by NOAA Ocean Exploration and NIWA, with co-funding from Woods Hole Oceanographic Institution, Scripps Oceanographic Institution, and the University of Hawai'i. We thank the reviewers for their time and helpful suggestions

Conflict of interest

The authors declare that the research was conducted in the absence of any commercial or financial relationships that could be construed as a potential conflict of interest.

Publisher's note

References

Alcock, A., and Anderson, A. R. S. (1894). Natural history notes from H.M. Royal Indian Marine Survey Steamer "Investigator", commander C.F. Oldham, R.N., commanding. - Series II, No. 14. An account of a recent collection of deep-sea Crustacea from the Bay of Bengal and Laccadive Sea. *J. Asiatic Soc. Bengal (2) (Natural History)* 63, 141–185.

Baco, A. R., Rowden, A. A., Levin, L. A., Smith, C. R., and Bowden, D. A. (2010). Initial characterization of cold seep faunal communities on the New Zealand Hikurangi margin. *Mar. Geol.* 272, 251–259. doi: 10.1016/j.margeo.2009.06.015

Bankevich, A., Nurk, S., Antipov, D., Gurevich, A. A., Dvorkin, M., Kulikov, A. S., et al. (2012). SPAdes: a new genome assembly algorithm and its applications to single-cell sequencing. *J. Comput. Biol.* 19, 455–477. doi: 10.1089/cmb.2012.0021

Bolger, A. M., Lohse, M., and Usadel, B. (2014). Trimmomatic: a flexible trimmer for Illumina sequence data. *Bioinformatics* 30, 2114–2120. doi: 10.1093/bioinformatics/btu170

Camacho, C., Coulouris, G., Avagyan, V., Ma, N., Papadopoulos, J., Bealer, K., et al. (2009). BLAST+: architecture and applications. *BMC Bioinf.* 10, 421. doi: 10.1186/1471-2105-10-421

DecaNet eds (2024). DecaNet. Accessed through: World Register of Marine Species. Available online at: https://www.decanet.info/aphia.php?p=taxdetails&id=1214590 (Accessed August 1, 2024).

de Saint Laurent, M. (1973). Sur la systématique et la phylogénie des Thalassinidea: définition des familles des Callianassidae et des Upogebiidae et diagnose de cinq genres nouveaux. *Comptes Rendus Hebdomadaires Séances l'Académie Des. Sci. Paris* 277, 513–516.

Dworschak, P. C., and Cunha, M. R. (2007). A new subfamily, Vulcanocalliacinae n.subfam., for *Vulcanocalliax arutyunovi* n.gen,. n.sp. from a mud volcano in the Gulf of Cadiz (Crustacea, Decapoda, Callianassidae). *Zootaxa* 1460, 35–46. doi: 10.11646/zootaxa.1460.1

Greinert, J., Lewis, K. B., Bialas, J., Pecher, I. A., Rowden, A., Bowden, D. A., et al. (2010). Methane seepage along the Hikurangi Margin, New Zealand: Overview of studies in 2006 and 2007 and new evidence from visual, bathymetric and hydroacoustic investigations. *Mar. Geol.* 272, 6–25. doi: 10.1016/j.margeo.2010.01.017

Kearse, M., Moir, R., Wilson, A., Stones-Havas, S., Cheung, M., Sturrock, S., et al. (2012). Geneious Basic: an integrated and extendable desktop software platform for the organization and analysis of sequence data. *Bioinformatics* 28, 1647–1649. doi: 10.1093/bioinformatics/bts199

Lin, F. J., Komai, T., and Chan, T. Y. (2007). First record of the thalassinidean genus *Callianopsis* de Saint Laurent 1973 (Decapoda, Ctenocheildae) in the West Pacific, with the description of a new species from Taiwan. *Crustaceana* 80, 1193–1203. Available at: http://www.jstor.org/stable/20107910.

Lörz, A.-N., Glenner, H., and Lützen, J. (2008). New records of Rhizocephala (Cirripedia) from New Zealand, including the first rhizocephalan records from hot vents and cold seeps. *Crustaceana* 81, 1013–1019. doi: 10.1163/156854008X354911

Lützen, J., Glenner, H., and A-Lörz, N. (2009). Parasitic barnacles (Cirripedia: Rhizocephala) from New Zealand off-shore waters. *New Z. J. Mar. Freshw. Res.* 43, 613–621. doi: 10.1080/00288330909510027

Manning, R. B., and Felder, D. L. (1991). Revision of the American callianassidae (Crustacea: decapoda: thalassinidea. *Proc. Biol. Soc. Washington* 104, 764–792.

Poore, G. C. B., and Ahyong, S. T. (2023). *Marine Decapod Crustacea - A Guide to Families and Genera of the World* (Clayton South, Australia: CSIRO Publishing).

Poore, G. C., Dworschak, P. C., Robles, R., Mantelatto, F. L., and Felder, D. L. (2019). A new classification of Callianassidae and related families (Crustacea: Decapoda: Axiidea) derived from a molecular phylogeny with morphological support. *Memoirs Museum Victoria* 78, 73–146. doi: 10.24199/j.mmv.2019.78.05

Poore, G. C. B., Dworschak, P. C., and Schnabel, K. (2022). *Articullichirus*, a new genus of ghost shrimp (Crustacea: Axiidea: Callichiridae) with two new species. *Memoirs Museum Victoria* 81, 123–133. doi: 10.24199/j.mmv.2022.81.05

Rathbun, M. J. (1902). Descriptions of new decapod crustaceans from the west coast of North America. *Proc. United States Natl. Museum* 24, 885–905. doi: 10.5479/si.00963801.1272.885

Robles, R., Dworschak, P. C., Felder, D. L., Poore, G. C. B., and Mantelatto, F. L. (2020). A molecular phylogeny of Callianassidae and related families (Crustacea: Decapoda: Axiidea) with morphological support. *Invertebrate Systematics* 34, 113–132. doi: 10.1071/IS19021

Robles, R., Tudge, C. C., Dworschak, P. C., Poore, G., and Felder, D. (2009). Molecular phylogeny of the Thalassinidea based on nuclear and mitochondrial genes. In: J. W. Martin, K. A. Crandall and D. L. Felder (Eds). *Crustacean Issues* Decapod crustacean phylogenetics. Boca Raton, FL, USA: CRC Press. 18, 309–326. doi: 10.1201/9781420092592-c15

Rose, R., Golosova, O., Sukhomlinov, D., Tiunov, A., and Prosperi, M. (2019). Flexible design of multiple metagenomics classification pipelines with UGENE. *Bioinformatics* 35, 1963–1965. doi: 10.1093/bioinformatics/bty901

Sakai, K. (2011). Axioidea of the world and a reconsideration of the Callianassoidea (Decapoda, Thalassinidea, Callianassida). *Crustaceana Monogr.* 13, 1–616. doi: 10.1163/9789047424185

Sakai, K., and Türkay, M. (1999). A new subfamily, Bathycalliacinae n. subfam., for *Bathycalliax geomar* n. gen., n. sp. from deep water cold seeps off Oregon, USA. *Senckenbergiana biologica* 79, 203–209.

Sakai, K., Türkay, M., Beuck, L., and Freiwald, A. (2015). A collection of the Infraorder Callianassidea (Decapoda, Pleocyemata) with one new genus and five new species from the Eastern Atlantic off Mauritania (R/V Maria S. Merian cruise MSM 16/3 "PHAETON"). *Mar. Biodiversity* 45, 113–133. doi: 10.1007/s12526-014-0227-2

Schnabel, K. E., Peart, R. A., Bradford-Grieve, J., Eagar, S., Hosie, A., and Buckeridge, J. (2023a). "Kingdom Animalia, Phylum Arthropoda, Subphylum Crustacea," in *The Marine Biota of New Zealand: Updating the New Zealand Inventory of Biodiversity to 2020*. Eds. M. Kelly, S. Mills, W. Nelson and M. Terezow (NIWA Biodiversity Memoir, Wellington), 412–445.

Schnabel, K., Rowden, A. A., and Poore, G. C. B. (2023b). A new species of *Arenallianassa* (Decapoda: Axiidea: Callianassidae) from hydrothermal vents with notes on its ecology and a redescription of *Arenallianassa arenosa* (Poore 1975). *Memoirs Museum Victoria* 82, 55–69. doi: 10.24199/j.mmv.2023.82.03

Webber, W. R., Fenwick, G. D., Bradford-Grieve, J. M., Eagar, S. H., Buckeridge, J. S., Poore, G. C. B., et al. (2010). "Subphylum Crustacea - shrimps, crabs, lobsters, barnacles, slaters, and kin," in *New Zealand Inventory of Biodiversity Volume 2. Chaetognatha, Ecdysozoa, Ichnofossils*. Ed. D. P. Gordon (Canterbury University Press, Christchurch), 98–232.

frontiers | Frontiers in Marine Science

TYPE Original Research
PUBLISHED 20 September 2024
DOI 10.3389/fmars.2024.1429314

OPEN ACCESS

EDITED BY
Rachael Peart,
National Institute of Water and Atmospheric Research (NIWA), New Zealand

REVIEWED BY
Ka Yan Ma,
Sun Yat-sen University, China
Danielle M. DeLeo,
Florida International University, United States

*CORRESPONDENCE
Jonas C. Geburzi
jonas.geburzi@leibniz-zmt.de

†PRESENT ADDRESSES
Paula C. Rodríguez-Flores,
Department of Invertebrate Zoology, National Museum of Natural History, Washington, DC, United States
Shahan Derkarabetian,
Department of Entomology, San Diego Natural History Museum, San Diego, CA, United States

RECEIVED 07 May 2024
ACCEPTED 30 August 2024
PUBLISHED 20 September 2024

CITATION
Geburzi JC, Rodríguez-Flores PC, Derkarabetian S and Giribet G (2024) From the shallows to the depths: a new probe set to target ultraconserved elements for Decapoda and other Malacostraca. *Front. Mar. Sci.* 11:1429314. doi: 10.3389/fmars.2024.1429314

From the shallows to the depths: a new probe set to target ultraconserved elements for Decapoda and other Malacostraca

Jonas C. Geburzi[1,2]*, Paula C. Rodríguez-Flores[2†], Shahan Derkarabetian[2†] and Gonzalo Giribet[2]

[1]Mangrove Ecology, Leibniz Center for Tropical Marine Research (ZMT), Bremen, Germany, [2]Museum of Comparative Zoology, Department of Organismic & Evolutionary Biology, Harvard University, Cambridge, MA, United States

Introduction: Since its introduction about a decade ago, target enrichment sequencing of ultraconserved elements (UCEs) has proven to be an invaluable tool for studies across evolutionary scales, and thus employed from population genetics, to historical biogeography as well as deep-time phylogenetics. Here, we present the first probe set targeting UCEs in crustaceans, specifically designed for decapods and tested beyond decapods in other malacostracan lineages.

Methods: Probes were designed using published genomes of nine decapod and one peracarid species, as well as raw Nanopore long reads of one additional brachyuran species. The final probe set consists of about 20,000 probes, targeting 1,384 unique UCE loci. We compiled a dataset across Malacostraca,as well as datasets of a deep-sea squat lobster genus, and an intertidal mangrove crab species, to test the probe set at different phylogenetic levels (i.e., class, order, genus, within species).

Results: Final mean UCE recovery from fresh samples across Malacostraca was 568 loci, with up to 847 and 658 loci recovered from decapod and non-decapod species, respectively. Final mean recovery from fresh samples in the genus- and within species-level datasets was 849 and 787 loci, respectively. Up to several hundreds of UCEs were recovered from historical museum specimens (10 to > 150 years old), that were included in all datasets. UCE-based phylogenies largely reflected the known relationships of the included taxa, and we were able to infer population differentiation based on >600 SNPs extracted from the species-level dataset.

Discussion: Our results showcase the versatility of this UCE probe set, yielding informative data from phylogenetic as well as population-genetic datasets. They demonstrate once more that UCEs are a promising technique for leveraging museum specimens for genomic studies, and overall highlight the probe set's potential for crustacean evolutionary studies.

KEYWORDS

Arthropoda, UCEs, Brachyura, phylogenomics, population genetics

1 Introduction

Ultraconserved elements (UCEs) are highly conserved genome regions that are present across many taxa. They are known to have regulatory expression functions in vertebrates, while being of exonic origin in arthropods (Faircloth et al., 2012; McCormack et al., 2012; Hedin et al., 2019). Since their discovery as syntenically conserved regions in the human, mouse and rat genomes (Bejerano et al., 2004), the use of UCEs for phylogenomic studies has rapidly increased, becoming a popular technique in the past few years (see references below). The increasing popularity of the UCEs approach relies on 1) the amount of generated data, since it allows to target between hundreds to thousands of orthologous loci, improving phylogenetic resolution and largely outperforming traditional multilocus sequencing; 2) in contrast to other genomic techniques such as transcriptomics, UCE sequencing allows to obtain historical DNA from ethanol preserved or dried specimens in museum collections (McCormack et al., 2012; Blaimer et al., 2016; Derkarabetian et al., 2019; Raxworthy and Smith, 2021); and, 3) unlike anchored hybrid enrichment (AHE; Lemmon et al., 2012), the full UCE probe set design and hybridization pipeline was originally published open source (Faircloth, 2017), allowing everybody to design baits to target their organisms of study.

UCEs have been used to reconstruct phylogenies for many taxa across the entire Tree of Life, and at multiple phylogenetic scales, from backbone phylogenies (e.g., Faircloth et al., 2013; Streicher and Wiens, 2017) to species-level or even population-level studies (e.g., Smith et al., 2014; Derkarabetian et al., 2018, 2022). The versatility of UCEs at different evolutionary scales relies on the sequencing of UCEs flanking regions, with a higher proportion of variable sites when increasing the distance from the highly conserved core of the UCE (Faircloth et al., 2012). This allows generation of conserved datasets useful for phylogenomic reconstruction at higher taxonomic levels, as well as the possibility to extract single nucleotide polymorphisms (SNPs) from each single locus, showing an efficacy comparable to microsatellites and ddRAD, for population genomics (Vinciguerra et al., 2019; Glon et al., 2021).

UCE probe sets are currently available for several invertebrate taxa, and at different levels of divergence, from phylum to genus-level: e.g., anthozoans (Cnidaria) (Quattrini et al., 2018), hexacorals (Cnidaria, Anthozoa) (Cowman et al., 2020), heterobranchs (Mollusca, Gastropoda) (Moles and Giribet, 2021), velvet worms (Onychophora) (Sato et al., 2024a), bivalves (Mollusca, Bivalvia) (González-Delgado et al., 2024) and for multiple arthropod taxa, including many groups of insects and arachnids (Starrett et al., 2017; Zhang et al., 2019, and references therein). Within arthropods, the most comprehensive probe set was designed for Arachnida, a group spanning more than 500 million years of evolution (Starrett et al., 2017). However, despite this huge divergence, this probe set has proven to be very useful across all chelicerate groups and across a variety of phylogenetic levels (e.g., Hedin et al., 2020; Ballesteros et al., 2021; Boyer et al., 2022; de Miranda et al., 2024; Sato et al., 2024b).

A major component of Earth's biodiversity is represented by the crustaceans of the class Malacostraca. This group has a long evolutionary history, and like arachnids, probably started to diversify at least 500 million years ago (Schram, 1982; Schwentner et al., 2017; Bernot et al., 2023). It is the largest class of non-hexapod crustaceans, with more than 30,000 described species classified into 17 orders. Malacostracans display great morphological disparity, including multiple body forms such as shrimp-like, crab-like, lobster-like, with a bivalved carapace, mantis-like, conglobated forms, etc. This group has received much attention due to its ancient origin, morphological disparity and ecological diversity. However, although clearly monophyletic, the scarcity of genomic studies has hampered the understanding of the phylogenetic placement of many malacostracan groups (e.g., Schwentner et al., 2018; Bernot et al., 2023; Höpel et al., 2022). Additionally, within Malacostraca, decapods and peracarids are considered hyperdiverse taxa with independent radiations to the land and fresh waters (e.g., Hou et al., 2014; Wolfe et al., 2019, 2023; Tsang et al., 2022). They have colonized extreme environments in both marine and terrestrial habitats, such as anchialine caves, hydrothermal vents or hadal trenches (e.g., Gonzalez et al., 2020; Patel et al., 2020; Swan et al., 2021), and therefore represent a model group for several disciplines in evolutionary biology.

Genomic resources to tackle malacostracan and decapod relationships first focused on phylotranscriptomics (Schwentner et al., 2017, 2018; Lozano-Fernandez et al., 2019), but transcriptomes are expensive to generate, require fresh tissues,

and the analytical pipelines are complex due to the need of an orthology-assignment step. Wolfe et al. (2019) thus turned to sequence capture techniques and generated a large dataset for decapods by developing a new anchored hybrid enrichment (AHE) kit for decapod phylogenetics designed from existing genomic and transcriptomic sequences. However, UCEs appear to have become the most popular tool for invertebrate phylogenomics now, with regular publications of new invertebrate UCE probe sets following Faircloth's (2017) open source pipeline (see e.g. van der Sprong et al., 2024). We thus turned to UCEs for their versatility and open access, as, despite the rapid growth of UCEs to study the evolution of arthropod lineages, no crustacean probe set is currently available.

The use of target capture sequencing of UCEs in crustacean research can offer multiple benefits at various levels. Firstly, it can aid in resolving phylogenetic uncertainties in Malacostraca, providing insights into the evolutionary relationships of this diverse group of crustaceans. Secondly, it can improve phylogenetic resolution for the study of explosive radiations and other evolutionary events at different scales, ranging from intraspecific to interspecific levels. Finally, this approach can be especially valuable in cases where access to living specimens is limited and expensive, such as with deep-sea samples. By utilizing historical collections, researchers can leverage this technique to solve taxonomic questions using molecular methods, thereby advancing our understanding of this fascinating group of organisms and adding value to the extensive museum collections of deep-sea fauna and regions of the world where collecting is no longer feasible.

Here we present a new probe set targeting UCEs for Decapoda and other lineages of Malacostraca, which is also the first UCE probe set for any crustacean lineage to date. We tested this probe set *in-silico* and *in-vitro* by hybridization to DNA samples obtained from all major decapod lineages as well as several non-decapod Malacostraca. Our tests demonstrate the efficacy of the probe set at different taxonomic scales, regularly recovering hundreds to more than 1,000 loci across Malacostraca, including dozens to hundreds of loci from historical samples (collection dates 1865 to 2012)

TABLE 1 Genome quality (contig N50 and BUSCO score as % completeness) and UCE recovery from *in-silico* samples: raw locus recovery with 65/65 % coverage/identity percentage thresholds (UCEs raw), and number of loci retained in 50% and 70% occupancy matrices after trimming and filtering.

Higher taxonomy	Species	GenBank accession No.	Contig N50	BUSCO	UCEs raw	UCEs 50%	UCEs 70%
Brachyura: Portunidae	*Callinectes sapidus*	GCA 020233015.1	9.3	94.6	1026	784	100
Brachyura: Portunidae	*Portunus trituberculatus*	GCA 017591435.1	4100.0	95.9	1112	850	108
Brachyura: Oregoniidae	***Chionoecetes opilio***	**GCA 016584305.1**	**149.6**	**95.3**	**1155**	**837**	**102**
Brachyura: Varunidae	***Eriocheir sinensis***	**GCA 013436485.1**	**3200.0**	**96.6**	**1167**	**863**	**107**
Anomura: Coenobitidae	***Birgus latro***	**GCA 018397915.1**	**5.3**	**59.6**	**1196**	**840**	**107**
Anomura: Lithodidae	*Paralithodes camtschaticus*	GCA 018397895.1	5.8	47.2	949	682	88
Astacidea: Cambaridae	*Procambarus clarkii*	GCA 020424385.2	217.7	97.1	1156	828	105
Astacidea: Nephropidae	***Homarus americanus***	**GCA 018991925.1**	**133.3**	**96.4**	**1190**	**852**	**109**
Astacidea: Parastacidae	*Cherax destructor*	GCA 009830355.1	80.9	82.6	1023	744	104
Achelata: Palinuridae	***Panulirus ornatus***	**GCA 018397875.1**	**5.4**	**72.5**	**1175**	**836**	**106**
Caridea: Atyidae	*Caridina multidentata*	GCA 002091895.1	0.8	24.8	919	680	101
Caridea: Palaemonidae	***Macrobrachium nipponense***	**GCA 015104395.1**	**255.0**	**42.8**	**994**	**682**	**82**
Dendrobranchiata: Penaeidae	***Penaeus japonicus***	**GCA 017312705.2**	**132.8**	**95.9**	**1098**	**845**	**107**
Isopoda: Armadillidiidae	*Armadillidium vulgare*	GCA 004104545.1	38.4	88.6	840	569	90
Isopoda: Cirolanidae	*Bathynomus jamesi*	GCA 023014485.1	586.5	93.9	805	567	90
Isopoda: Idoteidae	*Idotea balthica*	GCA 023373965.1	6.1	76.7	704	509	85
Amphipoda: Hyalidae	*Parhyale hawaiensis*	GCA 001587735.2	10.4	94.4	851	556	95
Amphipoda: Hyalellidae	***Hyalella azteca***	**GCA 000764305.4**	**112.9**	**95.5**	**1015**	**665**	**107**

(Continued)

TABLE 1 Continued

Higher taxonomy	Species	GenBank accession No.	Contig N50	BUSCO	UCEs raw	UCEs 50%	UCEs 70%
Amphipoda: Gammaridae	*Gammarus roeseli*	GCA 016164225.1	4.7	36.0	946	619	99
Branchiopoda: Artemiidae	*Artemia franciscana*	GCA 019857095.1	61.1	52.3	381	143	29
Copepoda: Temoridae	*Eurytemora affinis*	GCA 000591075.2	67.7	94.4	452	115	25

Species in bold were used for probe set design.

in our test datasets. The new probe set should thus provide a valuable resource for population-level to phylogenomic studies across Malacostraca.

2 Materials and methods

2.1 Taxon sampling

The publicly available genomes cover the majority of infraorders within Decapoda. For the probe set design, we used seven genomes from across the Decapoda tree of life, with a focus on the most diverse group, the true crabs (Brachyura), our main focal taxon. The mitten crab *Eriocheir sinensis* (Brachyura, Grapsoidea) was chosen as the base genome for its high level of completeness; *Birgus latro* (Anomura), *Chionoecetes opilio* (Brachyura), *Homarus americanus* (Astacidea), *Macrobrachium nipponense* (Caridea), *Panulirus ornatus* (Achelata) and *Penaeus japonicus* (Dendrobranchiata) were used as exemplar taxa. The peracarid *Hyalella azteca* (Amphipoda) was used as the outgroup taxon. See Table 1 for genome quality scores and accession numbers of all genomes used for probe set design and *in-silico* testing. Additionally, we added novel Oxford Nanopore raw reads (unassembled) of a third crab species, *Aratus pisonii* (Brachyura, Grapsoidea), to the probe set design pipeline. For this, we extracted high-molecular weight DNA from leg muscle tissue of a specimen (voucher no. MCZ:IZ:162234; collected on April 2021 on N Hutchinson Island, FL, fixed in liquid Nitrogen and stored at -80° C), using a custom high-salt extraction protocol, followed by chloroform-isoamyl-alcohol purification. The DNA sample was sequenced on a PromethION platform and basecalled with Guppy 5.0.11, yielding 29.6 Gbases across 64.7 million reads with a read N50 of 827 bases (reads available at BioProject PRJNA988117, accession numbers SRX20952170 – SRX20952177).

We downloaded 13 additional crustacean genomes from NCBI to test the probe set *in-silico*. These included seven decapod, four peracarid, and two non-malacostracan genomes (one branchiopod and one copepod), to also assess performance and efficacy of the probe set on other crustacean taxa beyond Malacostraca (Table 1).

For the *in-vitro* test of the probe set, we compiled 41 samples from the collections of the Museum of Comparative Zoology, Cambridge, MA (MCZ), the Smithsonian National Museum of Natural History, Washington DC (USNM), and the Muséum national d'Histoire naturelle, Paris (MNHN), focusing on Decapoda, but also including representatives of Peracarida (Amphipoda, Cumacea, Isopoda), Euphausiacea, Stomatopoda, Phyllocarida, and Branchiopoda (Table 2). Ten of these samples were obtained from "historical" museum specimens with degraded DNA, i.e., collected more than 10 years ago, and stored in 70% ethanol at room temperature. The historical samples covered a range of collection years between 1865 and 2012, and were included to assess UCE locus recovery and utility of the probe set for phylogenetic studies of crustacean specimens from museum collections. These 41 *in-vitro* and 21 *in-silico* malacostracan samples combined are subsequently referred to as the "Malacostraca dataset".

Furthermore, we compiled two additional datasets to assess the efficacy of the probe set at shallower taxonomic levels, i.e. its potential to recover variation among closely related species and populations of a single species: a set of 10 samples representing 6 species of the squat lobster family Eumunididae (Anomura) from the Western Indian Ocean (*E. bispinata*, *E. capillata*, *E. minor*, *E. multispina*, *E. similior* and *E. spiridonovi*), collected between 1972 and 2017, including historical specimens from the MNHN, and the California Academy of Sciences, San Francisco (CAS) (the "*Eumunida* dataset" in the following, Supplementary Table S1); and 30 specimens of the mangrove crab *Aratus pisonii* (Brachyura, Sesarmidae), collected between 1859 and 2021 in southeastern Florida, including historical specimens from the MCZ, USNM, the American Museum of Natural History, New York (AMNH) and the Florida Museum of Natural History, Gainesville (UF) (the "*Aratus* dataset" in the following, Supplementary Table S2).

2.2 Probe set design and synthesis

We used PHYLUCE version 1.7.1 (Faircloth, 2016) to design the probe set, following the tutorial on https://phyluce.readthedocs.io/en/latest/tutorials/tutorial-4.html (also see Faircloth, 2017). The downloaded genomes and *A. pisonii* raw reads were converted to FASTA format and file headers were modified for compatibility with the PHYLUCE pipeline using SeqIO, available on Bioconda (Grüning et al., 2018). Copies of the genomes in 2bit format, required further downstream in the pipeline, were created using faToTwoBit (Kent, 2002). ART (Huang et al., 2012) was then used to simulate 100-bp short reads with 200-bp insert size (150 standard deviation) from all exemplar genomes and the *A. pisonii* long reads, covering the base genome approximately 2X. These simulated reads were individually aligned to the base genome using STAMPY (Lunter and Goodson, 2011), identifying putatively conserved loci with less than 5% sequence divergence to the base genome.

TABLE 2 Assembly and UCE extraction summary statistics for the *in-vitro* samples in the Malacostraca dataset, with collection accession numbers (see main text for collection codes), collection years, raw reads, proportion of on-target reads (i.e. reads mapped to a UCE probe), assembled contigs, raw UCE loci recovered from contigs, the length of the raw UCE loci, and final numbers of UCEs in 50% and 70% taxon coverage matrices after trimming and filtering.

Higher taxonomy	Species	Voucher	Year	Reads	% reads on target	Contigs	UCEs raw	Locus length (bp)			UCEs 50%	UCEs 70%
								mean	min	max		
Brachyura												
Dynomenidae	*Metadynomene* sp.	MCZ:IZ:153343	2019	2,879,274	0.55	83,578	1,166	611.8	236	1,157	847	107
Gecarcinidae	*Gecarcinus ruricola*	MCZ:IZ:46902	2003	186,296	1.80	1,982	48	258.0	80	496	29	6
Grapsidae	*Pachygrapsus transversus*	MCZ:IZ:61995	2004	6,500,430	3.46	38,220	1,069	455.0	227	3,619	741	97
Percnidae	*Percnon planissimum*	MCZ:IZ:163892	2022	38,706,346	2.16	463,250	657	1,399.9	394	5,678	528	80
Portunidae	*Callinectes sapidus*	MCZ:IZ:23424	2010	7,036,308	0.06	94,335	290	329.4	80	6,602	16	2
Sesarmidae	*Aratus pisonii*	MCZ:IZ:161758	2021	7,077,520	7.79	239,522	1,031	1,503.0	77	10,525	788	103
	Aratus pisonii	MCZ:IZ:6197	1865	2,275,666	41.19	2552	5	212.6	80	257	3	1
	Armases cinereum	MCZ:IZ:162859	2021	26,878,648	4.08	417,860	744	1,217.5	245	5,048	589	94
Trapeziidae	*Trapezia rufopunctata*	MCZ:IZ:163860	2022	8,798,622	2.94	108,611	847	1,622.1	247	3,786	656	96
Varunidae	*Eriocheir sinensis*	MCZ:IZ:68008	1932	3,466,502	15.61	10,746	40	265.5	79	493	13	1
Xanthidae	*Actaeodes tomentosus*	MCZ:IZ:163780	2022	33,281,628	1.47	794,710	243	1,146.9	269	2,115	198	42
	Cymo melanodactylus	MCZ:IZ:163854	2022	28,583,220	0.90	578,024	601	841.8	205	4,203	463	70
Anomura												
Eumunididae	*Eumunida* cf. *pacifica*	MCZ:IZ:153356	2019	17,174,134	1.48	510,382	1,051	1,255.2	81	5,316	793	107
	Eumunida pacifica	MNHN-IU-2014-23737	1991	11,783,584	1.43	110,384	975	398.7	229	6,054	656	86
	Pseudomunida fragilis	MCZ:IZ:151084	2018	3,070,266	1.69	84,402	965	1,275.2	229	6,592	730	102
Galatheidae	*Coralliogalathea parva*	MCZ:IZ:163893	2022	45,563,018	0.68	355,095	612	1,091.5	240	6,396	466	76
	Galathea platycheles	MCZ:IZ:163971	2022	41,649,784	0.57	733,875	510	1,118.5	280	2,322	412	71
Munididae	*Grimothea quadrispina*	MCZ:IZ:139215	2016	57,233,300	1.52	1,108,273	531	873.5	235	1,528	415	66
Munidopsidae	*Munidopsis lentigo*	USNM 1487884	2012	44,612,328	0.86	423,853	1,000	1,043.2	232	8,073	748	99
Paguridae	*Porcellanopagurus* sp.	MNHN-IU-2021-7149	2021	1,612,206	0.71	4,229	108	295.9	80	575	65	13
Porcellanidae	*Euceramus transversilineatus*	MCZ:IZ:30775	2011	8,243,738	2.84	82,661	735	498.0	194	1,815	550	81

(Continued)

10.3389/fmars.2024.1429314

TABLE 2 Continued

Higher taxonomy	Species	Voucher	Year	Reads	% reads on target	Contigs	UCEs raw	Locus length (bp)			UCEs 50%	UCEs 70%
								mean	min	max		
Axiidea												
Axiidae	Axiidae sp. 1	MCZ:IZ:150640	2016	19,780,698	1.07	138,693	957	650.3	229	4,892	664	92
	Axiidae sp. 2	MCZ:IZ:163883	2022	14,444,094	0.67	157,219	837	1,083.0	229	13,111	623	96
Astacidea												
Cambaridae	*Procambarus clarkii*	MCZ:IZ:68053	2015	8,523,920	0.86	188,529	913	819.6	276	5,449	675	98
Nephropidae	*Homarus americanus*	MCZ:IZ:162632	2019	3,711,656	11.27	55,790	918	1,672.0	323	8,079	711	96
Polychelida												
Polychelidae	*Pentacheles laevis*	MCZ:IZ:19151	2012	23,839,132	1.17	181,358	669	1,161.5	232	6,871	528	95
Caridea												
Alpheidae	*Synalpheus* sp.	MCZ:IZ:163842	2022	5,357,062	0.30	134,448	1,131	679.3	229	1,712	797	106
Palaemonidae	*Zenopontonia soror*	MCZ:IZ:163834	2022	7,638,680	1.05	98,044	1,018	1,131.9	231	4,138	768	103
Stenopodidea												
Stenopodidae	*Stenopus hispidus*	MCZ:IZ:163857	2022	14,546,840	2.11	417,365	842	890.0	186	1,933	602	89
Dendrobranchiata												
Penaeidae	*Penaeus japonicus*	MCZ:IZ:9630	1933	3,143,632	20.76	4,698	38	251.4	80	393	3	x
Sergestidae	*Robustosergia robusta*	MCZ:IZ:46338	2014	38,537,050	0.67	541,292	441	1,296.3	230	4,106	349	62
Euphausiacea												
Euphausiidae	*Euphausia pacifica*	MCZ:IZ:148541	2018	3,829,828	0.48	86,011	828	1,034.8	157	7,162	573	90
Stomatopoda												
Gonodactylidae	*Gonodactylellus* sp.	MCZ:IZ:163794	2022	25,116,804	0.76	311,979	906	1,052.6	230	5,658	658	96
Isopoda												
Armadillidiidae	*Armadillidium vulgare*	MCZ:IZ:28779	2007	1,755,378	8.17	18,254	204	293.4	80	2,604	31	6
Idoteidae	*Idotea balthica*	MCZ:IZ:150668	2018	7,471,644	0.69	154,544	799	1,175.0	235	10,191	612	97
Amphipoda												
Hyalellidae	*Hyalella azteca*	MCZ:IZ:78322	1969	3,291,524	9.15	2,767	123	276.4	80	1,039	3	1

(Continued)

10.3389/fmars.2024.1429314

TABLE 2 Continued

Higher taxonomy	Species	Voucher	Year	Reads	% reads on target	Contigs	UCEs raw	Locus length (bp)			UCEs 50%	UCEs 70%
								mean	min	max		
Amphipoda												
Maeridae	Maeridae sp.	MCZ:IZ:163784	2022	16,162,444	0.44	278,164	820	986.1	140	2,381	571	89
Cumacea												
	Cumacea sp.	MCZ:IZ:742248	2015	12,128,034	0.01	215,981	454	927.6	83	2,948	285	48
Lophogastrida												
Gnathophausiidae	*Gnathophausia zoea*	MCZ:IZ:46341	2014	4,117,104	1.70	41,250	500	324.0	80	911	348	51
Leptostraca												
Nebaliidae	*Nebalia* sp.	MCZ:IZ:126457	2004	2,658,028	0.32	5,896	72	278.2	79	586	14	2
Anostraca												
Artemiidae	*Artemia franciscana*	MCZ:IZ:58866	2001	6,014,170	4.18	32,021	196	283.9	79	487	111	27
mean fresh				**19,390,527**	**1.75**	**307,115**	**762**	**1,040.7**	**212**	**4,926**	**568**	**84**
mean total				**15,089,769**	**3.89**	**227,094**	**632**	**828.8**	**183**	**4,081**	**454**	**69**

"x": not included in the final matrix.
Mean values for fresh samples, and across all samples at the end of the table are highlighted in bold.

10.3389/fmars.2024.1429314

Unmapped reads were removed from the alignment files using the view function in SAMtools (Li et al., 2009), and the cleaned alignments were converted to BED format, sorted by position along scaffolds, and proximate contigs were merged using BEDTools (Quinlan and Hall, 2010). Finally, phyluce_probe_strip_masked_loci_from_set in PHYLUCE was used to filter out putatively conserved loci that are repetitive regions, by removing all contigs shorter than 80 bp and where more than 25% of the base genome were masked.

Based on these pairwise alignment files, an SQLite database was created to query conserved loci shared across several taxa. From this database, we identified those loci shared between the base genome and six out of seven exemplar genomes, and extracted sequences corresponding to these loci from the base genome, buffered to 160 bp, with phyluce_probe_get_genome_sequences_from_bed. For each of these sequences, two 120-bp probes with 40 bp overlap were designed to achieve 3X tiling density at the center of the conserved locus. Potentially problematic probes with more than 25% masked bases, below 30% or above 70% GC content, as well as potential duplicate probes with more than 50% coverage and identity were subsequently removed, to create a temporary probe set.

To design the final probe set, the temporary probes were aligned back to all exemplar genomes, now also including the outgroup *Hyalella azteca*, with a minimum identity of 50%. Sequences of 180 bp length were extracted from the targeted conserved loci in all taxa and written to FASTA files. Another SQLite database with the matches of the temporary probes to conserved loci across all taxa was created and used to identify loci that were recovered by a temporary probe in at least seven out of the nine taxa (7 exemplar, 1 outgroup, 1 base genome). For each of these loci, two 120-bp probes with 3X tiling density were designed from all taxa, filtered and duplicates removed as described above. *In-silico* tests of the UCE probe set were performed by assessing locus recovery across a range of decapod and non-decapod crustacean genomes, using phyluce_assembly_match_contigs_to_probes after aligning the probe set to these genomes (see Table 1).

The concatenated probe set file was sent to Arbor BioSciences, where final tests of the design were performed before synthesizing the probes. Each probe was BLASTed against the base genome, and hybridization was simulated under standard myBaits® (Arbor BioSciences, MI, USA) conditions, to identify and remove non-specific probes, as well as probes targeting over-represented regions.

2.3 DNA extraction, library preparation and UCE sequence capture

Genomic DNA was extracted from muscle tissue dissected from the pleon or one to several walking legs in the case of large-bodied specimens, from an entire set of legs, or from the whole body in the case of small-bodied specimens (e.g., Peracarida, Branchiopoda). For fresh specimens (collected at most 20 years ago, preserved in ca. 95% EtOH, and preserved at -20 °C) we used the Qiagen DNeasy Blood and Tissue kit following the manufacturer's protocol, with final elution between 100 and 200 µL in ddH_2O, depending on the amount of starting material. For older museum specimens (collected more than 10 years ago, preserved in 70–80% EtOH and stored at room temperature), we followed the protocol of Tin et al. (2014) for DNA extraction from degraded historical specimens using silica-based magnetic beads, with some in-lab modifications (Derkarabetian et al., 2019), and a final elution volume between 20 and 70 µL in ddH_2O. These samples are below referred to as "historical" samples. All extractions were quantified on a Qubit 2.0 fluorometer using a dsDNA High Sensitivity kit (Life Technologies, Inc.).

Libraries were prepared using the KAPA HyperPlus kit, following the manufacturer's protocol with some in-lab modifications (in parts described in Derkarabetian et al., 2019; Moles and Giribet, 2021), particularly for the historical samples. We used up to 250 ng of DNA as input material; however, input from historical samples was usually much lower (down to 4 ng). Fresh samples, as well as more recently collected historical samples, were enzymatically fragmented to a target length of 500–700 bp, using 5 µL KAPA Fragmentation Enzyme, 2.5 µL KAPA Fragmentation Buffer (10X) and 17.5 µL DNA sample for a final volume of 25 µL, with incubation times between 3 and 8 min at 37°C. Fragmentation times for samples of different age and DNA content were optimized by visualizing fragmentation results on an Agilent 2200 TapeStation. Older historical samples did not require fragmentation as they were naturally degraded, and 25 µL of the eluted DNA went directly into end-repair and A-tailing. End-repair and A-tailing was conducted using the KAPA HyperPlus enzyme mix for fresh, enzymatically fragmented samples, and KAPA HyperPrep enzyme mix for historical, naturally fragmented samples, with 30 min incubation at 65°C. This step was immediately followed by adapter ligation, using 10 µM universal iTru stubs and 45 min incubation at 20°C for fresh, high-input samples, and 5 µM stubs and up to 60 min incubation at 20°C for historical and low-input samples. A post-ligation cleanup was carried out using freshly prepared Serapure SpeedBeads (Rohland and Reich, 2012) with 0.8X beads for fresh, and up to 3X beads for old and low-input samples. Fifteen µL of ligated libraries were used in library amplification, with 25 µL 2X KAPA HiFi HotStart ReadyMix, 5 µL individual i5/i7 dual indexing adaptors (Glenn et al., 2019), and the following thermal protocol: 45 s at 98°C, 10–18 cycles of 15 s at 98°C, 30 s at 60°C, 60 s at 72°C (number of cycles adjusted to Qubit measures of post-ligation DNA concentration), and 5 min at 72°C final extension. Amplified libraries were purified with SpeedBeads (1X for high-, 3X for low-input samples), quantified, and pooled into equimolar batches of eight samples with 250 ng DNA per sample. If necessary, pools were speed-vacuumed to a final volume of 14 µL.

Hybridization followed the myBaits® Hybridization Capture for Targeted NGS manual v 5.01 with the following modifications: Hybridization time for pools of fresh samples was 24 h at 60°C, for pools of historical and low-input samples we used a touchdown-protocol with 4 h at 62°C, 16 h at 60°C and 4 h at 55°C. These settings decrease hybridization specificity, but increase hybridization yield, in particular for degraded samples. Fifteen µL of hybridized pools were amplified for 14–18 cycles using the same thermal protocol as described above, purified with

AMPure beads (1.8X for pools of high-, 3X for pools of low-input samples), quantified on a Qubit 2.0, and size estimated on an Agilent TapeStation 2200. A final 1X bead cleanup was performed on pools where adapter-dimers were present. Amplified, hybridized pools were pooled in equimolar amounts and sequenced on an Illumina NovaSeq platform (paired-end, 150 bp) at the Bauer Core Facility, Faculty of Arts and Sciences, Harvard University.

2.4 Bioinformatics and phylogenetic analyses

Raw Illumina reads for the Malacostraca dataset were demultiplexed and processed using PHYLUCE version 1.7.2 following the workflow in the online tutorial. Adapters and low-quality bases were removed with illumiprocessor (Faircloth, 2013), which implements trimmomatic (Bolger et al., 2014). Contigs were assembled with SPAdes version 3.15.5 (Prjibelski et al., 2020) using the "–careful" option to reduce the number of mismatches and indels. Probes were matched to the assembled contigs with phyluce_assembly_match_contigs_to_probes, with a 65% threshold value for minimum locus coverage and identity. UCE sequences from all taxa were extracted to individual FASTA files per locus, including incomplete loci that were recovered only in a subset of the taxa. At this step, we also included contigs from the 22 genomes used for probe set design and *in-silico* tests, "harvested" with phyluce_probe_slice_sequence_from_genomes (see Table 1 for UCE recovery summary statistics for these samples). Extracted sequences were aligned with MAFFT (Katoh and Standley, 2013), and alignments were trimmed with GBlocks (Castresana, 2000; Talavera and Castresana, 2007), using very conservative settings, i.e. –b1 0.5 –b2 0.85 –b3 4 –b4 8, suitable for phylogenetic analyses on high taxonomic levels. We built >50% and >70% occupancy matrices, meaning that a UCE was included if present at least in 50% and 70% of taxa, respectively. In order to evaluate the effect of slower evolving UCEs on the resolution of deeper nodes, we additionally created a matrix containing the 25% most conserved UCEs (224 loci) by ordering the alignments of the 50% occupancy matrix by pairwise identity and selecting the 25% with the highest identity scores. These matrices were prepared in Geneious Prime version 2023.0.1 (Kearse et al., 2012). A further cleaning step was carried out with CIAlign (Tumescheit et al., 2022), to crop long gaps in sequence ends (threshold –crop_ends_mingap_perc 0.02) and to remove paralogous and outlier sequences (threshold –remove_diver gent_minperc 0.65). All alignments with historical samples were additionally inspected manually in Geneious Prime, further removing non-orthologous sequences and potential contaminations.

Phylogenies for the Malacostraca dataset were estimated using the concatenated >50% and >70% occupancy matrices, as well as the 25% conserved loci matrix in IQ-TREE version 2.2.0 (Minh et al., 2020a), with model selection using ModelFinder (Kalyaanamoorthy et al., 2017) and an ultrafast bootstrap (Hoang et al., 2018) with 1500 replicates. We ran IQ-TREE on partitioned matrices, using the implemented terrace aware approach (Chernomor et al., 2016) and PartitionFinder (Lanfear et al., 2012), and calculated gene- and site-concordance factors (gCF and sCF; Minh et al., 2020b; Mo et al., 2023) as additional measures of nodal support. The resulting consensus trees were visualized with iTOL version 6.7.4 (Letunic and Bork, 2021), and edited in Inkscape version 1.2.

Assembly, UCE extraction and alignment for the *Eumunida* and *Aratus* datasets (Supplementary Tables S1, S2) followed the same pipeline as above. We used less conservative trimming settings for GBlocks (–b1 0.5 –b2 0.5 –b3 6 –b4 6 for the *Eumunida* dataset, –b1 0.5 –b2 0.5 –b3 10 –b4 4 for the *Aratus* dataset, respectively), but a slightly higher threshold for outlier removal with CIAlign (–remove_divergent_minperc 0.75), reflecting the shallower taxonomic level of these datasets. We built 50% occupancy matrices for downstream analysis of both datasets. In addition to assembly and UCE recovery statistics for the *Eumunida* and *Aratus* datasets, we assessed recovery of genetic variation on species- and population-level via "smilograms" using the PHYLUCE function phyluce_align_get_smilogram_from_alignments on both datasets. "Smilograms" visualize the frequency of base variations across UCE loci in relation to the distance from the alignment center, usually showing increasing variability in the flanking regions compared to the UCE core. Furthermore, we reconstructed a phylogeny for the *Eumunida* dataset using IQ-TREE as described above. To analyze the *Aratus* dataset, we called single-nucleotide polymorphisms (SNPs) from the 50% matrix using SNP-sites version 2.5.1 (Page et al., 2016), and randomly selected one SNP per UCE-locus using custom scripts. We assessed population structure by performing a discriminant analysis of principal components (DAPC; Jombart et al., 2010) with adegenet version 2.1.10 (Jombart and Ahmed, 2011) and estimated population differentiation (pairwise and population-specific F_{ST} values using hierfstat version 0.5 (Goudet and Jombart, 2022).

3 Results

3.1 UCE recovery and probe set efficacy

The final probe set after filtering and final testing included 20,304 probes targeting 1,384 loci. For the Malacostraca dataset, trimmed Illumina reads of the *in-vitro* samples were assembled to a mean number of 227,094 contigs per sample (range 1,982–1,108,273). Mean raw UCE locus recovery per sample was 632 across all samples (range 5–1,166), with the oldest sample in the dataset, *Aratus pisonii*, collected in 1865, recovering the lowest number of loci. When considering only fresh samples (collection date 2012 or later), mean raw UCE locus recovery was 785 (range 243–1166). Mean locus length across all *in-vitro* Malacostraca samples was 829 bp (range of mean per sample 213–1,627 bp), again with the oldest sample having the shortest mean UCE length (see Table 2 for detailed assembly and UCE extraction statistics of the *in-vitro* samples). Across malacostracan orders, locus recovery from fresh and *in-silico* samples was generally highest within Decapoda. Still, the probe set recovered > 800 loci from Euphausiacea and Stomatopoda, 454–1015 loci from various Peracarida, and even 381 and 452 loci from the non-malacostracan Copepoda (*Eurytemora affinis*) and Branchiopoda (*Artemia franciscana*), respectively, which

were included as outgroups (Figure 1; Tables 1, 2). The trimmed and revised 50% occupancy matrix of the Malacostraca dataset contained 897 UCE loci with a mean length of 230 ± 8 bp per locus. The mean number of loci per sample in this matrix was 527 (range 3–863, Tables 1, 2). The concatenated alignment had a length of 206,250 bp and contained 100,102 informative sites, with a mean number of 112 informative sites per locus. The 70% occupancy matrix of the Malacostraca dataset contained 110 UCE loci with a mean length of 268 ± 30 bp per locus. The mean number of loci per sample in this matrix was 77 (range 1–109, Tables 1, 2). The concatenated alignment had a length of 29,518 bp and contained 14,651 informative sites, with a mean number of 133 informative sites per locus.

For the *Eumunida* dataset, SPAdes assembly of the trimmed Illumina reads resulted in a mean number of 124,439 contigs (range 3,014–745,615). Mean raw UCE locus recovery was 685 across all samples (range 34–1,115), of which on average 600 loci were retained in the final 50% occupancy matrix (range 20–941). Mean locus length across all samples was 581 bp (range of mean per sample 190–1,339 bp), again with the oldest sample having the shortest mean locus length (Supplementary Table S1).

Lastly, the 30 samples in the *Aratus* dataset yielded mean of 828,724 assembled contigs from the trimmed Illumina reads (range 6,259–1,671,386). Mean raw UCE locus recovery was 654 (range 21–1,017), of which on average 530 loci were retained in the final 50% occupancy matrix (range 10–828). Mean UCE locus length per sample was 1,441 bp (range 213–1,622 bp). When considering only the fresh samples in this dataset (all collected in 2021), mean raw and final locus recovery was 941 and 530 loci, respectively. See Supplementary Table S2 for detailed assembly and UCE extraction summary statistics for this dataset.

Across all three datasets, UCE locus recovery and mean locus length clearly decreased with increasing sample age (Figure 2). Still, the probe set recovered 5–26 loci from the three oldest specimens (*Aratus pisonii*, MCZ: IZ:6194 [two specimens], and MCZ: IZ:6197 [1 specimen], collected 164 and 158 years ago, respectively), of which 3–15 loci were retained in the final matrices after trimming and manual inspection. Mean UCE lengths for these oldest samples were likewise among the lowest across all samples, ranging between 213 and 262 bp (compare Table 2; Supplementary Tables S1, S2). At the same time, UCE recovery and length showed considerable variation across the more recent historical, as well as the fresh specimens, reflecting differences in specimen preservation and storage (see Discussion for details).

Further exploration of the *Eumunida* and *Aratus* datasets indicated that the targeted UCE loci are also informative at species and population levels. Sequence variation, as visualized by "smilograms", generally increased with distance from the UCE core region, showing a

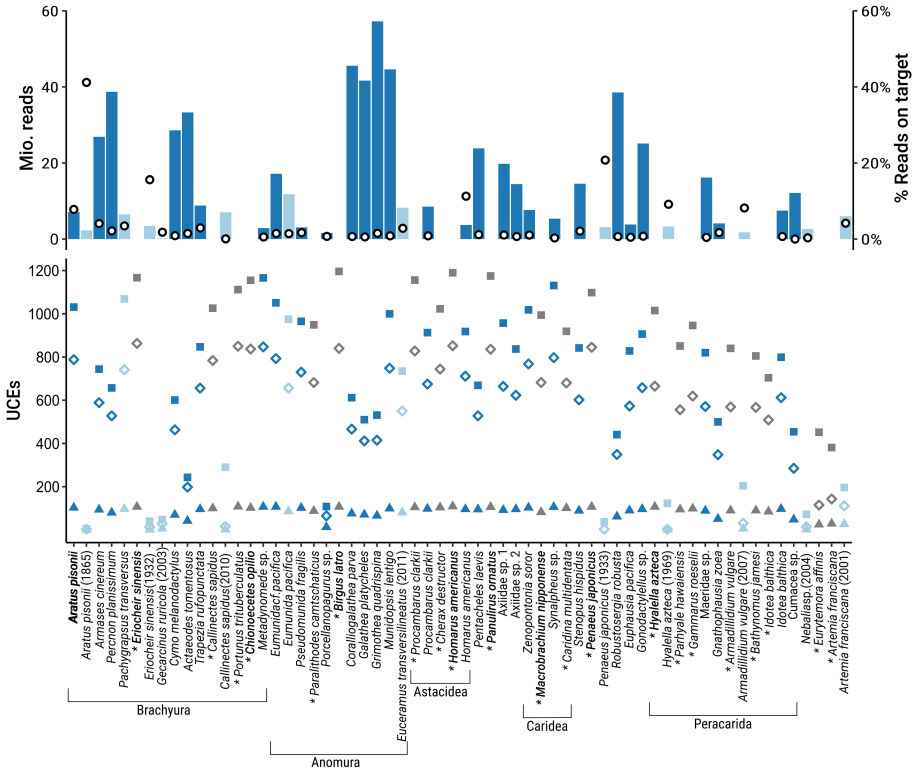

FIGURE 1
Reads and UCE recovery by species in the Malacostraca dataset. Top: number of raw illumina reads (bars) and percentage of on-target reads (open circles). Bottom: number of raw UCEs (squares), UCEs in the 50% occupancy matrix (open diamonds), and UCEs in the 70% occupancy matrix (triangles). Dark blue: fresh samples, light blue: historical samples (collected before 2013), grey: *in-silico* samples. Species used for probe set design are in bold.

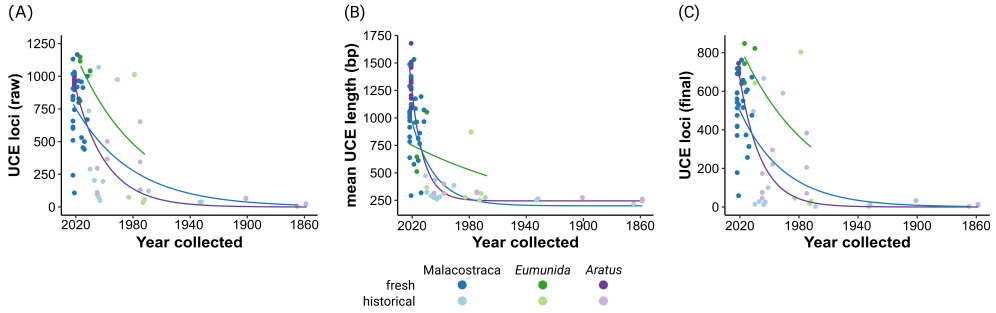

FIGURE 2
Relationship between sample age and UCE locus recovery and mean UCE locus length across the three datasets used in this study. **(A)** Number of raw (unaligned) UCE loci recovered by PHYLUCE. **(B)** Mean raw UCE length per sample. **(C)** Number of loci in final 50% occupancy matrices. Exponential trend lines fitted using nonlinear least squares regression. 'Historical' refers to samples collected before 2013. Note the different scales on the y-axis.

bimodal/W-shaped distribution for the *Eumunida* subset (Figure 3A) and a more typical, U-shaped distribution for the *Aratus* dataset (Figure 3B). The trimmed and revised 50% occupancy matrix of Western Indian Ocean *Eumunida* spp. (six species, ten samples, see Supplementary Table S1) included 24,983 informative sites at a total length of 785,344 bp across 1,045 loci. The phylogeny derived from the *Eumunida* dataset showed congruent relationships among the six species included, with full support for almost all nodes, and the historical samples placed at their expected positions (Figure 4). We extracted 680 SNPs from the 50% occupancy matrix of the *Aratus* dataset (i.e., one SNP randomly sampled from each UCE locus containing SNPs). The four oldest samples in the dataset (collected in 1859 and 1901, respectively; see Supplementary Table S2) were removed before further analysis due to high amounts of missing data. The DAPC analysis (no. of retained PCAs = 8, no. of retained discriminant functions = 5) revealed only little structure in the genetic data, with five of the six sampling populations clustering closely together (Figure 5). The proportion of specimens assigned to their actual sampling population based on posterior probabilities estimated by DACP was 0.77 over the entire dataset, ranging between 0.6 and 1 for the six populations (compare Supplementary Figure S3). In line with the DAPC results, estimates of population differentiation were low overall (overall F_{ST} = 0.0176) as well as between populations, with just one population (Highland Beach, 3 specimens collected in 1975) showing signs of weak differentiation (pairwise F_{ST} > 0.05; Supplementary Table S3).

3.2 UCE phylogeny of the Malacostraca

Maximum-likelihood analyses of the different matrices (50% and 70% occupancy thresholds, 25% most conserved loci) recovered fully resolved phylogenies of the included taxa (Figure 5; Supplementary Figures S1, S2). All matrices recovered Decapoda as monophyletic, with Euphausiacea, represented by *Euphausia pacifica*, as their sister group (forming the clade Eucarida), and Stomatopoda, represented by *Gonodactylellus* sp., as the sister group of Eucarida. The relationships within Decapoda were largely congruent between the different matrices: Dendrobranchiata were recovered as the sister group to all other decapod infraorders (the clade Pleocyemata). Pleocyemata were divided in two monophyletic groups, i.e. Caridea + Stenopodidea, and the 'reptant' groups (Achelata + Anomura + Astacidea + Axiidea + Brachyura + Polychelida). Axiidea clustered with a clade Astacidea + Achelata + Polychelida, and the two remaining groups, Anomura and

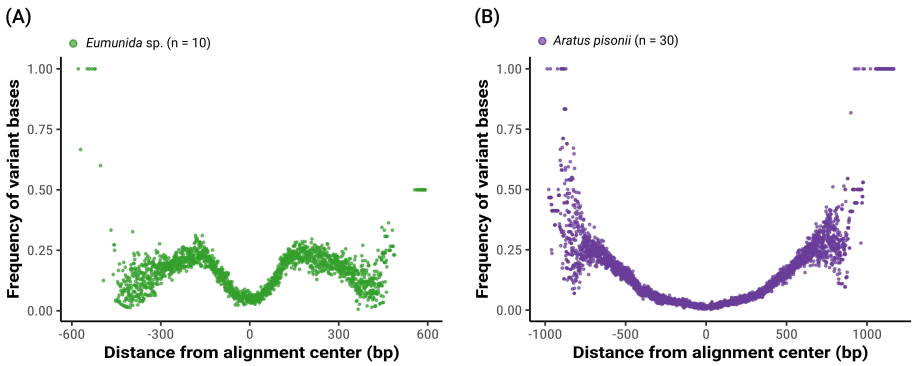

FIGURE 3
Species- and population-level genetic variation captured by the UCE probe set, shown as the frequency of variant bases in relation to their distance from the center of alignment. Variation data extracted from trimmed 50% occupancy matrices. **(A)** "Smilogram" for a dataset of six *Eumunida* species (10 specimens) from the Western Indian Ocean. **(B)** "Smilogram" for a dataset of 30 *Aratus pisonii* specimens collected in southeastern Florida.

10.3389/fmars.2024.1429314

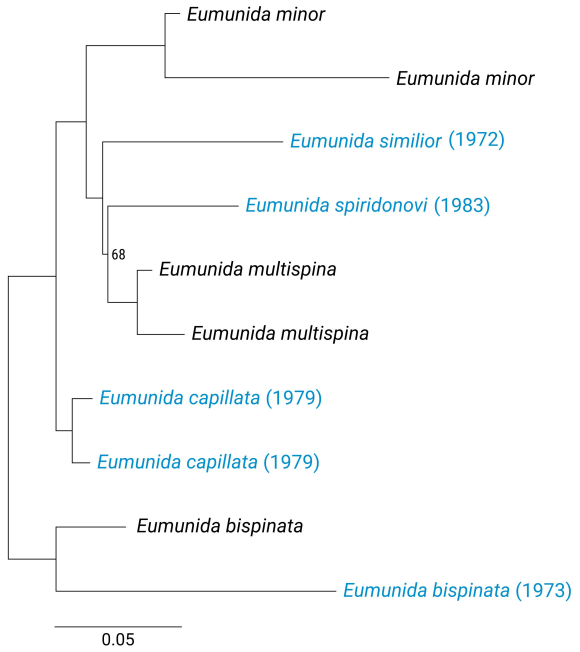

FIGURE 4
UCE-derived phylogenies (maximum likelihood) for six *Eumunida* species from the Western Indian Ocean, based on a 50% occupancy matrix of a 10-specimen dataset. Historical samples (collection year in parentheses) are highlighted in blue, and bootstrap values are given for nodes with support <100%.

Brachyura, formed a second monophyletic group of reptant decapods. Within Brachyura, all matrices supported an early diverging position of Dromioidea (*Metadynomede* sp.) with respect to the other groups, and also recovered the two major clades within the Eubrachyura, i.e., Heterotremata (*Actaeodes*, *Callinectes*, *Chionoecetes*, *Cymo*, *Portunus*, and *Trapezia*) and Thoracotremata (*Aratus*, *Armases*, *Eriocheir*, *Gecarcinus*, *Pachygrapsus*, and *Percnon*) (Figure 4; Supplementary Figures S1, S2). Incongruencies between the results based on the three data sets within Decapoda relate to the position of historical samples (see below). Relationships towards the base of the tree (i.e. outside Decapoda) were less stable, with varying topologies between data matrices. Peracarida is not monophyletic, irrespective of the analyzed data matrix, however, Isopoda and Amphipoda were each recovered as monophyletic in all topologies, and Lophogastrida (represented by *Gnathophausia zoea*) was always recovered as sister group to a clade containing Amphipoda + Stomatopoda + Eucarida. Leptostraca (*Nebalia* sp.) was recovered as sister group to Malacostraca only in the 50% occupancy matrix (Figure 6), while it clustered with Euphausiacea in the 70% occupancy matrix and in the one with the 25% most conserved UCEs (Supplementary Figures S1, S2). Likewise, Cumacea was recovered either as sister group to Isopoda (50% occupancy matrix, Figure 6), as sister group to all other Malacostraca (70% occupancy matrix, Supplementary Figure S2), or as sister group to all Malacostraca excluding Isopoda (25% most conserved UCEs matrix, Supplementary Figure S1).

The instability at the base of the malacostracan UCE phylogeny was also reflected by lower support for several of the deeper nodes in all topologies. The nodes grouping the major clades of the Peracarida, as well as Peradarida and Decapoda received low bootstrap (bs) support in the 50% (bs <80), and particularly the 70% occupancy matrix (bs <40), as well as gene concordance factors (gCF) mostly < 20. Also within Decapoda, gCF values were low for several of the deeper nodes (e.g., 3.19 in the 50% occupancy matrix for the node grouping Dendrobranchiata and Pleocyemata, and 6.92 for the node grouping Brachyura + Anomura and the other

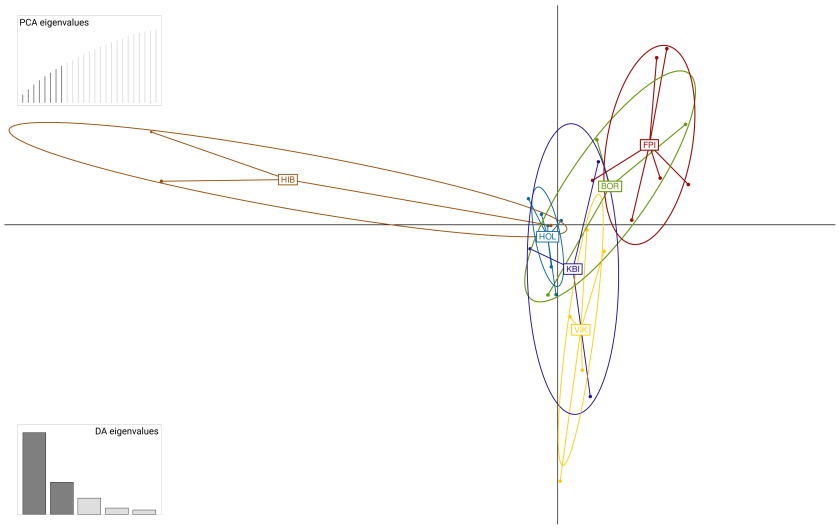

FIGURE 5
Discriminant analysis of principal components (DAPC) for 30 specimens of *Aratus pisonii*, sampled from six populations in southeastern Florida, based on a matrix of 680 SNPs. Population codes: BRO, Boca Raton; FPI, Fort Pierce; HIB, Highland Beach; HOL, Hollywood; KBI, Key Biscayne; VIK, Virginia Key.

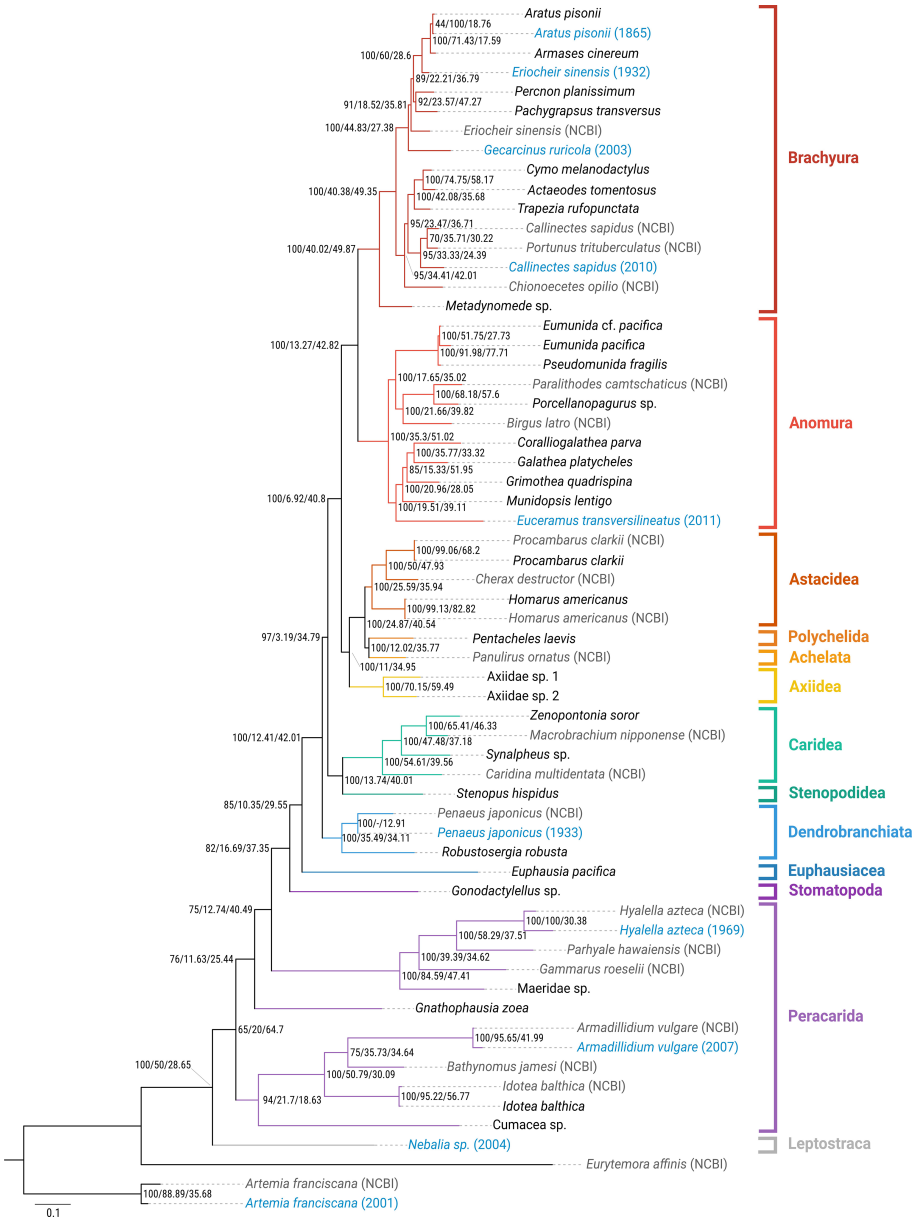

FIGURE 6
Phylogenetic hypothesis (maximum likelihood) for Malacostraca, based on a 50% occupancy matrix of 897 UCE loci. Historical samples are indicated in blue, with collection years in parentheses. *In-silico* samples (NCBI) are indicated in gray. Bootstrap values and concordance factors are shown for all nodes (bs/gCF/sCF).

'reptant' decapods; Figure 6), indicating that only few individual gene trees supported these nodes, despite high bootstrap support. Overall, all phylogenies showed a tendency towards decreasing nodal support (bs, and particularly gCF) in deeper nodes, and for those clades including historical samples.

The historical samples included in the dataset were largely placed at their expected positions in the phylogeny, despite a strong decrease of the number of retained loci with sample age (compare Table 2; Figure 6; Supplementary Figures S1, S2). The historical *Aratus pisonii*, *Armadillidium vulgare*, *Artemia franciscana*, *Hyalella azteca* and *Penaeus japonicus* samples (only included in the 50% occupancy matrix) clustered with their conspecific fresh or *in-silico* samples, respectively. In the 70% occupancy matrix the historical *Callinectes sapidus* and *Eriocheir sinensis* samples clustered with their conspecific *in-silico* samples, while the almost 20 year-old *Nebalia* sample, the only representative of Leptostraca in our analysis, was recovered as the sister group to all other Malacostraca only in the 50% occupancy matrix, but clustered with *Euphausia pacifica* in the 70% occupancy matrix and with the 25% most conserved UCEs.

4 Discussion

In this study, we present a newly designed UCE probe set initially tailored towards Decapoda, but resulting in a much broader applicability across Malacostraca. We further illustrate its

applicability and effectiveness at different evolutionary scales, down to the level of populations. Over the past few years, UCEs have emerged as valuable markers for phylogenomic reconstruction and population studies due to their ability to provide large numbers of homologous loci, and to make use of fragmented DNA, as typically found in historical museum specimens. While UCE probe sets have been developed for many major taxa (e.g., Faircloth et al., 2012, 2013; Smith et al., 2014; Starrett et al., 2017; Quattrini et al., 2018; Moles and Giribet, 2021; Goulding et al., 2023; Sato et al., 2024a; van der Sprong et al., 2024), no probe set was available for any crustacean. Our research addresses this gap by introducing a specialized UCE probe set for investigating the intricate diversity within Malacostraca, with a specific emphasis on the diverse order Decapoda. It is important to note here that another study using a similar approach, anchored hybrid enrichment (AHE) has been available for a while (Wolfe et al., 2019), but such approach does not allow the easy incremental addition of samples since AHE was designed from the onset to be a proprietary technology (Lemmon et al., 2012) while UCEs operated under an open source paradigm (Faircloth et al., 2012).

We identified almost 1,400 highly conserved genomic regions between taxa of the hyperdiverse Malacostraca, and designed about 20,000 probes to target these UCEs. We tested the efficacy of this new genomic resource on three datasets representing various levels of phylogenetic depth. The mean number of UCE loci recovered from our main Malacostraca dataset of 31 fresh, 10 historical and 21 genome-derived *in-silico* samples (743 raw and 621 final loci in the 50% occupancy matrix, respectively), as well as mean locus length (742 bp in the raw, and 230 bp in the 50% occupancy matrix after GBlocks trimming, respectively), and the proportion of informative sites in the final alignment (48.5%) were comparable to similar-sized UCE probe sets for other invertebrate groups (e.g., Starrett et al., 2017; Quattrini et al., 2018; Moles and Giribet, 2021). Locus recovery of our probe set was also comparable to the Wolfe et al. (2019) AHE kit for Decapoda (max. 410 loci in a 60% matrix of a 94 species-dataset), while requiring a much smaller number of probes for this performance (about 20,000 *vs.* >50,000). It should be noted that we achieved these recovery statistics with a comparatively high proportion of historical samples in the dataset. When including fresh and in-silico samples only, locus recovery increased to a mean of 853 loci per sample in the raw, and 621 loci per sample in the final 50% occupancy matrix.

All the datasets analyzed in this study demonstrated the capability of the new probe set to capture sequence data from historical specimens, regularly highlighted as a key asset of UCEs in studies targeting various invertebrate and vertebrate taxa. We were able to recover up to 25 loci from specimens collected in 1859 (i.e., 164 years old), which are to our knowledge among the oldest used in targeted UCE sequencing studies (compare Derkarabetian et al., 2019; González-Delgado et al., 2024), and up to 68 loci from specimens collected in 1901 (see Supplementary Tables S1, S2). While the number of loci from historical specimens dropped considerably during alignment trimming and revisions, the retained loci were still informative enough to put most historical specimens to their expected phylogenetic position (Figure 6). At the same time, we observed very low locus recovery in a few samples collected less than 20 years ago (e.g. *Callinectes sapidus*, MCZ: IZ:23424, coll. 2010: 16 loci in 50% occupancy matrix, or *Porcellanopagurus* sp., MNHN-IU-2021-7149, coll. 2021: 65 loci in 50% occupancy matrix). A likely cause for the apparent lack of a clearer correlation between sample age and locus recovery is vastly varying collection, preservation, specimen size, and storage history among collection events of "standard" museum specimens, which are still mostly focused on preserving external morphology. Particularly in hard-bodied crustaceans like crabs, soft tissues usually used for DNA extraction may quickly degrade due to slow ethanol penetration through the exoskeleton, if it is not manually perforated (own observations). As fixation and storage history of specimens are oftentimes unknown and/or not reported in collection databases, the use of historical specimens for sequencing experiments will inevitably include the risk of selecting specimens that are unsuitable for molecular work (compare e.g., Wandeler et al., 2007; Bernstein and Ruane, 2022; González-Delgado et al., 2024).

Our data furthermore showed a notable broad-range applicability of the probe set across Decapoda, and even beyond, on Malacostraca. With the probe set design strongly focused on Decapoda, we consequently recovered the highest numbers of loci from samples within this group (49.1–62.4% of the total probe set for the in-silico samples, and 4.7–61.2% of the total probe set for fresh *in-vitro* samples in the 50% matrix), which also achieved better phylogenetic resolution and support. However, between 450 and > 1,000 loci were recovered from fresh or in-silico Euphausiacea, Stomatopoda, and several Peracarida, and still between about 200 and 450 loci from fresh and in-silico Copepoda and Branchiopoda. Capture efficiency for fresh non-decapod Malacostracan samples in the 50% matrix was 25.1%–47.4%. Thus, the probe set performed well across a vastly divergent group, spanning at least 540 million years of evolution (compare Bernot et al., 2023). In this respect, the Decapoda probe set appeared equivalent to the Arachnida probe set, spanning a similarly divergent lineage (Starrett et al., 2017), corroborating Bossert and Danforth's (2018) findings on the universal character of UCEs. Yet, denser sampling within these outgroups to Decapoda will be needed to assess the information contained in these UCEs. At the other end of the spectrum of phylogenetic depth, the genus- (*Eumunida* sp.) and within species-level (*Aratus pisonii*) datasets showed increasing sequence variability in UCE locus alignments with increasing distance from the UCE core region, as expected (compare Figure 3). UCE capture efficiency for fresh samples in the 50% matrices of these datasets was 51.7%–68.1% (*Eumunida* dataset, n=4) and 55.3%–59.8% (*Aratus* dataset, n=18), respectively. Moreover, the UCE data fully resolved the phylogenetic relationships among the Western Indian Ocean *Eumunida* species with high support. The population genetic analysis of the evolutionary shallow *Aratus* dataset showcased the presence of SNPs in hundreds of loci captured by the probe set. While the apparent lack of geographic structure might be expected from a species with planktonic larval dispersal on such a restricted geographic range, the slight genetic differentiation detected between the oldest and the more recent specimens might hint at some temporal structure in the genetic data. Despite a relatively low proportion of variable sites in the final alignments of the *Eumunida* and *Aratus* datasets (3.1% and 2.2%, respectively), our data thus indicate the potential of the probe set for e.g., biogeographic or population genomic studies on genus- and species-level datasets. Future studies with larger datasets, as well as optimized locus trimming and filtering settings towards improved

recovery of variable sites from UCE flanking regions, will further explore this potential.

The UCE-based malacostracan phylogeny demonstrated the utility of our probe set across several phylogenetic levels. Overall, the tree topologies derived from the three occupancy matrices agreed well with recent malacostracan phylogenies based on transcriptomes (Bernot et al., 2023) and mitogenomes (Höpel et al., 2022). Specifically, the focal group for probe set design, Decapoda, was recovered as monophyletic with full support by all, and most of the internal relationships within the order were congruent with Wolfe et al.'s (2019) phylogeny based on anchored hybrid enrichment (AHE) data–the only other genomic approach to crustacean phylogenetics other than transcriptomics. The only major discrepancy to previously published decapod phylogenies was the clustering of Axiidea in a clade with Astacidea, Polychelida and Achelata, instead of clustering with Anomura + Brachyura (e.g., Shen et al., 2015; Wolfe et al., 2019). However, there were some limitations regarding incongruent topologies on the deeper nodes of the Malacostraca phylogeny, most likely due to the antiquity of the group and the strong bias towards decapod taxa in both probe set design and testing, and also because taxon sampling was not optimized for non-decapod malacostracans. Further testing of this UCE set beyond Decapoda was beyond the scope of this study and remains to be further tested.

The historical samples included in the Malacostraca dataset were mostly recovered at their expected positions in the phylogenies, with single exceptions across the three matrices, e.g., *Eriocheir sinensis* (coll. 1932), and *Callinectes sapidus* (coll. 2010) not clustering with their respective conspecific *in-silico* samples in the 25% conserved loci and 50% matrices, or *Nebalia* sp. (coll. 2004) clustering with Euphausiidae in the 25% conserved loci and 70% matrices. Low DNA quantities and natural DNA degradation by biochemical processes (particularly oxidation and hydrolysis) do not only reduce locus recovery and locus lengths of historical samples (see above), but make them more prone to contamination, sequencing and assembly errors (compare McCormack et al., 2016; Derkarabetian et al., 2019). The misplacement of some historical samples may well be due to either, or a combination, of these factors. Alternatively stochastic effects of the low number and short length of recovered UCE loci may also play a role. The lower number of UCEs recovered from historical and non-decapod samples is also a potential cause for the incongruencies between tree topologies and the reduced support for many of the deeper nodes, as it reduces the number and length of single-locus trees that contain these nodes. Similarly, DNA degradation may lead to the incorporation and eventual accumulation of erroneous bases, particularly towards the edges of UCE loci, where assembly coverage is lower. While most of these erroneous bases should have been removed by the per-locus alignment trimming (see section 2.4 Bioinformatics and phylogenetic analyses), they are sometimes difficult to tell apart from "valid" mutations, leading to long branches. Finally, there is the possibility of misidentification of the GenBank *in-vitro* samples.

Regarding the deeper malacostracan phylogeny, the UCE loci recovered Leptostraca as the sister group to the remaining Malacostraca (only in the 50% occupancy matrix), as well as a clade including Stomatopoda, Euphausiacea and Decapoda (in all matrices), in line with the findings of Bernot et al. (2023) and Höpel et al. (2022). Peracarida, on the other hand, were not recovered as monophyletic. While their monophyly has been occasionally disputed (Richter and Scholtz, 2001; Poore, 2005; and references therein), morphological and multilocus phylogenies, as well as mitogenomic and phylotranscriptomic studies support a monophyletic Peracarida (Spears et al., 2005; Schwentner et al., 2018; Bernot et al., 2023; Höpel et al., 2022). A potential explanation for lacking monophyly of Peracarida in our data could be insufficient taxon sampling within the group (only one sample from each Cumacea and Lophogastrida, and no representatives of Mysida, Tanaidacea, and Thermosbaenacea), and strong taxon sampling bias towards Decapoda (particularly Anomura and Brachyura) in the Malacostraca dataset (compare Bernot et al., 2023). Furthermore, the fact that Peracarida were represented only by one amphipod genome in our probe set design might have caused a decrease in the number of loci that can resolve the deeper nodes within this group, which is almost as speciose as the Decapoda. We would like to stress, however, that the intention of this study was not to fully resolve phylogenetic relationships among and within malacostracan orders, but rather to provide a proof of concept, and a demonstration of the performance and utility of this new UCE probe set. Future analyses including more outgroup and ingroup taxa will focus on peracarid relationships to further test this clade.

Overall, our data provide strong evidence for the versatility of the UCE probe set we present in this study, mostly within the focal group of probe set design for Decapoda, but also shows potential across the highly divergent Malacostraca. They highlight the universality of the targeted probes and their ability to recover deep phylogenetic relationships, and genetic variation from taxonomically shallow datasets alike. They furthermore demonstrate the utility of the probe set to extract informative sequence data from historical museum specimens. This is particularly beneficial for studies including rare, or difficult to sample species, such as deep-sea crustaceans, as many of them will only be available as historical museum specimens. Therefore, we expect our probe set to become a valuable and affordable resource for targeted sequencing studies across multiple taxonomic levels and along varying lines of research, including biodiversity research and conservation genetics (e.g., Derkarabetian et al., 2022; Benham and Bowie, 2023). This probe set should therefore allow researchers to explore a wide range of evolutionary and population studies within one of the most diverse and economically significant marine invertebrate taxa.

Data availability statement

The datasets presented in this study can be found in online repositories. The names of the repository/repositories and accession number(s) can be found below: https://www.ncbi.nlm.nih.gov/, PRJNA988117, Harvard Dataverse, https://doi.org/10.7910/DVN/WASGMF.

Ethics statement

The manuscript presents research on animals that do not require ethical approval for their study.

Author contributions

JG: Writing – review & editing, Writing – original draft, Visualization, Methodology, Investigation, Funding acquisition, Formal analysis, Data curation, Conceptualization. PR-F: Writing – review & editing, Writing – original draft, Investigation, Funding acquisition, Formal analysis, Data curation. SD: Writing – review & editing, Methodology, Conceptualization. GG: Writing – review & editing, Supervision, Resources, Funding acquisition, Conceptualization.

Funding

The author(s) declare financial support was received for the research, authorship, and/or publication of this article. Funding for this study was provided by a Walter-Benjamin postdoctoral fellowship from the Deutsche Forschungsgemeinschaft (DFG, German Research Foundation) to JG (project number 447933028), by a Biodiversity Postdoctoral Fellowship from the Museum of Comparative Zoology, Harvard University (MCZ) to PR-F, as well as by Putnam Expedition Grants from the MCZ to JG and PR-F for collecting specimens in Florida and on Guam. Lab work and sequencing were financially supported by internal funds from the MCZ.

Acknowledgments

We thank Claire Hartmann of the Bauer Core Facility at Harvard University for her great help in troubleshooting and optimizing sequencing results. Héctor Torrado and David Combosch supported us during field work on Guam, as did Linnea and Sinikka Lennartz during field work in Florida. The historical specimens used in this study were provided in addition to the Museum of Comparative Zoology, by the Muséum national d'Histoire naturelle, the US National Museum of Natural History, the Florida Museum of Natural History, and the California Academy of Sciences, and we thank all curators who generously granted our loan and sampling requests including Laure Corbari, Paula Martin-Lefèvre, Martha Nizinski, Gustav Paulay, Christina Piotrowski, and Karen Reed. PR-F is grateful for Laure Corbari's and Paula Martin-Lefèvre's hospitality during her stays at the crustacean collection of the MNHN in Paris.

Conflict of interest

The authors declare that the research was conducted in the absence of any commercial or financial relationships that could be construed as a potential conflict of interest.

Publisher's note

Supplementary material

The Supplementary Material for this article can be found online at: https://www.frontiersin.org/articles/10.3389/fmars.2024.1429314/full#supplementary-material

SUPPLEMENTARY FIGURE 1
Phylogenetic hypothesis (maximum-likelihood) for Malacostraca, based on a partitioned analysis of the 25% most conserved loci in the 50% occupancy matrix of the Malacostraca dataset (224 UCEs, selected by average pairwise identity among samples). Historical samples are in blue (with collection years), in-silico samples "(NCBI)" are in grey. For each node, bootstrap value, gene- and site-concordance factors are given (bs/gCF/sCF).

SUPPLEMENTARY FIGURE 2
Phylogenetic hypothesis (maximum-likelihood) for Malacostraca, based on a partitioned analysis of a 70% occupancy matrix of 110 UCEs. Historical samples are in blue (with collection years), in-silico samples "(NCBI)" are in grey. For each node, bootstrap value, gene- and site-concordance factors are given (bs/gCF/sCF).

SUPPLEMENTARY FIGURE 3
Posterior probabilities of population assignment of the specimens in the *Aratus* dataset, based on DAPC results. Colors represent assignment probability from 1 (red) to 0 (white), blue crosses indicate the actual sampling population.

SUPPLEMENTARY TABLE 1
Assembly and UCE extraction summary statistics for the *Eumunida* dataset, including the number of assembled contigs, the number of raw UCE loci recovered from contigs, the length of the raw UCE loci, and the final number of UCE loci in a 50% occupancy matrix after trimming and filtering. Small letters appended to voucher numbers (a or b) denote different individuals from multi-specimen lots.

SUPPLEMENTARY TABLE 2
Assembly and UCE extraction summary statistics for the *Aratus* dataset, including sampling locality, the number of assembled contigs, the number of raw UCE loci recovered from contigs, the length of the raw UCE loci, and the final number of UCE loci in a 50% occupancy matrix after trimming and filtering. Small letters appended to voucher numbers (a to e) denote different individuals from multi-specimen lots. Specimens with an asterisk were excluded from the SNP analysis due to high amounts of missing data.

SUPPLEMENTARY TABLE 3
SNP-based pairwise FST values between six populations of *Aratus pisonii* in southeastern Florida (the *Aratus* dataset). The values in the last column (Population-specific FST) indicate whether the contribution of a specific population to the overall population differentiation is higher (population-specific FST > 0) or lower (population-specific FST < 0) than the mean contribution across all populations.

References

Ballesteros, J. A., Setton, E. V. W., Santibáñez-López, C. E., Arango, C. P., Brenneis, G., Brix, S., et al. (2021). Phylogenomic resolution of sea spider diversification through integration of multiple data classes. *Mol. Biol. Evol.* 38, 686–701. doi: 10.1093/molbev/msaa228

Bejerano, G., Pheasant, M., Makunin, I., Stephen, S., Kent, W. J., Mattick, J. S., et al. (2004). Ultraconserved elements in the human genome. *Science* 304, 1321–1325. doi: 10.1126/science.1098119

Benham, P. M., and Bowie, R. C. K. (2023). Natural history collections as a resource for conservation genomics: Understanding the past to preserve the future. *J. Hered.* 114, 367–384. doi: 10.1093/jhered/esac066

Bernot, J. P., Owen, C. L., Wolfe, J. M., Meland, K., Olesen, J., and Crandall, K. A. (2023). Major revisions in pancrustacean phylogeny and evidence of sensitivity to taxon sampling. *Mol. Biol. Evol.* 40, msad175. doi: 10.1093/molbev/msad175

Bernstein, J. M., and Ruane, S. (2022). Maximizing molecular data from low-quality fluid-preserved specimens in natural history collections. *Front. Ecol. Evol.* 10. doi: 10.3389/fevo.2022.893088

Blaimer, B. B., Lloyd, M. W., Guillory, W. X., and Brady, S. G. (2016). Sequence capture and phylogenetic utility of genomic ultraconserved elements obtained from pinned insect specimens. *PloS One* 11, e0161531. doi: 10.1371/journal.pone.0161531

Bolger, A. M., Lohse, M., and Usadel, B. (2014). Trimmomatic: a flexible trimmer for Illumina sequence data. *Bioinformatics* 30, 2114–2120. doi: 10.1093/bioinformatics/btu170

Bossert, S., and Danforth, B. N. (2018). On the universality of target-enrichment baits for phylogenomic research. *Methods Ecol. Evol.* 9, 1453–1460. doi: 10.1111/2041-210X.12988

Boyer, S. L., Dohr, S. R., Tuffield, M. S., Shu, Y., Moore, C. D., Hahn, K. M., et al. (2022). Diversity and distribution of the New Zealand endemic mite harvestman genus *Aoraki* (Arachnida, Opiliones, Cyphophthalmi, Pettalidae), with the description of two new species. *Invertebr. Syst.* 36, 372–387. doi: 10.1071/IS21044

Castresana, J. (2000). Selection of conserved blocks from multiple alignments for their use in phylogenetic analysis. *Mol. Biol. Evol.* 17, 540–552. doi: 10.1093/oxfordjournals.molbev.a026334

Chernomor, O., von Haeseler, A., and Minh, B. Q. (2016). Terrace aware data structure for phylogenomic inference from supermatrices. *Syst. Biol.* 65, 997–1008. doi: 10.1093/sysbio/syw037

Cowman, P. F., Quattrini, A. M., Bridge, T. C. L., Watkins-Colwell, G. J., Fadli, N., Grinblat, M., et al. (2020). An enhanced target-enrichment bait set for Hexacorallia provides phylogenomic resolution of the staghorn corals (Acroporidae) and close relatives. *Mol. Phylogenet. Evol.* 153, 106944. doi: 10.1016/j.ympev.2020.106944

de Miranda, G. S., Kulkarni, S. S., Tagliatela, J., Baker, C. M., Giupponi, A. P. L., Labarque, F. M., et al. (2024). The rediscovery of a relict unlocks the first global phylogeny of whip spiders (Amblypygi). *Syst. Biol.* 73, 495–505. doi: 10.1093/sysbio/syae021

Derkarabetian, S., Benavides, L. R., and Giribet, G. (2019). Sequence capture phylogenomics of historical ethanol–preserved museum specimens: Unlocking the rest of the vault. *Mol. Ecol. Resour.* 19, 1531–1544. doi: 10.1111/1755-0998.13072

Derkarabetian, S., Paquin, P., Reddell, J., and Hedin, M. (2022). Conservation genomics of federally endangered *Texella* harvester species (Arachnida, Opiliones, Phalangodidae) from cave and karst habitats of central Texas. *Conserv. Genet.* 23, 401–416. doi: 10.1007/s10592-022-01427-9

Derkarabetian, S., Starrett, J., Tsurusaki, N., Ubick, D., Castillo, S., and Hedin, M. (2018). A stable phylogenomic classification of Travunioidea (Arachnida, Opiliones, Laniatores) based on sequence capture of ultraconserved elements. *ZooKeys* 760, 1–36. doi: 10.3897/zookeys.760.24937

Faircloth, B. C. (2013). *Illumiprocessor: a trimmomatic wrapper for parallel adapter and quality trimming*. Available at: https://github.com/faircloth-lab/illumiprocessor. doi: 10.6079/J9ILL.

Faircloth, B. C. (2016). PHYLUCE is a software package for the analysis of conserved genomic loci. *Bioinformatics* 32, 786–788. doi: 10.1093/bioinformatics/btv646

Faircloth, B. C. (2017). Identifying conserved genomic elements and designing universal bait sets to enrich them. *Methods Ecol. Evol.* 8, 1103–1112. doi: 10.1111/2041-210X.12754

Faircloth, B. C., McCormack, J. E., Crawford, N. G., Harvey, M. G., Brumfield, R. T., and Glenn, T. C. (2012). Ultraconserved elements anchor thousands of genetic markers spanning multiple evolutionary timescales. *Syst. Biol.* 61, 717–726. doi: 10.1093/sysbio/sys004

Faircloth, B. C., Sorenson, L., Santini, F., and Alfaro, M. E. (2013). A phylogenomic perspective on the radiation of ray-finned fishes based upon targeted sequencing of ultraconserved elements (UCEs). *PloS One* 8, e65923. doi: 10.1371/journal.pone.0065923

Glenn, T. C., Nilsen, R. A., Kieran, T. J., Sanders, J. G., Bayona-Vásquez, N. J., Finger, J. W., et al. (2019). Adapterama I: universal stubs and primers for 384 unique dual-indexed or 147,456 combinatorially-indexed Illumina libraries (iTru & iNext). *PeerJ* 7, e7755. doi: 10.7717/peerj.7755

Glon, H., Quattrini, A., Rodríguez, E., Titus, B. M., and Daly, M. (2021). Comparison of sequence-capture and ddRAD approaches in resolving species and populations in hexacorallian anthozoans. *Mol. Phylogenet. Evol.* 163, 107233. doi: 10.1016/j.ympev.2021.107233

Gonzalez, B., Martínez, A., Institute for Water Research and Italian National Research Council, , Olesen, J., Truskey, S. B., et al. (2020). Anchialine biodiversity in the Turks and Caicos Islands: New discoveries and current faunal composition. *Int. J. Speleol.* 49, 71–86. doi: 10.5038/1827-806X.49.2.2316

González-Delgado, S., Rodríguez-Flores, P. C., and Giribet, G. (2024). Testing ultraconserved elements (UCEs) for phylogenetic inference across bivalves (Mollusca: Bivalvia). *Mol. Phylogenet. Evol.* 198, 108129. doi: 10.1016/j.ympev.2024.108129

Goudet, J., and Jombart, T. (2022). hierfstat: estimation and tests of hierarchical F-statistics. Available online at: https://CRAN.R-project.org/package=hierfstat. (Accessed August 15, 2024).

Goulding, T. C., Strong, E. E., and Quattrini, A. M. (2023). Target-capture probes for phylogenomics of the Caenogastropoda. *Mol. Ecol. Resour.* 23, 1372–1388. doi: 10.1111/1755-0998.13793

Grüning, B., Dale, R., Sjödin, A., Chapman, B. A., Rowe, J., Tomkins-Tinch, C. H., et al. (2018). Bioconda: sustainable and comprehensive software distribution for the life sciences. *Nat. Methods* 15, 475–476. doi: 10.1038/s41592-018-0046-7

Hedin, M., Derkarabetian, S., Alfaro, A., Ramírez, M. J., and Bond, J. E. (2019). Phylogenomic analysis and revised classification of atypoid mygalomorph spiders (Araneae, Mygalomorphae), with notes on arachnid ultraconserved element loci. *PeerJ* 7, e6864. doi: 10.7717/peerj.6864

Hedin, M., Foldi, S., and Rajah-Boyer, B. (2020). Evolutionary divergences mirror Pleistocene paleodrainages in a rapidly-evolving complex of oasis-dwelling jumping spiders (Salticidae, *Habronattus tarsalis*). *Mol. Phylogenet. Evol.* 144, 106696. doi: 10.1016/j.ympev.2019.106696

Hoang, D. T., Chernomor, O., von Haeseler, A., Minh, B. Q., and Vinh, L. S. (2018). Ufboot2: improving the ultrafast bootstrap approximation. *Mol. Biol. Evol.* 35, 518–522. doi: 10.1093/molbev/msx281

Höpel, C. G., Yeo, D., Grams, M., Meier, R., and Richter, S. (2022). Mitogenomics supports the monophyly of Mysidacea and Peracarida (Malacostraca). *Zool. Scr.* 51, 603–613. doi: 10.1111/zsc.12554

Hou, Z., Sket, B., and Li, S. (2014). Phylogenetic analyses of Gammaridae crustacean reveal different diversification patterns among sister lineages in the Tethyan region. *Cladistics* 30, 352–365. doi: 10.1111/cla.12055

Huang, W., Li, L., Myers, J. R., and Marth, G. T. (2012). ART: a next-generation sequencing read simulator. *Bioinformatics* 28, 593–594. doi: 10.1093/bioinformatics/btr708

Jombart, T., and Ahmed, I. (2011). *adegenet 1.3-1* : new tools for the analysis of genome-wide SNP data. *Bioinformatics* 27, 3070–3071. doi: 10.1093/bioinformatics/btr521

Jombart, T., Devillard, S., and Balloux, F. (2010). Discriminant analysis of principal components: A new method for the analysis of genetically structured populations. *BMC Genet.* 11, 94. doi: 10.1186/1471-2156-11-94

Kalyaanamoorthy, S., Minh, B. Q., Wong, T. K. F., von Haeseler, A., and Jermiin, L. S. (2017). ModelFinder: fast model selection for accurate phylogenetic estimates. *Nat. Methods* 14, 587–589. doi: 10.1038/nmeth.4285

Katoh, K., and Standley, D. M. (2013). Mafft multiple sequence alignment software version 7: improvements in performance and usability. *Mol. Biol. Evol.* 30, 772–780. doi: 10.1093/molbev/mst010

Kearse, M., Moir, R., Wilson, A., Stones-Havas, S., Cheung, M., Sturrock, S., et al. (2012). Geneious Basic: An integrated and extendable desktop software platform for the organization and analysis of sequence data. *Bioinformatics* 28, 1647–1649. doi: 10.1093/bioinformatics/bts199

Kent, W. J. (2002). BLAT—The BLAST-like alignment tool. *Genome Res.* 12, 656–664. doi: 10.1101/gr.229202

Lanfear, R., Calcott, B., Ho, S. Y. W., and Guindon, S. (2012). Partitionfinder: combined selection of partitioning schemes and substitution models for phylogenetic analyses. *Mol. Biol. Evol.* 29, 1695–1701. doi: 10.1093/molbev/mss020

Lemmon, A. R., Emme, S. A., and Lemmon, E. M. (2012). Anchored hybrid enrichment for massively high-throughput phylogenomics. *Syst. Biol.* 61, 727–744. doi: 10.1093/sysbio/sys049

Letunic, I., and Bork, P. (2021). Interactive Tree Of Life (iTOL) v5: an online tool for phylogenetic tree display and annotation. *Nucleic Acids Res.* 49, W293–W296. doi: 10.1093/nar/gkab301

Li, H., Handsaker, B., Wysoker, A., Fennell, T., Ruan, J., Homer, N., et al. (2009). The sequence alignment/map format and SAMtools. *Bioinforma. Oxf. Engl.* 25, 2078–2079. doi: 10.1093/bioinformatics/btp352

Lozano-Fernandez, J., Giacomelli, M., Fleming, J. F., Chen, A., Vinther, J., Thomsen, P. F., et al. (2019). Pancrustacean evolution illuminated by taxon-rich genomic-scale data sets with an expanded remipede sampling. *Genome Biol. Evol.* 11, 2055–2070. doi: 10.1093/gbe/evz097

Lunter, G., and Goodson, M. (2011). Stampy: A statistical algorithm for sensitive and fast mapping of Illumina sequence reads. *Genome Res.* 21, 936–939. doi: 10.1101/gr.111120.110

McCormack, J. E., Faircloth, B. C., Crawford, N. G., Gowaty, P. A., Brumfield, R. T., and Glenn, T. C. (2012). Ultraconserved elements are novel phylogenomic markers that resolve placental mammal phylogeny when combined with species-tree analysis. *Genome Res.* 22, 746–754. doi: 10.1101/gr.125864.111

McCormack, J. E., Tsai, W. L. E., and Faircloth, B. C. (2016). Sequence capture of ultraconserved elements from bird museum specimens. *Mol. Ecol. Resour.* 16, 1189–1203. doi: 10.1111/1755-0998.12466

Minh, B. Q., Hahn, M. W., and Lanfear, R. (2020b). New methods to calculate concordance factors for phylogenomic datasets. *Mol. Biol. Evol.* 37, 2727–2733. doi: 10.1093/molbev/msaa106

Minh, B. Q., Schmidt, H. A., Chernomor, O., Schrempf, D., Woodhams, M. D., von Haeseler, A., et al. (2020a). IQ-TREE 2: new models and efficient methods for phylogenetic inference in the genomic era. *Mol. Biol. Evol.* 37, 1530–1534. doi: 10.1093/molbev/msaa015

Mo, Y. K., Lanfear, R., Hahn, M. W., and Minh, B. Q. (2023). Updated site concordance factors minimize effects of homoplasy and taxon sampling. *Bioinformatics* 39, btac741. doi: 10.1093/bioinformatics/btac741

Moles, J., and Giribet, G. (2021). A polyvalent and universal tool for genomic studies in gastropod molluscs (Heterobranchia). *Mol. Phylogenet. Evol.* 155, 106996. doi: 10.1016/J.YMPEV.2020.106996

Page, A. J., Taylor, B., Delaney, A. J., Soares, J., Seemann, T., Keane, J. A., et al. (2016). SNP-sites: rapid efficient extraction of SNPs from multi-FASTA alignments. *Microb. Genomics* 2, e000056. doi: 10.1099/mgen.0.000056

Patel, T., Robert, H., D'Udekem D'Acoz, C., Martens, K., De Mesel, I., Degraer, S., et al. (2020). Biogeography and community structure of abyssal scavenging Amphipoda (Crustacea) in the Pacific Ocean. *Biogeosciences* 17, 2731–2744. doi: 10.5194/bg-17-2731-2020

Poore, G. C. B. (2005). Peracarida: monophyly, relationships and evolutionary success. *Nauplius* 13, 1–27.

Prjibelski, A., Antipov, D., Meleshko, D., Lapidus, A., and Korobeynikov, A. (2020). Using SPAdes *de novo* assembler. *Curr. Protoc. Bioinforma.* 70, e102. doi: 10.1002/cpbi.102

Quattrini, A. M., Faircloth, B. C., Dueñas, L. F., Bridge, T. C. L., Brugler, M. R., Calixto-Botía, I. F., et al. (2018). Universal target-enrichment baits for anthozoan (Cnidaria) phylogenomics: New approaches to long-standing problems. *Mol. Ecol. Resour.* 18, 281–295. doi: 10.1111/1755-0998.12736

Quinlan, A. R., and Hall, I. M. (2010). BEDTools: a flexible suite of utilities for comparing genomic features. *Bioinformatics* 26, 841–842. doi: 10.1093/bioinformatics/btq033

Raxworthy, C. J., and Smith, B. T. (2021). Mining museums for historical DNA: advances and challenges in museomics. *Trends Ecol. Evol.* 36, 1049–1060. doi: 10.1016/j.tree.2021.07.009

Richter, S., and Scholtz, (2001). Phylogenetic analysis of the malacostraca (Crustacea). *J. Zool. Syst. Evol. Res.* 39, 113–136. doi: 10.1046/j.1439-0469.2001.00164.x

Rohland, N., and Reich, D. (2012). Cost-effective, high-throughput DNA sequencing. *Genome Res.* 22, 939–946. doi: 10.1101/gr.128124.111

Sato, S., Derkarabetian, S., Lord, A., and Giribet, G. (2024a). An ultraconserved element probe set for velvet worms (Onychophora). *Mol. Phylogenet. Evol.* 197, 108115. doi: 10.1016/j.ympev.2024.108115

Sato, S., Derkarabetian, S., Valdez-Mondragón, A., Pérez-González, A., Benavides, L. R., Daniels, S. R., et al. (2024b). Under the hood: Phylogenomics of hooded tick spiders (Arachnida, Ricinulei) uncovers discordance between morphology and molecules. *Mol. Phylogenet. Evol.* 193, 108026. doi: 10.1016/j.ympev.2024.108026

Schram, F. R. (1982). "The fossil record and evolution of Crustacea," in *The Biology of the Crustacea*, vol. 1, ed. L. G. Abele (New York City, NY: Academic Press), 93–147.

Schwentner, M., Combosch, D. J., Pakes Nelson, J., and Giribet, G. (2017). A phylogenomic solution to the origin of insects by resolving crustacean-hexapod relationships. *Curr. Biol.* 27, 1818–1824.e5. doi: 10.1016/j.cub.2017.05.040

Schwentner, M., Richter, S., Rogers, D. C., and Giribet, G. (2018). Tetraconatan phylogeny with special focus on Malacostraca and Branchiopoda: highlighting the strength of taxon-specific matrices in phylogenomics. *Proc. R. Soc B Biol. Sci.* 285, 20181524. doi: 10.1098/rspb.2018.1524

Shen, X., Tian, M., Yan, B., and Chu, K. (2015). Phylomitogenomics of malacostraca (Arthropoda: crustacea). *Acta Oceanol. Sin.* 34, 84–92. doi: 10.1007/s13131-015-0583-1

Smith, B. T., Harvey, M. G., Faircloth, B. C., Glenn, T. C., and Brumfield, R. T. (2014). Target capture and massively parallel sequencing of ultraconserved elements for comparative studies at shallow evolutionary time scales. *Syst. Biol.* 63, 83–95. doi: 10.1093/SYSBIO/SYT061

Spears, T., DeBry, R. W., Abele, L. G., and Chodyla, K. (2005). Peracarid monophyly and interordinal phylogeny inferred from nuclear small-subunit ribosomal DNA sequences (Crustacea: Malacostraca: Peracarida). *Proc. Biol. Soc Wash.* 118, 117–157. doi: 10.2988/0006-324X(2005)118[117:PMAIPI]2.0.CO;2

Starrett, J., Derkarabetian, S., Hedin, M., Bryson, R. W., McCormack, J. E., and Faircloth, B. C. (2017). High phylogenetic utility of an ultraconserved element probe set designed for Arachnida. *Mol. Ecol. Resour.* 17, 812–823. doi: 10.1111/1755-0998.12621

Streicher, J. W., and Wiens, J. J. (2017). Phylogenomic analyses of more than 4000 nuclear loci resolve the origin of snakes among lizard families. *Biol. Lett.* 13, 20170393. doi: 10.1098/rsbl.2017.0393

Swan, J. A., Jamieson, A. J., Linley, T. D., and Yancey, P. H. (2021). Worldwide distribution and depth limits of decapod crustaceans (Penaeoidea, Oplophoroidea) across the abyssal-hadal transition zone of eleven subduction trenches and five additional deep-sea features. *J. Crustac. Biol.* 41, 1–13. doi: 10.1093/jcbiol/ruaa102

Talavera, G., and Castresana, J. (2007). Improvement of phylogenies after removing divergent and ambiguously aligned blocks from protein sequence alignments. *Syst. Biol.* 56, 564–577. doi: 10.1080/10635150701472164

Tin, M. M. Y., Economo, E. P., and Mikheyev, A. S. (2014). Sequencing degraded DNA from non-destructively sampled museum specimens for RAD-tagging and low-coverage shotgun phylogenetics. *PloS One* 9, e96793. doi: 10.1371/journal.pone.0096793

Tsang, C. T. T., Schubart, C. D., Chu, K. H., Ng, P. K. L., and Tsang, L. M. (2022). Molecular phylogeny of Thoracotremata crabs (Decapoda, Brachyura): Toward adopting monophyletic superfamilies, invasion history into terrestrial habitats and multiple origins of symbiosis. *Mol. Phylogenet. Evol.* 177, 107596. doi: 10.1016/j.ympev.2022.107596

Tumescheit, C., Firth, A. E., and Brown, K. (2022). CIAlign: A highly customisable command line tool to clean, interpret and visualise multiple sequence alignments. *PeerJ* 10, e12983. doi: 10.7717/peerj.12983

van der Sprong, J., de Voogd, N. J., McCormack, G. P., Sandoval, K., Schätzle, S., Voigt, O., et al. (2024). A novel target-enriched multilocus assay for sponges (Porifera): Red Sea Haplosclerida (Demospongiae) as a test case. *Mol. Ecol. Resour.* 24, e13891. doi: 10.1111/1755-0998.13891

Vinciguerra, N. T., Tsai, W. L. E., Faircloth, B. C., and McCormack, J. E. (2019). Comparison of ultraconserved elements (UCEs) to microsatellite markers for the study of avian hybrid zones: a test in *Aphelocoma* jays. *BMC Res. Notes* 12, 456. doi: 10.1186/s13104-019-4481-z

Wandeler, P., Hoeck, P. E. A., and Keller, L. F. (2007). Back to the future: museum specimens in population genetics. *Trends Ecol. Evol.* 22, 634–642. doi: 10.1016/j.tree.2007.08.017

Wolfe, J. M., Ballou, L., Luque, J., Watson-Zink, V. M., Ahyong, S. T., Barido-Sottani, J., et al. (2023). Convergent adaptation of true crabs (Decapoda: Brachyura) to a gradient of terrestrial environments. *Syst. Biol.* 73, 247–262. doi: 10.1093/sysbio/syad066

Wolfe, J. M., Breinholt, J. W., Crandall, K. A., Lemmon, A. R., Lemmon, E. M., Timm, L. E., et al. (2019). A phylogenomic framework, evolutionary timeline and genomic resources for comparative studies of decapod crustaceans. *Proc. R. Soc B Biol. Sci.* 286, 20190079. doi: 10.1098/rspb.2019.0079

Zhang, Y. M., Williams, J. L., and Lucky, A. (2019). Understanding UCEs: a comprehensive primer on using ultraconserved elements for arthropod phylogenomics. *Insect Syst. Divers.* 3, 1–12. doi: 10.1093/ISD/IXZ016

frontiers | Frontiers in Marine Science

TYPE Original Research
PUBLISHED 30 October 2024
DOI 10.3389/fmars.2024.1380594

OPEN ACCESS

EDITED BY
Rachael Peart,
National Institute of Water and Atmospheric Research (NIWA), New Zealand

REVIEWED BY
Jörundur Svavarsson,
University of Iceland, Iceland
Amy Driskell,
Smithsonian National Museum of Natural History (SI), United States

*CORRESPONDENCE
Anchita Casaubon
anchita.casaubon@senckenberg.de

RECEIVED 01 February 2024
ACCEPTED 19 September 2024
PUBLISHED 30 October 2024

CITATION
Casaubon A and Riehl T (2024) Shape matters: investigating the utility of geometric morphometric techniques in the deep-sea isopod family Macrostylidae (Isopoda: Asellota). *Front. Mar. Sci.* 11:1380594. doi: 10.3389/fmars.2024.1380594

Shape matters: investigating the utility of geometric morphometric techniques in the deep-sea isopod family Macrostylidae (Isopoda: Asellota)

Anchita Casaubon[1,2]* and Torben Riehl[1,2]

[1]Department of Marine Zoology, Section Crustacea, Senckenberg Institute and Natural History Museum Frankfurt, Frankfurt am Main, Germany, [2]Institute for Ecology, Diversity and Evolution, Goethe University Frankfurt, Frankfurt am Main, Germany

Accurate taxonomic classification of deep-sea taxa is often impeded by the presence of highly morphologically similar but genetically distinct species. This issue is particularly pronounced in the isopods of the deep-sea family Macrostylidae, which exhibit remarkably low morphological variation despite significant genetic diversity. In this study, we present the first application of geometric morphometric techniques to 41 specimens across five species of deep-sea macrostylid isopods collected from Icelandic waters. Our results suggest that geometric morphometric techniques can effectively discriminate between macrostylid species. These techniques, hence, promise to be an important addition to the toolset of macrostylid taxonomists.

KEYWORDS

BIOICE, geometric morphometrics, integrative taxonomy, macrostylid, Iceland, IceAGE

1 Introduction

Geometric morphometrics has emerged as an important addition to the taxonomic toolset (Mutanen and Pretorius, 2007; Ludoški et al., 2008; Francuski et al., 2009; Roggero et al., 2013; Mitrovski-Bogdanović et al., 2014; Siriwut et al., 2015; Karanovic et al., 2016; Li et al., 2016; Grinang et al., 2019). This approach combines multivariate statistics with Cartesian coordinates to quantify shape variation, making it effective for identifying the subtle morphological differences that traditional taxonomic approaches may overlook (see e.g., Fukami et al., 2004; Bridge et al., 2023). Numerous studies have successfully applied geometric morphometric techniques to investigate cryptic species (usually defined as co-occurring species indistinguishable by the human eye despite high genetic distinctness), discovering new taxa, and identifying new taxonomically informative traits across a wide range of taxa (insects: Mutanen and Pretorius, 2007; Ludoški et al., 2008; Francuski et al., 2009; centipedes: Siriwut et al., 2015; copepods: Karanovic et al., 2016; decapods: Grinang et al., 2019; Lovrenčić et al.,

2020; Casaubon et al., 2023; ostracods: Ligios and Gliozzi, 2012; tardigrades: Fontoura and Morais, 2011). However, the application of geometric morphometrics is completely lacking for some taxonomic groups, including the deep-sea isopod family Macrostylidae Hansen, 1916.

The family Macrostylidae, comprising a single genus *Macrostylis* Sars, 1864, includes isopods with a global distribution spanning sublittoral (*M. spinifera* Sars, 1864, found at approximately 4 m) to hadal zones (*M. mariana* Mezhov, 1993, found at approximately 11,000 m) (Mezhov, 1992; Menzies, 1962; Brandt, 2002; 2004; Riehl et al., 2012). Despite an extensive distribution and significant molecular divergence, macrostylid isopods exhibit remarkably low morphologic variation (Riehl, 2014). Additionally, these isopods display varying degrees of sexual dimorphism, with copulatory (terminal) males having pronounced morphological differences from both subadult and females (Riehl et al., 2012), further complicating species diagnoses and allocation of conspecifics based solely on morphology.

Historically, macrostylid taxonomy has relied heavily on the comparative analysis of morphological characters and their linear measurements and ratios (Mezhov, 2003; Brandt, 2004; Vey and Brix, 2009; Riehl et al., 2012; Riehl and Brandt, 2013). Recent research on macrostylid isopods has increasingly employed integrative taxonomic techniques that combine molecular genetics and traditional morphometrics (Riehl et al., 2012; Riehl and Brandt, 2013; Bober et al., 2018). However, there are no known studies employing geometric morphometric techniques on Macrostylidae or other deep-sea isopods. This study represents the first application of geometric morphometric techniques in macrostylid taxonomy, aiming to: 1) evaluate the efficacy of these methods, and 2) to investigate various species of macrostylid isopods.

2 Materials and methods

Five species of macrostylid isopods (Figure 1) were used in this study: *M. spinifera* Sars, 1864, *M.* sp. aff. *spinifera, M. subinermis* Hansen, 1916, *M. longiremis* Hansen, 1916, and *M. magnifica* Wolff, 1962. The specimens used here (Table 1) were collected during research campaigns for several projects spanning from 1992 to 2014, including the BIOICE project (Benthic Invertebrates of Icelandic Waters; Brix and Svavarrson, 2010; Brattegard et al., 2019; Steingrímsson et al., 2020), the IceAGE project (Icelandic Marine Animals: Genetics and Ecology, 2008), and the PolySkag project (Polychaetes in coastal areas of the Skaggerak, 2014; Oug et al., 2015). All specimens analyzed here are deposited in the collections at the Senckenberg Natural History Museum in Frankfurt, Germany.

Initial species identifications were based on established taxonomic descriptions of macrostylid isopods (Sars, 1864, 1899; Meinert, 1890; Hansen 1916; Wolff, 1962). While there is some genetic data (16S and 18S, unpublished data) for macrostylids from the IceAGE and PolySkag projects, specimens collected during the BIOICE expedition lack genetic data due to the use of formaldehyde as a preservative.

A total of 41 subadult (preparatory) and adult (copulatory) specimens were used in geometric morphometric analyses. Only female isopods were used as they are more abundant in collections (Riehl et al., 2012) and are difficult to distinguish using morphology alone (Riehl et al., 2012), making them ideal candidates for use in geometric morphometric analyses.

The pleotelson was chosen as it is an important diagnostic character when used in conjunction with other morphological characters. It is also easier to position and photograph in a standard view compared to the third pereopod ischium or the operculum. As such, each pleotelson was photographed in dorsal view using a Leica M165C stereomicroscope equipped with a Leica DMC5400 20 Megapixel color CMOS camera. Images were saved in TIFF format using the Leica Application Suite (LAS X). The tpsUtil (Rohlf, 2015) program was used to prepare the images for landmarking and the tpsDig (Rohlf, 2015) program was used to digitize landmarks and semilandmarks. MorphoJ 1.07a (Klingenberg, 2011) was used for all subsequent analyses.

Though there are a few studies that have applied geometric morphometric techniques to isopod taxa (Santamaria et al., 2013; Ismail 2021; Kamilari and Sfenthourakis, 2009; Kim et al., 2021), to our knowledge none have focused on macrostylid isopods. Previous studies on isopod taxa have focused primarily on body shape, on pleopodal appendages (Kamilari and Sfenthourakis, 2009), or have employed destructive techniques (Bertin et al., 2002). Here, we selected homologous landmarks across macrostylid species that captured the most amount of shape variation using non-destructive techniques. Additionally, given the pleotelson is a symmetrical character (Schultz, 1969) and an excessive number of landmarks can reduce statistical power (Rufino et al., 2006; Mitteroecker et al., 2013), we selected three landmarks and 66 semi-landmarks comprising half of the pleotelson (Figure 2). Landmark 1 (lmk1) represents the point where the lateral pleotelson outline meets the 7th pereonite. Landmark 2 (lmk2) represents the midpoint of the posterior apex of the pleotelson, the position and shape of which appears to vary widely between macrostylids (e.g., *M. spinifera* vs. *M. subinermis*). Landmark 3 (lmk3) represents the maximum curvature of the point where the uropod inserts into the pleotelson (see arrow in Figure 2). The semi-landmarks are anchored between lmk 1 and lmk 2 and capture the lateral and posterior margins of the pleotelson.

A Procrustes superimposition method was used to standardize landmark data and generate Procrustes shape coordinates by translating, scaling, and rotating the raw coordinate data (Adams and Otárola-Castillo, 2013). The Procrustes shape coordinates generated were then used for principal component analyses (PCA) and canonical variate analyses (CVA). A PCA was performed to visualize and quantify pleotelson shape variation. The PCA created a morphospace (Figure 3) for visualizing shape variation, with each point representing the pleotelson shape of a macrostylid isopod. Points closer together on the PCA morphospace indicate more similar shapes, while points farther away indicate more dissimilar shapes. A CVA with a permutation test for pairwise distances (10,000

FIGURE 1
Female macrostylid isopods used in the present study. **(A)** *Macrostylis longiremis*; **(B)** *M. subinermis*; **(C)** *M. magnifica*; **(D)** *M.* sp. aff. *spinifera*; **(E)** *M. spinifera*.

TABLE 1 Macrostylid specimens examined for the application of geometric morphometric techniques in this study.

Expedition	Voucher	Species	Cruise ID	Station no.	Depth 1 (m)	Depth 2 (m)	Sampling Gear
BIOICE 2648	BiMa 1218	*M. longipes*	HM-1-94	14	1306	1310	RP sledge
BIOICE 2648	BiMa 1219	*M. longipes*	HM-1-94	14	1306	1310	RP sledge
BIOICE 2648	BiMa 1220	*M. longipes*	HM-1-94	14	1306	1310	RP sledge
BIOICE 2648	BiMa 1513	*M. longipes*	HM-1-94	14	1306	1310	RP sledge
BIOICE 2648	BiMa 1514	*M. longipes*	HM-1-94	14	1306	1310	RP sledge
BIOICE 2648	BiMa 1517	*M. longipes*	HM-1-94	14	1306	1310	RP sledge
BIOICE 2412	BiMa 935	*M. longipes*	B-9-93	562	1170	1174	detr. sledge (Sneli)
BIOICE 2465	BiMa 793	*M. longiremis*	B-9-93	584	180	–	detr. sledge (Sneli)
BIOICE 2465	BiMa 794	*M. longiremis*	B-9-93	584	180	–	detr. sledge (Sneli)
BIOICE 2465	BiMa 796	*M. longiremis*	B-9-93	584	180	–	detr. sledge (Sneli)
BIOICE 2465	BiMa 798	*M. longiremis*	B-9-93	584	180	–	detr. sledge (Sneli)
BIOICE 2465	BiMa 799	*M. longiremis*	B-9-93	584	180	–	detr. sledge (Sneli)

(Continued)

TABLE 1 Continued

Expedition	Voucher	Species	Cruise ID	Station no.	Depth 1 (m)	Depth 2 (m)	Sampling Gear
BIOICE 2585	BiMa 864	*M. longiremis*	HM-1-93	43	450	450	RP sledge
BIOICE 2585	BiMa 872	*M. longiremis*	HM-1-93	43	450	450	RP sledge
BIOICE 2585	BiMa 875	*M. longiremis*	HM-1-93	43	450	450	RP sledge
BIOICE 2863	BiMa 01*	*M. magnifica*	B-8-96	–	–	–	–
BIOICE 2863	BiMa 02*	*M. magnifica*	B-8-96	734	2399	2399	RP sledge
BIOICE 2863	BiMa 04*	*M. magnifica*	B-8-96	734	2399	2399	RP sledge
BIOICE 2863	BiMa 06*	*M. magnifica*	B-8-96	734	2399	2399	RP sledge
BIOICE 2863	BiMa 07*	*M. magnifica*	B-8-96	734	2399	2399	RP sledge
BIOICE 2863	BiMa 09*	*M. magnifica*	B-8-96	734	2399	2399	RP sledge
BIOICE 2904	BiMa 904	*M. n.* sp. *1*	B-8-96	473	1057	1067	RP sledge
BIOICE 2410	BiMa 1436	*M. n.* sp. *1*	B-9-93	561	1074	1075	RP sledge
BIOICE 2410	BiMa 1439	*M. n.* sp. *1*	B-9-93	561	1074	1075	RP sledge
BIOICE 2410	BiMa 1440	*M. n.* sp. *1*	B-9-93	561	1074	1075	RP sledge
BIOICE 2410	BiMa 1441	*M. n.* sp. *1*	B-9-93	561	1074	1075	RP sledge
BIOICE 2983	BiMa 79	*M. spinifera*	B-8-96	503	174	179	RP sledge
BIOICE 2983	BiMa 81	*M. spinifera*	B-8-96	503	175	179	RP sledge
BIOICE 2983	BiMa 82	*M. spinifera*	B-8-96	503	175	179	RP sledge
BIOICE 2983	BiMa 83	*M. spinifera*	B-8-96	503	175	179	RP sledge
BIOICE 2983	BiMa 84	*M. spinifera*	B-8-96	503	175	179	RP sledge
BIOICE 2983	BiMa 85	*M. spinifera*	B-8-96	503	175	179	RP sledge
BIOICE 2983	BiMa 86	*M. spinifera*	B-8-96	503	175	179	RP sledge
BIOICE 2983	BiMa 87	*M. spinifera*	HM-1-93	43	450	450	RP sledge
Polyskag 2014	PMa 15	*M. spinifera*	–	–	–	–	–
Polyskag 2014	PMa 16	*M. spinifera*	–	–	–	–	–
IceAGE	iMacro 21	*M. longipes*	M85-3	–	–	–	–
IceAGE	iMacro 37	*M. longipes*	M85-3	–	–	–	–

iterations) was performed to analyze interspecific shape variation in the pleotelson. The CVA (Figure 4) maximized the distance between individuals of different groups (i.e., species) while minimizing the distance between individuals of the same groups.

The Procrustes and Mahalanobis distances (Table 2) generated from the CVA were used to determine the statistical significance of the permutation tests. The Procrustes distance measured the absolute magnitude of shape deviation (Klingenberg and Monteiro, 2005), while the Mahalanobis distance measured how different an individual species was from others (Klingenberg and Monteiro, 2005).

Finally, a Procrustes ANOVA (analysis of variance; pANOVA) was conducted to assess the significance of pleotelson shape variation between the macrostylids studied here. The significance level (p-value) for all analyses was set to 0.05, with p-values less than 0.05 considered statistically significant.

3 Results

The results of the pANOVA revealed significant differences in pleotelson shape between macrostylid species ($p < 0.0001$; Table 2). The first two principal components accounted for 80.9% (PC1 53.3%, PC2 27.6%) of total variance. A scatter plot of the first two principal components (Figure 3) showed *M. spinifera* and *M.* sp. aff. *spinifera* clustering together but not overlapping in their distribution in the negative PC axis, *M. subinermis* forming its own distinct cluster in the positive PC axis, and *M. magnifica* slightly overlapping with *M. longiremis* in the positive PC axis. The first principal component accounted for most of the morphological variation and primarily showed changes in the posterolateral margins and the positioning of the pleotelson posterior apex. The pleotelson shape of species on the negative PC1, i.e., *M. spinifera*

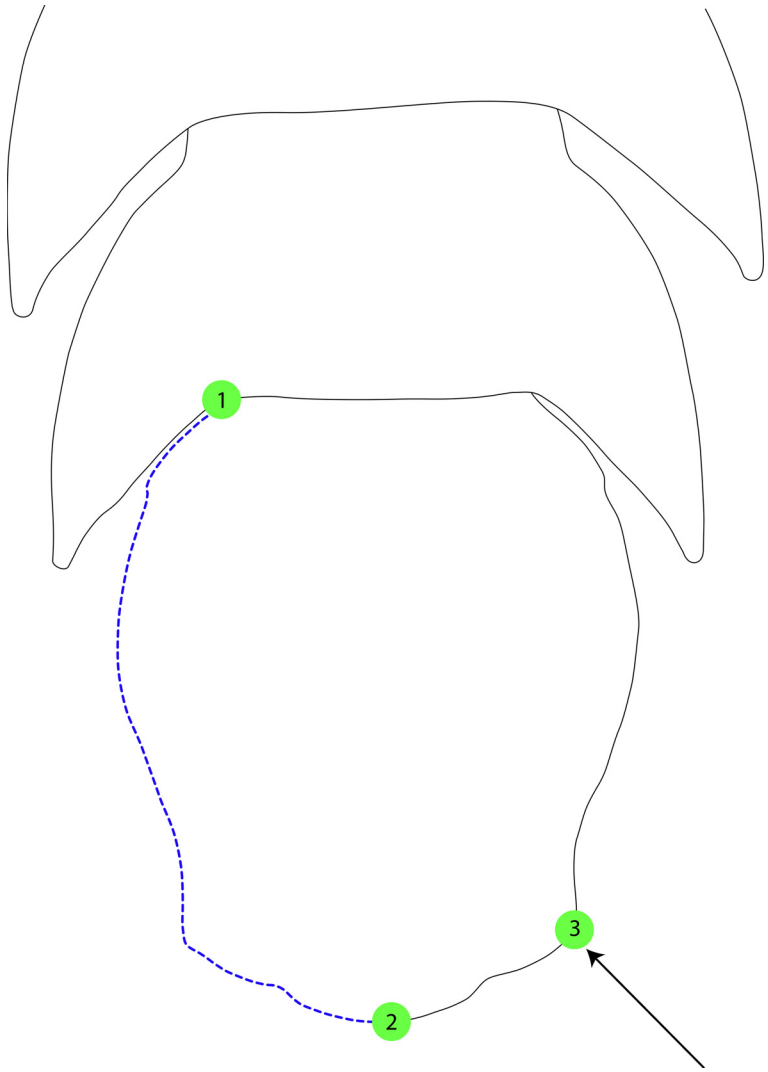

FIGURE 2
Landmarks and semi-landmarks on the pleotelson of *Macrostylis* spp. identified for use in geometric morphometric analyses. Closed red dots denote landmarks (n = 2), dashed blue lines denote the curve along which the semi-landmarks were placed.

and *M.* sp. aff. *spinifera*, was more hourglass shaped with a waist. The posterolateral margins and the posterior apex of these two species are very different from the remaining species clustered on the positive PC2 axis. The second principal component primarily showed changes in the lateral margins and overall pleotelson shape.

The first two canonical variates accounted for 98.3% (CV1 96.0%, CV2 2.26%) of total variance. A scatter plot of the first two canonical variates (Figure 4) showed all five species completely separated. *Macrostylis spinifera* and *M.* sp. aff. *spinifera* clustered closely together but did not overlap in the positive CV1 axis, *M. subinermis* and *M. longiremis* overlapped in their distribution in the negative CV1 axis while *M. magnifica* clustered by itself in the extreme negative CV1 axis. On average, the species on the positive extremes, i.e., *M. spinifera* and *M.* sp. aff. *spinifera*, were characterized by an hourglass shaped pleotelson with a waist while the species on the negative extremes, i.e., *M. magnifica*, *M. subinermis*, and *M. longiremis*, were characterized by a pleotelson with more parallel lateral margins. Similarly, the second canonical variate (CV2) axis also demonstrated shape changes in the posterior end of the pleotelson, with the species on the positive extremes having a less pronounced waist, compared to the isopods on the negative extremes having a more pronounced waist.

4 Discussion

Our application of geometric morphometric techniques to the pleotelson of macrostylid isopods successfully differentiated between the five species studied here, revealing subtle morphological differences even between highly morphologically similar taxa. Despite their high levels of genetic divergence, macrostylid isopods exhibit remarkable morphological homogeneity (Riehl and Brandt, 2010; Riehl and Brandt, 2013) significantly impeding accurate species diagnoses and complicating efforts at taxonomic reorganization. Our

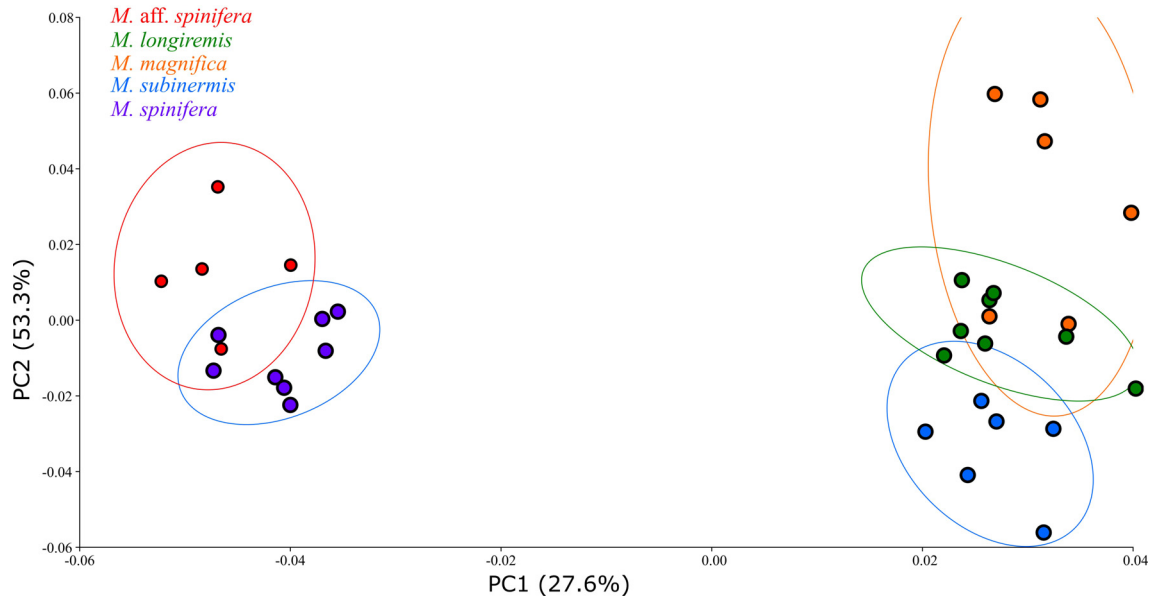

FIGURE 3
Scatter plot of the principal component analysis (PCA) performed on macrostylid isopods along the first two principal axes. Isopod specimens (dots) are colored by species.

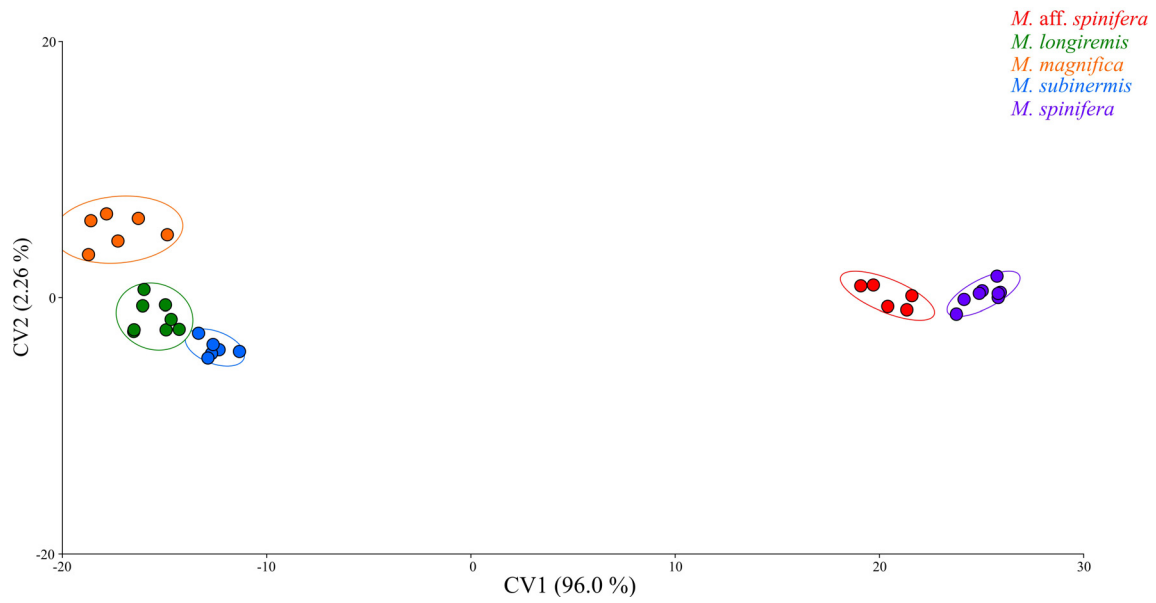

FIGURE 4
Canonical variate analysis (CVA) plot of pleotelson shape data of the macrostylid species used in the present study.

results demonstrate that geometric morphometric techniques are excellent at detecting the subtle morphological differences that separate species which are highly morphologically similar.

As a prime example, the lack of overlap between *M. spinifera* and *M.* sp. aff. *spinifera* was unexpected given the high morphological similarity their females exhibit. Instead, geometric morphometric techniques clearly discriminated the two species. The distinction between *M. spinifera* and *M.* sp. aff. *spinifera* is ostensible in their males. The males of *M.* sp. aff. *spinifera* have strikingly elongated sixth

TABLE 2 Procrustes ANOVA for the pleotelson shape of all species used in this study.

Effect	SS	MS	df	F	p
Individual	0.05985144	0.0001133550	528	9.23.55	< 0.0001
Residual	0.01778706	0.0000048125	3696	-	-

SS, sum of squares; MS, mean squares (i.e., SS divided by df); df, degree of freedom.

and seventh pereopods that closely resemble those of *M. longipes*. However, this rather strong expression of sexual dimorphism impedes allocation of conspecific male and female specimens (see also, e.g., Riehl et al., 2012); without the application of geometric morphometrics or genetics, the females may easily be taken for *M. spinifera* by an unexperienced identifier while the males may be identified either as *M. longipes*, or as a separate species without conspecific females in the samples. Interestingly, Hansen (1916) was the first one to report variation within *M. spinifera*. He remarked on an "atypical form" of a female macrostylid collected from the Davis Strait, which differed from the "typical form" of *M. spinifera* in its pleotelson shape along with differences in other morphological characters. More recently, a Bayesian phylogenetic reconstruction using 16S mitochondrial DNA from macrostylids recovered *M. spinifera* in two clades (Riehl, 2014). Hansen's (1916) remarks on a different form of *M. spinifera*, coupled with phylogenetic results (Riehl 2014, unpublished chapter[1]) suggest that there may be more than one species hidden under *M. spinifera*. As shown here, an approach integrating geometric morphometrics is useful for further investigating the morphological differences between females of these two species.

While our results demonstrated a successful application of geometric morphometric techniques, our study was limited in several respects. First, we were restricted by a small sample size ($N = 5–10$) for all species excluding *M. spinifera*. A small sample size is correlated with an increased risk of type II error and reduces the power of the statistical analyses being undertaken (Columb and Atkinson, 2016). Second, because of a limited number of specimens available to us and the enormous and cost-prohibitive sampling efforts required to collect deep-sea specimens, we avoided dissections or any techniques that would physically damage specimens. As such, this study was limited to only the pleotelson as it was the easiest to standardize without dissection. Still our results demonstrate the potential of geometric morphometrics as a powerful tool in macrostylid taxonomy, highlighting efficiency and applicability without the necessity of time-consuming and specimen-harming preparation.

Our findings introduce a promising new direction for research in macrostylid taxonomy and suggest that geometric morphometric techniques are a useful addition to the existing set of tools used in this field. As shown here, geometric morphometric techniques are especially useful for elucidating shape differences between female macrostylid isopods, which can be difficult to differentiate using traditional morphology. Within the scope of macrostylid taxonomy, we expect that future studies will integrate these techniques in their approach and expand the use of geometric morphometrics to not only assess other diagnostically informative body parts, such as the fossosome and the operculum but also assess the efficacy of new taxonomic characters in macrostylid taxonomy. Outside the scope of macrostylid taxonomy, geometric morphometric techniques may be applicable to other deep-sea isopod families to support taxonomic efforts. Geometric morphometric techniques may also be useful in other deep-sea asellotes that face similar difficulties in efforts at taxonomic reorganization (Raupach et al., 2009; Brix et al., 2011).

Data availability statement

The original contributions presented in the study are included in the article/supplementary material. Further inquiries can be directed to the corresponding author.

Ethics statement

The manuscript presents research on animals that do not require ethical approval for their study.

Author contributions

AC: Data curation, Formal analysis, Investigation, Methodology, Validation, Visualization, Writing – original draft, Writing – review & editing. TR: Data curation, Funding acquisition, Writing – review & editing.

Funding

The author(s) declare financial support was received for the research, authorship, and/or publication of this article. The present study is part of the Ph.D. project of the first author conducted in the framework of the Senckenberg Ocean Species Alliance (SOSA), which is a research and conservation program funded through a philanthropic donation. This is SOSA contribution #24.

Acknowledgments

We are grateful to Jörundur Svavarsson for his hospitality and support during a stay of TR at the University of Iceland and for providing the isopod material from the BIOICE expedition. We are thankful to Andreas H.J. Kelch for his assistance with the pleotelson illustration used in the present paper. We thank the two reviewers for their comments and suggestions. We are thankful to Nicolas Casaubon for his insightful comments and invaluable support. Lastly, we are thankful to Dr. Angelika Brandt and the teams of the Senckenberg Crustacea section and the Senckenberg Ocean Species Alliance (SOSA) for their invaluable support.

Conflict of interest

The authors declare that the research was conducted in the absence of any commercial or financial relationships that could be construed as a potential conflict of interest.

Publisher's note

References

Adams, D. C., and Otárola-Castillo, E. (2013). geomorph: an r package for the collection and analysis of geometric morphometric shape data. *Methods Ecol. Evol.* 4, 393–399. doi: 10.1111/2041-210X.12035

Bertin, A., et al. (2002). Quantification of sexual dimorphism in *Asellus aquaticus* (Crustacea: Isopoda) using outline approaches. *Biol. J. Linn. Soc.* 77, 523–533. doi: 10.1046/j.1095-8312.2002.00125.x

Bober, S., et al. (2018). New Macrostylidae (Isopoda) from the Northwest Pacific Basin described by means of integrative taxonomy with reference to geographical barriers in the abyss. *Zoological J. Linn. Soc.* 182, 549–603. doi: 10.1093/zoolinnean/zlx042

Brandt, A. (2002). Desmostylis gerdesi, a new species (Isopoda: Malacostraca) from kapp norvegia, weddell sea, antarctica. *Proc. Biol. Soc. Washington* 115 (3), 616–627.

Brandt, A. (2004). New deep-sea species of Macrostylidae (Asellota: Isopoda: Malacostraca) from the Angola Basin off Namibia, South West Africa. *Zootaxa* 448, 1. doi: 10.11646/zootaxa.448.1.1

Brattegard, T., Steingrímsson, S.A., Svavarsson, J., Helgason, G.V., Gudmundsson, G., Sneli, J.A., et al. (2019). *BIOICE: The Benthic Invertebrates of Icelandic waters stationlist* (Marine Data Archive).

Bridge, T. C. L., Cowman, P. F., Quattrini, A. M., Bonito, V. E., Sinniger, F., Harii, S., et al. (2023). A tenuis relationship: traditional taxonomy obscures systematics and biogeography of the "Acropora tenuis" (Scleractinia: Acroporidae) species complex. *Zoological J. Linn. Soc.* 202, 1–24. doi: 10.1093/zoolinnean/zlad062

Brix, S., Riehl, T., and Leese, F. (2011). First genetic data for species of the genus haploniscus richardso(Isopoda: Asellota: Haploniscidae) from neighbouring deep-sea basins in the south atlantic. *Zootaxa* 2838 (1), 79–84.

Brix, S., and Svavarsson, J. (2010). Distribution and diversity of desmosomatid and nannoniscid isopods (Crustacea) on the greenland–Iceland–Faeroe ridge. *Polar Biol.* 33, 515–530.

Casaubon, A., Hultgren, K. M., Murray, C., Hanscom, R. J., and Hurt, C. (2023). Application of integrative taxonomy combining phylogenetic and geometric morphometric techniques in a snapping shrimp (*Alpheus*) species complex (Decapoda: Caridea: Alpheidae). *J. Crustacean Biol.* 43. doi: 10.1093/jcbiol/ruad078

Columb, M., and Atkinson, M. (2016). Statistical analysis: sample size and power estimations. *BJA Educ.* 16, 159–161. doi: 10.1093/bjaed/mkv034

Fontoura, P., and Morais, P. (2011). Assessment of traditional and geometric morphometrics for discriminating cryptic species of the *Pseudechiniscus suillus* complex (Tardigrada, Echiniscidae). *J. Zoological Systematics Evolutionary Res.* 49, 26–33. doi: 10.1111/j.1439-0469.2010.00594.x

Francuski, L., Vujić, A., Kovačević, A., Ludoški, J., and Milankov, V. (2009). Identification of the species of the *Cheilosia variabilis* group (Diptera, Syrphidae) from the Balkan Peninsula using wing geometric morphometrics, with the revision of status of C. melanopa redi Vujic 1996. *Contributions To Zool. - CONTRIB ZOOL* 78, 129–140. doi: 10.1163/18759866-07803004

Fukami, H., Budd, A. F., Paulay, G., Solé-Cava, A., Allen Chen, C., Iwao, K., et al. (2004). Conventional taxonomy obscures deep divergence between Pacific and Atlantic corals. *Nature* 427, 832–835. doi: 10.1038/nature02339

Grinang, J., Das, I., and Ng, P. K. L. (2019). Geometric morphometric analysis in female freshwater crabs of Sarawak (Borneo) permits addressing taxonomy-related problems. *PeerJ* 7, e6205. doi: 10.7717/peerj.6205

Hansen, H. J. (1916). The order isopoda. *Danish Ingolf Expedition Copenhagen* 3 (5), l–262.

Ismail, T. G. (2021). Seasonal shape variations, ontogenetic shape changes, and sexual dimorphism in a population of land isopod *Porcellionides pruinosus*: a geometric morphometric study. *J. Basic Appl. Zoology* 82, 1–15. doi: 10.1186/s41936-021-00209-y

Kamilari, M., and Sfenthourakis, S. (2009). A morphometric approach to the geographic variation of the terrestrial isopod species *Armadillo tuberculatus* (Isopoda: Oniscidea). *J. Zoological Systematics Evolutionary Res.* 47 (3), 219–226. doi: 10.1111/j.1439-0469.2008.00510.x

Karanovic, T., Djurakic, M., and Eberhard, S. M. (2016). Cryptic species or inadequate taxonomy? Implementation of 2D geometric morphometrics based on integumental organs as landmarks for delimitation and description of copepod taxa. *Systematic Biol.* 65, 304–327. doi: 10.1093/sysbio/syv088

Kim, J., Kim, J., Lee, W., and Karanovic, I. (2021). The first insight into the patterns of size and shape variation of a microcerberid isopod. *Water* 13, 515. doi: 10.3390/w13040515

Klingenberg, C. P., and Monteiro, L. R. (2005). Distances and directions in multidimensional shape spaces: implications for morphometric applications. *Systematic Biol.* 54 (4), 678–688. doi: 10.1080/10635150590947258

Klingenberg, C. P. (2011). MorphoJ: an integrated software package for geometric morphometrics. *Mol. Ecol. Resour.* 11, 353–357. doi: 10.1111/j.1755-0998.2010.02924.x

Li, L., Qi, Y., Yang, Y., and Bai, M. (2016). A new species of *Falsopodabrus* Pic characterized with geometric morphometrics (Coleoptera, Cantharidae). *ZooKeys* 614), 97–112. doi: 10.3897/zookeys.614.6156

Ligios, S., and Gliozzi, E. (2012). The genus cyprideis jones 1857 (Crustacea, Ostracoda) in the Neogene of Italy: A geometric morphometric approach. *Rev. Micropaléontologie* 55, 171–207. doi: 10.1016/j.revmic.2012.09.002

Lovrenčić, L., Pavić, V., Majnarić, S., Abramović, L., Jelić, M., and Maguire, I. (2020). Morphological diversity of the stone crayfish – traditional and geometric morphometric approach. *Knowledge Manage. Aquat. Ecosyst.* 421), 1. doi: 10.1051/kmae/2019042

Ludoški, J., Francuski, L., Vujić, A., and Milankov, V. (2008). The *Cheilosia canicularis* group (Diptera: Syrphidae): Species delimitation and evolutionary relationships based on wing geometric morphometrics. *Zootaxa* 1825, 40–50. doi: 10.11646/zootaxa.1825.1.4

Meinert, F. V. A. (1890). Crustacea Malacostraca. *Videnskabelige udbytte af kanonbaden "Hauchs Dogter"*, 147–230 (In Danish).

Menzies, R. J. (1962). The isopods of abyssal depths in the atlantic ocean. *Columbia Univ. Press Vema Res. Ser.* 1, 79–206.

Mezhov, B. V. (1992). Two new species of the genus macrostylis GO sar(Crustacea isopoda asellota macrostylidae) from the antarctic. *Arthropoda Selecta* 1 (2), 83–87.

Mezhov, B. V. (1993). Three new species of macrostylis GO sar(Crustacea isopoda asellota macrostylidae) from the pacific ocean. *Arthropoda Selecta* 2 (3), 3–9.

Mezhov, B. V. (2003). *New abyssal species of the genus* Macrostylis *G.O. Sars 1864 (Crustacea: Isopoda: Macrostylidae) from the northwestern part of the Indian Ocean*. 12 (1), 1–8.

Mitrovski-Bogdanović, A., Tomanović, Ž., Mitrović, M., Petrović, A., Ivanović, A., Žikić, V., et al. (2014). The *Praon dorsale–yomenae* s.str. complex (Hymenoptera, Braconidae, Aphidiinae): Species discrimination using geometric morphometrics and molecular markers with description of a new species. *Zoologischer Anzeiger - A J. Comp. Zool.* 253, 270–282. doi: 10.1016/j.jcz.2014.02.001

Mitteroecker, P., Gunz, P., Windhager, S., and Schaefer, K. (2013). A brief review of shape, form, and allometry in geometric morphometrics, with applications to human facial morphology. *Hystrix* 24, 59. doi: 10.4404/hystrix-24.1-6369

Mutanen, M., and Pretorius, E. (2007). Subjective visual evaluation vs. traditional and geometric morphometrics in species delimitation: A comparison of moth genitalia. *Systematic Entomol.* 32, 371–386. doi: 10.1111/j.1365-3113.2006.00372.x

Oug, E., Christiansen, M. E., Dobbe, K., Rønning, A. H., Bakken, T., and Kongsrud, J. A. (2015). Mapping of marine benthic invertebrates in the oslofjord and the skagerrak: sampling data of museum collections from 1950–1955 and from recent investigations. doi: 10.5324/fn.v35i0.1944

Raupach, M. J., Mayer, C., Malyutina, M., and Wägele, J. W. (2009). Multiple origins of deep-sea asellota (Crustacea: Isopoda) from shallow waters revealed by molecular data. *Proc. R. Soc. B: Biol. Sci.* 276 (1658), 799–808.

Riehl, T. (2014). A phylogenetic approach to the classification of macrostylid isopods and faunal linkages between the deep sea and shallow-water environments (Doctoral dissertation, Hamburg, Germany, Universität Hamburg). doi: 10.13140/RG.2.1.3989.6084

Riehl, T., and Brandt, A. (2010). Descriptions of two new species in the genus Macrostylis Sars 1864 (Isopoda, Asellota, Macrostylidae) from the Weddell Sea (Southern Ocean), with a synonymisation of the genus *Desmostylis* Brandt 1992 with Macrostylis. *ZooKeys* 57), 9–49. doi: 10.3897/zookeys.57.310

Riehl, T., and Brandt, A. (2013). Southern ocean macrostylidae reviewed with a key to the species and new descriptions from maud rise. *Zootaxa* 3692 (1), 160–203.

Riehl, T., Wilson, G., and Hessler, R. (2012). New Macrostylidae Hansen 1916 (Crustacea: Isopoda) from the Gay Head-Bermuda transect with special consideration of sexual dimorphism. *Zootaxa* 3277, 1–26. doi: 10.11646/zootaxa.3277.1.1

Roggero, A., Giachino, P. M., and Palestrini, C. (2013). A new cryptic ground beetle species from the Alps characterised via geometric morphometrics. *Contributions to Zool.* 82, 171–183. doi: 10.1163/18759866-08204002

Rohlf, F. (2015). The Tps series of software. *Hystrix* 26, 1–4. doi: 10.4404/hystrix-26.1-11264

Rufino, M. M., Abelló, P., and Yule, A. B. (2006). Geographic and gender shape differences in the carapace of liocarcinus depurator (Brachyura: Portunidae) using geometric morphometrics and the influence of a digitizing method. *J. Zoology* 269 (4), 458–465.

Santamaria, C. A., Mateos, M., Taiti, S., DeWitt, T. J., and Hurtado, L. A. (2013). A complex evolutionary history in a remote archipelago: phylogeography and morphometrics of the Hawaiian endemic *ligia* isopods. *PloS One* 8, e85199. doi: 10.1371/journal.pone.0085199

Sars, G. O. (1864). Om en anomal Gruppe af Isopoder. *Forhandlinger i Videnskaps-selskabet i Christiania* 1863, 205–221.

Sars, G. O. (1899). *An account of the crustacea of norway: with short descriptions and figures of all the species: Isopoda*. Ed. A. Cammermeyer (Bergen: Bergen Museum).

Schultz, G. A. (1969). How to know the marine isopod crustaceans.

Siriwut, W., Edgecombe, G.D., Sutcharit, C., and Panha, S. (2015). The centipede genus *scolopendra* in Mainland Southeast Asia: molecular phylogenetics, geometric morphometrics and external morphology as tools for species delimitation. *PloS One* 10, e0135355. doi: 10.1371/journal.pone.0135355

Steingrímsson, S. A., Gudmundsson, G., and Helgason, G. V. (2020). The BIOICE station and sample list: revised compilation, March 2020. *Zenodo*. doi: 10.5281/zenodo.3728257

Vey, A., and Brix, S. (2009). *Macrostylis* cerritus sp. nov., a new species of Macrostylidae (Isopoda: Asellota) from the Weddell Sea, Southern Ocean. *Zootaxa* 2096. doi: 10.11646/zootaxa.2096.1.21

Wolff, T. (1962). The systematics and biology of bathyal and abyssal Isopoda Asellota. *Galathea Rep.* 6, 1–320.

Frontiers in Marine Science

Explores ocean-based solutions for emerging global challenges

The third most-cited marine and freshwater biology journal, advancing our understanding of marine systems and addressing global challenges including overfishing, pollution, and climate change.

Discover the latest Research Topics

See more →

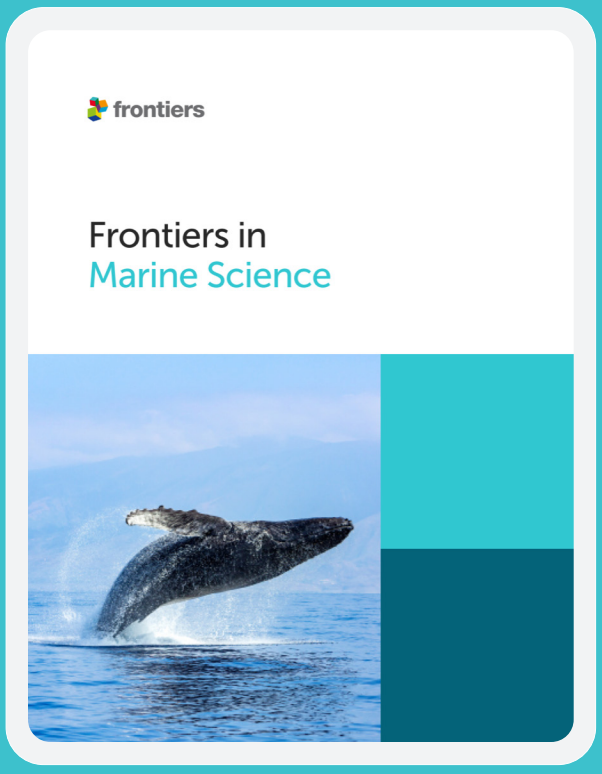

Frontiers

Avenue du Tribunal-Fédéral 34
1005 Lausanne, Switzerland
frontiersin.org

Contact us

+41 (0)21 510 17 00
frontiersin.org/about/contact